

Advances

in Clinical and Experimental Medicine

MONTHLY ISSN 1899-5276 (PRINT) ISSN 2451-2680 (ONLINE)

www.advances.umed.wroc.pl

2020, Vol. 29, No. 4 (April)

Impact Factor (IF) – 1.227
Ministry of Science and Higher Education – 40 pts.
Index Copernicus (ICV) – 155.19 pts.



WROCLAW
MEDICAL UNIVERSITY

Advances
in Clinical and Experimental
Medicine



Advances in Clinical and Experimental Medicine

ISSN 1899-5276 (PRINT)

ISSN 2451-2680 (ONLINE)

www.advances.umed.wroc.pl

MONTHLY 2020
Vol. 29, No. 4
(April)

Advances in Clinical and Experimental Medicine is a peer-reviewed open access journal published by Wrocław Medical University. Its abbreviated title is Adv Clin Exp Med. Journal publishes original papers and reviews encompassing all aspects of medicine, including molecular biology, biochemistry, genetics, biotechnology, and other areas. It is published monthly, one volume per year.

Editorial Office

ul. Marcinkowskiego 2–6
50-368 Wrocław, Poland
Tel.: +48 71 784 11 36
E-mail: redakcja@umed.wroc.pl

Publisher

Wrocław Medical University
Wybrzeże L. Pasteura 1
50-367 Wrocław, Poland

© Copyright by Wrocław Medical University,
Wrocław 2020

Online edition is the original version of the journal

Editor-in-Chief

Maciej Bagłaż

Vice-Editor-in-Chief

Dorota Frydecka

Editorial Board

Piotr Dziągłiel
Marian Klinger
Halina Milnerowicz
Jerzy Mozrzymas

Thematic Editors

Marzenna Bartoszewicz (microbiology)
Marzena Dominiak (dentistry)
Paweł Domosławski (surgery)
Maria Ejma (neurology)
Jacek Gajek (cardiology)
Mariusz Kuształ
(nephrology and transplantology)
Rafał Matkowski (oncology)
Ewa Milnerowicz-Nabzdyk (gynecology)
Katarzyna Neubauer (gastroenterology)
Marcin Ruciński (basic sciences)
Robert Śmigiel (pediatrics)
Paweł Tabakow (experimental medicine)
Anna Wiela-Hojeńska
(pharmaceutical sciences)
Dariusz Wołowicz (internal medicine)

International Advisory Board

Reinhard Berner (Germany)
Vladimir Bobek (Czech Republic)
Marcin Czyz (UK)
Buddhadeb Dawn (USA)
Kishore Kumar Jella (USA)

Secretary

Katarzyna Neubauer

Piotr Ponikowski
Marek Sąsiadek
Leszek Szenborn
Jacek Szepietowski

Statistical Editors

Dorota Diakowska
Leszek Noga
Lesław Rusiecki

Technical Editorship

Paulina Kunicka
Marek Misiak

English Language Copy Editors

Eric Hilton
Sherill Howard Pociecha
Jason Schock
Marcin Tereszewski

Pavel Kopel (Czech Republic)
Tomasz B. Owczarek (USA)
Ivan Rychlík (Czech Republic)
Anton Sculean (Switzerland)
Andriy B. Zimenkovsky (Ukraine)

Editorial Policy

Advances in Clinical and Experimental Medicine (Adv Clin Exp Med) is an independent multidisciplinary forum for exchange of scientific and clinical information, publishing original research and news encompassing all aspects of medicine, including molecular biology, biochemistry, genetics, biotechnology and other areas. During the review process, the Editorial Board conforms to the "Uniform Requirements for Manuscripts Submitted to Biomedical Journals: Writing and Editing for Biomedical Publication" approved by the International Committee of Medical Journal Editors (www.ICMJE.org/). The journal publishes (in English only) original papers and reviews. Short works considered original, novel and significant are given priority. Experimental studies must include a statement that the experimental protocol and informed consent procedure were in compliance with the Helsinki Convention and were approved by an ethics committee.

For all subscription-related queries please contact our Editorial Office:
redakcja@umed.wroc.pl

For more information visit the journal's website:
www.advances.umed.wroc.pl

Pursuant to the ordinance No. 134/XV R/2017 of the Rector of Wrocław Medical University (as of December 28, 2017) from January 1, 2018 authors are required to pay a fee amounting to 700 euros for each manuscript accepted for publication in the journal Advances in Clinical and Experimental Medicine.

„Podniesienie poziomu naukowego i poziomu umiędzynarodowienia wydawanych czasopism naukowych oraz upowszechniania informacji o wynikach badań naukowych lub prac rozwojowych – zadanie finansowane w ramach umowy 784/p-DUN/2017 ze środków Ministra Nauki i Szkolnictwa Wyższego przeznaczonych na działalność upowszechniającą naukę”.



Indexed in: MEDLINE, Science Citation Index Expanded, Journal Citation Reports/Science Edition, Scopus, EMBASE/Excerpta Medica, Ulrich's™ International Periodicals Directory, Index Copernicus

Typographic design: Monika Kołęda, Piotr Gil
DTP: Wydawnictwo UMW
Cover: Monika Kołęda
Printing and binding: EXDRUK

Contents

Original papers

- 423 Hajer Foddha, Nadia Bouzidi, Abdelhak Foddha, Saoussen Chouchene, Rahma Touhami, Nadia Leban, Mohamed Faouzi Maatoug, Habib Gamra, Salima Ferchichi, Jemni Ben Chibani, Amel Haj Khelil
Single nucleotide polymorphisms of *SCN5A* and *SCN10A* genes increase the risk of ventricular arrhythmias during myocardial infarction
- 431 Jingtang Li, Guanxiang Liao, Zhisheng Long, Peng Qiu, Linghua Ding, Long Xiong
Study of PLGA microspheres loaded with pOx/PEI nanoparticles for repairing bone defects in vivo and in vitro
- 441 Michał Wolańczyk, Joanna Bladowska, Anna Kołtowska, Anna Pokryszko-Dragan, Przemysław Podgórski, Sławomir Budrewicz, Marek Szaśiadek
Diffusion tensor imaging of normal-appearing cervical spinal cords in patients with multiple sclerosis: Correlations with clinical evaluation and cerebral diffusion tensor imaging changes. Preliminary experience
- 449 Yusuf Özay, Dilay Ozek, Filiz Yıldırım, Zuhaf Yıldırım
The effect of diabetes on vitreous levels of adiponectin and inflammatory cytokines in experimental rat model
- 453 Yaşar Turan, Vahit Demir
The relation of endocan and galectin-3 with ST-segment resolution in patients with ST-segment elevation myocardial infarction
- 459 Xiangyuan Wen, Hai Huang, Canbin Wang, Jianghui Dong, Xuezhi Lin, Fuming Huang, Hua Wang, Liping Wang, Shicai Fan
Comparative biomechanical testing of customized three-dimensional printing acetabular-wing plates for complex acetabular fractures
- 469 Anna Pokryszko-Dragan, Karol Marschollek, Aleksandra Chojko, Magdalena Karasek, Adam Kardys, Paweł Marschollek, Ewa Gruszka, Marta Nowakowska-Kotas, Sławomir Budrewicz
Social participation of patients with multiple sclerosis
- 475 Mehmet Güli Çetinçakmak, Salih Hattapoğlu, Murat Söker, Faysal Ekici, Kamil Yılmaz, Cemil Göya, Cihad Hamidi
Evaluation of the relationship between splenic iron overload and liver, heart and muscle features evident on T2*-weighted magnetic resonance imaging
- 481 Natalia Alicja Świątoniowska-Lonc, Agnieszka Sławuta, Krzysztof Dudek, Katarzyna Jankowska, Beata Katarzyna Jankowska-Polańska
The impact of health education on treatment outcomes in heart failure patients
- 493 Yuxiang Dai, Shufu Chang, Shen Wang, Yi Shen, Chenguang Li, Zheyong Huang, Hao Lu, Juying Qian, Lei Ge, Qibing Wang, Feng Zhang, Junbo Ge
The preservation effect of coronary collateral circulation on left ventricular function in chronic total occlusion and its association with the expression of vascular endothelial growth factor A
- 499 Mazen Al-Essa, Gursev Dhaunsi
Receptor-mediated attenuation of insulin-like growth factor-1 activity by galactose-1-phosphate in neonate skin fibroblast cultures: Galactosemia pathogenesis

Reviews

- 505 Magdalena Liszewska-Kapłon, Mateusz Strózik, Łukasz Kotarski, Maciej Bałaj, Lidia Hirnle
Mayer–Rokitansky–Küster–Hauser syndrome as an interdisciplinary problem
- 513 Katarzyna Dyga, Maria Szczepańska
IgA vasculitis with nephritis in children

Single nucleotide polymorphisms of *SCN5A* and *SCN10A* genes increase the risk of ventricular arrhythmias during myocardial infarction

Hajer Fodhda^{1,2,A–D,F}, Nadia Bouzidi^{1,B}, Abdelhak Fodhda^{3,A–C}, Saoussen Chouchene^{4,B}, Rahma Touhami^{1,2,B}, Nadia Leban^{1,E}, Mohamed Faouzi Maatoug^{3,B}, Habib Gamra^{3,B}, Salima Ferchichi^{1,B}, Jemni Ben Chibani^{1,E}, Amel Haj Khelil^{1,2,C–F}

¹ Laboratory of Biochemistry and Molecular Biology, Faculty of Pharmacy, University of Monastir, Tunisia

² Higher Institute of Biotechnology, University of Monastir, Tunisia

³ Department of Cardiology, Fattouma Bourguiba University Hospital of Monastir, Tunisia

⁴ Department of Hematology, Fattouma Bourguiba University Hospital of Monastir, Tunisia

A – research concept and design; B – collection and/or assembly of data; C – data analysis and interpretation;

D – writing the article; E – critical revision of the article; F – final approval of the article

Advances in Clinical and Experimental Medicine, ISSN 1899–5276 (print), ISSN 2451–2680 (online)

Adv Clin Exp Med. 2020;29(4):423–429

Address for correspondence

Hajer Fodhda

E-mail: hajer.fodhda@hotmail.fr

Funding sources

None declared

Conflict of interest

None declared

Received on September 8, 2019

Reviewed on November 11, 2019

Accepted on January 21, 2020

Published online on April 24, 2020

Cite as

Fodhda H, Bouzidi N, Fodhda A, et al. Single nucleotide polymorphisms of *SCN5A* and *SCN10A* genes increase the risk of ventricular arrhythmias during myocardial infarction.

Adv Clin Exp Med. 2020;29(4):423–429.

doi:10.17219/acem/116750

DOI

10.17219/acem/116750

Copyright

© 2020 by Wrocław Medical University

This is an article distributed under the terms of the Creative Commons Attribution 3.0 Unported (CC BY 3.0)

(<https://creativecommons.org/licenses/by/3.0/>)

Abstract

Background. Coronary artery disease (CAD) and its ultimate consequence – myocardial infarction (MI) – are major causes of sudden cardiac death (SCD). Previous studies have demonstrated the role of genetic polymorphisms in the risk of SCD and ventricular arrhythmia (VA) during MI.

Objectives. To investigate the association between single nucleotide polymorphisms (SNPs) of genes implicated in congenital cardiac arrhythmias and the risk of developing VA in the context of MI.

Material and methods. We performed a case–control study in which we genotyped 4 SNPs (rs11708996, rs10428132, rs9388451, and rs2200733) in 469 subjects using amplification refractory mutation system (ARMS) and a polymerase chain reaction–restriction fragment length polymorphism (PCR–RFLP). These SNPs are located in the *SCN5A*, *SCN10A*, *HEY2*, and *PITX2* genes, respectively. We first compared 70 patients who had developed VA in the context of MI with 141 healthy controls; next, we compared VA patients with 258 MI patients who did not develop VA during a 1-year follow up. The statistical analyses were adjusted for sex and age.

Results. Compared to the controls, 2 polymorphisms were significantly associated with the development of VA during MI, located in *SCN5A* rs11708996 ($p = 0.001$) and *SCN10A* rs10428132 ($p = 0.001$). Similar results were found when comparing VA cases with patients without VA. No associations of *HEY2* and *PITX2* polymorphisms were observed.

Conclusions. Our results suggest that the rs11708996 and rs10428132 polymorphisms of the *SCN5A* and *SCN10A* genes may contribute to an elevated risk of developing VA in the context of MI. The associated alleles or genotypes may be used to predict the risk, and thus prevent eventual SCD.

Key words: single nucleotide polymorphism, myocardial infarction, ventricular arrhythmia, sudden cardiac death

Introduction

In the last decade, there have been notable advances in the study of the mechanisms responsible for increased risk of arrhythmia and sudden cardiac death (SCD). In 5–10% of all cases, SCD occurs in patients with congenital rhythm disorders with normal heart structure.¹ However, SCD is mainly described in the setting of structural heart disease resulting from ventricular arrhythmias (VA), particularly ventricular fibrillation (VF).

Ventricular arrhythmia most commonly occurs early in ischemia, and patients presenting acute myocardial infarction (MI) and VA show a high risk of mortality.^{2,3} In nearly 10% of cases, VA occurs within the first hours following the MI symptoms.^{4,5}

Recognition of the genetic substrate underlying normal and abnormal electrical behavior in congenital arrhythmias has provided remarkable insight into the molecular basis of cardiac electrophysiology. The variants described may be of use in the general framework of all types of arrhythmias. It has been shown that some variants in the *SCN5A* gene can be considered a genetic risk for some acquired arrhythmias. The original causes can be heart failure, MI or coronary artery disease (CAD).⁶ The input of *SCN5A* mutations under ischemic conditions has been examined. In fact, the first sodium channel mutation to be associated with the development of an arrhythmic event during acute ischemia (G400A) was discovered in a patient who developed 6 episodes of VA within the first 12 h.⁷

Brugada syndrome (BrS) is a primary electrical heart disease with a high risk of VF and SCD.⁸ Some studies suggest that BrS and VA during MI are the result of a similar electrophysiological substrate, and sometimes the 2 diseases are confused.^{9,10} In this context, the genetic background of some congenital rhythm disorders could serve as a marker of arrhythmia in common cardiac diseases.

Single nucleotide polymorphisms (SNPs) that may play a role in high risk of VA and SCD diseases like atrial fibrillation (AF)¹¹ and BrS have been identified by genome-wide association studies (GWAS) on the *PITX2*,¹² *SCN5A*, *SCN10A*, and *HEY2* genes.¹³ More recently, some of them have been involved in Brs,¹⁴ long QT syndrome and SCD.¹⁵

In this in mind, we designed a case–control study using 4 SNPs previously associated with BrS (rs11708996, rs10428132 and rs9388451) and AF (rs2200733) to test their influence on the physiopathology of cardiac arrhythmias in patients with structural heart disease, aiming at finding a genetic marker that could be used as a general predictor of SCD.

Material and methods

Features of the populations studied

We enrolled a sample of patients with MI who developed VA (VA⁺) and compared them to a group of controls. The definition of MI is based on the European Society of Cardiology (ESC) 2018 diagnostic criteria¹⁶ and was diagnosed using coronary angiogram. Ventricular arrhythmia is defined as the presence of documented ventricular tachycardia (VT) or VF after AMI. The VA can be sustained VT/VF when its lasts more than 30 s of consecutive beats, or non-sustained VT/VF, defined as more than 5 consecutive beats lasting below 30 s, or VT/VF that must be terminated by immediate defibrillation due to hemodynamic instability. Over a follow-up period of 1 year, we also included patients who died from SCD of presumed arrhythmic origin.

A total of 481 unrelated Tunisian patients were admitted to the Department of Cardiology at the University Hospital of Monastir (Tunisia) for a suspected MI between October 2014 and June 2015. For this study, we considered

Table 1. Amplification conditions for SNP genotyping

SNP	Primers	Type of PCR	PCR conditions	Fragment length (bp)
rs2200733	F: 5'GCCTGCTTGGGTGGATGAAT3' R: 5'CCAGAGGCTCTATGGGATG3'	RFLP-PCR	94°C for 10 min, 35 cycles of: –94°C for 30 s, –60°C for 30 s, –72°C for 1 min 72°C for 10 min	CC: 415 + 246 C/T: 661 + 415 + 246 T/T: 661
rs11708996	F: 5'TGTTGACAGGTTGTGGAAC3' F: 5'TGTTGACAGGTTGTGGAAG3' R: 5'CCAGTTTCCCCTATGACTAA3'	ARMS-PCR	94°C for 10 min, 35 cycles of: –94°C for 30 s, –55°C for 30 s, –72°C for 1 min 72°C for 10 min	235
rs10428132	F: 5'TTAGCTCACTTATTCTCAA33' F: 5'TTAGCTCACTTATTCTCAAC33' R: 5'GAGGAGAAGCAATGCTATT33'			328
rs9388451	F: 5'TAGTGTGAAGACAAAATCC33' F: 5'TAGTGTGAAGACAAAATCCC33' R: 5'TGTGGTGGTGAAGATAGACA33'			400

SNP – single nucleotide polymorphism; PCR – polymerase chain reaction; ARMS-PCR – amplification refractory mutation system PCR; RFLP-PCR – restriction fragment length polymorphism PCR.

those with confirmed diagnoses of MI (n = 328) and, in this group, those who developed VA during a follow-up period of 1 year (n = 70). In order to reinforce our study, we compared the VA⁺ group to a sample of MI patients with no history of arrhythmic events (VA⁻; n = 258). Informed consent was obtained from all the patients included in the study. In the control cohort, 141 volunteer blood donors were recruited from the Blood Bank at the University Hospital of Mahdia (Tunisia). Inclusion criteria restricted the control group to those with no history of congenital or acquired cardiac arrhythmia and no family history of SCD.

SNP genotyping

Genomic DNA was extracted in all subjects from peripheral blood leukocytes using standard protocols. The SNPs associated with BrS (rs11708996, rs10428132 and rs9388451) were genotyped using a polymerase chain reaction-restriction fragment length polymorphism (PCR-RFLP). The one associated with AF (rs2200733) was genotyped using MboI restriction fragment length polymorphism (RFLP) PCR. All the details of the amplification conditions are summarized in Table 1.

Statistical analysis

Data distribution was checked with the Kolmogorov–Smirnov normality test. Parameters with normal distribution were presented as means ± standard deviation (SD), and compared using Student's t-test. If there were more than 2 groups, the analysis of variance (ANOVA) procedure was followed by post-hoc tests. Parameters that showed non-normal distribution were presented as median (min–max); comparisons of more than 2 groups were done using one-way

ANOVA (Kruskal–Wallis test) followed by the Mann–Whitney U test. Categorical data was summarized as frequencies or percentages and compared in cross tables using Pearson's χ^2 test. The IBM SPSS Statistics for Windows v. 22 software (IBM Corp., Armonk, USA) was used for all these tests.

Allelic distributions were compared using two-sided independent-sample Student's t-tests using Epi Info v. 1.4.3 software (Centers for Disease Control and Prevention, Atlanta, USA). Genotype frequencies between the case group and the control group were compared using the χ^2 test. The χ^2 goodness-of-fit test was employed to identify whether the genotype distributions fulfilled the Hardy–Weinberg equilibrium. Crude and adjusted genotyping associations in codominant, dominant and recessive models were analyzed with logistic regression analysis. These tests were assessed using SNPStats online software (<https://bioinfo.iconcologia.net/SNPstats>).¹⁷

Results with a p-value <0.05 were considered statistically significant. The relative risk was presented as odds ratios (OR) with 95% confidence intervals (95% CI).

Results

Clinical features of the study populations

The clinical history and demographic characteristics of the patients and controls are summarized in Table 2. The age and sex ratios were significantly different between the VA⁺ patients and the controls (p < 0.001). Myocardial infarction seems to occur more often in smoking men at advanced age. No significant differences were found between the patient groups in terms of age or gender. The MI patients with ST elevation (STEMI) were more likely

Table 2. Clinical history and demographic characteristics of the patients and controls

Characteristics	Controls (114)	MI patients (328)		p-value
		VA ⁻ (258)	VA ⁺ (70)	
Age [years]	44 (21–76)	57 (31–88)	54 (27–83)	<0.001 ^{a*} 0.075 ^b
Gender (male %)	42.5	80.6	90	<0.001 ^{a*} 0.066 ^b
Smokers (%)	8.9	55.4	40	<0.001 ^{a*} 0.047 ^{b*}
Personal history of VA (%)	0	0	15.1	ns
Victims of SCD (%)	0	0	34.2	ns
Family history of SCD (%)	0	4.6	11.1	0.036 ^{b*}
ST-elevation myocardial infarction (%)	0	40.8	71.4	<0.001 ^{b*}
Peak troponin I levels [ng/mL]	0.00	0.86 (0.00–483.9)	14.35 (0.01–468.8)	<0.001 ^{b*}
Time of occurrence of VA event (%): – 6 months – 1 year			71.4% 28.6%	ns

Age and peak troponin I levels are shown as median (min–max); a – comparison of control vs VA⁺ patients; b – comparison of VA⁺ vs VA⁻ patients; * statistically significant differences; ns – not significant; MI – myocardial infarction; VA – ventricular arrhythmia; SCD – sudden cardiac death.

Table 3. Case-control study comparing minor allele frequencies between healthy controls and VA+ MI patients

SNP (minor allele)	Healthy controls (141)	MI patients VA+ (70)	p-value	OR (95% CI)
<i>SCN5A</i> rs11708996 (C)	0.15	0.27	0.001*	2.18 (1.33–3.60)
<i>SCN10A</i> rs10428132 (T)	0.10	0.21	0.001*	2.46 (1.39–4.36)
<i>HEY2</i> rs9388451 (C)	0.32	0.39	0.07	1.36 (0.89–2.07)
<i>PITX2</i> rs2200733 (T)	0.26	0.25	0.47	0.95 (0.59–1.52)

Allelic data is presented as proportions; * statistically significant differences; MI – myocardial infarction; SNP – single nucleotide polymorphism; VA – ventricular arrhythmia; OR – odds ratio; 95% CI – 95% confidence interval.

Table 4. Genotypic distributions of rs11708996 and rs10428132 in controls and in VA+ MI patients in crude and adjusted analyses under different inheritance models

SNP	Inheritance model	Genotypes	Controls n (%)	VA+ MI patients n (%)	Crude analysis		Adjusted analysis (by age and gender)	
					OR (95% CI)	p-value	OR (95% CI)	p-value
rs11708996 (<i>SCN5A</i>)	codominant	G/G	103 (73)	42 (60)	1.00	0.003*	1.00	<0.001*
		G/C	35 (24.8)	18 (25.7)	1.26 (0.64–2.47)		1.23 (0.55–2.75)	
		C/C	3 (2.1)	10 (14.3)	8.17 (2.14–31.19)		19.23 (3.31–111.85)	
	dominant	G/G vs G/C-C/C	103 vs 38	42 vs 28	1.81 (0.99–3.31)	0.057	2.01 (0.97–4.17)	0.058
	recessive	G/G-G/C vs C/C	138 vs 3	60 vs 10	7.67 (2.04–28.85)	<0.001*	18.16 (3.17–103.97)	<0.001*
rs10428132 (<i>SCN10A</i>)	codominant	G/G	117 (83)	46 (65.7)	1.00	0.016*	1.00	0.038*
		G/T	21 (14.9)	19 (27.1)	2.30 (1.13–4.67)		2.84 (1.20–6.71)	
		T/T	3 (2.1)	5 (7.1)	4.24 (0.97–18.46)		2.51 (0.47–13.52)	
	dominant	G/G vs G/T-T/T	117 vs 24	46 vs 24	2.54 (1.31–4.92)	0.005*	2.78 (1.26–6.16)	0.011*
	recessive	G/G-G/T vs T/T	183 vs 3	65 vs 5	3.54 (0.82–15.26)	0.084	2.78 (1.26–6.16)	0.39

* statistically significant differences; MI – myocardial infarction; SNP – single nucleotide polymorphism; VA – ventricular arrhythmia; OR – odds ratio; 95% CI – 95% confidence interval.

to present VA than those without ST elevation (NSTEMI), especially in the first 6 months after the event. The mean peak of troponin I levels was significantly more elevated in VA+ patients. Coronary angiograms showed one-vessel disease in the vast majority of patients (73.47%), and no significant differences between the 2 groups were found in this respect.

Genetic analysis

The genotype distribution in the groups examined was concordant with the Hardy–Weinberg equilibrium (all $p > 0.05$). Table 3 shows the results of *HEY2*, *SCN5A*, *SCN10A* and *PITX2* allele frequencies. The minor alleles of *SCN5A* (rs11708996, G > C) and *SCN10A* (rs10428132, G > T) significantly increased the risk of arrhythmia

in patients with MI (*SCN5A*: $p = 0.001$; OR = 2.18 and *SCN10A*: $p = 0.001$; OR = 2.46). There was no significant relationship between *HEY2* (rs9388451, T > C) and *PITX2* (rs2200733, C > T) SNPs and the risk of developing VA.

Genotype distributions

Genotype distributions for the 2 SNPs that showed significant association are described in Table 4. Genotype frequencies were compared using crude analyses and analyses adjusted by age and gender, under different inheritance models.

The results of the crude analyses revealed that the CC genotype of *SCN5A* rs11708996 is significantly associated with the occurrence of arrhythmia under the recessive ($p < 0.001$; OR = 7.67) and codominant ($p = 0.003$; OR = 8.17) models. The TT genotype of *SCN10A* rs10428132

Table 5. Association analyses using allelic frequencies of VA⁺ and VA⁻ MI patients

SNP (minor allele)	VA ⁺ MI patients (70)	VA ⁻ MI patients (258)	p-value	OR (95% CI)
<i>SCN5A</i> rs11708996 (C)	0.27	0.19	0.019*	1.58 (1.03–2.44)
<i>SCN10A</i> rs10428132 (T)	0.21	0.12	0.006*	1.94 (1.19–3.17)
<i>HEY2</i> rs9388451 (C)	0.39	0.31	0.056	1.39 (0.94–2.05)
<i>PITX2</i> rs2200733 (T)	0.25	0.23	0.29	1.12 (0.72–1.73)

* statistically significant differences; MI – myocardial infarction; SNP – single nucleotide polymorphism; VA – ventricular arrhythmia; OR – odds ratio; 95% CI – 95% confidence interval.

showed an association with the arrhythmic group under the codominant ($p = 0.016$; OR = 2.30) and the dominant ($p = 0.005$; OR = 2.54) models. The adjusted analyses reinforce these associations (Table 4).

Allelic associations of the 4 SNPs between the 2 cohorts of MI patients (VA⁺ and VA⁻) revealed significant differences between the proportions of the C allele of *SCN5A* rs11708996 ($p = 0.019$; OR = 1.58) and the T allele of *SCN10A* rs10428132 ($p = 0.006$; OR = 1.94). In fact, the frequencies of these 2 alleles are increased in the group of VA⁺ patients (Table 5). Subsequent analyses of the genotypic associations showed no significant differences between the 2 groups.

Discussion

Many studies have suggested that the risk of fatal arrhythmias may be modulated by genetically determined variants in several genes, especially those responsible for the expression of ion channels.¹⁸ In this work, we selected 4 SNPs that are reported to be associated with certain forms of cardiac death. We investigated whether any of these genetic markers are of predictive value in assessing the risk of developing arrhythmia and SCD in patients with MI. Three of them were reported to have a strong association with BrS in a GWAS that located them in the *SCN5A*, *SCN10A* and *HEY2* genes.¹³ The 4th SNP is located near the *PITX2* gene and was reported to be strongly associated with lone atrial fibrillation.¹²

Our results showed that 2 of the 4 SNPs are significantly associated with the risk of developing VA in the context of MI. The first association is observed with rs11708996, located in intron 21 of the *SCN5A* gene. The C allele frequencies are significantly higher in VA⁺ MI patients compared to healthy controls and VA⁻ MI cases. A previous study showed that rs11708996 is associated with significant electrocardiographic changes in ST elevation, PR interval and QRS duration, which may explain the effect in arrhythmic patients.¹⁹ The *SCN5A* gene encodes the alpha subunit of the cardiac sodium channels responsible for the rapid upstroke of cardiac action potential, and plays a central role in the excitability of myocardial cells.²⁰

Mutations in *SCN5A* are associated with a broad spectrum of inherited cardiac arrhythmias, such as long QT syndrome type III,²¹ BrS,²² idiopathic VF,²³ sudden infant death syndrome,²⁴ and cardiac conduction defects.²⁵ Many studies have found associations between common polymorphisms in the *SCN5A* gene and SCD in acquired heart diseases^{26,27}; however, a minority focused on VA and SCD in the context of MI.

Investigations performed in a very heterogeneous cohort of cardiac death victims showed that, compared to controls, the CC genotype of the *SCN5A* rs117205200 polymorphism was significantly associated with ischemic heart disease ($p = 0.012$; OR = 1.45).²⁸ Other investigations screened the *SCN5A* gene in cases of sudden cardiac arrest associated with CAD, and found that the proportion of synonymous and non-synonymous nucleotide changes was higher in the case subjects than in the controls. However, none of these SNPs had an association with the disease.²⁹ These 2 studies prove the effect of *SCN5A* gene polymorphisms in acquired heart rhythm disorder.

The 2nd association is found with rs10428132, located in intron 14 of the *SCN10A* gene, which is adjacent to *SCN5A* on chromosome 3p21–22. Recent studies have shown that the sodium channel isoform Nav1.8 coded by *SCN10A*, besides being expressed in cardiac neurons,³⁰ is expressed in the working myocardium and the specialized conduction system,³¹ indicating a possible role for Nav1.8 in cardiac electrical function. However, any genetic implication of this protein in SCD remains undetected, probably due to the fact that the Nav1.8 protein is expressed more in the central and peripheral nervous systems than in the heart. That is why the *SCN10A* gene is not yet included in the panel of arrhythmia and SCD diagnosis in the vast majority of cardiogenetic centers.¹⁴ Our result concerning the association of the *SCN10A* gene polymorphism with arrhythmia constitutes a novel element that could help in the diagnosis of SCD based on this gene and Nav1.8 protein.

Furthermore, the SNP rs6801957, which is in high linkage disequilibrium ($r^2 = 0.97$) with rs10428132, has been reported to alter a highly conserved nucleotide within a consensus T-box-binding site (*TBX5* and *TBX3*), which functionally affects the *SCN5A/SCN10A* enhancer.³²

TBX5 drives *SCN5A* expression to regulate the functioning of the cardiac conduction system.³³ Further studies are required to determine whether the effects of rs10428132 on conduction and arrhythmia are mediated through regulation of *SCN5A*, *SCN10A* or both.

In this paper, 21.3% of MI patients developed VA after a 1 year follow-up. These results are consistent with those found in a large cohort of MI patients, showing that early arrhythmic complications occur in nearly 9.3% of patients with MI, and in 22.3% of patients after a follow-up of 5 years.⁵ The results of the association analyses of the 2 SNPs in *SCN5A* and *SCN10A* with MI VA⁺ patients showed strong p-values and OR when compared to healthy controls. This could indicate that the population of MI VA⁻ patients is still at risk of developing VA.

Genetic similarities between VA during MI and BrS found for the first time in this paper may be explained by the fact that both clinical entities are the result of similar electrophysiological substrates, and both can result in SCD. In addition, studies have shown that ST segment elevation during acute MI recapitulates features of BrS and may be the result of closely coupled phase 2 reentrant extrasystoles.¹⁰

Regarding *HEY2* polymorphisms, rs9388451 showed no association with VA patients ($p = 0.07$). Bezzina et al. were the first to report association between rs9388451 and BrS.¹³ The risk allele of this SNP has also been found in association with cardiac arrest/VA in the larger UK Biobank population, indicating a possible pathological role of this allele in cardiac arrhythmia.¹⁹ The effect of this SNP on cardiac conduction may be explained by its location near the *HEY2* gene, encoding a transcriptional repressor that is important in the development of the cardiovascular system.³⁴ Experiments in *HEY2* knock-out embryos showed abnormal right ventricle morphology and a spectrum of postnatal cardiomyopathies.³⁵ Our results concerning the lack of association for this SNP are near the threshold of significance ($p = 0.05$). This may be due, first, to the small number of MI VA⁺ patients and, second, to the fact that the MI VA⁻ population is still at risk of developing VA.

As for rs2200733, it also showed no association with the MI VA⁺ patients compared to the healthy controls ($p = 0.47$). This SNP is located 150 kb upstream of the *PITX2* gene that codes for transcription factors playing an important role in the embryonic development of heart left-right symmetry.³⁶ *PITX2* is also implicated in the development of the pulmonary vein myocardium, which is a major source of atrial arrhythmogenesis.³⁷ The rs2200733 SNP is well-established to be at risk of developing AF³⁸ and SCD.³⁹ The study by Lahtinen et al. supports a joint genetic pathway between AF and VF, or at least abnormal cardiac function.³⁹ No association between rs2200733 and the risk of VA was found in the Tunisian population (this study). Our results are in agreement with a case-control study that found no association between 24 common genetic variants, including rs2200733, related to AF and the risk of VF in the setting of first STEMI.⁴⁰









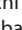


Our results support the idea that cardiac electrical abnormalities may be the result of variations in genes coding ion channels. On the other hand, our study shows that SNPs in genes involved in embryonic cardiogenesis, previously associated with congenital heart rhythm diseases, are not associated with acquired heart rhythm disorders.

Conclusions

The study was conducted on a small sample size, due to the very critical nature of the clinical situation. The inclusion criteria were highly restricted in an effort to maintain the homogeneity of the cohort. On the other hand, the practical and clinical significance of the associated polymorphisms in *SCN5A* and *SCN10A* remains an open question. These observations need to be further confirmed by a larger number of VA⁺ patients and deeper genetic explorations that can be correlated to clinical characteristics.

The major strength of this study is the originality of the concept and the results. In fact, we are the first to carry out an association study of 4 polymorphisms, previously associated to BrS and AF, with VA in the context of MI. We found that *SCN5A* rs11708996 and *SCN10A* rs10428132 are significantly associated with the risk of VA in MI patients. In addition, we demonstrated novel genetic similarities between VA in acquired heart disease and BrS. Based on these novel findings, we hypothesize that variations in genes coding for cardiac ion channels or modulating their expression, which are currently used to stratify arrhythmic risk in patients with inherited syndromes of SCD, may also be associated with the occurrence of VA during MI. Our results may enable us to distinguish patients who are genetically susceptible to developing VA and SCD. This could make them more aware of their situation and could orient their clinicians toward better treatments. In addition, further study of the functional consequences of these variants on cardiac electrophysiology may lead to important advances in our understanding of the mechanisms underlying SCD and could ultimately lead to novel therapeutic approaches.

ORCID iDs

Hajer Foddha  <https://orcid.org/0000-0003-1490-3772>
 Nadia Bouzidi  <https://orcid.org/0000-0003-3722-7279>
 Abdelhak Foddha  <https://orcid.org/0000-0002-7325-9158>
 Saoussen Chouchene  <https://orcid.org/0000-0003-1428-9856>
 Rahma Touhami  <https://orcid.org/0000-0002-6558-4292>
 Nadia Leban  <https://orcid.org/0000-0002-5913-7795>
 Mohamed Faouzi Maatoug  <https://orcid.org/0000-0003-1062-6712>
 Habib Gamra  <https://orcid.org/0000-0001-8758-5766>
 Salima Ferchichi  <https://orcid.org/0000-0002-1532-066X>
 Jemni Ben Chibani  <https://orcid.org/0000-0003-3575-610X>
 Amel Haj Khelil  <https://orcid.org/0000-0001-5404-2116>

References

1. Priori SG, Aliot E, Blomstrom-Lundqvist C, et al. Task Force on Sudden Cardiac Death, European Society of Cardiology. Summary of recommendations. *Ital Heart J Suppl.* 2002;3(10):1051–1065.

2. Henkel DM, Witt BJ, Gersh BJ, et al. Ventricular arrhythmias after acute myocardial infarction: A 20-year community study. *Am Heart J*. 2006;151(4):806–812.
3. Khairy P, Thibault B, Talajic M, et al. Prognostic significance of ventricular arrhythmias post-myocardial infarction. *Can J Cardiol*. 2003;19(12):1393–1404.
4. Spooner PM, Albert C, Benjamin EJ, et al. Sudden cardiac death, genes, and arrhythmogenesis: Consideration of new population and mechanistic approaches from a National Heart, Lung, and Blood Institute workshop, Part II. *Circulation*. 2001;103(20):2447–2452.
5. Jabbari R, Engstrom T, Glinge C, et al. Incidence and risk factors of ventricular fibrillation before primary angioplasty in patients with first ST-elevation myocardial infarction: A nationwide study in Denmark. *J Am Heart Assoc*. 2015;4(1):e001399.
6. Maekawa K, Saito Y, Ozawa S, et al. Genetic polymorphisms and haplotypes of the human cardiac sodium channel alpha subunit gene (SCN5A) in Japanese and their association with arrhythmia. *Ann Hum Genet*. 2005;69(Pt 4):413–428.
7. Hu D, Viskin S, Oliva A, et al. Genetic predisposition and cellular basis for ischemia-induced ST-segment changes and arrhythmias. *J Electrocardiol*. 2007;40(6 Suppl):S26–S29.
8. Brugada P, Brugada J. Right bundle branch block, persistent ST segment elevation and sudden cardiac death: A distinct clinical and electrocardiographic syndrome. A multicenter report. *J Am Coll Cardiol*. 1992;20(6):1391–1396.
9. Indik JH, Ott P, Butman SM. Syncope with ST-segment abnormalities resembling Brugada syndrome due to reversible myocardial ischemia. *Pacing Clin Electrophysiol*. 2002;25(8):1270–1273.
10. Di Diego JM, Fish JM, Antzelevitch C. Brugada syndrome and ischemia-induced ST-segment elevation: Similarities and differences. *J Electrocardiol*. 2005;38(4 Suppl):14–17.
11. Benjamin EJ, Wolf PA, D'Agostino RB, Silbershatz H, Kannel WB, Levy D. Impact of atrial fibrillation on the risk of death: The Framingham Heart Study. *Circulation*. 1998;98(10):946–952.
12. Gudbjartsson DF, Arnar DO, Helgadóttir A, et al. Variants conferring risk of atrial fibrillation on chromosome 4q25. *Nature*. 2007;448(7151):353–357.
13. Bezzina CR, Barc J, Mizusawa Y, et al. Common variants at SCN5A-SCN10A and HEY2 are associated with Brugada syndrome, a rare disease with high risk of sudden cardiac death. *Nat Genet*. 2013;45(9):1044–1049.
14. Monasky MM, Micaglio E, Vicedomini G, et al. Comparable clinical characteristics in Brugada syndrome patients harboring SCN5A or novel SCN10A variants. *Europace*. 2019;21(10):1550–1558.
15. Neubauer J, Wang Z, Rougier JS, et al. Functional characterization of a novel SCN5A variant associated with long QT syndrome and sudden cardiac death. *Int J Legal Med*. 2019;133(6):1733–1742.
16. Nunez-Gil IJ, Riha H, Ramakrishna H. Review of the 2017 European Society of Cardiology's Guidelines for the Management of Acute Myocardial Infarction in Patients Presenting with ST-Segment Elevation and Focused Update on Dual Antiplatelet Therapy in Coronary Artery Disease Developed in Collaboration with the European Association for Cardio-Thoracic Surgery. *J Cardiothorac Vasc Anesth*. 2019;33(8):2334–2343.
17. Sole X, Guino E, Valls J, Iniesta R, Moreno V. SNPStats: A web tool for the analysis of association studies. *Bioinformatics*. 2006;22(15):1928–1929.
18. Nattel S, Frelin Y, Gaborit N, Louault C, Demolombe S. Ion-channel mRNA-expression profiling: Insights into cardiac remodeling and arrhythmic substrates. *J Mol Cell Cardiol*. 2010;48(1):96–105.
19. Andreasen L, Ghouse J, Skov MW, et al. Brugada syndrome-associated genetic loci are associated with J-point elevation and an increased risk of cardiac arrest. *Front Physiol*. 2018;9:894.
20. Balsler JR. Structure and function of the cardiac sodium channels. *Cardiovasc Res*. 1999;42(2):327–338.
21. Wang Q, Shen J, Splawski I, et al. SCN5A mutations associated with an inherited cardiac arrhythmia, long QT syndrome. *Cell*. 1995;80(5):805–811.
22. Chen Q, Kirsch GE, Zhang D, et al. Genetic basis and molecular mechanism for idiopathic ventricular fibrillation. *Nature*. 1998;392(6673):293–296.
23. Akai J, Makita N, Sakurada H, et al. A novel SCN5A mutation associated with idiopathic ventricular fibrillation without typical ECG findings of Brugada syndrome. *FEBS Lett*. 2000;479(1–2):29–34.
24. Ackerman MJ, Siu BL, Sturmer WQ, et al. Postmortem molecular analysis of SCN5A defects in sudden infant death syndrome. *JAMA*. 2001;286(18):2264–2269.
25. Schott JJ, Alshinawi C, Kyndt F, et al. Cardiac conduction defects associate with mutations in SCN5A. *Nat Genet*. 1999;23(1):20–21.
26. Burke A, Creighton W, Mont E, et al. Role of SCN5A Y1102 polymorphism in sudden cardiac death in blacks. *Circulation*. 2005;112(6):798–802.
27. Splawski I, Timothy KW, Tateyama M, et al. Variant of SCN5A sodium channel implicated in risk of cardiac arrhythmia. *Science*. 2002;297(5585):1333–1336.
28. Marcsa B, Denes R, Voros K, et al. A common polymorphism of the human cardiac sodium channel alpha subunit (SCN5A) gene is associated with sudden cardiac death in chronic ischemic heart disease. *PLoS One*. 2015;10(7):e0132137.
29. Stecker EC, Sono M, Wallace E, Gunson K, Jui J, Chugh SS. Allelic variants of SCN5A and risk of sudden cardiac arrest in patients with coronary artery disease. *Heart Rhythm*. 2006;3(6):697–700.
30. Verkerk AO, Remme CA, Schumacher CA, et al. Functional Nav1.8 channels in intracardiac neurons: The link between SCN10A and cardiac electrophysiology. *Circ Res*. 2012;111(3):333–343.
31. Yang T, Atack TC, Stroud DM, Zhang W, Hall L, Roden DM. Blocking Scn10a channels in heart reduces late sodium current and is antiarrhythmic. *Circ Res*. 2012;111(3):322–332.
32. van den Boogaard M, Wong LY, Tessadori F, et al. Genetic variation in T-box binding element functionally affects SCN5A/SCN10A enhancer. *J Clin Invest*. 2012;122(7):2519–2530.
33. Arnolds DE, Liu F, Fahrenbach JP, et al. TBX5 drives Scn5a expression to regulate cardiac conduction system function. *J Clin Invest*. 2012;122(7):2509–2518.
34. Fischer A, Gessler M. Hey genes in cardiovascular development. *Trends Cardiovasc Med*. 2003;13(6):221–226.
35. Sakata Y, Kamei CN, Nakagami H, Bronson R, Liao JK, Chin MT. Ventricular septal defect and cardiomyopathy in mice lacking the transcription factor CHF1/Hey2. *Proc Natl Acad Sci U S A*. 2002;99(25):16197–16202.
36. Franco D, Campione M. The role of Pitx2 during cardiac development: Linking left-right signaling and congenital heart diseases. *Trends Cardiovasc Med*. 2003;13(4):157–163.
37. Mommersteeg MT, Brown NA, Prall OW, et al. Pitx2c and Nkx2-5 are required for the formation and identity of the pulmonary myocardium. *Circ Res*. 2007;101(9):902–909.
38. Olesen MS, Nielsen MW, Haunso S, Svendsen JH. Atrial fibrillation: The role of common and rare genetic variants. *Eur J Hum Genet*. 2014;22(3):297–306.
39. Lahtinen AM, Noseworthy PA, Havulinna AS, et al. Common genetic variants associated with sudden cardiac death: The FinSCDgen study. *PLoS One*. 2012;7(7):e41675.
40. Jabbari R, Glinge C, Jabbari J, et al. A common variant in SCN5A and the risk of ventricular fibrillation caused by first ST-segment elevation myocardial infarction. *PLoS One*. 2017;12(1):e0170193.

Study of PLGA microspheres loaded with pOsx/PEI nanoparticles for repairing bone defects in vivo and in vitro

Jingtang Li^{B-D,F}, Guanxiang Liao^{B,C,F}, Zhisheng Long^{B,C,F}, Peng Qiu^{B,F}, Linghua Ding^{C,F}, Long Xiong^{A,C,E,F}

Department of Orthopedics, Jiangxi Provincial People's Hospital Affiliated to Nanchang University, China

A – research concept and design; B – collection and/or assembly of data; C – data analysis and interpretation; D – writing the article; E – critical revision of the article; F – final approval of the article

Advances in Clinical and Experimental Medicine, ISSN 1899–5276 (print), ISSN 2451–2680 (online)

Adv Clin Exp Med. 2020;29(4):431–440

Address for correspondence

Long Xiong
E-mail: xionglong1234@126.com

Funding sources

This study was supported by Jiangxi Provincial Youth Fund (20161BAB215258) and the general plan of Jiangxi Provincial Department of Health (No. 20165030)

Conflict of interest

None declared

Received on March 29, 2019

Reviewed on October 1, 2019

Accepted on January 21, 2020

Published online on May 4, 2020

Abstract

Background. Autogenous or allogenic bone transplantation is the main treatment for bone defects and nonunions. However, the shortcomings of autogenous or allogenic bone transplantation limit its wide application in clinical use.

Objectives. This study investigated the effect of poly(lactic-co-glycolic acid) (PLGA) microspheres loaded with pOsterix (pOsx)/polyethylenimine (PEI) nanoparticles in repairing bone defects and explored its mechanism.

Material and methods. Poly(lactic-co-glycolic acid) microspheres loaded with pOsx/PEI nanoparticles were constructed. The Osx transfection effect was detected by fluorescence quantitative PCR and western blotting methods. 3-(4,5)-dimethylthiazoliazol-2-yl-4-methylcarbazole (MTT) and flow cytometry methods were used to detect cell proliferation. The collagen I (Col-1), osteopontin (OPN) and osteocalcin (OC) expression levels were detected using real-time polymerase chain reaction (RT-PCR) and western blotting methods. Bone defect model was constructed. Bone repair was detected using X-ray, hematoxylin and eosin (H&E) staining, and Mason staining methods.

Results. PLGA@pOsx/PEI has transfection effect both in vitro and in vivo, does not affect cell proliferation and is safe for cells. PLGA@pOsx/PEI could promote the expression of Col-1, OPN and OC in vitro and in vivo. PLGA@pOsx/PEI could promote osteogenesis in vivo.

Conclusions. PLGA@pOsx/PEI with high Osx expression could promote the expression of OC, OPN, and COL-1. PLGA@pOsx/PEI can be used as a material for repairing bone defects and can promote bone formation. These results provide a theoretical and practical basis for its further clinical application.

Key words: bone defect, pOsx/PEI nanoparticles, PLGA microspheres

Cite as

Li J, Liao G, Long Z, Qiu P, Ding L, Xiong L. Study of PLGA microspheres loaded with pOsx/PEI nanoparticles for repairing bone defects in vivo and in vitro. *Adv Clin Exp Med.* 2020;29(4):431–440. doi:10.17219/acem/116752

DOI

10.17219/acem/116752

Copyright

© 2020 by Wrocław Medical University
This is an article distributed under the terms of the Creative Commons Attribution 3.0 Unported (CC BY 3.0) (<https://creativecommons.org/licenses/by/3.0/>)

Introduction

Autogenous or allogenic bone transplantation is the main treatment for bone defects and nonunions in clinical practice. However, the shortcomings of autogenous or allogenic bone transplantation limit its wide application.^{1–4} Bone repair using bone tissue engineering technology is a possible way to solve the problem of bone defect treatment.^{5–8} There are 2 kinds of bone tissue engineering techniques: in vivo and in vitro. In vitro bone tissue engineering technology has several shortcomings, which limits its application. Firstly, the construction is complex and expensive with a long operating cycle; it does great damage to patients. Secondly, the proportion of bone marrow mesenchymal stem cells to bone marrow cells in elderly patients decreases correspondingly, the cell proliferation rate decreases and the osteogenesis ability in vivo decreases significantly. Thirdly, exogenous osteogenic factors are easily lost and inactivated in vivo with short duration, low potency and high cost; it may induce an immune response.^{9,10}

Bone morphogenetic protein 2 (BMP-2) is a classic bone growth factor.^{11,12} In BMP-2 promoting osteogenesis signaling pathway, Nakashima et al. found transcription factor Osterix (*Osx*) in mice in 2002.¹³ Osterix is a highly specific transcription factor of osteoblasts located downstream of BMP-2. Bone morphogenetic protein 2 promotes osteogenesis through *Osx*. Osterix regulates the expression of many important late phenotypes and functional proteins of osteoblasts, such as collagen I, osteopontin, salivary protein and osteocalcin, and synthesizes matrix to produce mineralization reaction to achieve bone formation. Osterix has zinc finger structure and is a specific transcription factor of osteoblasts. Osterix is expressed in all osteoblasts. Bone morphogenetic protein 2 has a positive regulation on *Osx* in the process of osteoblasts differentiation. Osterix is one of the most important transcription factors found to regulate osteoblast differentiation, and its expression level is used as a marker for osteoblast differentiation. At the same time, *Osx* can promote the differentiation of preosteoblasts into mature and functional osteoblasts. Osterix has the most specific effect on bone formation.^{14–16} There would be no bone formation and regeneration without *Osx*.^{17–19}

Vectors that can be used to transfer therapeutic genes into target cells include viral and non-viral vectors. However, viral vectors have a limited size and number of genes, poor targeting specificity, and many undesirable side effects.^{20,21} Nanotechnology has created a new non-viral vector system, in which polyethylenimine (PEI) is an effective cationic carrier with high gene transfection rate and low adverse reactions.^{22–26} Polyethylenimine nanoparticles have been used as *Osx* plasmid (p*Osx*) carriers. Although they are beneficial to cell binding, uptake and transfection, p*Osx*/PEI nanoparticles are easily degraded and destroyed by tissue fluids. In order to make p*Osx*/PEI nanoparticles release slowly in the bone defect area and be effective for a longer period of time, we are looking for

a drug sustained-release carrier, poly(lactic-co-glycolic acid) (PLGA), which is biodegradable, is a good membrane slow-release carrier and promotes bone growth.²⁷ PLGA@pBMP-2/PEI nanoparticles were successfully used to transfect cells and promote osteoblast differentiation.²⁸

There are few reports on the use of *Osx* in the treatment of bone defects. In this study, PLGA microspheres were successfully prepared to encapsulate p*Osx*/PEI nanoparticles. Bone regeneration, bone repair ability and excessive osteogenesis of PLGA microspheres were studied in cell and animal models. The related mechanisms were studied to provide a theoretical basis for its clinical application and to open up a new treatment method for bone defects.

Material and methods

Experimental cells and animals

The mouse osteoblastic cell line MC3T3-E1 cells were purchased from Beijing Beina Biological Technology Co., Ltd. (Beijing, China) (BNCC339285). MC3T3-E1 cells were cultured in α -MEM containing 10% fetal bovine serum (FBS) and 1% penicillin-streptomycin (Hyclone, Logan, USA) in a humidified, 95% air, 5% CO₂ atmosphere at 37°C. They were divided into control group, PLGA@PEI group (transfected with 10 μ L PLGA@PEI suspension for 7 days), and PLGA@p*Osx*/PEI group (transfected with 10 μ L PLGA@p*Osx*/PEI suspension for 7 days).

Japanese big-ear rabbits were purchased from Nanchang Longping Rabbit Industry Co., Ltd. (Nanchang, China). They were maintained in a temperature-controlled room (22–26°C) with 12-h light/dark cycles, with continuous access to food and water. All animal experiments were conducted according to the Principles of Laboratory Animal Care (National Society for Medical Research in China).

Experimental reagents and instruments

Poly(lactic-co-glycolic acid) (P133293, Aladdin); PEI (408727, sigma); PVA (P105126, Aladdin); DMEM Completely High Sugar Culture Medium (NanJing KeyGen Biotech Co., Ltd. KGM12800S-500); Cell Cycle Staining Kit (CCS102, MultiSciences (Lianke) Biotech Co., Ltd.); Mouse ALP biochemical detection Kit (A059-2, NanJing Jiancheng bioengineering Institute); Trizol Reagent (CW0580S, Beijing ComWin Biotech Co.,Ltd.); Ultrapure RNA extraction kit (CW0581M, Beijing ComWin Biotech Co.,Ltd.); HiFiScript cDNA synthesis Kit (CW2569M, Beijing ComWin Biotech Co.,Ltd.); UltraSYBR Mix (CW0957M, Beijing ComWin Biotech Co.,Ltd.); RIPA Cell lysis buffer (C1053, Beijing Applygen Co.,Ltd.); PVDF membrane (IPVH00010, Millipore); Hypersensitive luminescent liquid (RJ239676, Thermo Fisher); Mouse Monoclonal Anti-GAPDH (TA-08, Beijing ZSGB-BIO Co.,Ltd.); Horseradish Enzyme Labeled Goat Anti-Rat IgG (H+L) (ZB-2305, Beijing

ZSGB-BIO Co.,Ltd.); Rabbit Polyclonal Anti-Osteocalcin (OC) (OM266698, OmnimAbs, 1/500); Rabbit Polyclonal Anti-Osteopontin (OPN) (AF0227, Affinity, 1/500); Rabbit Polyclonal Anti-Collagen I (Cbfet1) (bs-0578R, Bioss, 1/100); Rabbit Polyclonal Anti-Osterix (Osx) (bs-1110R, Bioss, 1/100); Masson's Trichrome Stain Kit (G1340, Solarbio); NovoCyte™ Flow cytometry (NovoCyte 2060R, ACEA Hangzhou Biosciences Inc.); Microplate Reader (RT-6100, Rayto); fluorescent quantitative PCR instrument (CFX Connect™, Bio-Rad Shanhhai Laboratories); Protein vertical electrophoresis instrument (DYY-6C, Beijing 61 instrument factory); Ultra High Sensitivity Chemiluminescence Imaging System (Chemi Doc™ XRS+, Bio-Rad Shanhhai Laboratories); Microscope (CX41 Olympus); Paraffin slicer for biological tissues (BQ-318D, Hubei Bona Medical Technology Co., Ltd.).

Preparation of PLGA@PEI and PLGA@pOsx/PEI microspheres

Polyvinyl alcohol (PVA) solution (6%) was prepared, 200 mg PLGA was dissolved in 10 mL dichloromethane solution by double emulsion solvent evaporation method. Osterix vector (180 µg) and PEI (191.25 µg, N/p = 8) were dissolved in 3 mL water. The 3 mL vector complex was added to the above PLGA solution and stirred for 10 s at 5,000 rpm with a hand-held homogenizer to form colostrum solution. Colostrum solution was quickly poured into 3% PVA solution (10 mL), and stirred at 10,000 rpm under ice bath for 10 s to form double emulsion solution. The double emulsion solution was poured into 500 mL of 0.5% PVA solution and stirred by magnetic force for 2 h at room temperature. The residual organic solvents were removed by vacuum distillation after 6 h and centrifuged at 5,000 rpm for 15 min. Poly(lactico-glycolic acid) microspheres loaded with pOsx/PEI powders were obtained by deionized water washing 3 times and freeze-drying of precipitation. They were stored at 4°C. The blank PLGA microspheres and the PLGA microspheres containing only PEI were prepared using the same method.

Cell transfection

MC3T3-E1 cells were pre-incubated with α-MEM containing 10% FBS overnight in 6-well plates at a density of 5×10^5 cells per well. The microspheres could be transfected when the cells adhered completely.

The microsphere suspension prepared in advance was placed in the water-bath ultrasound instrument for 10–20 min, and the microsphere suspension was added to 6-well plates after it was fully dispersed (10 µL/well).

MTT detection

Cell viability was determined by MTT reduction assay. In brief, MC3T3-E1 cells transfected with microspheres for 7 days in each group were digested with 0.25% trypsin (containing 0.02% EDTA) and collected respectively.

They were preincubated with α-MEM containing 10% FBS overnight in 96-well plates at a density of 5×10^3 cells per well. According to the experimental design, cells in each well were added 10 µL of MTT without light. The cells were incubated at 37°C for 4 h, the supernatants were removed, and the formazan crystals were dissolved in 100 µL of dimethyl sulfoxide (DMSO). Absorbance was recorded at a wavelength of 490 nm and reference wavelength of 630 nm using a microplate reader (Bio-Rad, Foster, USA).

Detection of cell cycle by flow cytometry

Cell suspension was centrifuged at 2,500 rpm for 3 min and the supernatant was discarded. The precipitation was fixed with 1 mL absolute ethanol for more than 2 h at 4°C, centrifuged with 8,000 rpm for 3 min, and the supernatant was discarded. The precipitation was washed with phosphate-buffered saline (PBS) and stained with 1 mL DNA staining solution at room temperature for 30 min. The cells were detected and analyzed by flow cytometry.

Alkaline phosphatase activity detection

MC3T3-E1 cells were treated with the indicated agents according to the experimental design. Alkaline phosphatase (ALP) activity was detected using ALP activity detection Kit according to the manufacturer's instructions. The values of OD at 520 nm were determined using enzyme-labeled instrument.

Construction of repairing bone defect of rabbit model

Rabbits were weighed and injected with 1% sodium pentobarbital at a dose of 30 mg/kg through an ear vein. The rabbit was fixed on the operating table with its forelimb hair removed and the operation area was wiped with iodophor 3 times. A towel was spread at the start of the operation. The skin was incised with a blunt separation of muscles, the radius was exposed and a defect of about 1.5 cm in length was created in the middle part of the radius. PLGA@pOsx/PEI and PLGA@PEI microspheres were filled into the bone defect site and sutured layer by layer. Penicillin (80,000 units per day) was injected intramuscularly 3 days after operation, and the wound was observed for any signs of infection. The rabbits were divided into the Model group, the PLGA group, the PLGA@PEI group, and the PLGA@pOsx/PEI group. Bone repair was detected using X-ray after 60 and 90 days, and bone defect repair tissues were taken for detection.

RNA extraction and qRT-PCR

The total RNA was extracted using Ultrapure RNA kit according to the manufacturer's protocol. Total RNA (1 µg) was subjected to reverse transcription using HiFiScript

Table 1. Primers used in this study

Gene	Primers (5'-3')	Product length [bp]	Annealing temperature [°C]
<i>Osx</i>	F: GGGAAAGGAGGCACAAAG R: AGGAAATGAGTGAGGGAAGG	174	56.0
<i>OPN</i>	F: CTGATGAGACCGTCACTGCT R: TGCCCTTTCCGTTGTG	273	57.3
<i>OC</i>	F: GGAGGGCAATAAGGTAGTGAA R: CCATAGATGCGTTTGTAGGC	162	56.8
<i>Col-1</i>	F: CTACTIONAGCCGTCTGTGCCT R: GCTTCTTTTCTTGGGGTT	63	58.6
<i>GAPDH</i>	F: GCAAGTTCAACGGCACAG R: CGCCAGTAGACTCCACGAC	141	58.0

cDNA synthesis Kit. Real-time polymerase chain reaction (RT-PCR) were performed using SYBR Green PCR Master Mix. At the end of each reaction, a melting curve analysis was performed to confirm the absence of primer dimers. Glyceraldehyde 3-phosphate dehydrogenase (*GAPDH*) gene was used as an internal control for normalization of RNA quantity and quality differences in all samples. Quantifications of target genes mRNA was performed using the $2^{-\Delta\Delta C_t}$ method. Primers' sequences were listed in Table 1.

Western blotting method

The cells were lysed with lysis solution (Sigma-Aldrich, St. Louis, USA) at 4°C overnight. They were centrifuged with 10,000 rpm/min at 4°C for 10 min. The supernatant was collected. Total proteins were extracted and the protein concentration was determined using BCA Protein Assay Kit. Proteins (50 µg per lane) were separated using 12% sodium dodecyl sulfate and polyacrylamide gel electrophoresis (SDS-PAGE). Proteins were then electrotransferred to a polyvinylidene fluoride (PVDF) membrane (Amersham Biosciences, Piscataway, USA). The PVDF membrane was rinsed with Tris buffered saline (TBS) for 10–15 min, placed in TBS/T blocking buffer containing 5% (w/v) of skimmed milk powder and incubated at room temperature for 2 h following the addition of an appropriate dilution of primary antibodies. The membrane was then 3 times rinsed with TBST (5–10 min/wash) and then incubated at room temperature for 1 h with horseradish peroxidase-labeled secondary antibody (1:50,000; Abcam, Cambridge, UK; diluted with TBST containing 0.05% (w/v) skimmed milk powder). The membrane was then rinsed 3 times with TBST (5–10 min/wash). Protein bands were detected using an enhanced chemiluminescence kit (Perkin-Elmer Inc., Waltham, USA) and quantified as the ratio to *GAPDH*. Quantification was performed using Quantity One software (Bio-Rad Laboratories, Inc., Hercules, USA).

Hematoxylin and eosin staining test

The tissues were taken and washed with PBS, fixed with 4% paraformaldehyde solution and embedded in paraffin. They were cut into 5-µm slices and stained with hematoxylin and eosin (H&E) using conventional method. The sections were deparaffinized with 2 changes of xylene, 10 min each; they were re-hydrated in 2 changes of absolute alcohol, 5 min each; 95% alcohol for 2 min and 70% alcohol for 2 min; they were washed briefly in distilled water and stained in Harris hematoxylin solution for 8 min, washed in running tap water for 5 min, differentiated in 1% acid alcohol for 30 s, washed in running tap water for 1 min and blued in 0.2% ammonia water or saturated lithium carbonate solution for 30 s–1 min, washed in running tap water for 5 min, rinsed in 95% alcohol, 10 dips; counterstained in eosin-phloxine solution for 30 s–1 min and dehydrated in 95% alcohol, 2 changes of absolute alcohol, 5 min each. They were cleared in 2 changes of xylene, 5 min each and mounted with xylene based mounting medium. The samples were observed under an optical microscope.

Masson staining test

The tissues were washed with running water and dehydrated with 70%, 80% and 90% ethanol solutions, respectively. They were treated with mixtures of equivalent pure alcohol and xylene for 15 min, xylene I for 15 min and II for 15 min (until transparent). They were put in the mixture of xylene and paraffin for 15 min, then put in paraffin I and paraffin II for 50–60 min, respectively. The paraffin embedding tissues were sliced and stained using Masson's Trichrome Stain Kit (Solarbio, Beijing, China) according to the manuals.

Statistical analysis

The data was analyzed using the IBM SPSS Statistics for Windows v. 19.0 software (IBM Corp., Armonk, USA). The normality of probability distribution was approved using Kolmogorov–Smirnov test. One-way analysis of variance (ANOVA) and t-test were used for comparison between groups. A p-value <0.05 was considered to indicate a statistically significant difference.

Results

Cell transfection efficiency

Compared with the control group, the expression in *Osx* in the PLGA@p*Osx*/PEI group was significantly higher than that in the control group (Fig. 1, mRNA expression $p = 0.003$, protein expression $p = 0.021$).

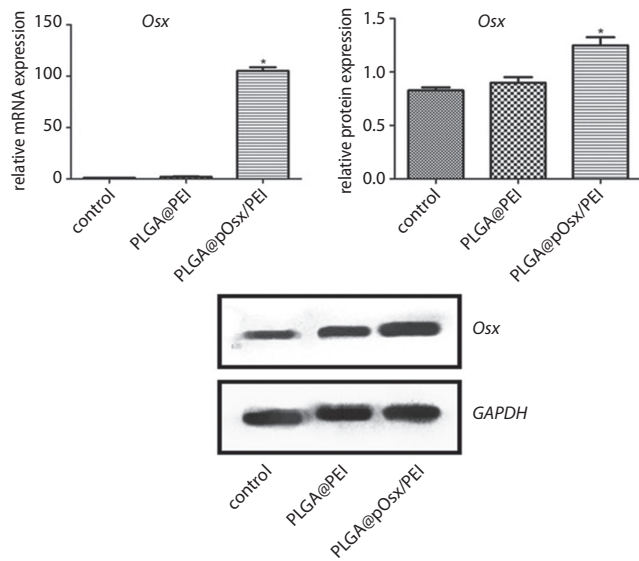


Fig. 1. Validation of cell transfection efficiency

*mRNA expression (p = 0.003) and protein expression (p = 0.021) vs control.

Effects of PLGA@pOsx/PEI on cell proliferation

As shown in Fig. 2, compared with the control group, there was no significant difference in cell proliferation and cell cycle in other groups.

Effect of PLGA@pOsx/PEI on cell osteogenesis

As shown in Fig. 3A, ALP activity in the PLGA@pOsx/PEI group was significantly higher than in the control group (p = 0.027). As shown in Fig. 3B, the expression levels of *Col-1*, *OPN* and *OC* in the PLGA@pOsx/PEI group were significantly higher than those in the control group (p = 0.009).

Osterix expression in vivo

As shown in Fig. 4, compared with the model, the mRNA expression of *Osx* in the PLGA@pOsx/PEI group increased significantly at 60 (p = 0.037) and 90 days (p = 0.004), the *Osx* protein expression in the PLGA@pOsx/PEI group also increased significantly at 60 (p = 0.017) and 90 days (p = 0.012).

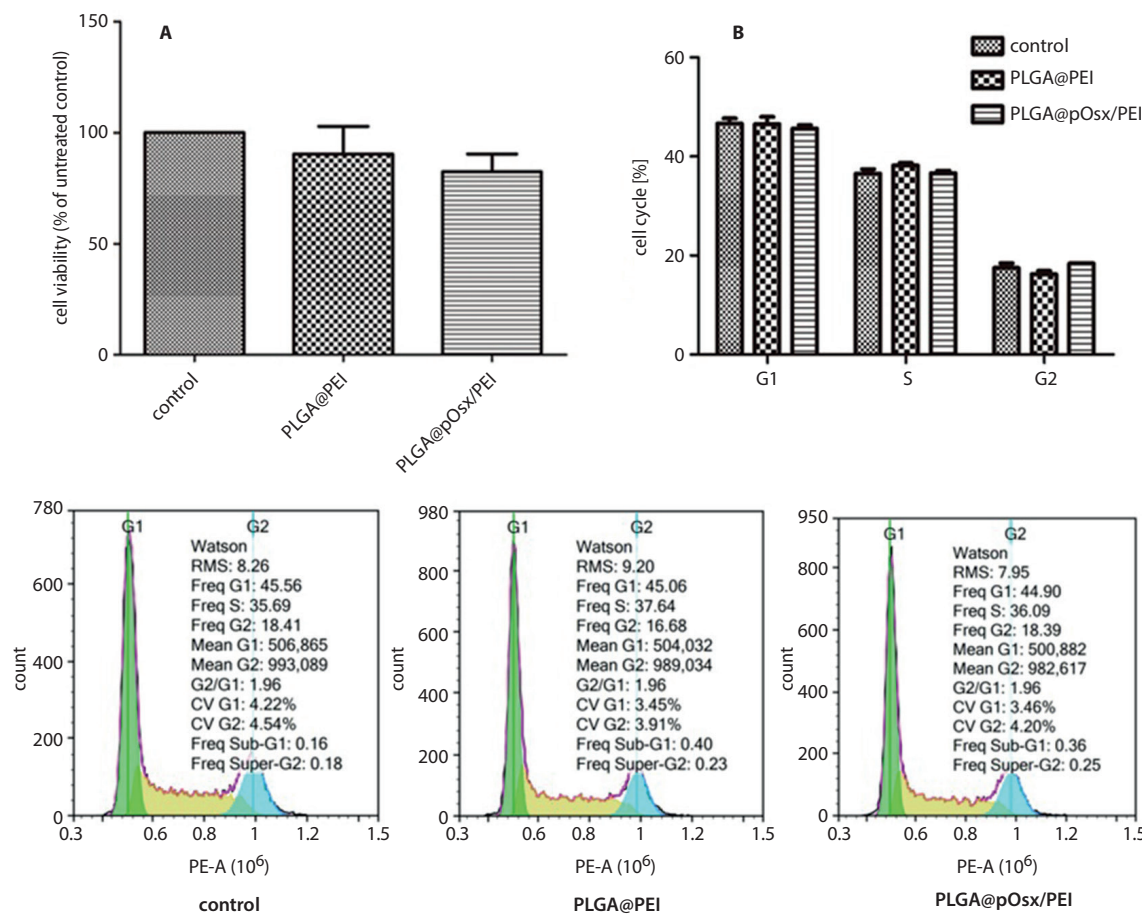


Fig. 2. PLGA@pOsx/PEI had no effects on cell proliferation

A – results of cell proliferation; B – results of cell cycles.

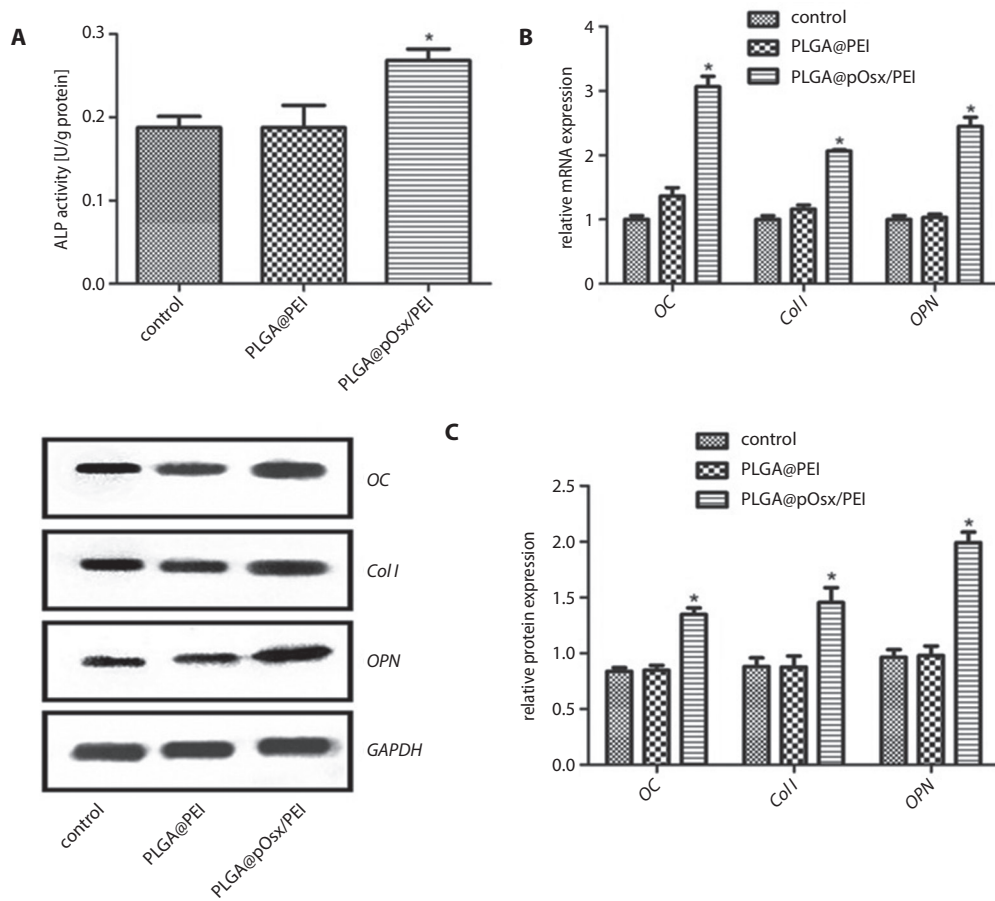


Fig. 3. Effect of PLGA@pOsx/PEI on cell osteogenesis

A – ALP activity in different groups (* $p = 0.027$ vs control); B, C – *Col-1*, *OPN* and *OC* expression levels in different groups (* $p = 0.009$ vs control).

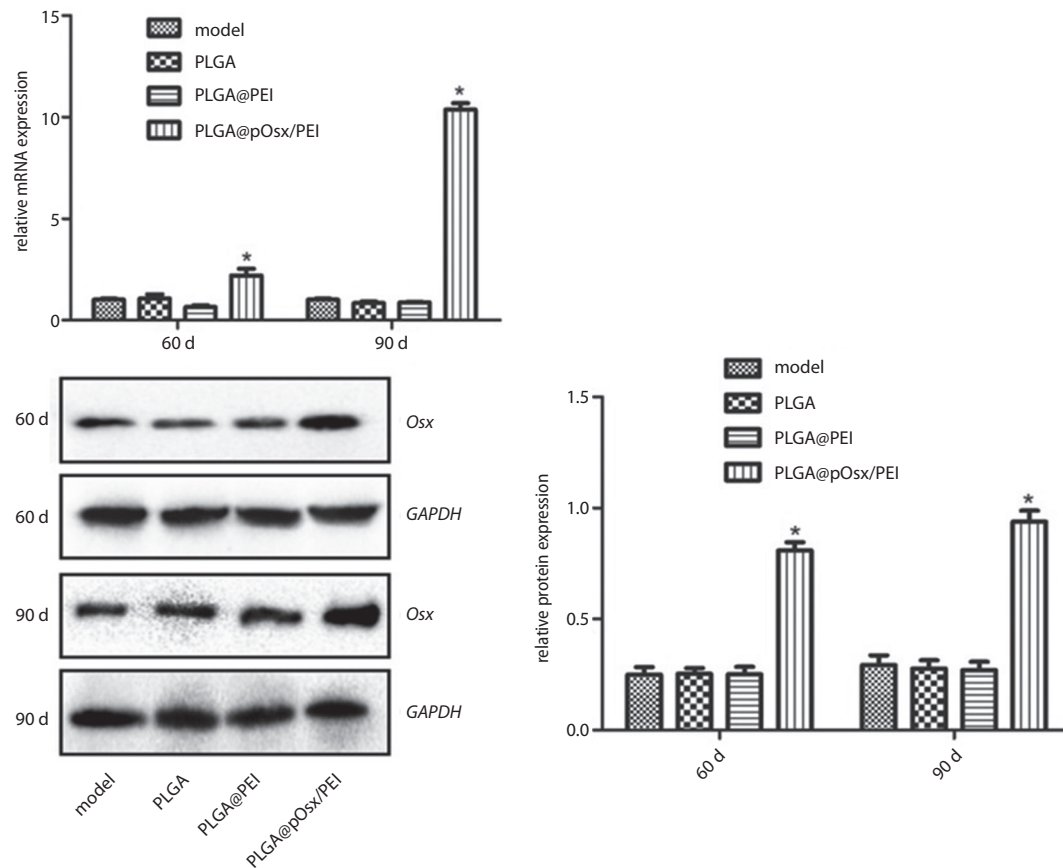


Fig. 4. *Osx* expression in vivo

Compared with that of the model group, the mRNA expression of *Osx* in the PLGA@pOsx/PEI group increased significantly at 60 ($p = 0.037$) and 90 days ($p = 0.004$), the *Osx* protein expression in the PLGA@pOsx/PEI group also increased significantly at 60 ($p = 0.017$) and 90 days ($p = 0.012$).

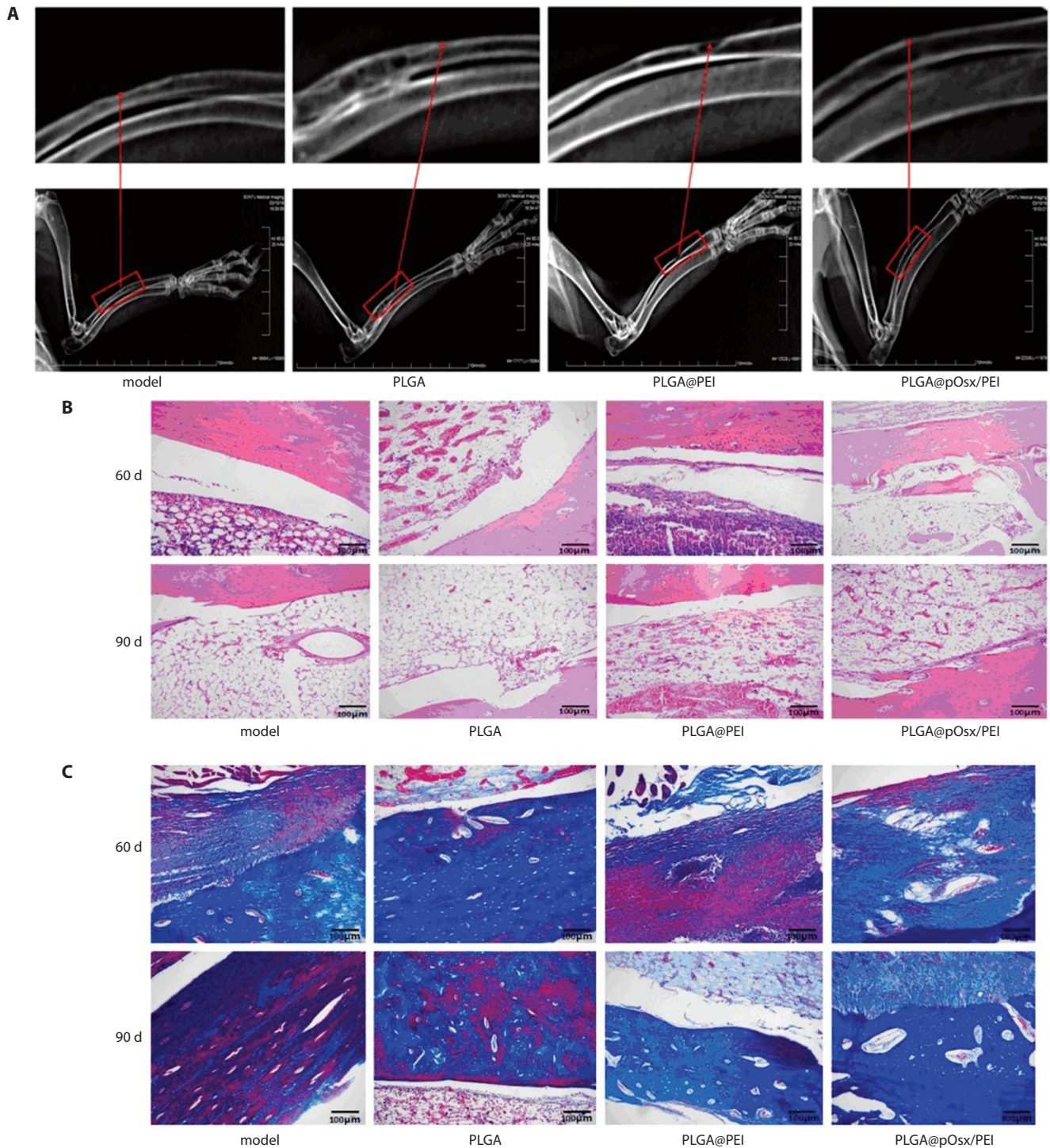


Fig. 5. PLGA@pOsx/PEI microspheres promoted osteogenesis in vivo
 A – H-ray results; B – H&E staining results; C – Masson staining results.

PLGA@pOsx/PEI microspheres promoted osteogenesis in vivo

As shown in Fig. 5A, there were significant bone defects in the model group, the PLGA group and the PLGA@PEI group. The enlarged area was obviously rough and uneven. In the PLGA@pOsx/PEI group, the boundary between

the defect and the autogenous bone was blurred, and the enlarged area was smooth and uniform.

As shown in Fig. 5B, the model group, the PLGA group and the PLGA@PEI group were loosely connected at 60 and 90 days of experiment with intermittent spaces between them. In the PLGA@pOsx/PEI group, new bone was formed, and the defect tissue was closely bound to the surrounding bone.

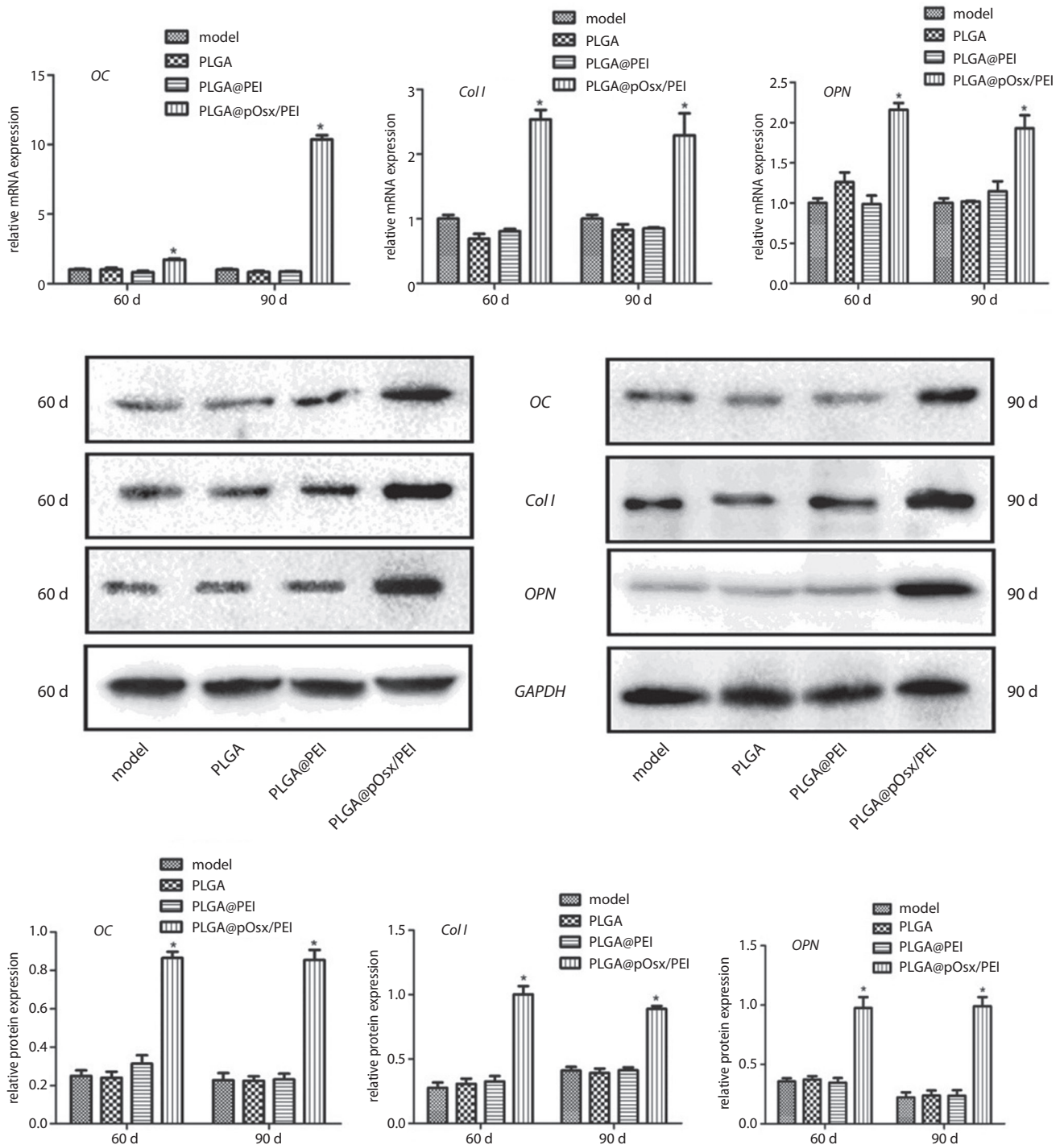


Fig. 6. The effect of PLGA@pOsx/PEI on the expression of *COL-1*, *OPN* and *OC* in vivo

Compared with that of the model group, the mRNA expression of *OC*, *Col-1* and *OPN* in the PLGA@pOsx/PEI group increased significantly at 60 ($p = 0.041$, $p = 0.023$, $p = 0.038$ respectively) and 90 days ($p = 0.003$, $p = 0.020$, $p = 0.037$, respectively), the protein expressions of *OC*, *Col-1* and *OPN* in the PLGA@pOsx/PEI group also increased significantly at 60 ($p = 0.025$, $p = 0.031$, $p = 0.034$, respectively) and 90 days ($p = 0.024$, $p = 0.022$, $p = 0.036$, respectively).

Figure 5C shows that in the model group, the PLGA and the PLGA@PEI groups, fibroblasts proliferated and collagen fibers increased but were arranged irregularly at 60 and 90 days of experiment. In the PLGA@pOsx/PEI group, fibroblasts proliferated, collagen fibers increased, the arrangement tended to be regular, and inflammatory cells decreased.

PLGA@pOsx/PEI promoted *Col-1*, *OPN* and *OC* expression in vivo

As shown in Fig. 6, the mRNA expression of *OC*, *Col-1* and *OPN* in the PLGA@pOsx/PEI group was significantly higher than those in the model group at 60 ($p = 0.041$, $p = 0.023$, $p = 0.038$, respectively) and 90 days ($p = 0.003$,

$p = 0.020$, $p = 0.037$, respectively). The protein expressions of OC, Col-1 and OPN in PLGA@pOsx/PEI group were also significantly higher than those in model group at 60 ($p = 0.025$, $p = 0.031$, $p = 0.034$, respectively) and 90 days ($p = 0.024$, $p = 0.022$, $p = 0.036$, respectively).

Discussion

Bone defects caused by acute trauma, congenital deformity, benign and malignant tumors, bone infection and nonunion of fracture need to be repaired surgically. Bone substitute materials include synthetic scaffolds, natural bio-derived scaffolds, and composite scaffolds. The tissue engineering scaffolds made of single scaffolds often have some unavoidable defects, cannot meet the normal physiological needs of the human body, and limit their clinical application.^{8,29} The PLGA@pOsx/PEI material used in this study has a high gene transfection rate and can release the pOsx/PEI nanoparticles slowly in the local bone defect for a longer time.

In this study, PLGA@PEI material was used to wrap *Osx* in cells and animals, and *Osx* expression in cells and animals was significantly increased. These results suggested that this method had a high gene transfection rate. There was no significant difference in cell proliferation and cell cycle between groups. Therefore, the material had good biocompatibility and no toxic effect on the growth and proliferation of MC3T3-E1 osteoblasts.

The synthesis and secretion of ALP is an important marker of osteoblast differentiation and maturation and has been widely used as a marker of osteoblast identification. It has the function of hydrolyzing organic phosphoric acid and can increase local phosphate concentration, degrade calcification inhibitors in microenvironment, combine and transport calcium ions, and start the calcification process.³⁰ This study showed that ALP activity was significantly increased in the PLGA@pOsx/PEI group. The overexpression of *Osx* not only promotes the differentiation and mineralization of bone marrow stromal stem cells into osteoblasts, but also increases ALP activity and mineralized nodule formation in muscle satellite cells.³¹ Our result suggested that *Osx* had a promoting effect on directional osteogenic differentiation.

Osteocalcin (OC), osteopontin (OPN) and collagen I (COL-I) are important osteoblast-related cytokines secreted and synthesized by osteoblasts, which can be used as indicators for evaluating the functional status of osteoblasts. Collagen I provides a framework for cell adhesion and calcium deposition, and the *COL-I* expression in cells can be used as an index for evaluating the functional status of osteoblasts.³² Osteocalcin is an extracellular matrix protein and an important osteogenic factor for maintaining bone matrix calcification and normal mineralization rate. Osteocalcin is one of the markers of matrix mineralization of osteoblasts and is instrumental in maintaining

normal mineralization rate and calcification process of bone matrix.³³ Osteopontin is an important osteogenic factor in maintaining the mineralization and absorption of bone matrix, participating in the process of bone formation and bone remodeling, and also a marker of osteoblasts. Osteopontin can be synthesized and secreted by many kinds of cells. It is an important chemokine in cell adhesion in vivo. It participates in many metabolic processes, such as bone metabolism, invasion and metastasis of tumors, inflammatory reaction and immunity. It can stimulate the proliferation and calcification of osteoblasts.^{34–36} Our study found that PLGA@pOsx/PEI could promote the expression of OC, OPN and COL-I. These results suggested that *Osx* could promote osteoblast differentiation by affecting the expression of characteristic proteins related to osteoblast differentiation. The results of X-ray and histopathological findings were consistent with the above conclusions. These results suggested that the overexpression of *Osx* promoted new bone formation.

Conclusions

The study confirmed that the overexpression of *Osx* could promote the expression of OC, OPN and COL-I. PLGA@pOsx/PEI can be used as a material for repairing bone defects, which could promote bone formation and provide a theoretical and practical basis for further clinical application.

ORCID iDs

Jingtang Li  <https://orcid.org/0000-0003-2652-7161>
 Guanxiang Liao  <https://orcid.org/0000-0003-4010-9062>
 Zhisheng Long  <https://orcid.org/0000-0001-6239-0591>
 Peng Qiu  <https://orcid.org/0000-0003-0289-0134>
 Linghua Ding  <https://orcid.org/0000-0002-4040-9519>
 Long Xiong  <https://orcid.org/0000-0003-1674-9174>

References

- Dimitriou R, Jones E, McGonagle D, et al. Bone regeneration: Current concepts and future directions. *BMC Med*. 2011;9:66. doi:10.1186/1741-7015-9-66
- Athanasίου VT, Papachristou DJ, Panagopoulos A, et al. Histological comparison of autograft, allograft-DBM, xenograft, and synthetic grafts in a trabecular bone defect: An experimental study in rabbits. *Med Sci Monit*. 2010;16(1):BR24–BR31.
- Brydone AS, Meek D, Maclaine S. Bone grafting, orthopaedic biomaterials, and the clinical need for bone engineering. *Proc Inst Mech Eng H*. 2010;224(12):1329–1343. doi:10.1243/09544119JHEM770
- Oryan A, Alidadi S, Moshiri A, et al. Bone regenerative medicine: classic options, novel strategies, and future directions. *J Orthop Surg Res*. 2014;9(1):18. doi:10.1186/1749-799X-9-18
- Amini AR, Laurencin CT, Nukavarapu SP. Bone tissue engineering: Recent advances and challenges. *Crit Rev Biomed Eng*. 2012;40(5):363–408.
- Liu M, Zeng X, Ma C, et al. Injectable hydrogels for cartilage and bone tissue engineering. *Bone Res*. 2017;5:17014. doi:10.1038/boneres.2017.14.
- Zhang Y, Ma W, Zhan Y, et al. Nucleic acids and analogs for bone regeneration. *Bone Res*. 2018;6:37. doi:10.1038/s41413-018-0042-7
- Yi H, Ur Rehman F, Zhao C, et al. Recent advances in nano scaffolds for bone repair. *Bone Res*. 2016;4:16050. doi:10.1038/boneres.2016.50

9. Bhattacharjee P, Kundu B, Naskar D, et al. Silk scaffolds in bone tissue engineering: An overview. *Acta Biomater.* 2017;63:1–17. doi:10.1016/j.actbio.2017.09.027
10. Wubneh A, Tsekoura EK, Ayranci C, et al. Current state of fabrication technologies and materials for bone tissue engineering. *Acta Biomater.* 2018;80:1–30. doi:10.1016/j.actbio.2018.09.031
11. Carreira AC, Lojudice FH, Halcsik E, et al. Bone morphogenetic proteins: Facts, challenges, and future perspectives. *J Dent Res.* 2014;93(4):335–345. doi:10.1177/0022034513518561
12. Ronga M, Fagetti A, Canton G, et al. Clinical applications of growth factors in bone injuries: Experience with BMPs. *Injury.* 2013;44(Suppl1):S34–S39. doi:10.1016/S0020-1383(13)70008-1
13. Nakashima K, Zhou X, Kunkel G, et al. The novel zinc finger-containing transcription factor osterix is required for osteoblast differentiation and bone formation. *Cell.* 2002;108(1):17–29.
14. Liang GS, Chen WC, Yin CC, et al. Effect of total ravinoids of herba epimedium on BMP-2/RunX2/OSX signaling pathway during osteogenic differentiation of bone marrow mesenchymal stem cells. *Zhongguo Zhong Xi Yi Jie He Za Zhi.* 2016;36(5):614–618.
15. Yang G, Yuan G, MacDougall M, et al. BMP-2 induced Dspp transcription is mediated by Dlx3/Osx signaling pathway in odontoblasts. *Sci Rep.* 2017;7(1):10775. doi:10.1038/s41598-017-10908-8
16. Cooley MA, Harikrishnan K, Opperl JA, et al. Fibulin-1 is required for bone formation and Bmp-2-mediated induction of Osterix. *Bone.* 2014;69:30–38. doi:10.1016/j.bone.2014.07.038
17. Sinha KM, Zhou X. Genetic and molecular control of osterix in skeletal formation. *J Cell Biochem.* 2013;114(5):975–984. doi:10.1002/jcb.24439
18. Feng JQ, Zhang H, Qin C. Letter to the Editor: Osterix regulates tooth root formation in a site-specific manner. *J Dent Res.* 2015;94(9):1326. doi:10.1177/0022034515593744
19. Mizoguchi T, Pinho S, Ahmed J, et al. Osterix marks distinct waves of primitive and definitive stromal progenitors during bone marrow development. *Dev Cell.* 2014;29(3):340–349. doi:10.1016/j.devcel.2014.03.013
20. Yin H, Kanasty RL, Eltoukhy AA, et al. Non-viral vectors for gene-based therapy. *Nat Rev Genet.* 2014;15(8):541–555. doi:10.1038/nrg3763
21. Ibraheem D, Elaissari A, Fessi H. Gene therapy and DNA delivery systems. *Int J Pharm.* 2014;459(1–2):70–83. doi:10.1016/j.ijpharm.2013.11.041
22. Xun MM, Liu YH, Guo Q, et al. Low molecular weight PEI-appended polyesters as non-viral gene delivery vectors. *Eur J Med Chem.* 2014;78:118–125. doi:10.1016/j.ejmech.2014.03.050
23. Yan X, Zhang Y, Zhang H, et al. Amphiphilic polyethylenimine (PEI) as highly efficient non-viral gene carrier. *Org Biomol Chem.* 2014;12(12):1975–1982. doi:10.1039/c3ob42279h
24. Shen J, Xu R, Mai J, et al. High capacity nanoporous silicon carrier for systemic delivery of gene silencing therapeutics. *ACS Nano.* 2013;7(11):9867–9880. doi:10.1021/nn4035316
25. Elsbahy M, Nazarali A, Foldvari M. Non-viral nucleic acid delivery: Key challenges and future directions. *Curr Drug Deliv.* 2011;8(3):235–244.
26. Patnaik S, Gupta KC. Novel polyethylenimine-derived nanoparticles for in vivo gene delivery. *Expert Opin Drug Deliv.* 2013;10(2):215–228. doi:10.1517/17425247.2013.744964
27. Kempen DH, Lu L, Hefferan TE, et al. Retention of in vitro and in vivo BMP-2 bioactivities in sustained delivery vehicles for bone tissue engineering. *Biomaterials.* 2008;29(22):3245–3252. doi:10.1016/j.biomaterials.2008.04.031
28. Qiao C, Zhang K, Jin H, et al. Using poly(lactic-co-glycolic acid) microspheres to encapsulate plasmid of bone morphogenetic protein 2/polyethylenimine nanoparticles to promote bone formation in vitro and in vivo. *Int J Nanomedicine.* 2013;8:2985–2995. doi:10.2147/IJN.S45184
29. Mao C, Pan W, Shao X, et al. The clearance effect of tetrahedral dna nanostructures on senescent human dermal fibroblasts. *ACS Appl Mater Interfaces.* 2019;11(2):1942–1950. doi:10.1021/acsami.8b20530
30. Daltaban O, Saygun I, Bal B, et al. Gingival crevicular fluid alkaline phosphatase levels in postmenopausal women: effects of phase I periodontal treatment. *J Periodontol.* 2006;77(1):67–72. doi:10.1902/jop.2006.77.1.67
31. Ding LZ, Teng X, Zhang ZB, et al. Mangiferin inhibits apoptosis and oxidative stress via BMP2/Smad-1 signaling in dexamethasone-induced MC3T3-E1 cells. *Int J Mol Med.* 2018;41(5):2517–2526. doi:10.3892/ijmm.2018.3506
32. Shen H, Wang J, Min J, et al. Activation of TGF-beta1/alpha-SMA/Col I profibrotic pathway in fibroblasts by galectin-3 contributes to atrial fibrosis in experimental models and patients. *Cell Physiol Biochem.* 2018;47(2):851–863. doi:10.1159/000490077
33. Brady KP, Dushkin H, Fornzler D, et al. A novel putative transporter maps to the osteosclerosis (oc) mutation and is not expressed in the OC mutant mouse. *Genomics.* 1999;56(3):254–261. doi:10.1006/geno.1998.5722
34. Martins CM, de Azevedo Queiroz IO, Ervolino E, et al. RUNX-2, OPN and OCN expression induced by grey and white mineral trioxide aggregate in normal and hypertensive rats. *Int Endod J.* 2018;51(6):641–648. doi:10.1111/iej.12876
35. Byeon H, Lee SD, Hong EK, et al. Long-term prognostic impact of osteopontin and Dickkopf-related protein 1 in patients with hepatocellular carcinoma after hepatectomy. *Pathol Res Pract.* 2018;214(6):814–820. doi:10.1016/j.prp.2018.05.002
36. Zhang Q, Lin S, Zhang T, et al. Curved microstructures promote osteogenesis of mesenchymal stem cells via the RhoA/ROCK pathway. *Cell Prolif.* 2017;50(4):e12356. doi:10.1111/cpr.12356

Diffusion tensor imaging of normal-appearing cervical spinal cords in patients with multiple sclerosis: Correlations with clinical evaluation and cerebral diffusion tensor imaging changes. Preliminary experience

Michał Wolańczyk^{1,A–D,F}, Joanna Bładowska^{1,A,B}, Anna Kołtowska^{1,A–D}, Anna Pokryszko-Dragan^{2,E,F}, Przemysław Podgórski^{1,B,E}, Sławomir Budrewicz^{2,E,F}, Marek Sąsiadek^{1,A–F}

¹ Department of General Radiology, Interventional Radiology and Neuroradiology, Wrocław Medical University, Poland

² Department of Neurology, Wrocław Medical University, Poland

A – research concept and design; B – collection and/or assembly of data; C – data analysis and interpretation;

D – writing the article; E – critical revision of the article; F – final approval of the article

Advances in Clinical and Experimental Medicine, ISSN 1899–5276 (print), ISSN 2451–2680 (online)

Adv Clin Exp Med. 2020;29(4):441–448

Address for correspondence

Anna Kołtowska
E-mail: annakoltowska02@gmail.com

Funding sources

Supported by Wrocław Medical University (grant No. ST.C270.17.041).

Conflict of interest

None declared

Received on May 26, 2019

Reviewed on June 4, 2019

Accepted on January 21, 2020

Published online on May 5, 2020

Cite as

Wolańczyk M, Bładowska J, Kołtowska A, et al. Diffusion tensor imaging of normal-appearing cervical spinal cords in patients with multiple sclerosis: Correlations with clinical evaluation and cerebral diffusion tensor imaging changes. Preliminary experience. *Adv Clin Exp Med.* 2020;29(4):441–448. doi:10.17219/acem/116754

DOI

10.17219/acem/116754

Copyright

© 2020 by Wrocław Medical University

This is an article distributed under the terms of the Creative Commons Attribution 3.0 Unported (CC BY 3.0) (<https://creativecommons.org/licenses/by/3.0/>)

Abstract

Background. Several studies have identified changes in the spinal cord DTI measurements in patients with multiple sclerosis (MS). However, correlations between changes in DTI parameters in normal appearing cervical spine and neurological findings have not been clearly established.

Objectives. To determine whether diffusion tensor imaging (DTI) measurements such as fractional anisotropy (FA) and apparent diffusion coefficient (ADC) are sufficiently sensitive in detecting microstructure alterations in normal-appearing spinal cords in patients with MS and whether they reflect these patients' clinical disability.

Material and methods. Fifteen patients diagnosed with relapsing-remitting MS (RRMS) with normal-appearing cervical spinal cords on plain MRI and 11 asymptomatic volunteers were enrolled in the study. Overall, 75 cervical spinal segments were analyzed. The regions of interest were drawn from the entire spinal cord cross-section and in the normal-appearing white matter tracts: the superior and inferior cerebellar peduncles and the posterior limbs of the internal capsules. Neurological deficit and the level of disability were evaluated using the Expanded Disability Status Scale (EDSS), the timed 25-foot walk test (T25FW) and the 9-hole peg test (9HPT) for manual dexterity.

Results. A significant difference ($p < 0.05$) in FA values between patients with MS and the control group was found at levels C2 ($p = 0.047$) and C3 ($p = 0.023$). No significant changes in ADC values were found. There was correlation between FA and ADC values in selected white matter tracts and at particular spinal cord levels. We also observed significant correlations between diffusion tensor imaging parameters and manual dexterity.

Conclusions. Our preliminary results may suggest that the spinal cord's structural loss is the dominant factor in the inflammatory/demyelinating component in patients with MS. Diffusion tensor imaging changes in the spinal cord correlate with brain DTI changes. Manual functioning seems to be more affected than walking.

Key words: disability, walking, multiple sclerosis, spinal cord, diffusion tensor imaging

Introduction

Multiple sclerosis (MS) is a chronic disease with a complex background, which is associated with the processes of immune-mediated inflammatory demyelination and axonal loss within the central nervous system (CNS). Multifocal damage to the brain and spinal cord, which develops over time in a relapsing-remitting or less frequently progressive manner, results in a diversity of symptoms and signs of neurological deficit, eventually leading to disability.

Magnetic resonance imaging (MRI) has become the modality of choice for detecting and assessing MS lesions within both the brain and the spinal cord, due to its sensitivity in detecting focal white matter lesions. However, changes observed in plain MRI often do not correlate with patients' clinical presentation, which is called the clinical–radiological paradox or mismatch. On the other hand, MS lesions might not be visible in the spinal cord due to its small volume, despite clinical signs of spinal cord impairment.¹

Diffusion tensor imaging (DTI) is a method which is sensitive to microstructure alterations even within the normal-appearing brain and spinal cord, which enables quantitative assessment of changes almost at the cellular level. The main DTI parameters are fractional anisotropy (FA) and apparent diffusion coefficient (ADC). Fractional anisotropy is a biomarker of white matter integrity, and lower FA values indicate impairment of the white matter fibers' integrity; ADC is a measure of diffusivity which therefore increases over the course of inflammatory/demyelinating processes.²

Several studies have identified changes in the spinal cord DTI measurements in patients with MS.^{3–10} However, correlations between changes in DTI parameters and neurological findings have not been clearly established.^{1,11–14} Some of these studies were not controlled trials. Moreover, relationships between quantitative clinical indices and DTI parameters within normal-appearing spinal cords have not been closely explored.

The aim of this preliminary study was to determine whether quantitative DTI measurements in normal-appearing spinal cords of patients with MS are sensitive in detecting alterations to its microstructure and whether these values are related to the patients' disability indices. Another objective was to assess whether DTI values in normal-appearing spinal cords correlate with the corresponding cerebral ones (within the cortico-spinal and cerebello-spinal tracts).

Material and methods

The study was comprised of 15 patients diagnosed with relapsing-remitting MS (RRMS) according to the current McDonald criteria¹⁵ (14 women and 1 man; age range: 28–48 years, mean age: 35.45 years) and 11 asymptomatic volunteers as control subjects (CS) with no history of neurological disorder (10 women and 1 man; age range:

28–48 years, mean age: 34.2 years). In patients with MS, the duration of illness ranged from 3 to 15 years (mean: 7.06 years). The EDSS results were 1–4 (mean: 2.26). All the patients and controls were right-handed.

The inclusion criterion for the study group was a lack of MS plaques or any other focal lesions in the spinal cord. The exclusion criteria were as follows: acute MS relapse and corticosteroid treatment within 3 months prior to inclusion in the study, the presence of marked cervical spine degenerative disease, previous spinal surgery or any incidental findings seen on plain MRI which would potentially suggest a neurological disorder.

The study was performed in accordance with the guidelines of the local University Ethics Committee for conducting research involving humans. All subjects provided their written informed consent to participate in this study according to the Helsinki Declaration, and the study was approved by the Local Commission of Bioethics.

MRI and DTI protocol

The MRI examinations were performed with a 1.5T MRI (SignaHdx; GE Medical Systems, Chicago, USA) with a maximum gradient amplitude of 33 mT/m, a 120 mT/m/s slew rate and a 16-channel HNS coil. The MRI protocol for cervical spinal cord study consisted of sagittal T1-weighted images, sagittal and axial T2-weighted images and sagittal T2-weighted FAT SAT images, followed by axial DTI sequence. Acquisition of DTI was based on single-shot spin-echo echo-planar imaging (SE/EPI) with the following settings: TR 10,000 ms; TE 100 ms, 160 × 160 mm field of view (FOV), 96 × 96 mm matrix, 1.6 × 1.6 mm in-plane image resolution, 4 mm axial slices parallel to the intervertebral disk space, no gap and 2 acquisitions. The examination frame was adjusted to cover the length of the spinal cord from vertebrae C1 to C7. Diffusion was measured along 15 non-collinear directions using *b* values of 0 s/mm² and 1,000 s/mm². The acquisition time of the sequence was about 7 min.

In all patients, a conventional brain MRI was performed according to the standard protocol used in our department¹⁶: sagittal and coronal T2 FRFSE sequences, axial T1 SE, T2 FSE and FLAIR sequences, axial DWI SE/EPI sequence and gadolinium-enhanced 3D-FSPGR sequence. The brain DTI acquisitions were performed using an axial single-shot spin-echo echo-planar imaging sequence (SE/EPI) along 25 different diffusion-encoding directions. For each direction, 2 *b* values were used: 0 and 1,000 s/mm² (4-mm slice thickness, no gap, TR 8,500 ms; TE 100,8 ms, 260 × 208 mm field of view, 128 × 128 mm matrix and 2 excitations). The acquisition time of DTI in each subject was 7.31 min.¹⁶

Image analysis

The image analysis was performed according to previously described methods.¹⁷ Plain MRIs of the cervical spine

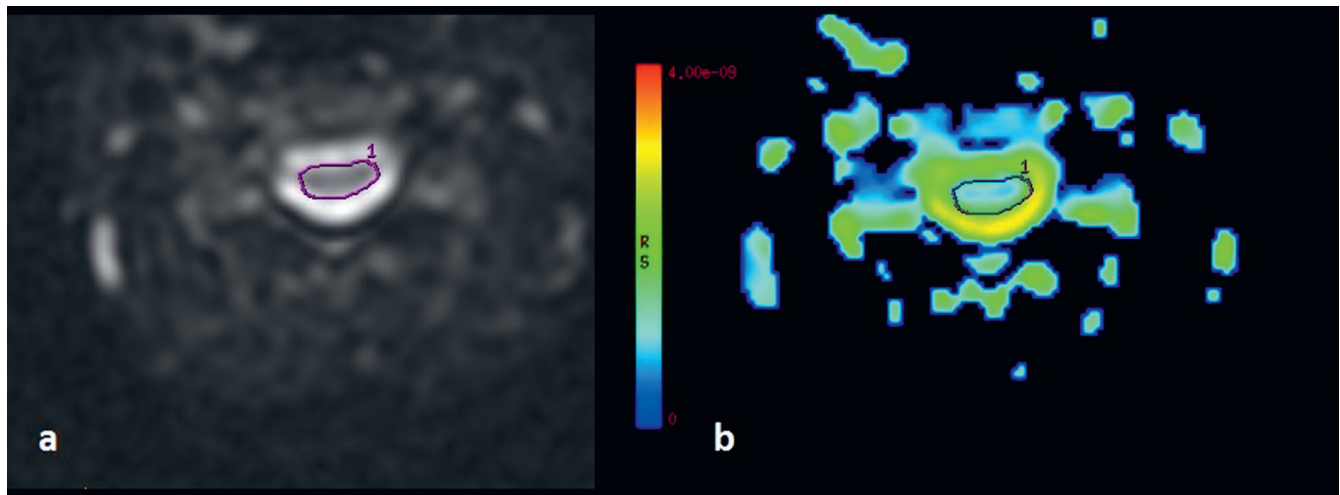


Fig. 1. Positioning of the regions of interest (ROI): a) b0 image and b) FA map. Each ROI was drawn manually over the entire axial cross-section of the cervical spinal cord, according to the most accurate axial b0 image

and brains of the 15 patients and 11 age-matched control subjects were analyzed by 2 independent readers (M.W. and J.B.), who were blinded to the clinical results. Image post-processing was done using the Functool software (GE ADW 4.6 workstation; GE Healthcare). Apparent diffusion coefficient (ADC) and fractional anisotropy (FA) axial maps were generated; FA and ADC values at the selected spine segments and brain regions were calculated based on these axial maps.

The regions of interest (ROIs) were drawn over the entire axial spinal cord cross-section, according to the most accurate axial B0 image¹⁷ at about half of the height of each vertebral body, as shown in Fig. 1.

All levels with significant artifacts were excluded from further analysis. The vast majority of artifacts were found at level C7; therefore, we decided to exclude all C7 levels from further evaluation. In total, 75 spinal segments were analyzed.

Diffusion tensor imaging measurements in the brain were performed by placing ROIs of 10 mm² in the following normal-appearing white matter regions: the right and left superior cerebellar peduncles (SCPR and SCPL), the right and left inferior cerebellar peduncles (ICPR and ICPL) and the right and left posterior limbs of the internal capsules (pyramidal cortico-spinal tracts (CSTs)) (PLICR and PLICL).

Clinical data

The type and duration of MS (duration of illness) were determined based on the patients' medical records. All patients underwent neurological examination, and their neurological deficit and level of disability were evaluated using the Expanded Disability Status Scale (EDSS).¹⁸ Functional tests¹⁹ were also performed to assess particular aspects of disability: the timed 25-foot walk (T25FW) for ambulation (the time needed to walk a distance of 25 feet,

with an average of the results from 2 trials) and the 9-hole peg test (9HPT) for manual dexterity (the time needed to insert 9 pegs into holes and remove them using one hand, with an average of the results from 2 consecutive trials for the dominant and non-dominant hand).

Statistical analysis

Comparisons of the FA and ADC values of the same cervical spinal cord levels among all groups were performed using Student's t-test and the Mann–Whitney test. Correlations between spinal cord DTI parameters and clinical results, as well as DTI values in selected brain regions, were estimated using Pearson's correlation coefficient. STATISTICA v. 10 software (StatSoft, Inc., Tulsa, USA) was used for statistical calculations; a p-value <0.05 was considered statistically significant.

Results

There were no significant differences in age ($p = 0.66$) or sex distribution between patients with MS and the control group.

Comparison of FA and ADC values in the spinal cord between patients with MS and the control group

The FA and ADC values at different levels (C1–C6) of the cervical spinal cord in patients with MS and controls, as well as statistical differences in these parameters between the 2 groups, are shown in Tables 1 and 2.

In the MS group, the mean FA values ranged from 0.570 (C6 level) to 0.644 (C3 level) and the mean ADC values ranged from 0.947 (C1 level) to 1.078 (C6 level) ($\times 0.001 \text{ mm}^2/\text{s}$). In the controls, the mean FA values ranged

Table 1. Mean FA values within the spinal cords of patients with MS and the control group

Cervical spine level	Mean FA in MS group	Mean FA in controls	p-value
C1	0.635	0.641	0.884
C2	0.639	0.708	0.047
C3	0.644	0.694	0.023
C4	0.604	0.636	0.425
C5	0.599	0.650	0.062
C6	0.570	0.632	0.068

Statistically significant differences are marked in bold; MS – multiple sclerosis; FA – fractional anisotropy.

from 0.632 (C6 level) to 0.708 (C2 level) and the mean ADC values ranged from 1.009 (C3 level) to 1.058 (C4 level) ($\times 0.001 \text{ mm}^2/\text{s}$). Significantly lower FA values ($p < 0.05$) were found at levels C2 and C3 in patients with MS than in the control subjects (Table 1). There were no significant changes in ADC values between the studied groups (Table 2).

Correlations of DTI measurements in the spinal cord with outcomes of clinical evaluation in patients with MS

The outcomes of clinical evaluation of each patient are shown in Table 3. Correlations between mean DTI values in the spinal cord and clinical outcomes in the MS group are presented in Table 4.

Table 2. Mean ADC values within the spinal cords of patients with MS and the control group

Cervical spine level	Mean ADC in MS group	Mean ADC in controls	p-value
C1	0.947	1.030	0.417
C2	1.060	1.010	0.310
C3	1.045	1.009	0.399
C4	1.026	1.058	0.467
C5	1.048	1.029	0.632
C6	1.078	1.014	0.211

FA – fractional anisotropy; ADC – apparent diffusion coefficient.

Significant negative correlations between the mean FA values in the spinal cord and the 9HPT test results were found at levels C4 and C5, for both the dominant and non-dominant hands.

There was also a significant negative correlation between FA values at level C6 and the 9HPT test results for the dominant hand. No significant positive correlations between mean FA values in the spinal cord and clinical results were observed.

Significant positive correlations between the ADC values in the spinal cord and the 9HPT test results for the non-dominant hand were found at levels C1, C2, C3, C4 and C6, and for the dominant hand at levels C4 and C6. The ADC values at levels C4 and C5 also positively correlated with a longer duration of illness. There were no significant negative correlations between the mean ADC values in the spinal cord and the clinical outcomes.

Table 3. Clinical evaluation of patients with MS

Patient	T25FW [s]	9HPT with dominant hand [s]	9HPT with non-dominant hand [s]	EDSS	Duration of illness [years]
1	5.6	19.6	21.3	1	3
2	5.3	21.3	20.6	1.5	7
3	4.9	20.5	22.4	3	11
4	4.0	16.6	17.2	3	5
5	4.2	23.6	28.9	1.5	8
6	6.1	21.5	27.3	4	5
7	7.1	31.7	32.5	1.5	14
8	4.8	33.2	31.4	2	8
9	5.2	29.1	29.3	3.5	15
10	6.4	19.3	21.4	2.5	3
11	4.6	20.2	21.7	2.5	10
12	5.4	21.5	19.2	2	3
13	5.2	18.1	16.6	2	5
14	4.0	19.2	19.1	1.5	6
15	5.7	19.8	17.3	2.5	3
Median	5.2	20.5	21.4	2.0	6.0

T25FW – timed 25-foot walk test; 9HPT – 9-hole peg test; EDSS – Expanded Disability Status Scale.

Table 4. Correlations between mean DTI values in the spinal cord and clinical outcomes in patients with MS

Cervical spine level		T25FW		9HPT, dominant hand		9HPT, non-dominant hand		EDSS		Duration of illness	
		PCC	p-value	PCC	p-value	PCC	p-value	PCC	p-value	PCC	p-value
C1	FA	-0.5412	0.086	-0.2914	0.385	-0.4049	0.217	-0.4199	0.198	-0.0756	0.825
	ADC	0.4674	0.147	0.4371	0.179	0.6382	0.035	0.3044	0.363	0.1898	0.576
C2	FA	0.1809	0.595	-0.2524	0.454	-0.5221	0.099	-0.0977	0.775	-0.256	0.447
	ADC	0.3854	0.242	0.47	0.145	0.6613	0.027	0.2189	0.518	0.1284	0.707
C3	FA	-0.2639	0.433	-0.483	0.132	-0.555	0.076	-0.3941	0.230	-0.2735	0.416
	ADC	-0.009	0.979	0.5829	0.060	0.6373	0.035	0.3232	0.332	0.4583	0.156
C4	FA	-0.1142	0.738	-0.8626	0.001	-0.7529	0.007	-0.0811	0.813	-0.5435	0.084
	ADC	0.1294	0.705	0.8897	0.001	0.8287	0.002	0.041	0.905	0.6583	0.028
C5	FA	-0.0863	0.801	-0.8467	0.001	-0.7209	0.012	-0.0654	0.848	-0.4814	0.134
	ADC	-0.0573	0.867	0.0534	0.876	0.3643	0.271	0.5587	0.074	0.1901	0.576
C6	FA	-0.2115	0.533	-0.6287	0.038	-0.4551	0.160	0.2392	0.479	-0.212	0.531
	ADC	-0.1285	0.707	0.7331	0.010	0.6859	0.020	-0.1958	0.564	0.7921	0.004

Statistically significant differences are marked in bold; C1–C6 – levels of the cervical spinal cord; FA – fractional anisotropy values; ADC – apparent diffusion coefficient values; EDSS – expanded disability status scale score; T25FW – timed 25-foot walk test; 9HPT – 9-hole peg test; PCC – Pearson correlation coefficient.

Correlations between mean DTI parameters in the spinal cord and selected white matter tracts

Within the white matter tracts, the mean FA values ranged from 0.570 to 0.658, and for selected white matter locations the values were as follows: ICPR – 0.57; ICPL – 0.64; SCPR – 0.59; SCPL – 0.60; PLICR – 0.65; and PLICL – 0.66 (Table 5).

Significant positive correlations were found between the mean FA values in SCPR and the FA values in the spinal cord at level C2, between FA values in ICPL and FA values in the spinal cord at levels C4 and C5, and between FA values in PLICL and FA values in the spinal cord at level C6, which means that spinal FA values were lower in patients with lower FA values in the cerebral white matter tracts.

Within the brain regions which were analyzed, the mean ADC values ranged from 0.71 to 1.26, and for the selected locations the values were as follows: ICPR – 0.87; ICPL – 0.77; SCPR – 1.26; SCPL – 1.11; PLICR – 0.71; and PLICL – 0.72.

Significant positive correlations were found between the mean ADC values in PLICR and the ADC values in the spinal cord at levels C1, C3 and C4, between the ADC values in PLICL and the ADC values in the spinal cord at levels C2 and C3, and between the ADC values in ICPL and the ADC values in the spinal cord at level C4, which means that ADC values in the spinal cord were higher in patients with higher ADC values in the cerebral white matter tracts.

There were no significant negative correlations found between ADC values in the spinal cord and ADC values in the examined brain regions.

Table 5. Correlations between mean FA values in the spinal cord (levels C1 to C6) and brain white matter tracts

Cervical spina level FA value	ICPR FA		ICPL FA		SCPR FA		SCPL FA		PLICR FA		PLICL FA	
	PCC	p-value	PCC	p-value	PCC	p-value	PCC	p-value	PCC	p-value	PCC	p-value
C1 FA	0.128	0.708	0.1733	0.610	0.3392	0.307	0.135	0.692	0.0724	0.833	0.4236	0.194
C2 FA	-0.0937	0.784	0.4463	0.169	0.6157	0.044	0.4477	0.167	0.3157	0.344	0.1656	0.627
C3 FA	0.1592	0.640	0.295	0.378	0.0674	0.844	-0.1179	0.730	-0.012	0.972	0.2659	0.429
C4 FA	0.1959	0.564	0.6405	0.034	0.2448	0.468	-0.209	0.537	0.1347	0.693	0.193	0.570
C5 FA	0.215	0.526	0.6381	0.035	0.2697	0.423	-0.1817	0.593	0.284	0.397	0.3444	0.300
C6 FA	0.2397	0.478	0.2797	0.405	-0.1359	0.690	-0.4744	0.140	0.4093	0.211	0.6947	0.018

Statistically significant differences are marked in bold; C1–C6 – levels of the cervical spinal cord; FA – fractional anisotropy values; SCPR/SCPL – right/left superior cerebellar peduncles; ICPR/ICPL – right/left inferior cerebellar peduncles; PLICR/PLICL – right/left posterior limbs of internal capsules; PCC – Pearson correlation coefficient.

Table 6. Correlations between mean ADC values in the spinal cord (levels C1 to C6) and the brain

Cervical spinal level ADC value	ICPR ADC		ICPL ADC		SCPR ADC		SCPL ADC		PLICR ADC		PLICL ADC	
	PCC	p-value	PCC	p-value	PCC	p-value	PCC	p-value	PCC	p-value	PCC	p-value
C1 ADC	0.2717	0.419	0.1413	0.679	0.0607	0.859	-0.3826	0.246	0.652	0.030	0.489	0.127
C2 ADC	0.3103	0.353	0.2404	0.476	0.1777	0.601	-0.2385	0.480	0.5552	0.076	0.6661	0.025
C3 ADC	-0.0518	0.880	0.5132	0.106	0.0808	0.813	-0.5963	0.053	0.8303	0.002	0.7517	0.008
C4 ADC	0.1448	0.671	0.6652	0.026	-0.1176	0.731	-0.5598	0.073	0.7026	0.016	0.4697	0.145
C5 ADC	-0.3967	0.227	-0.02	0.953	-0.2161	0.523	-0.3959	0.228	0.579	0.062	0.4795	0.136
C6 ADC	-0.087	0.799	0.4599	0.155	-0.4038	0.218	-0.5568	0.075	0.5435	0.084	0.1459	0.669

Statistically significant differences are marked in bold; C1–C6 – levels of the cervical spinal cord; ADC – apparent diffusion coefficient values; SCPR/SCPL – right/left superior cerebellar peduncles; ICPR/ICPL – right/left inferior cerebellar peduncles; PLICR/PLICL – right/left posterior limbs of internal capsules; PCC – Pearson correlation coefficient.

Discussion

Because MS onset mainly occurs in young adults, and due to the long-term and highly variable course of the disease, there is a need to diagnose and possibly predict at an early stage the extent of damage to the CNS and its clinical consequences.²⁰ Early DTI changes reflect microstructural changes found at almost the cellular level, and FA value could potentially be a noninvasive biomarker for detecting subtle axonal lesions which may precede focal demyelination likely appearing later on as MS plaques on T2 sequences.

In this study, we investigated quantitative DTI indices such as FA and ADC values, measured at different levels of normal-appearing cervical spinal cords and in selected normal-appearing cerebral white matter tracts. This data correlated with functional measures of the degree of overall disability (EDSS), ambulation (T25FW) and manual dexterity (9HPT). Spinal cord atrophy is a well-known contributor to disability^{3,21}; however, the conventional indices of spinal cord atrophy reflect tissue loss that is more likely to be irreversible. Measuring DTI parameters within a normal-appearing spinal cord may have the advantage of detecting potentially reversible changes which are not visible on conventional MRI scans.

Significant differences in FA values between patients with MS with normal-appearing spinal cords and controls were found at spinal levels C2 and C3. These results are in agreement with previous DTI studies showing decreased FA values in both normal-appearing spinal cords and in T2-visible lesions in the spinal cords of subjects with MS.^{6–10} On the other hand, we found no significant differences between the ADC values of the studied groups. Lower FA values in MS reflect axonal impairment, which corresponds to functional discontinuity of the axons and, by definition, is a more specific measurement than ADC, which increases due to the inflammatory/demyelinating processes. Therefore, our results may suggest that the axonal loss within the spinal cords of patients with MS is more pronounced than the inflammatory-demyelinating

component. The other mechanism which could contribute to the lower FA values is Wallerian degeneration. However, the patients have no visible demyelinating lesions in the spinal cord – only the brain lesions; therefore, it seems rather unlikely.

Our results suggest a correlation between ADC values at levels C4 and C6 and the duration of illness, since the spinal ADC values appear to be higher in patients with a longer duration of illness. This may reflect increasing neuronal damage with a longer duration of disease.

In the next part of our study, we analyzed FA and ADC values of the spinal cord as related to various measurements of disability in the course of MS. Our data showed significant FA and ADC correlations with manual dexterity, as measured with the 9HPT. Particularly pronounced correlations were found between the higher ADC values in the spinal cord and manual dexterity at the levels of C1, C2, C3 and C6. Correlations between FA values and manual dexterity parameters were found only at levels C4 and C5.

Walking dysfunction is a relatively common problem in patients with MS, yet there is still a poor understanding of the possible neuronal substrate of walking.^{4,5,14} In this study, we did not find any significant correlations of DTI parameters in the spinal cord with the timed 25-foot walk test (T25FW) or the Expanded Disability Status Scale (EDSS). The EDSS score is strongly affected by ambulation ability, so the lack of correlations for both the EDSS and the T25FW is consistent. Our results seem to suggest that a loss of neuronal integrity within the cervical spinal cord is associated with greater impairment in manual dexterity than in walking ability.

The vast majority of available studies investigating the relationships between clinical parameters and DTI changes in patients with MS are primarily focused on the brain and not on the spinal cord. Hubbard et al.¹⁴ evaluated different DTI values of the corticospinal tract, including mean diffusivity (MD), radial diffusivity (RD), axial diffusivity (AD) and FA and their relationships with ambulation test scores (the T25FW and the 6-minute walk test).¹⁴ Although they found some significant correlations

between the walking test results and RD and AD values, none were observed for FA values in the corticospinal tract, which seems to be consistent with our results.

Additionally, we investigated the relationships between DTI values in the spinal cord and corresponding pathways in the brain. A significant correlation was observed between lower FA values in the inferior cerebellar peduncle (ICP) and at levels C4 and C5 of the spinal cord. Such an association may suggest neuronal disintegration along the posterior spinocerebellar tract, running predominantly through the ICP. A significant correlation was also noted between the lower FA values in the superior cerebellar peduncle (SCP) and level C2 of the spinal cord, which in turn may be related to changes in the integrity of the anterior spinocerebellar tract.^{22,23} A considerable positive correlation was found between ADC values within the ICP and level C4 of the spinal cord, with corresponding higher ADC values in both regions. Although this correlation was found only at 1 level, it might suggest the involvement of the spinocerebellar tracts by disease, which could contribute to MS-related disability.

Our study also revealed correlations between ADC values within the spinal cord (levels C1, C2, C3 and C4) and in both posterior limbs of the internal capsules (PLICs). This association may depend on the anatomical structure of the pyramidal tracts, as more than half of their fibers terminate in the cervical spinal cord to supply the upper extremities.²³ In comparison to other studies which evaluated cervical spinal cord changes at 1 or 2 levels of the cervical spinal cord,^{9,34–36} our study provides an assessment of pathological changes within a wider range of the cervical spinal cord (levels C1 to C6), which renders a more comprehensive look into changes that may contribute to clinical dysfunction.

As a preliminary report, our study features a number of limitations. The small sample size is likely to limit the statistical significance of the findings. Additionally, the use of ROIs encircling the cross-sectional area of the spinal cord— instead of particular columns – might have possibly created a bias in the observed structure–function relationships, although we believe this approach provides us with a more comprehensive view of spinal cord changes, assessing both white matter and grey matter. This approach has been already discussed in the literature, including our previous experience.¹⁷ Besides, it has been shown that MS affects both white matter and grey matter; therefore, the impairment of all spinal cord structures is calculated with our method. The involvement of the spinal cord grey matter (GM) in MS had already been recognized by the turn of the 20th century, which is discussed in a study by Schlaeger et al.²⁴ Other authors have reported a similar reduction of both grey matter and white matter cross-sectional cervical cord areas in advanced, progressive MS, with a predominance of GM loss.^{26–33}


Nevertheless, the results seem to be interesting and to encourage further investigation. They suggest the need to explore spinal cord-specific pathological processes, mainly

with regard to clinical disability in patients with a normal-appearing spinal cord on plain MRI. Studies on a larger base of material, using an improved DTI evaluation protocol, may improve our understanding of the inflammatory and neurodegenerative processes underlying disability in MS.

Conclusions

Our preliminary findings show significant differences in FA values between the normal-appearing spinal cords of patients with MS and healthy controls. These may suggest that the structural loss within the spinal cords of patients with MS is of greater importance than the inflammatory-demyelinating component. The initial loss of neuronal integrity within the cervical spinal cord seems to influence manual dexterity more than walking function. Further studies are necessary to establish the role of DTI measures as biomarkers of the subtle alterations in the spinal cord integrity of patients with MS and their clinical and prognostic relevance.

ORCID iDs

Michał Wolańczyk  <https://orcid.org/0000-0002-4296-3353>
 Joanna Bładowska  <https://orcid.org/0000-0003-0597-8457>
 Anna Kołtowska  <https://orcid.org/0000-0003-2508-9817>
 Anna Pokryszko-Dragan  <https://orcid.org/0000-0002-5203-112X>
 Przemysław Podgórski  <https://orcid.org/0000-0002-9303-8432>
 Sławomir Budrewicz  <https://orcid.org/0000-0002-2044-6347>
 Marek Szaśiadek  <https://orcid.org/0000-0003-3627-118X>

References

- Oh J, Saidha S, Chen M, et al. Spinal cord quantitative MRI discriminates between disability levels in multiple sclerosis. *Neurology*. 2013;80(6):540–547. doi:10.1212/WNL.0b013e31828154c5
- Banaszek A, Bładowska J, Podgórski P, Szaśiadek MJ. Role of diffusion tensor MR imaging in degenerative cervical spine disease: A review of the literature. *Clin Neuroradiol*. 2016;26(3):265–276. doi:10.1007/s00062-015-0467-y
- Filippi M, Bozzali M, Horsfield MA, et al. A conventional and magnetization transfer MRI study of the cervical cord in patients with MS. *Neurol*. 2000;54(1):207–213.
- Hobart JC, Riazi DL, Lamping R, Fitzpatrick R, Thompson AJ. Measuring the impact of MS on walking ability: The 12-Item MS Walking Scale (MSWS-12). *Neurology*. 2003;60(1):31–36.
- Motl RW. Ambulation and multiple sclerosis. *Phys Med Rehabil Clin N Am*. 2013;24(2):325–336.
- Agosta F, Benedetti B, Rocca MA, et al. Quantification of cervical cord pathology in primary progressive MS using diffusion tensor MRI. *Neurology*. 2005;64(4):631–635.
- Benedetti B, Valsasina P, Judica E, et al. Grading cervical cord damage in neuromyelitis optica and MS by diffusion tensor MRI. *Neurology*. 2006;67(1):161–163.
- Ciccarelli O, Wheeler-Kingshott CA, McLean MA, et al. Spinal cord spectroscopy and diffusion-based tractography to assess acute disability in multiple sclerosis. *Brain*. 2007;130(Pt 8):2220–2231.
- Hesseltine SM, Law M, Babb J, et al. Diffusion tensor imaging in multiple sclerosis: Assessment of regional differences in the axial plane within normal-appearing cervical spinal cord. *AJNR Am J Neuroradiol*. 2006;27(6):1189–1193.
- Raz E, Bester M, Sigmund EE, et al. A better characterization of spinal cord damage in multiple sclerosis: A diffusional kurtosis imaging study. *AJNR Am J Neuroradiol*. 2013;34(9):1846–1852. doi:10.3174/ajnr.A3512

11. von Meyenburg J, Wilm BJ, Weck A, et al. Spinal cord diffusion-tensor imaging and motor-evoked potentials in multiple sclerosis patients: Microstructural and functional asymmetry. *Radiology*. 2013;267(3):869–879. doi:10.1148/radiol.13112776
12. Oh J, Zackowski K, Chen M, et al. Multi-parametric MRI correlates of sensor motor function in the spinal cord in multiple sclerosis. *Mult Scler*. 2013;19(4):427–435. doi:10.1177/1352458512456614
13. Pardini M, Yaldizli Ö, Sethi V. Motor network efficiency and disability in multiplesclerosis. *Neurology*. 2015;85(13):1115–1122. doi:10.1212/WNL
14. Hubbard EA, Wetter NC, Sutton BP. Diffusion tensor imaging of the corticospinal tract and walking performance in multiple sclerosis. *J Neurol Sci*. 2016;15:225–231. doi:10.1016/j.jns.2016.02.044
15. Thompson AJ, Banwell BL, Barkhof F, et al. Diagnosis of multiple sclerosis: 2017 revisions of the McDonald criteria. *Lancet Neurol*. 2018;17(2):162–173. doi:10.1016/S1474-4422(17)30470-2
16. Banaszek A, Bładowska J, Pokryszko-Dragan A, Podemski R, Sasiadek MJ. Evaluation of the degradation of the selected projectile, commissural and association white matter tracts within normal appearing white matter in patients with multiple sclerosis using diffusion tensor MR imaging: A preliminary study. *Pol J Radiol*. 2015;80:457–463. doi:10.12659/PJR.894661
17. Banaszek A, Bładowska J, Szewczyk P, Podgorski P, Sasiadek M. Usefulness of diffusion tensor MR imaging in the assessment of intramedullary changes of the cervical spinal cord in different stages of degenerative spine disease. *Eur Spine J*. 2014;23(7):1523–1530. doi:10.1007/s00586-014-3323-x
18. Kurtzke JF. Rating neurologic impairment in multiple sclerosis: An expanded disability status scale (EDSS). *Neurology*. 1983;33(11):1444–1452.
19. Fischer JS, Rudick RA, Cutter GR, Reingold SC. The Multiple Sclerosis Functional Composite Measure (MSFC): An integrated approach to MS clinical outcome assessment. National MS Society Clinical Outcomes Assessment Task Force. *Mult Scler*. 1999;5(4):244–250.
20. Johns P. *Clinical Neuroscience*. New York, NY: Elsevier; 2014.
21. Nijeholt GJ, Bergers E, Kamphorst W, et al. Post-mortem high-resolution MRI of the spinal cord in multiple sclerosis: A correlative study with conventional MRI, histopathology and clinical phenotype. *Brain*. 2001;124(Pt 1):154–166.
22. Tovar-Moll F, Evangelou IE, Chiu AW, et al. Diffuse and focal corticospinal tract disease and its impact on patient disability in multiple sclerosis. *J Neuroimaging*. 2015;25(2):200–206.
23. Kahle W, Frotscher M. *Color Atlas of Human Anatomy*. Vol. 3. Nervous System and Sensory Organs. 7th ed. New York, NY: Thieme; 2015.
24. Schlaeager R, Papinutto N, Panara V, et al. Spinal cord gray matter atrophy correlates with multiple sclerosis disability. *Ann Neurol*. 2014;76(4):568–580. doi:10.1002/ana.24241
25. Dejerine J. Etude sur la sclérose en plaques cérébrospinale à forme de sclérose latérale amyotrophique. *Rev de Méd*. 4:193;1884.
26. Brauer L. Muskelatrophie bei multipler Sklerose. *Neuro Centralbl*. 17:635;1898.
27. Bouchaud S. Sclérose en plaques avec amyotrophique. *J de Neurol*. 5:348;1900.
28. Lejonne MP. Contribution à l'étude des atrophies musculaires dans la sclérose en plaques. Thèse de Paris: G. Steinheil; 1903.
29. Davison C, Goodhart SP, Lander J. Multiple sclerosis and amyotrophies. *Arch Neur Psych*. 1934;31(2):270–289. doi:10.1001/archneurpsyc.1934.02250020058003
30. Gilmore CP, Donaldson I, Bö L, Owens T, Lowe J, Evangelou N. Regional variations in the extent and pattern of grey matter demyelination in multiple sclerosis: A comparison between the cerebral cortex, cerebellar cortex, deep grey matter nuclei and the spinal cord. *J Neurol Neurosurg Psychiatry*. 2009;80(2):182–187.
31. Gilmore CP, DeLuca GC, Bö L, et al. Spinal cord neuronal pathology in multiple sclerosis. *Brain Pathol*. 2009;19(4):642–649.
32. Gilmore CP, DeLuca GC, Bö L, et al. Spinal cord atrophy in multiple sclerosis caused by white matter volume loss. *Arch Neurol*. 2005;62(12):1859–1862.
33. Bjartmar C, Kidd G, Mörk S, Rudick R, Trapp BD. Neurological disability correlates with spinal cord axonal loss and reduced N-acetyl aspartate in chronic multiple sclerosis patients. *Ann Neurol*. 2000;48(6):893–901.
34. Oh J, Sotirchos ES, Saidha S. Relationships between quantitative spinal cord MRI and retinal layers in multiple sclerosis. *Neurology*. 2015;84(7):720–728. doi:10.1212/WNL
35. Klineova S, Farber R, Saiote C, et al. 2016. Relationship between timed 25-foot walk and diffusion tensor imaging in MS. *Mult Scler J Exp Transl Clin*. 2016;2:2055217316655365. doi:10.1177/2055217316655365
36. Fritz NE, Kellera J, Calabresid PA, Zackowskia KM. Quantitative measures of walking and strength provide insight into brain cortico-spinal tract pathology in multiple sclerosis. *Neuroimage Clin*. 2017;14:490–498. doi:10.1016/j.nicl.2017.02.006

The effect of diabetes on vitreous levels of adiponectin and inflammatory cytokines in experimental rat model

Yusuf Özyay^{1,A,B}, Dilay Ozek^{2,A}, Filiz Yıldırım^{3,A–F}, Zuhâl Yıldırım^{4,A–F}

¹ Department of Medical Biology, Faculty of Medicine, Adiyaman University, Turkey

² Second Ophthalmology Clinic, Ankara Numune Education and Research Hospital, Turkey

³ Clinic of Internal Medicine, Polatlı Duatepe Government Hospital, Ankara, Turkey

⁴ Etimesgut Public Health Laboratory, Ankara, Turkey

A – research concept and design; B – collection and/or assembly of data; C – data analysis and interpretation; D – writing the article; E – critical revision of the article; F – final approval of the article

Advances in Clinical and Experimental Medicine, ISSN 1899–5276 (print), ISSN 2451–2680 (online)

Adv Clin Exp Med. 2020;29(4):449–452

Address for correspondence

Filiz Yıldırım

E-mail: drfyildirim@yahoo.com

Funding sources

None declared

Conflict of interest

None declared

Received on December 19, 2018

Reviewed on December 29, 2018

Accepted on December 2, 2019

Published online on April 28, 2020

Abstract

Background. Diabetic retinopathy is one of the most common eye diseases faced by diabetic patients. It is a slow-progressing complication that results from damage to the blood vessels of the retina.

Objectives. To investigate the role of adiponectin and inflammatory cytokines in the vitreous of diabetic rats.

Material and methods. The study was conducted in 3–4-month-old male albino Wistar rats (180–240 g). The animals were divided into 2 groups (n = 40 in each group): the diabetes group and the control group. A single dose of streptozotocin (STZ) (45 mg/kg) in citrate buffer (0.1 M; pH 4.5) was intraperitoneally (ip.) injected into the diabetes group rats. A single dose of citrate buffer was injected ip. into the control group rats. All subjects were sacrificed under intramuscular (im.) Na-thiopental (50 mg/kg) anesthesia. The rats' eyelids were opened with an eye speculum and vitreous samples were collected with 20G needles 4 mm posterior to the limbus. The levels of vitreous adiponectin, tumor necrosis factor α (TNF- α), interferon γ (INF- γ), and matrix metalloproteinase (MMP)-2 and -9 were determined using a solid-phase sandwich enzyme-linked immunosorbent assay (ELISA).

Results. The levels of adiponectin, TNF- α , INF- γ , MMP-2, and MMP-9 in the rat vitreous were significantly higher in the diabetes group than in the control group (p < 0.05).

Conclusions. Elevated adiponectin, TNF- α , and INF- γ levels in the vitreous may be diagnostically useful in diabetic retinopathy, and inflammatory cytokines in the vitreous may be pathogenically important in this concentration.

Key words: inflammation, diabetes mellitus, adiponectin, vitreous

Cite as

Özyay Y, Ozek D, Yıldırım F, Yıldırım Z. The effect of diabetes on vitreous levels of adiponectin and inflammatory cytokines in experimental rat model. *Adv Clin Exp Med.* 2020;29(4):449–452. doi:10.17219/acem/115004

DOI

10.17219/acem/115004

Copyright

© 2020 by Wrocław Medical University

This is an article distributed under the terms of the Creative Commons Attribution 3.0 Unported (CC BY 3.0) (<https://creativecommons.org/licenses/by/3.0/>)

Introduction

Diabetic retinopathy (DR) is one of the most common eye diseases faced by diabetic patients. It is a slow-progressing complication that results from damage to the blood vessels of the retina. In the initial stages of DR, the disease may remain asymptomatic, but eventually, if left untreated, can result in blindness.¹ The development of retinopathy is directly related to the duration of diabetes: within 10 years of diabetes, about 50% of patients will develop it, and within 20–25 years nearly 90% of diabetic patients will have some stage of retinopathy.^{2,3}

Diabetes is known to display a strong inflammatory component. Circulating levels of endothelial leucocyte adhesion molecule-1 (E-selectin), intercellular adhesion molecule-1 (ICAM-1), and vascular cell adhesion molecule-1 (VCAM-1) have been demonstrated to be increased in type 2 diabetes patients.⁴ The complex pathology of DR involves upregulation of inflammatory molecules, adhesion molecules, and pro-inflammatory cytokines, which play critical roles in the pathogenesis of DR. Increased vitreous levels of certain pro-inflammatory cytokines have been described.^{5–7} The sophisticated inflammatory and chemotactic cascades may be linked to the breakdown of the vascular barrier, which may be one further mechanism contributing to the development of DR.⁸

Adiponectin is a novel protein product of the adipose tissue, sometimes described as adipocytokines. Adiponectin is a plasma protein that was discovered a few years ago. It is produced exclusively and abundantly in adipose tissue and circulates at relatively high concentration.⁹ According to current data, adiponectin has powerful metabolic effects, including exacerbation of insulin sensitivity, reduction of hepatic glucose production, and lowered gluconeogenesis.¹⁰ In addition, plasma adiponectin levels were found to be negatively correlated with body mass index (BMI) and fat content, suggesting that fat mass may exert negative feedback on adiponectin production, and thus may negatively modulate the process of atherogenesis.¹¹

The study evaluated the effects of inflammatory cytokine and adiponectin in diabetic rat vitreous.

Material and methods

Inducing experimental diabetes

The rats were administered a single dose of 45 mg/kg streptozotocin (STZ) intraperitoneal (ip.) injection, dissolved in 1 mL 0.1 M cold citrate tampon with a pH of 4.5.¹² The rats fasted for 18 h prior to the STZ administration. Fasting blood glucose levels were measured 48 h after the administration. Those with fasting blood glucose levels exceeding 250 mg/dL were considered diabetic and included in the diabetic group. The study was carried out

according to the Dumlupinar University Laboratory Animal Welfare and Ethical Committee Regulations.

Control group (n = 40): A single dose of citrate buffer was injected ip.

Diabetes group (n = 40): Diabetes was induced by a single dose of STZ (45 mg/kg) injected ip. Following diabetes inducement, fasting blood glucose levels were periodically monitored for 2 weeks. Diabetes stabilization was anticipated.

All subjects were sacrificed under intramuscular (im.) Na-thiopental (50 mg/kg) anesthesia. The rats' eyelids were opened with an eye speculum. Vitreous samples were collected with 20G needles 4 mm posterior to the limbus. The vitreous samples were stored at -80°C until the analyses were carried out.

Biochemical analyses

Rat vitreous tumor necrosis factor α (TNF- α), interferon γ (INF- γ), matrix metalloproteinase (MMP)-2, and MMP-9 were determined using a solid-phase sandwich enzyme-linked immunosorbent assay (ELISA).

Statistical analysis

The data was presented as mean \pm standard deviation (SD). Statistical analyses were carried out using the Kruskal–Wallis test and the Mann–Whitney U test (SPSS for Windows v. 15.0; SPSS Inc., Chicago, USA). Values of $p < 0.05$ were taken to be significant.

Results

The study was conducted in 3–4-month-old male albino Wistar rats (180–240 g). The animals were divided into 2 groups (n = 40 in each group): The diabetes group and the control group.

The levels of adiponectin, TNF- α , INF- γ , MMP-2, and MMP-9 in the vitreous were significantly higher in the diabetes group than in the control group ($p < 0.05$; Table 1).

Table 1. Adiponectin, TNF- α , INF- γ , MMP-2, and MMP-9 levels in the vitreous of the diabetic and control groups (mean \pm SD)

Groups	Diabetic group (n = 40)	Control group (n = 40)
Adiponectin [$\mu\text{g}/\text{mL}$]	17.32 \pm 5.39*	10.54 \pm 6.43
TNF- α [pg/mL]	11.69 \pm 3.83*	7.06 \pm 3.27
INF- γ [pg/mL]	86.18 \pm 35.19*	57.61 \pm 27.62
MMP-2 [ng/mL]	135.81 \pm 48.02*	95.40 \pm 46.19
MMP-9 [ng/mL]	14.18 \pm 4.80*	11.24 \pm 2.17

TNF- α – tumor necrosis factor α ; INF- γ – interferon γ ; MMP-2 – metalloproteinase; MMP-9 – metalloproteinase 9; * $p < 0.05$, as compared to the control group.

Discussion

Diabetic retinopathy is a retinal neovascular disease and a significant diabetic complication, whose development is strongly linked with hyperglycemia, dyslipidemia,¹³ and mitochondrial dysfunction accompanied by induced oxidative stress¹⁴ and associated with abnormal adiponectin levels. Clinically, diabetic retinopathy can be classified into non-proliferative retinopathy (phase 1) and proliferative retinopathy (phase 2), similar to retinopathy of prematurity. Hyperglycemia through metabolic changes leads to retinal vascular loss (phase 1). The incompletely vascularized retina is deprived of nutrition and oxygen, inducing pathological angiogenesis (phase 2). Adiponectin modifies these primary drivers of diabetic retinopathy. Abnormalities in the adiponectin pathway result in increased insulin resistance,¹⁵ and adiponectin gene polymorphisms are associated with retinopathy in diabetic patients.¹⁶

Adiponectin is a regulator of energy homeostasis and is widely recognized for its antidiabetic, anti-inflammatory, antiangiogenic, antiatherogenic, antihypertensive, and cardioprotective effects.^{17,18} Yilmaz et al. demonstrated that circulating levels of adiponectin are lower in both obesity and type 2 diabetes mellitus (T2DM).¹⁹ Moreover, T2DM patients with DR (proliferative as well as non-proliferative), show lower levels of adiponectin than matched patients without retinopathy. Additionally, hypoadiponectinemia is positively correlated with the severity of retinopathy in T2DM.²⁰ Recently, Costagliola et al. and Mao et al. analyzed the levels of vascular endothelial growth factor (VEGF) and adiponectin in the aqueous humor of patients with proliferative diabetic retinopathy (PDR), T2DM, and macular edema and found that they were significantly higher than those recorded in the control subjects.^{21,22}

Ziez et al. have shown elevated adiponectin levels in the serum of patients with type 2 diabetes and PDR.¹⁶ Hong et al. have shown that adiponectin levels are higher in obese and non-obese patients with proliferative retinopathy than in those without apparent retinopathy.²³ Kato et al. demonstrated that blood levels of adiponectin are elevated in patients with DR as well as a positive correlation with the severity of the disease.²⁴ Danna et al. showed that adiponectin levels in the aqueous humor are higher in PDR.²⁵ These elevated levels may be a protective mechanism in PDR.

In the present study, it was determined that the vitreous adiponectin levels were significantly higher in the diabetes group than in the control group. One possible explanation of this finding may be attributed to the increased blood retinal barrier permeability documented among patients with diabetes. Another possible explanation could be the local reparative response to endothelial dysfunction; in fact, adiponectin induces endothelial nitric oxide production *in vitro*.

Proliferative retinopathy is associated with elevated intravitreal concentrations of certain cytokines. Although

inflammatory cytokines are thought to play an important role in the pathogenesis of DR, the precise pathophysiological mechanisms have not yet been totally explained.²⁶

Tumor necrosis factor alpha is the primary pro-inflammatory cytokine. It is expressed by mast cells, fibroblasts, and endothelial cells in addition to neutrophils and macrophages; it has autocrine, paracrine, and endocrine effects on the target cells. This cytokine plays an important role in many biological processes, such as infection control, preparation of tissue for repair, increasing phagocytic activities, stimulation of keratinocyte migration to the wound, phagocytic activity, fibroblast proliferation and chemotaxis, and degradation of the extracellular matrix proteins.²⁷

Interferon gamma plays an important role in inflammation. It is an important immune regulator that has been shown to inhibit collagen synthesis by fibroblasts, resulting in delayed healing in incision wounds.²⁸

It was demonstrated that vitreous TNF- α levels are significantly higher in patients with proliferative retinopathy than in those without retinopathy, after adjusting for covariates.²³ In the study by Costagliola et al., TNF- α levels in tears were found to be highly correlated with the severity of retinopathy, which suggested that local TNF- α production has greater clinical significance.²⁹

It was demonstrated that TNF- α and IFN- γ levels were also lower in the vitreous than in the plasma in patients with DR.³⁰

In the present study, it was determined that vitreous TNF- α and IFN- γ levels were significantly higher in the diabetes group than in the control group.

Matrix metalloproteinases (MMPs) are a group of enzymes involved in physiological and pathogenic processes associated with extracellular matrix (ECM) remodeling. They play a central role in organ development and subsequent tissue remodeling as well as in inflammation and injury. Several studies have pointed out that MMPs may be involved in the pathogenesis of PDR and other vitreoretinal diseases, and that MMPs may play a role in the development of postoperative proliferative vitreoretinopathy.³¹

Previous studies have shown that MMP-2 and MMP-9 are present in the vitreous samples of patients with PDR, and that MMP-9 – but not MMP-2 – is elevated in PDR.^{32–34}

It has been demonstrated that among the 7 different MMPs examined, concentrations of only MMP-2 and MMP-9 were significantly higher in vitreous samples from PDR-affected eyes compared to those from nondiabetic eyes.³⁵

Previous studies have shown increased activity of both MMP-2 and MMP-9 in the epiretinal neovascular membrane of patients with PDR.^{36,37}

Patients with DR and animal models have demonstrated elevated MMP-2 and MMP-9 levels in the retina and the vitreous. Recent research has demonstrated that MMPs have a dual role in the development of DR: In the early

period of the disease (pre-neovascularization), MMP-2 and MMP-9 facilitate the apoptosis of retinal capillary cells, possibly via damaging the mitochondria, and in the later period, they help in neovascularization.³¹

In the present study, it was determined that vitreous MMP-2 and MMP-9 levels were significantly higher in the diabetes group than in the control group. In the study, we only used diabetic rat model so additional prospective studies and, possibly, randomized clinical trials may be helpful in confirming the results and hypotheses.

Conclusions

The results of this study suggest that the inflammatory-immune process, adiponectin, and MMPs play an important role in PDR pathogenesis and vessel damage. Moreover, the levels of various inflammatory biomarkers may add clinically relevant, predictive information to existing, well-established risk factors for PDR.

ORCID iDs

Yusuf Özyay  <https://orcid.org/0000-0003-3855-6197>
 Dilay Ozek  <https://orcid.org/0000-0002-2797-4759>
 Filiz Yıldırım  <https://orcid.org/0000-0003-3841-5335>
 Zuhal Yıldırım  <https://orcid.org/0000-0002-2808-7860>

References

- Frank RN. Diabetic retinopathy. *N Engl J Med*. 2004;350:48–58.
- Klein R, Klein BEK, Jensen SC, Moss SE. The relation of socioeconomic factors to the incidence of proliferative diabetic retinopathy and loss of vision. *Ophthalmology*. 1994;101:68–76.
- Chew EY. Epidemiology of diabetic retinopathy. *Hosp Med*. 2003;64:396–399.
- Stehower CD, Gall MA, Twisk JW, Knudsen E, Emeis JJ, Parving HH. Increased urinary albumin excretion, endothelial dysfunction, and chronic low-grade inflammation in type 2 diabetes progressive, interrelated, and independently associated with risk of death. *Diabetes*. 2002;51:1157–1165.
- Cicik E, Tekin H, Akar S, et al. Interleukin-8 nitric oxide and glutathione status in proliferative vitreoretinopathy and proliferative diabetic retinopathy. *Ophthalmic Res*. 2003;35:251–255.
- Kim SJ, Kim S, Park J, et al. Differential expression of vitreous proteins in proliferative diabetic retinopathy. *Curr Eye Res*. 2006;31:231–240.
- Hernandez C, Segura RM, Fonollosa A, Carrasco E, Francisco, Simo R. Interleukin-8, monocyte chemoattractant protein-1 and IL-10 in the vitreous fluid of patients with proliferative diabetic retinopathy. *Diabet Med*. 2005;22:719–722.
- Vinorez SA, Derevjani N, Mahlow J, Berkowitz BA, Wilson CA. Electron microscopic evidence for the mechanism of blood retinal barrier breakdown in diabetic rabbits: Comparison with magnetic resonance imaging. *Pathol Res Pract*. 1998;194:497–505.
- Esposito K, Pantilo A, Di-Palio C. Effects of weight loss and life style changes on vascular inflammatory markers in obese women. *J Am Med Assoc*. 2003;289:1799–1804.
- Pankowska E, Szalek M. Adiponectin as an adipose tissue hormone and its role in the metabolic syndrome and cardiovascular disease. *Endokrynol Diabetol Chor*. 2005;11(3):187–190.
- Aygun C, Senturk D, Hulogu S, Uraz S, Celebi A. Serum levels of hepatoprotective adiponectin in non alcoholic fatty liver disease. *Eur J Gastroenterol Hepatol*. 2006;18(2):175–180.
- Nicholas SB, Mauer M, Basgen JM, Aguiniga E, Chon Y. Effect of angiotensin II on glomerular structure in streptozotocin-induced diabetics rats. *Am J Nephrol*. 2004;24(5):549–556.
- Chang YC, Wu WC. Dyslipidemia and diabetic retinopathy. *Rev Diabet Stud*. 2013;10:121–132.
- Barot M, Gokulgandhi MR, Mitra AK. Mitochondrial dysfunction in retinal disease. *Curr Eye Res*. 2011;36:1069–1077.
- Lian K, Du C, Liu Y, et al. Impaired adiponectin signaling contributes to disturbed catabolism of branched-chain amino acids in diabetic mice. *Diabetes*. 2015;64:49–59.
- Zietz B, Buechler K, Kobuch K, Neumeier M, Scholmenrich A, Schaffer A. Serum levels of adiponectin are associated with diabetic retinopathy and with adiponectin gene mutations in Caucasian patients with diabetes mellitus type 2. *Exp Clin Endocrinol Diabetes*. 2008;116(9):532–536.
- Kawana J, Arora R. The role of adiponectin in obesity, diabetes and cardiovascular disease. *J Cardiometab Syndr*. 2009;4:44–49.
- Shen YY, Peake PW, Charlesworth JA. Review article: Adiponectin: Its role in kidney disease. *Nephrology (Carlton)*. 2008;13:528–534.
- Yilmaz MI, Sonmez A, Acikel C, et al. Adiponectin may play a part in the pathogenesis of diabetic retinopathy. *Eur J Endocrinol*. 2004;151(1):135–140.
- Misu H, Ishikura K, Kurita S, et al. Inverse correlation between serum levels of selenoprotein P and adiponectin in patients with type 2 diabetes. *PLoS One*. 2012;7(4):34952–34959.
- Costagliola C, Daniele A, dell’Omo R, et al. Aqueous humor levels of vascular endothelial growth factor and adiponectin in patients with type 2 diabetes before and after intravitreal bevacizumab injection. *Exp Eye Res*. 2013;110:50–54.
- Mao D, Peng H, Li Q, et al. Aqueous humor and plasma adiponectin levels in proliferative diabetic retinopathy patients. *Curr Eye Research*. 2012;37:803–808.
- Hong SB, Lee JJ, Kim SH, et al. The effects of adiponectin and inflammatory cytokines on diabetic vascular complications in obese and non-obese patients with type 2 diabetes mellitus. *Diabetes Res Clin Pract*. 2016;111:58–65.
- Kato K, Osawa H, Ochi M, et al. Serum total and high molecular weight adiponectin levels are correlated with the severity of diabetic retinopathy and neuropathy. *Clin Endocrinol*. 2008;68(3):442–449.
- Danna M, Peng H, Qiu Hong L, et al. Aqueous humor and plasma adiponectin levels in proliferative diabetic retinopathy patients. *Curr Eye Res*. 2012;37(9):803–808.
- Feigold KR, Grunfeld C. Role of cytokines in inducing hyperlipidemia. *Diabetes*. 1992;41:97–101.
- Wemer S, Grose R. Regulation of wound healing by growth factors and cytokines. *Physiol Rev*. 2003;83:835–870.
- Shen H, Yao P, Lee E, Greenhalgh D, Soulika AM. Interferon-gamma inhibits healing post scald burn injury. *Wound Repair Regen*. 2012;20:580–591.
- Costagliola C, Romano V, De Tollis M, et al. TNF-alpha levels in tears: A novel biomarker to assess the degree of diabetic retinopathy. *Mediators Inflamm*. 2013;2013:629529–629535.
- Koskela UE, Kuusisto SM, Nissinen AE, Savolainen MJ, Liinamaa MJ. High vitreous concentration of IL-6 and IL-8, but not of adhesion molecules in relation to plasma concentrations in proliferative diabetic retinopathy. *Ophthalmic Res*. 2013;49:108–114.
- Kowluru RA, Zhong Q, Santos JM. Matrix metalloproteinases in diabetic retinopathy: Potential role of MMP-9. *Expert Opin Investig Drugs*. 2012;21(6):797–805.
- De La Pazz MA, Itoh Y, Toth CA, Nagesa H. Matrix metalloproteinases and their inhibitors in human vitreous. *Invest Ophthalmol Vis Sci*. 1998;39:1256–1260.
- Kosano H, Okano T, Katsura Y, et al. ProMMP-9 (92 kDa gelatinase) in vitreous fluid of patients with proliferative diabetic retinopathy. *Life Sci*. 1999;64:2307–2315.
- Jin M, Kashiwagi K, Lizuka Y, Tanaka Y, Imai M, Tsukahara S. Matrix metalloproteinases in human diabetic and nondiabetic vitreous. *Retina*. 2001;21:28–33.
- Noda K, Ishida S, Inoue M, et al. Production and activation of matrix metalloproteinase-2 in proliferative diabetic retinopathy. *Invest Ophthalmol Vis Sci*. 2003;44(5):2163–2170.
- Giebel SJ, Menicucci G, McGuire PG, Das A. Matrix metalloproteinases in early diabetic retinopathy and their role in alteration of the blood-retinal barrier. *Lab Invest*. 2005;85:567–607.
- Das A, Mandal M, Chakraborti T, Mandal A, Chakraborti S. Isolation of MMP-2 from MMP-2/TIMP-2 complex: Characterization of the complex and the free enzyme in pulmonary vascular smooth muscle plasma membrane. *Biochim Biophys Acta*. 2004;1674:158–174.

The relation of endocan and galectin-3 with ST-segment resolution in patients with ST-segment elevation myocardial infarction

Yaşar Turan^{A–F}, Vahit Demir^{A–F}

Department of Cardiology, Faculty of Medicine, Bozok University, Yozgat, Turkey

A – research concept and design; B – collection and/or assembly of data; C – data analysis and interpretation; D – writing the article; E – critical revision of the article; F – final approval of the article

Advances in Clinical and Experimental Medicine, ISSN 1899–5276 (print), ISSN 2451–2680 (online)

Adv Clin Exp Med. 2020;29(4):453–458

Address for correspondence

Vahit Demir
E-mail: dr.vdemir@hotmail.com

Funding sources

This study was funded by the Scientific Research Projects of Bozok University in Yozgat, Turkey (2015TF/A203).

Conflict of interest

None declared

Acknowledgements

The authors would like to thank the Scientific Research Projects of Bozok University in Yozgat, Turkey, and paramedics in the study area.

Received on May 20, 2019

Reviewed on February 10, 2020

Accepted on February 10, 2020

Published online on April 28, 2020

Abstract

Background. ST-segment elevation myocardial infarction (STEMI) remains a leading cause of morbidity and mortality around the world. In patients with STEMI undergoing primary percutaneous coronary intervention (PPCI), electrocardiographic measures of ST-segment resolution (STR) may give information about the myocardial perfusion and poor prognosis.

Objectives. To investigate the relation of endocan and galectin-3 levels with STR in STEMI patients.

Material and methods. In this cross-sectional study, 98 consecutive patients undergoing PPCI for STEMI were enrolled. Synergy between percutaneous coronary intervention with taxus and cardiac surgery (SYNTAX) scores were recorded. Electrocardiograms were assessed at baseline and 60 min after PPCI. According to STR levels, patients undergoing PPCI (n = 98) were divided into complete STR group ($\geq 70\%$, n = 53) and incomplete STR group ($< 70\%$, n = 45).

Results. Serum glucose, total cholesterol, low-density lipoprotein cholesterol, SYNTAX score, endocan and galectin-3 levels were significantly higher and ejection fraction was significantly lower in the incomplete STR ($< 70\%$) group ($p < 0.05$ for all). Body mass index (BMI) ($p = 0.046$) and galectin-3 ($p = 0.037$) were independently associated with the SYNTAX score. Endocan ($p = 0.044$) and galectin-3 ($p = 0.017$) were independent predictors of incomplete STR.

Conclusions. In patients with STEMI, the levels of endocan and galectin-3 may be helpful in identifying patients with a higher risk of insufficient myocardial perfusion and worse clinical outcome after PPCI.

Key words: ST-segment elevation myocardial infarction, galectin-3, endocan, ST-segment resolution

Cite as

Turan Y, Demir V. The relation of endocan and galectin-3 with ST-segment resolution in patients with ST-segment elevation myocardial infarction. *Adv Clin Exp Med.* 2020;29(4):453–458. doi: 10.17219/acem/118126

DOI

10.17219/acem/118126

Copyright

© 2020 by Wrocław Medical University
This is an article distributed under the terms of the Creative Commons Attribution 3.0 Unported (CC BY 3.0) (<https://creativecommons.org/licenses/by/3.0/>)

Introduction

ST-segment elevation myocardial infarction (STEMI) is a form of coronary artery disease (CAD) that requires immediate and adequate attention to avoid deadly consequences. It may occur as a result of coronary thrombosis in an epicardial coronary artery, which is damaged by a chronic and inflammatory process known as atherosclerosis.¹ The high mortality rate of STEMI could be offset by providing sufficient blood flow to the damaged myocardium as quick as possible.² Primary percutaneous coronary intervention (PPCI) has become the more preferred treatment option for STEMI, over the past 2 decades, compared to thrombolysis.

Primary percutaneous coronary intervention aims to restore complete blood flow in the infarcted arteries in STEMI patients. However, good blood flow does not always indicate an effective microvasculature perfusion at the myocyte level.³ In other words, good angiographic blood flow is unfortunately not always accompanied by good clinical outcomes. ST-segment deviations may be good indicators of the myocyte physiology, and thus the preferable option is to determine the success of PPCI electrocardiographically (ECG) by measuring ST-segment resolution (STR).⁴ Previous data suggests that a sufficient STR may be predictive for clinical outcomes in STEMI patients undergoing PPCI.^{4,5}

Endocan or endothelial cell-specific molecule-1 is synthesized in the vascular endothelium and gives information about angiogenesis and endothelial cell functions.⁶ Endocan plays a key role in cell adhesion and is reported to be associated with endothelial dysfunction.⁷ In patients with STEMI, higher endocan levels on admission were reported to be associated with a worse cardiovascular outcome and high synergy between percutaneous coronary intervention with taxus and cardiac surgery (SYNTAX) score.⁸

Galectin-3 is a β -galactoside-binding lectin expressed by activated macrophages that regulates inflammation, ventricular remodeling and fibrosis.⁹ In addition, galectin-3 was also reported to have a prognostic value in patients with CAD, possibly related to its role in plaque destabilization.¹⁰ Moreover, an association between higher levels of galectin-3 and a lower ejection fraction, as well as higher mortality, was reported in patients diagnosed with acute coronary syndrome.¹¹

The specific pathophysiology of endocan and galectin-3's association with negative cardiovascular outcomes remains to be elucidated. The assessment of the predictors of incomplete STR in acute phase might be helpful in identifying the patients at high risk for ineffective coronary reperfusion. Aggressive treatment may be planned for these patients to recover sufficient coronary perfusion.

This study evaluated the concentrations of endocan and galectin-3 in patients with STEMI and determined the relation of these parameters with STR.

Methods

Study population

Ninety-eight patients with STEMI with symptoms for less than 12 h who had undergone coronary angiography and PPCI at the Department of Cardiology of Bozok University in Turkey were prospectively enrolled in this cross-sectional study. ST-segment elevation myocardial infarction diagnosis was based on the presence of prolonged chest pain and ST-segment elevation (in all leads other than V2–V3: ≥ 1 mm, in leads V2–V3: ≥ 2 mm in men ≥ 40 years; ≥ 2.5 mm in men < 40 years, or ≥ 1.5 mm in women regardless of age).¹² Exclusion criteria were the following: cardiogenic shock, ventricular tachycardia, ventricular fibrillation, thrombolysis within the last 24 h, oral anticoagulant therapy, indication for emergency coronary artery bypass grafting, active severe bleeding, uncontrolled hypertension, severe renal failure, and left bundle branch block. Routine treatment was initiated according to current STEMI guidelines. Information regarding risk factors, including age, gender, diabetes mellitus, hypertension, family history, and smoking status was obtained. Weights and heights of participants were measured. Body mass index (BMI) was calculated as (weight in kilograms)/(height in meters)². Transthoracic echocardiography was performed for each patient immediately after admission using a commercially available machine (Philips Logic Affiniti 50G machine; Philips, Amsterdam, Netherlands) with a broadband transducer. The study was conducted according to the Declaration of Helsinki. The ethics committee of Bozok University approved the study and informed consent was obtained from all patients.

Electrocardiogram

A standard 12-lead ECG was recorded in all patients at admission (baseline ECG) and 60 min after the completion of revascularization with PPCI. All ECGs were interpreted by an observer who was unaware of other patient data. ST-segment elevation in millivolt was calculated 20 ms after the J point. The sum of ST-segment elevations in leads I, aVL, and V1–V6 for noninferior infarction and in leads II, III, aVF, V5, and V6 for inferior infarction were calculated separately. ST-segment resolution was calculated by reducing the sum of the ST-segment elevation from the baseline ECG to the 60-min ECG and was expressed as a percentage. A decrease in the sum of ST-segment elevation by at least 70% was categorized as complete STR. Patients were divided into 2 groups according to the degree of STR: $< 70\%$ (incomplete resolution) and $\geq 70\%$ (complete resolution).

Coronary angiography

The SYNTAX score is the most commonly used anatomical scoring system worldwide to assess the complexity

of coronary lesions.¹³ The baseline coronary angiograms were evaluated to determine the SYNTAX score by an experienced interventional cardiologist unaware of the patients' clinical or laboratory results. The SYNTAX score was determined for all coronary lesions with >50% diameter stenosis in a vessel >1.5 mm based on SYNTAX score calculator 2.1 (www.syntaxscore.com).

Laboratory measurements

Samples were taken from the antecubital vein when the patients were admitted to the hospital. Serum endocan and galectin-3 levels have been shown to be higher in patients with a myocardial infarction than in the healthy population.^{14,15} Although the entire study group consisted of patients with an acute myocardial infarction, blood samples were collected as soon as possible at the first admission to the hospital, to minimize possible changes resulting from the myocardial infarction. The venous blood samples were drawn from the patients at admission to the hospital. The blood samples used for endocan and galectin-3 measurements were centrifuged and preserved in the freezer (−80°C). Enzyme-linked immunosorbent assay (ELISA) kit (YH-Biosearch, Shanghai, China) was used for measuring serum endocan and galectin-3 levels.

Statistical analysis

Data was analyzed using PASW Statistics for Windows v. 18.0 (SPSS Inc., Chicago, USA). Continuous variables were reported as mean ± standard deviation (SD) or range (min–max). Normally distributed variables were compared with Student's t-test, whereas non-normally distributed variables were compared with Mann–Whitney U test. Categorical variables were reported as percentages and counts and compared using the χ^2 test. Correlation of the SYNTAX score with study parameters was assessed by Pearson or Spearman's correlation analysis as appropriate.

A multivariate logistic regression analysis was used to identify the predictors of incomplete STR. Furthermore, a linear regression analysis was performed to find predictors of SYNTAX score in the study population. Variables that had $p < 0.2$ in the univariate analysis were included in the multivariable models. For all statistical tests, $p < 0.05$ was considered significant.

Results

Patients' demographic characteristics and baseline clinical data are presented in Table 1. According to STR levels,

Table 1. Demographic and clinical data of the participants

Characteristics	Incomplete STR <70% (n = 45)	Complete STR ≥70% (n = 53)	p-value
Age [years]	62.5 ±10.6	59.1 ±10.3	0.097
Gender, n (female/male)	9/36 (25)	8/45 (18)	0.354
BMI [kg/m ²]	28.74 ±4.93	29.15 ±4.62	0.678
Hypertension, n (%)	19/45 (42)	23/53 (47)	0.535
Diabetes mellitus, n (%)	16/45 (35)	15/53 (28)	0.290
Smoking, n (%)	24/45 (53)	25/53 (47)	0.343
Family history, n (%)	17/45 (37)	14/53 (28)	0.228
Systolic blood pressure [mm Hg]	120.6 ±20.2	119.2 ±18.6	0.737
Diastolic blood pressure [mm Hg]	74.3 ±12.6	73.5 ±12.0	0.740
Heart rate [bpm]	75.8 ±12.5	74.1 ±13.1	0.422
Initial troponin level [ng/mL]	13.211 (18–50.000)	9.169 (11–50.000)	0.574
Peak troponin level [ng/mL]	38.843 (19.900–50.000)	33.244 (11.900–50.000)	0.142
Serum glucose [mg/dL]	145 (87–524)	118 (60–557)	0.019
Serum creatinine [mg/dL]	0.91 ±0.21	0.88 ±0.24	0.422
Total cholesterol [mg/dL]	204.9 ±42.2	180.7 ±43.6	0.007
Triglyceride [mg/dL]	141 (73–798)	115 (71–379)	0.063
HDL-C [mg/dL]	37.04 ±7.2	39.68 ±8.1	0.137
LDL-C [mg/dL]	136.3 ±35.2	114.6 ±37.5	0.004
SYNTAX score	16.2 ±7.6	12.04 ±6.6	0.003
Ejection fraction (%)	46.4 ±8.5	49.8 ±6.5	0.039
Endocan [ng/mL]	2.41 ±0.48	1.90 ±0.69	<0.001
Galectin-3 [ng/mL]	5.25 ±1.06	4.46 ±1.00	<0.001

Continuous variables are presented as mean ±SD and range (min–max). Categorical variables are presented as n (%). STR – ST-segment resolution; BMI – body mass index; HDL-C – high-density lipoprotein cholesterol; LDL-C – low-density lipoprotein cholesterol.

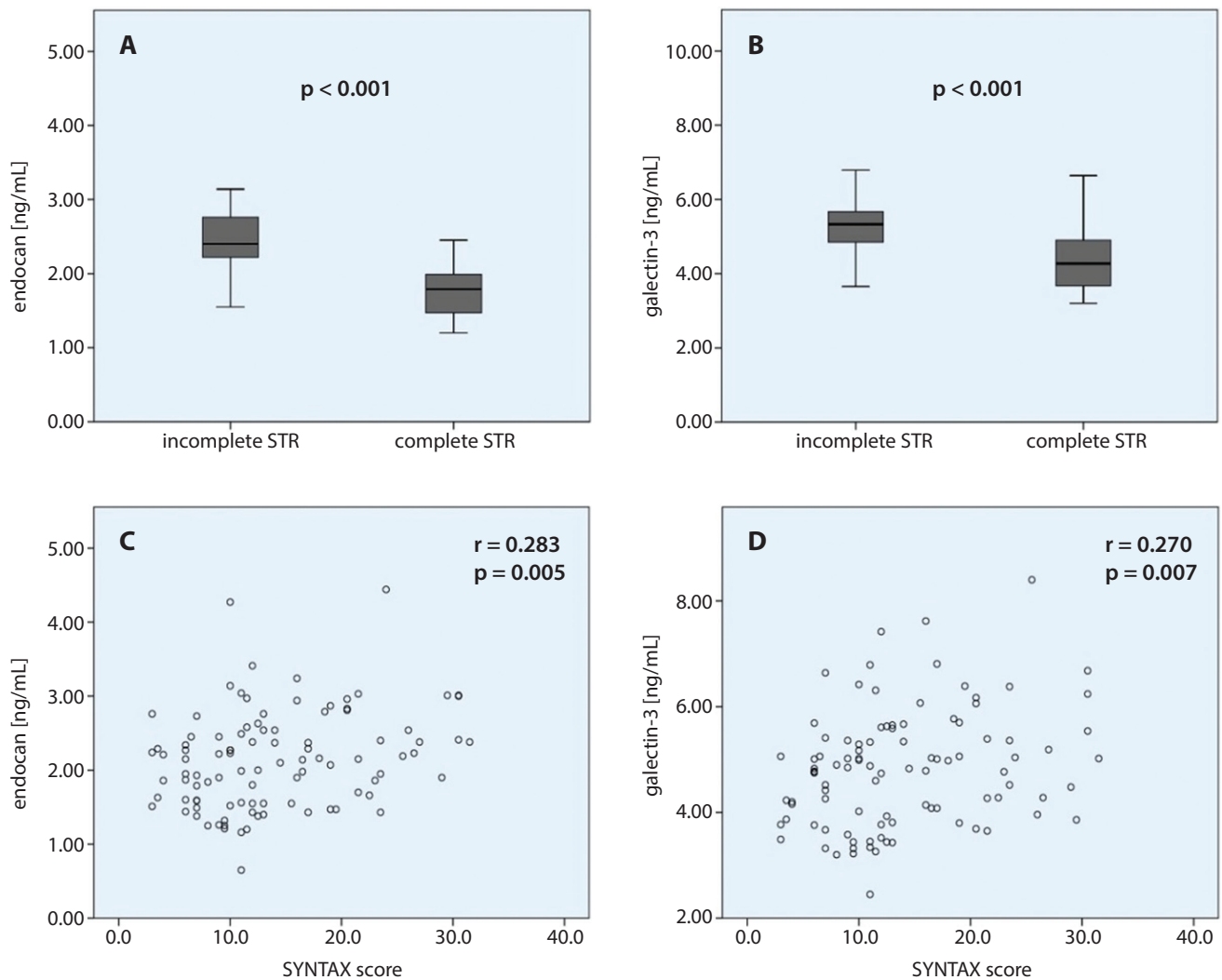


Fig. 1. A – comparison of endocan levels in the incomplete STR and complete STR groups; B – comparison of galectin-3 levels in the incomplete STR and complete STR groups; C – correlation between SYNTAX score and endocan; D – correlation between SYNTAX score and galectin-3

patients undergoing PPCI ($n = 98$) were divided into a complete STR group ($\geq 70\%$, $n = 53$) and an incomplete STR group ($< 70\%$, $n = 45$). Compared with the complete STR group, glucose, total cholesterol, low-density lipoprotein cholesterol (LDL-C), SYNTAX score, endocan and galectin-3 levels were significantly higher and the ejection fraction (EF) was significantly lower in the incomplete STR group ($p < 0.05$ for all) (Fig. 1). The 2 groups were similar regarding age, gender, BMI, and CAD risk factors, such as arterial hypertension, diabetes mellitus, family history, and smoking ($p \geq 0.05$ for all).

Correlation analysis showed that the SYNTAX score was positively correlated with BMI ($r = 0.227$, $p = 0.025$), peak troponin level ($r = 0.310$, $p = 0.03$), endocan ($r = 0.283$, $p = 0.005$), galectin-3 ($r = 0.270$, $p = 0.007$), and negatively correlated with EF ($r = -0.145$, $p = 0.010$) (Table 2) (Fig. 1).

Multivariate linear regression analysis revealed that BMI ($\beta = 0.196$, $p = 0.046$) and galectin-3 ($\beta = 0.212$, $p = 0.037$) were significantly associated with the SYNTAX score in patients with STEMI.

The results of multivariate logistic regression showed that in patients with STEMI, endocan (odds ratio (OR) = 0.406; 95% confidence interval (95% CI) = 0.169–0.976; $p = 0.044$) and galectin-3 (OR = 0.212; 95% CI = 0.084–2.752; $p = 0.017$) were significant predictors of incomplete STR ($< 70\%$) after PPCI.

Discussion

The main finding of the present study was that endocan and galectin-3 were independent predictors of incomplete STR ($< 70\%$) after PPCI in patients with STEMI. Furthermore, along with BMI, galectin-3 was an independent predictor of the SYNTAX score.

Vascular inflammation is an important process in the initiation and progression of atherosclerosis. The inflammatory process affects the endothelial functions starting in the early phases of atherosclerosis. Endothelial dysfunction can be interpreted as the early step of cardiovascular disease development. Endocan and galectin-3 have

Table 2. The correlation between SYNTAX score and clinical/demographic variables in STEMI patients

Variables	SYNTAX score	
	r	p-value
Age	0.188	0.064
BMI	0.227	0.025
Waist circumference	0.134	0.189
Heart rate	0.131	0.197
Systolic blood pressure	-0.182	0.075
Diastolic blood pressure	-0.077	0.454
Initial troponin level	0.093	0.370
Peak troponin level	0.310	0.030
Serum glucose	0.029	0.777
Serum creatinine	0.112	0.279
Total cholesterol	0.091	0.372
Triglyceride	0.109	0.284
HDL-C	-0.130	0.203
LDL-C	0.121	0.235
Ejection fraction	-0.145	0.010
Endocan	0.283	0.005
Galectin-3	0.270	0.007

SYNTAX – synergy between percutaneous coronary intervention with taxus and cardiac surgery; BMI – body mass index; HDL-C – high-density lipoprotein cholesterol; LDL-C – low-density lipoprotein cholesterol.

a significant role in the regulation of the inflammatory process and may be interpreted as markers of endothelial activation. Galectin-3 plays an important role in both acute and chronic phases of inflammation by many immune reactions such as neutrophil activation, migration of the inflammatory cells and apoptosis.¹⁵ Endocan causes endothelial dysfunction by promoting adhesion molecules and migration of leukocytes across the damaged endothelium.¹⁶ Later in this cascade, activated adhesion molecules may also secrete chemokines, which are essential for inflammatory reaction and the ultimate outcome is the acceleration of the atherosclerotic process.¹⁷

There are individual studies suggesting that increased levels of endocan⁸ and galectin-3¹⁸ are associated with CAD. In our study, which examined these biomarkers together, the results were consistent with the previous data. Although BMI, endocan and galectin-3 were significantly correlated with the SYNTAX score, only BMI and galectin-3 were independently associated with the SYNTAX score. Body mass index is reported to be a predictor of the extent and severity of coronary atherosclerosis.¹⁹ However, data about galectin-3 and SYNTAX score is relatively scarcer. Although both endocan and galectin-3 are associated with inflammation, galectin-3 has a complex relation with both acute and chronic phases of inflammation. Winter et al. suggested that galectin-3 was significantly related with premature myocardial infarctions, dyslipidemia and markers of inflammation.²⁰ In this manner,

galectin-3 may affect both plaque formation and plaque destabilization and this mechanism may explain the independent association of galectin-3 with the SYNTAX score. Galectin-3 may be interpreted as a novel biomarker that is independently associated with the complexity of coronary lesions.

The rupture of atherosclerotic plaque is the primary cause of STEMI. Through the complex mechanisms, including inflammation, oxidative stress and endothelial dysfunction, a cascade of events begins, leading to intimal thickening, development of plaque, eventually plaque rupture and clinical consequences.²¹ These mechanisms may also contribute to adverse outcomes during the follow-up of patients with a myocardial infarction.²²

Two types of ischemia induced microvascular damage have been classified based on the pathophysiology.²³ The first type is structural microvascular damage due to myocardial necrosis and the second type is functional microvascular damage in which the microvessels are intact and may be due to increased constriction of microvessels, edema, endothelial dysfunction or obstruction with platelets or neutrophils. Despite angiographically successful PPCI, lack of STR may be a good indicator of compromised tissue perfusion and more extensive myocardial damage.

As a novel finding, our results revealed that endocan and galectin-3 were independent predictors of incomplete STR in patients with STEMI. Besides the role of galectin-3 in inflammation, it also has effects on fibrosis and cardiac remodeling, thus galectin-3 is also reported to be associated with the development and worsening of heart failure.²⁴ The prognostic role of galectin-3 in CAD is a current issue. In this manner, galectin-3 was reported to be an independent predictor of advanced heart failure and 30-day mortality in patients with STEMI.^{11,25} In a prospective study with 1013 CAD patients, Maiolino et al. reported that galectin-3 was a strong independent predictor of cardiovascular mortality.¹⁰ The relation of endocan and worse cardiovascular outcomes after STEMI was reported.^{8,26} Ye et al. demonstrated that serum endocan was associated with coronary slow flow.²⁷ Qui et al. followed up 105 patients with STEMI for 3 months and reported that endocan was a predictor of major adverse cardiac events.²⁸

Although the previous data indicates that both endocan and galectin-3 are valuable markers in predicting worse cardiovascular outcomes, to the best of our knowledge, there is no data concerning the association of STR, endocan and galectin-3 levels in STEMI patients. Considering the functional microvascular damage mechanism one can conclude that microvascular endothelial dysfunction and inflammation may explain the poor myocardial perfusion observed after PPCI. Although the pathophysiologic mechanisms by which higher levels of endocan and galectin-3 increase the risk of incomplete STR after PPCI are not clearly understood, possible hypothesis of our findings could be that elevated levels of endocan and galectin-3, as indicators of endothelial dysfunction and inflammation,

may be surrogate markers of insufficient microvasculature perfusion at the myocyte level, which might contribute to incomplete STR.

The mechanism of the relationship between endocan, galectin-3 and cardiovascular mortality and morbidity is still unclear. Considering the association between endocan, galectin-3, endothelial dysfunction and inflammation, it can be proposed that insufficient coronary reperfusion related with elevated endocan and galectin-3 may be a potential pathophysiological mechanism of the adverse cardiovascular outcomes in patients with STEMI.


Our study had some limitations; it was a cross-sectional study with a limited number of patients and there was no control group. It reflects a single center experience and in our laboratory, there was an upper limit for troponin results. The levels of endocan and galectin-3 were evaluated only at admission and they were not evaluated after the acute phase of the myocardial infarction. ST-segment resolution may be helpful, but it cannot be accepted as a definitive parameter for the microvascular impairment like the invasive hemodynamic procedures. Longitudinal studies may be designed to determine the long-term influence of these parameters on cardiovascular outcome.

Conclusions

To our knowledge, ours is the first report describing endocan and independent association of galectin-3 with incomplete STR in patients with STEMI. Based on the relation of endocan and galectin-3 with endothelial dysfunction, oxidative stress and inflammation, it can be proposed that insufficient coronary reperfusion related with elevated endocan and galectin-3 may be a potential pathophysiological mechanism of the adverse cardiovascular outcomes in patients with STEMI. The levels of endocan and galectin-3 may be helpful in identifying patients with a higher risk of insufficient myocardial perfusions and worse clinical outcome.

ORCID iDs

Yaşar Turan  <https://orcid.org/0000-0002-2796-899X>

Vahit Demir  <https://orcid.org/0000-0001-8349-6651>

References

- Davies MJ. The pathophysiology of acute coronary syndromes. *Heart*. 2000;83:361–366.
- Carville S, Harker M, Henderson R, Gray H. Acute management of myocardial infarction with ST-segment elevation: Summary of NICE guidance. *BMJ*. 2013;347:f4006.
- Ito H, Okamura A, Iwakura K, et al. Myocardial perfusion patterns related to thrombolysis in myocardial infarction perfusion grades after coronary angioplasty in patients with acute anterior wall myocardial infarction. *Circulation*. 1996;93:1993–1999.
- Unikas R, Budrys P. Association between clinical parameters and ST-segment resolution after primary percutaneous coronary intervention in patients with acute ST-segment elevation myocardial infarction. *Medicina (Kaunas)*. 2016;52:156–162.
- McLaughlin MG, Stone GW, Aymong E, et al. Prognostic utility of comparative methods for assessment of ST-segment resolution after primary angioplasty for acute myocardial infarction: The Controlled Abciximab and Device Investigation to Lower Late Angioplasty Complications (CADILLAC) trial. *J Am Coll Cardiol*. 2004;44:1215–1223.
- Ozaki K, Toshikuni N, George J, et al. Serum endocan as a novel prognostic biomarker in patients with hepatocellular carcinoma. *J Cancer*. 2014;5:221–230.
- Balta S, Mikhailidis DP, Demirkol S, et al. Endocan – a novel inflammatory indicator in newly diagnosed patients with hypertension: A pilot study. *Angiology*. 2014;65:773–777.
- Kundi H, Balun A, Cicekcioglu H, et al. Admission endocan level may be a useful predictor for in-hospital mortality and coronary severity index in patients with st-segment elevation myocardial infarction. *Angiology*. 2017;68:46–51.
- Martinez-Martinez E, Calvier L, Fernandez-Celis A, et al. Galectin-3 blockade inhibits cardiac inflammation and fibrosis in experimental hyperaldosteronism and hypertension. *Hypertension*. 2015;66:767–775.
- Maiolino G, Rossitto G, Pedon L, et al. Galectin-3 predicts long-term cardiovascular death in high-risk patients with coronary artery disease. *Arterioscler Thromb Vasc Biol*. 2015;35:725–732.
- George M, Shanmugam E, Srivatsan V, et al. Value of pentraxin-3 and galectin-3 in acute coronary syndrome: A short-term prospective cohort study. *Ther Adv Cardiovasc Dis*. 2015;9:275–284.
- Thygesen K, Alpert JS, Jaffe AS, et al. Fourth universal definition of myocardial infarction (2018). *J Am Coll Cardiol*. 2018;72:2231–2264.
- Ong AT, Serruys PW, Mohr FW, et al. The SYNergy between percutaneous coronary intervention with TAXus and cardiac surgery (SYNTAX) study: Design, rationale, and run-in phase. *Am Heart J*. 2006;151:1194–1204.
- Qiu CR, Fu Q, Sui J, et al. Serum endothelial cell-specific molecule 1 (Endocan) levels in patients with acute myocardial infarction and its clinical significance. *Angiology*. 2017;68:354–359.
- Gucuk Ipek E, Akin Suljevic S, Kafes H, et al. Evaluation of galectin-3 levels in acute coronary syndrome. *Ann Cardiol Angeiol (Paris)*. 2016;65:26–30.
- Lee W, Ku SK, Kim SW, Bae JS. Endocan elicits severe vascular inflammatory responses in vitro and in vivo. *J Cell Physiol*. 2014;229:620–630.
- Jaipersad AS, Lip GY, Silverman S, Shantsila E. The role of monocytes in angiogenesis and atherosclerosis. *J Am Coll Cardiol*. 2014;63:1–11.
- Ozturk D, Celik O, Satilmis S, et al. Association between serum galectin-3 levels and coronary atherosclerosis and plaque burden/structure in patients with type 2 diabetes mellitus. *Coron Artery Dis*. 2015;26:396–401.
- Zhang B, Pei C, Zhang Y, Sun Y, Meng S. High resting heart rate and high BMI predicted severe coronary atherosclerosis burden in patients with stable angina pectoris by SYNTAX Score. *Angiology*. 2018;69:380–386.
- Winter MP, Wiesbauer F, Alimohammadi A, et al. Soluble galectin-3 is associated with premature myocardial infarction. *Eur J Clin Invest*. 2016;46:386–391.
- Daiber A, Xia N, Steven S, et al. New therapeutic implications of endothelial nitric oxide synthase (eNOS) function/dysfunction in cardiovascular disease. *Int J Mol Sci*. 2019;20:187.
- Zeller M, Korandji C, Guillard JC, et al. Impact of asymmetric dimethylarginine on mortality after acute myocardial infarction. *Arterioscler Thromb Vasc Biol*. 2008;28:954–960.
- Galiuto L. Optimal therapeutic strategies in the setting of post-infarct no reflow: The need for a pathogenetic classification. *Heart*. 2004;90:123–125.
- Salvagno GL, Pavan C. Prognostic biomarkers in acute coronary syndrome. *Ann Transl Med*. 2016;4:258.
- Tsai TH, Sung PH, Chang LT, et al. Value and level of galectin-3 in acute myocardial infarction patients undergoing primary percutaneous coronary intervention. *J Atheroscler Thromb*. 2012;19:1073–1082.
- Ziaee M, Mashayekhi S, Ghaffari S, Mahmoudi J, Sarbakhsh P, Garjani A. Predictive value of endocan based on TIMI risk score on major adverse cardiovascular events after acute coronary syndrome. *Angiology*. 2018;3319718815241.
- Ye MF, Zhao ZW, Luo YK, Dong XF, Yan YM. Elevated endocan concentration is associated with coronary slow flow. *Scand J Clin Lab Invest*. 2016;76:345–348.
- Qiu C, Sui J, Zhang Q, Wei P, Wang P, Fu Q. Relationship of endothelial cell-specific molecule 1 level in stress hyperglycemia patients with acute ST-segment elevation myocardial infarction: A pilot study. *Angiology*. 2016;67:829–834.

Comparative biomechanical testing of customized three-dimensional printing acetabular-wing plates for complex acetabular fractures

Xiangyuan Wen^{1,B,D–F}, Hai Huang^{1,B,F}, Canbin Wang^{1,C,F}, Jianghui Dong^{2,D–F},
Xuezhi Lin^{1,C,F}, Fuming Huang^{1,C,F}, Hua Wang^{1,A,F}, Liping Wang^{2,D–F}, Shicai Fan^{1,A,F}

¹ The Third Affiliated Hospital, Southern Medical University, Guangzhou, China

² UniSA Clinical & Health Sciences, UniSA Cancer Research Institute, University of South Australia, Adelaide, Australia

A – research concept and design; B – collection and/or assembly of data; C – data analysis and interpretation;
D – writing the article; E – critical revision of the article; F – final approval of the article

Advances in Clinical and Experimental Medicine, ISSN 1899–5276 (print), ISSN 2451–2680 (online)

Adv Clin Exp Med. 2020;29(4):459–468

Address for correspondence

Shicai Fan
E-mail: fanscyi@sohu.com

Funding sources

This study was funded by the Special Program of Guangdong Frontier and Key Technological Innovation (No. 2015B010125006), the National Natural Science Foundation of China (No. 81772428) and the Australian National Health and Medical Research Council (NHMRC) Fellowship (No. 1158402).

Conflict of interest

None declared

Received on September 24, 2019

Reviewed on October 15, 2019

Accepted on January 21, 2020

Published online on April 29, 2020

Abstract

Background. Three-dimensional (3D) printing of an acetabular wing-plate is a new minimally invasive surgical technique for complex acetabular fractures.

Objectives. To investigate the biomechanical stability of 3D printing acetabular wing-plates. The results were compared with 2 conventional fixation systems.

Material and methods. Eighteen fresh frozen cadaveric pelvises with both column fractures were randomly divided to 3 groups: A – ilioiastic plates fixation system; B – 3D printing plates; C – 2 parallel reconstruction plates fixation system. These constructions were loaded onto a biomechanical testing machine. Longitudinal displacement and stiffness values of the constructs were measured to estimate their stability.

Results. When the load force reached 700 N, Group A was superior to Group B in the longitudinal displacement of point 1 ($p > 0.05$). The longitudinal displacement of point 2 showed no significant differences among Groups A, B and C, and the displacement of the fracture line over point 3 showed no significant differences between Groups A and B ($p > 0.05$). The axial stiffness of Groups A, B and C were 122.4800 ± 8.8480 N/mm, 168.4830 ± 14.8091 N/mm and 83.1300 ± 3.8091 N/mm, respectively. Group B was significantly stiffer than A and C ($p < 0.05$). Loads at failure of internal fixation were 1378.83 ± 34.383 N, 1516.83 ± 30.896 N and 1351.00 ± 26.046 N for Groups A, B and C, respectively. Group B was significantly superior to Groups A and C ($p > 0.05$).

Conclusions. Customized 3D printing acetabular-wing plates provide stability for acetabular fractures compared to intraspecific buttressing fixation.

Key words: internal fixation, three-dimensional printing, acetabular fracture, biomechanical tests

Cite as

Wen X, Huang H, Wang C, et al. Comparative biomechanical testing of customized three-dimensional printing acetabular-wing plates for complex acetabular fractures. *Adv Clin Exp Med.* 2020;29(4):459–468. doi:10.17219/acem/116749

DOI

10.17219/acem/116749

Copyright

© 2020 by Wrocław Medical University

This is an article distributed under the terms of the Creative Commons Attribution 3.0 Unported (CC BY 3.0) (<https://creativecommons.org/licenses/by/3.0/>)

Introduction

Acetabular fractures are complex injuries and associated with significant morbidity and mortality.^{1,2} These injuries frequently occur in high-energy traumas and can lead to posttraumatic arthritis or disabilities.³ Due to the prolongation of human life span, coupled with the rise in the occurrence of osteoporosis, the incidence of acetabular fractures has distinctly increased.⁴ Culemann et al. found that the force required to displace an osteoporotic cadaveric fracture is significantly small.⁵ Therefore, it is necessary to find an effective treatment method for complex fractures of the acetabulum.

The medial boundary of the acetabulum is formed by the quadrilateral plate, and as a relatively thin bony structure, this area is more prone to fractures than the weight bearing areas. Fractures also occur under lower forces⁶ and appear as both-column, anterior column, and posterior hemi-transverse T-shaped fractures or posterior column and combined transverse fractures, often accompanied by quadrilateral plate fractures with medial displacement.⁷

In a previous study, Letournel confirmed that conservative fracture treatment was not satisfactory.⁸ Open reduction and internal fixation method are currently considered standard treatment for displaced acetabular fractures involving weight-bearing domains and fractures of the intra-articular fragment. Inadequate reduction and stabilization of quadrilateral plate fractures leads to incongruous joints and posttraumatic arthritis.⁹ The classic fixation technique is the ilioinguinal approach,¹⁰ which involves placing reconstruction plates at the pelvic margin and extending the screw distally to the posterior column. Although the current treatment protocol using multiple elongated or ace-shaped reconstruction plates and lag screws for the stabilization of the pelvic ring and hip joint has been shown to effectively reduce mortality, these fixators cause a high frequency of new morbidities.¹¹ Recently, studies have confirmed that early postoperative rehabilitation training is beneficial to joint function recovery; therefore,

a rigid fixation implant for acetabular fossa and pelvic rings that allows early mobilization is important for these injuries.¹² In a biomechanical study, Mehin et al. showed that locking plates may improve the management of acetabular fractures by eliminating the need for an interfragmentary lag screw, and they may be helpful in revision hip arthroplasty in patients with pelvic discontinuity.¹³ However, their study only loaded 250 N as an axial force, which did not meet the requirement of physiological weight-bearing conditions. These fixators were associated with multiple complications including pin site infection and fixator loosening. Besides the conventional reconstruction, bone plate mostly depends on the structure of the acetabulum and needs to be pre-contoured to bone surface before fixation.¹⁴ Utilizing reconstruction plates and more screws to maintain reduction during surgery is a potentially serious post-operative complication that may lead to post-traumatic osteoarthritis. In recent years, 3D printing technology has been widely used in orthopedics for internal implant manufacturing.^{14–16} It allows an individual plate to be designed for particular patients according to the fracture line and the surface of the acetabulum. A wing-shaped plate for both-column acetabulum fractures was designed (Fig. 1), and the pre-contoured shape, extended fix range, the oval screw hole and the angular stability were used to design the wing-shaped plate. However, prior to widespread adoption of these new concepts, a critical step in the systematic investigation of any new fixation strategy involves comparative biomechanical efficacy in a cadaveric model.

The aim of this study was to gather the evidence regarding the biomechanical stability of 3D printing acetabular-wing plates relative to 2 conventional fixation systems. Firstly, an effective method to produce personalized acetabular fracture plates was developed. Then, the displacement of the fracture line was measured and analyzed by applying stress on broken cadaver pelvises after internal fixation. Lastly, the stability of the 3D printed bone plate was evaluated by comparing the displacement of fracture line and stiffness with that of the traditional internal fixations.

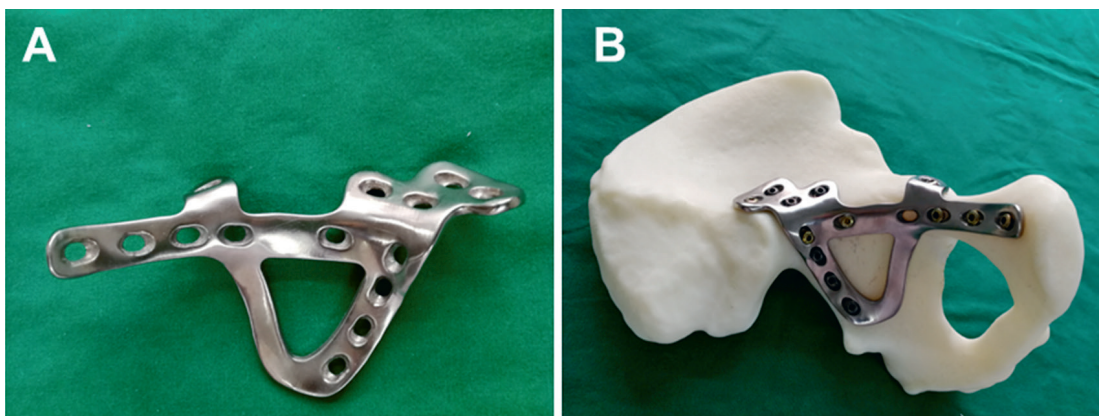


Fig. 1. 3D customized wing plates

A – 3D customized wing plates for use in complex acetabular fractures; B – preoperative design of 3D customized wing plates.

Material and methods

Specimen preparation

Nine male fresh frozen cadaveric pelvises were provided by the Department of Anatomy of the Southern Medical University in Guangzhou, China. Soft tissue and ligaments were removed from the surface, and the joint of the sacroiliac and the pubic bone were sawed. Eighteen hemipelvis samples were obtained after trimming. All donors or their next of kin provided written informed consent for the study. All specimens were visually and radiographically examined for evidence of abnormalities, and the bone mineral density was quantified using dual energy X-ray osteodensitometers prior to dissection. Each specimen revealed no signs of arthritis, malignancy or osteoporosis. We designed the proximal 1/3 of both femurs according to 3D specimen images obtained by using Mimics v. 19.0 (Materialise Software, Leuven, Belgium). Each hemipelvic area had an artificial proximal 1/3 of femurs to match. Each artificial femur was connected with the biomechanical testing machine.

We randomly divided the 18 specimens into 3 fixation groups (Fig. 2). In Group A, iliosciatic plating and 2 lag screws were used. In Group B, we used customized 3D printing acetabular-wing plates and 2 lag screws. In Group C, we used parallel reconstruction plates and 2 lag screws. The fixation experiments were performed in accordance with the relevant regulations and approved by the medical ethics committee of the Third Affiliated Hospital of Southern Medical University in Guangzhou, China.

Fracture models

A both-column acetabulum fracture was created with a saw according to the Judet–Letournel classification^{8,17} (Fig. 3). The 1st osteotomy line originated from the iliac crest through the quadrilateral surface to the brim of the incisura acetabula (points a–b). The 2nd osteotomy line ran from the ischial spine to the center of the quadrilateral surface (points c–d). The 3rd osteotomy line ran from the linear arcuate to the vertex of the great sciatic notch (points e–f). A fracture of the pubic bone was also created (point g).

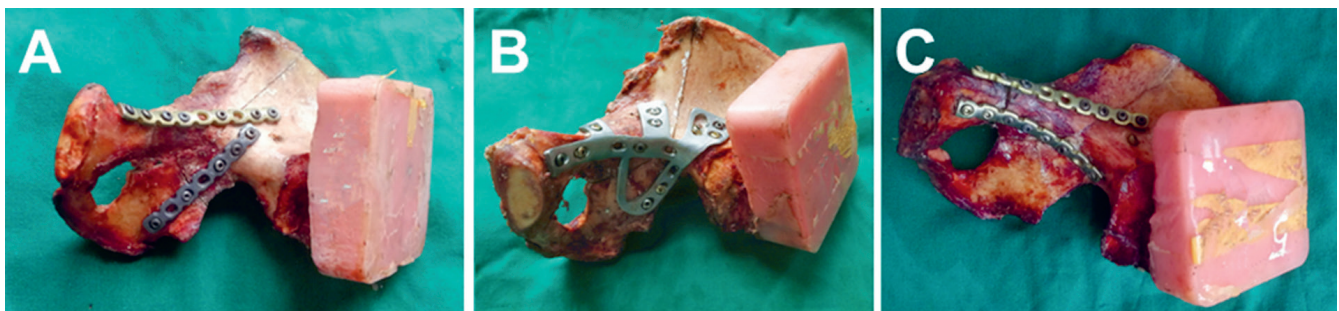


Fig. 2. Groups of different fixation constructs

A – Group A: iliosciatic plates and 2 screws; B – Group B: 3D printing customized bone plates and 2 lag screws; C – Group C: 2 parallel reconstruction plates and 2 lag screws.

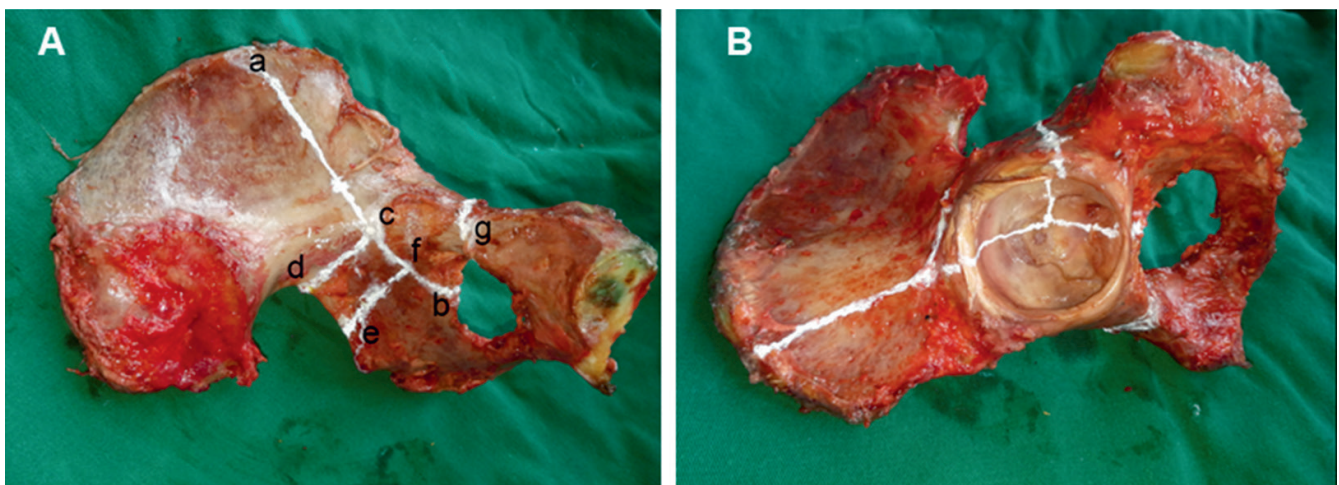


Fig. 3. Complex both-column acetabular fracture

A – the 1st osteotomy line originated from the iliac crest through the quadrilateral surface to the brim of the incisura acetabular (points a–b). The 2nd osteotomy line ran from the ischial spine to the center of the quadrilateral surface (points c–d). The 3rd osteotomy line ran from the linear arcuate to the vertex of the great sciatic notch (points e–f). A fracture of the pubic bone was also created (point g); B – the dorsal view of specimen with fracture line.

Design of the customized 3D-printing acetabular-wing plate

3D models of the specimens

A computed tomography (CT) was performed for each intact specimen, and data was obtained in the Digital Imaging and Communications in Medicine (DICOM) format. The CT data of the pelvis specimens was imported into the Materialise's interactive medical image control system (Mimics v. 19.0) and a 3D model was calculated according to the CT data. All data was stored as binary stereolithography (STL) data (Fig. 4).

Original shape of the customized bone plate

Binary STL data was imported into Geomagic® Studio v. 12.0 (3D Systems, Rock Hill, USA) and the location of the pelvic fracture line was used as a reference. The graphics of the bone plate was obtained according to the contralateral acetabulum surface morphology, the location and shape of the acetabulum fracture, and the placement of the bone plate area. The bone plate thickness (3 mm) and fitted the curved surface of the customized 3D bone plate model were set. The pelvic and bone plate models were derived in the STEP format (Fig. 4).

Fabrication of screw holes of the customized bone plate

Screw holes were added according to the shape and specifications of the screws. M3.5 compressive screws and

M6.5 pressure screws (generally used for conventional bone plates) were employed (Fig. 4).

Manufacturing the bone plate

Customized 3D printing acetabular-wing plates were manufactured using metal additive manufacturing technology. Processed data was imported into a self-developed DiMetal-100 metal 3D printing device. The final step involved heat and surface treatment. Samples were heated to 820°C for 3 h, incubated for 2 h, and cooled to 450°C in a furnace. The furnace was then opened and the samples were air-cooled. Surface treatment procedures included roll casting, oil cleaning, acid pickling, polishing, anodizing, cleaning, and disinfection.¹⁸ The properties of the customized bone plate were then evaluated (Fig. 4).

Biomechanical testing

Specimens were fixed in the stance position as previously described by Gillispie et al.¹⁹ According to the single inverted foot standing method, specimens were fixed using denture-based polymers. At the base of the biomechanical experimental machine (BOSE Corporation, Eden Prairie, USA), specimens were embedded and the upper end of the test machine was connected to the broken ends of the femoral shaft for biomechanical testing. Points 1, 2 and 3 on each specimen were marked as the displacement measurement points along the fracture line as shown in Fig. 5A. The 100 N preload was applied on 3 occasions and a 20 N/s rate was continually loaded to 700 N. Longitudinal displacement of the fracture was measured using

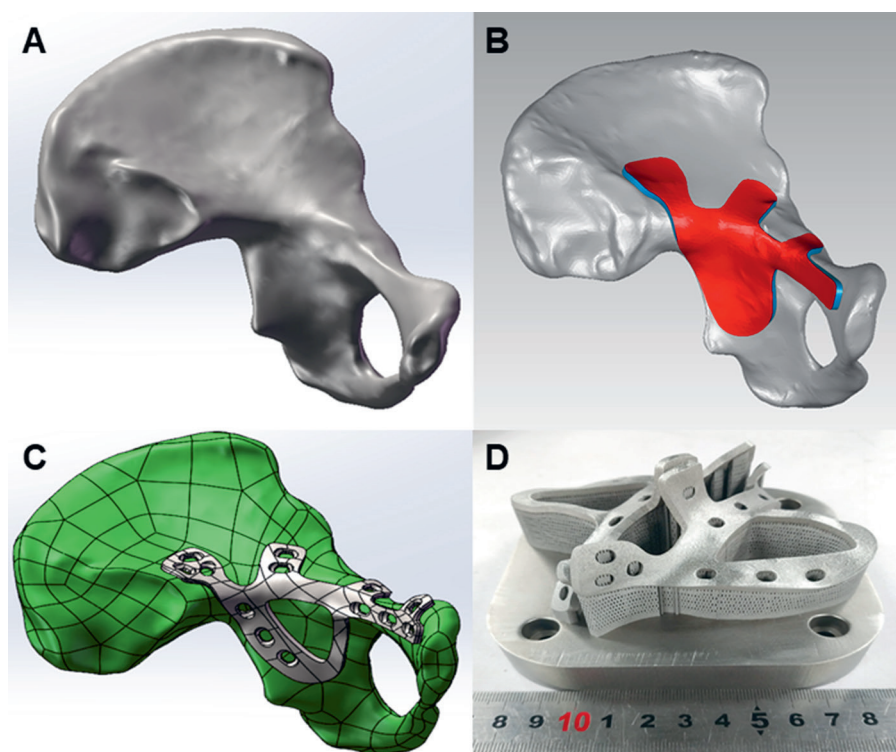


Fig. 4. Design process of 3D customized wing plates

A – 3D model of the specimens;
B – original shape of the customized bone plate;
C – fabrication of screw holes of the customized bone plate;
D – manufacturing the bone plate.

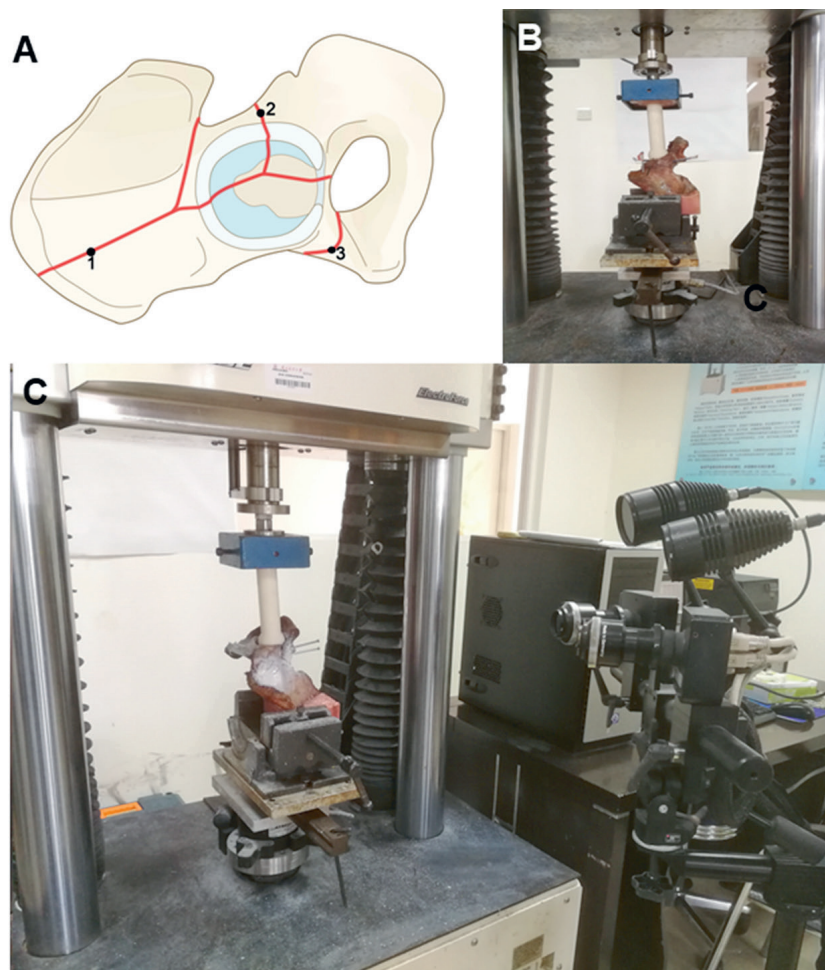


Fig. 5. The load cell and jig used to position the pelvis and femur

A – positions of the displacement at points 1–3 around the pelvis; B–C – biomechanical testing. Specimens were fixed in the stance position, fixed using denture-based polymers. Specimens were embedded and the upper end of the test machine was connected to the broken ends of the femoral shaft for biomechanical testing.

of internal fixation. No plates were broken and no screws were pulled out or broken at a force ≤ 700 N. As shown in Table 1 and Fig. 6, the significant difference of fracture displacement was presented when the loading force exceeded 500 N at point 1 region as well as point 3. However, no statistical significant displacement was displayed in each group at point 2 region. When the loading force reached 700 N (the average human body weight), the significant differences were shown between Groups B and A, B and C in the fracture line longitudinal displacement measurement of point 1 region. No significant differences between Group A and C occurred. The performance of Group B was superior to Groups A and C. The results of the fracture line longitudinal displacement measurement point 2 showed no significant differences among Groups A, B and C. And the results

a high-precision grating displacement sensor. Specimens were repeatedly loaded on 6 occasions and mean values were obtained. Stiffness was defined as the slope of the force vs the displacement curve.

of the fracture line longitudinal displacement measurement point 3 showed no significant differences between Groups A and B ($p > 0.05$), both of which were superior to the Group C ($p < 0.05$) (Fig. 7).

Results

Longitudinal displacement

The longitudinal displacement of each group of fractures under the same load was used to evaluate the stability

Axial stiffness

The axial stiffness of the internal fixation is reflected by its ability to resist deformation and maintain joint stability under axial loads. Using the formula: $S = F/\Delta L$ (S – axial stiffness, F – load, ΔL – deformation displacement) the axial stiffness of Groups A, B and C were 122.4800 ± 8.8480 N/mm,

Table 1. Mean displacement of different fixations in each point when under pressure

Loading force [N]		100	200	300	400	500	600	700	
Displacement [mm]	point 1	Group A	0.10 \pm 0.03	0.21 \pm 0.02	0.32 \pm 0.07	0.45 \pm 0.11	0.66 \pm 0.09	0.87 \pm 0.09	1.09 \pm 0.15
		Group B	0.10 \pm 0.03	0.20 \pm 0.06	0.30 \pm 0.10	0.38 \pm 0.10	0.44 \pm 0.10	0.50 \pm 0.11	0.62 \pm 0.08
		Group C	0.11 \pm 0.03	0.21 \pm 0.03	0.37 \pm 0.07	0.54 \pm 0.13	0.77 \pm 0.12	0.96 \pm 0.18	1.27 \pm 0.10
	point 2	Group A	0.12 \pm 0.03	0.28 \pm 0.05	0.44 \pm 0.08	0.65 \pm 0.12	0.83 \pm 0.10	1.10 \pm 0.14	1.44 \pm 0.09
		Group B	0.10 \pm 0.02	0.21 \pm 0.02	0.35 \pm 0.05	0.56 \pm 0.05	0.75 \pm 0.03	1.01 \pm 0.06	1.24 \pm 0.09
		Group C	0.15 \pm 0.02	0.31 \pm 0.04	0.54 \pm 0.07	0.73 \pm 0.09	0.99 \pm 0.12	1.31 \pm 0.07	1.62 \pm 0.06
	point 3	Group A	0.11 \pm 0.02	0.20 \pm 0.03	0.33 \pm 0.04	0.56 \pm 0.04	0.67 \pm 0.05	0.79 \pm 0.04	0.93 \pm 0.03
		Group B	0.09 \pm 0.02	0.18 \pm 0.03	0.31 \pm 0.03	0.49 \pm 0.05	0.63 \pm 0.06	0.74 \pm 0.07	0.87 \pm 0.05
		Group C	0.11 \pm 0.03	0.22 \pm 0.03	0.41 \pm 0.02	0.64 \pm 0.09	0.80 \pm 0.11	1.02 \pm 0.13	1.35 \pm 0.07

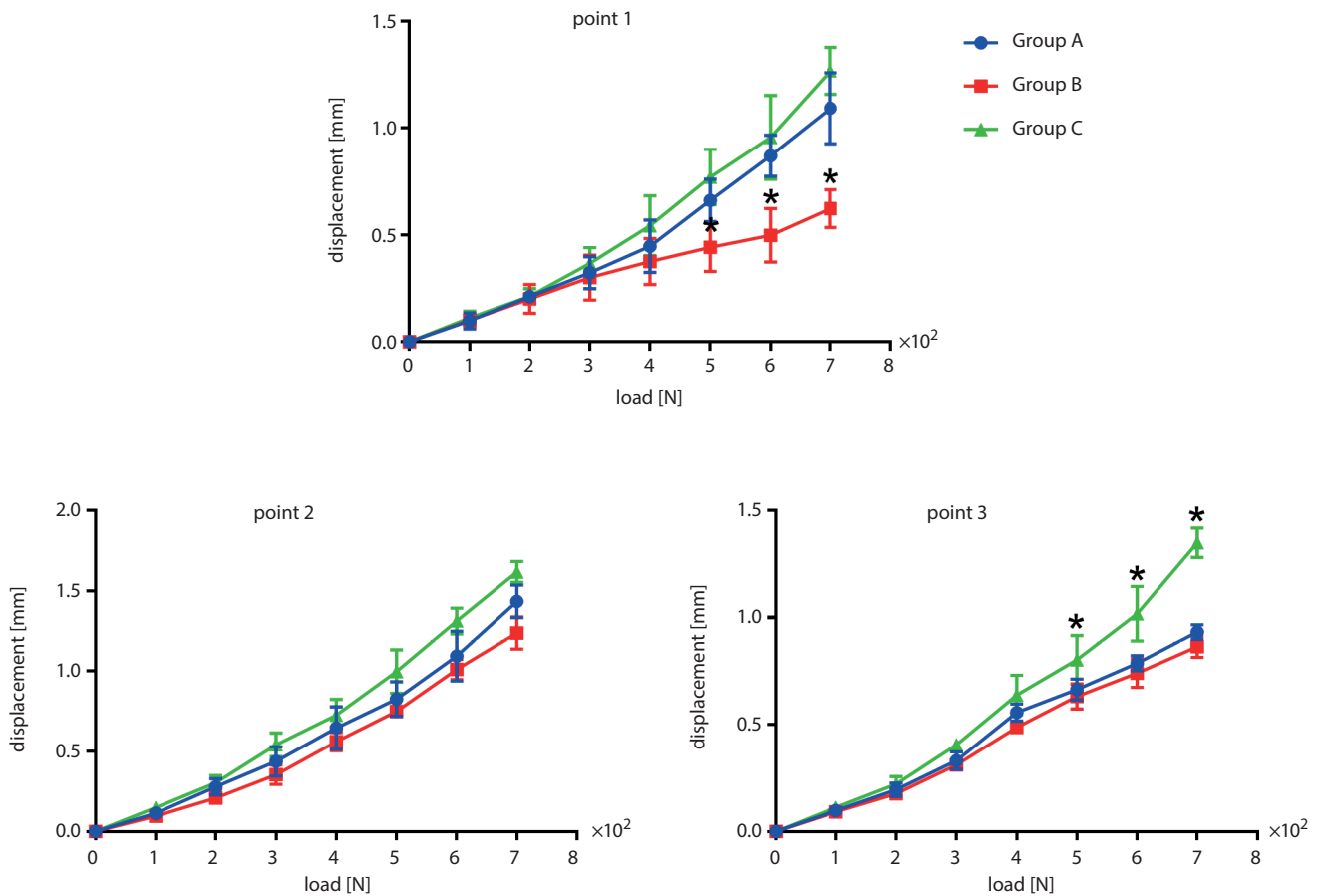


Fig. 6. Relationship between the displacement of the fracture line and the load force of the 3 points

* p < 0.05.

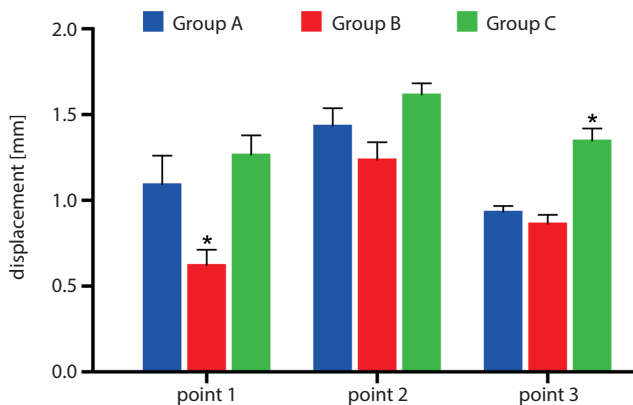


Fig. 7. Mean displacement for 3 groups in each point when the load force reached 700 N

* p < 0.05.

168.4830 ± 14.8091 N/mm and 83.1300 ± 3.8091 N/mm, respectively (Table 2). Group B was significantly stiffer than Groups A and C (p < 0.05) (Table 3).

Loads at failure of internal fixation

The dislocation of the articular surface fracture >3 mm was recognized as the internal fixation failure standard.^{7,20}

Table 2. Mean stiffness values and standard deviations for different fixation modalities at a load of 700 N

Groups	n	Stiffness [N/mm]	
		mean ±SD	95% CI
Group A	6	122.4800 ± 8.8480	113.1946, 131.7654
Group B	6	468.4830 ± 14.8091	152.8771, 183.9595
Group C	6	83.1300 ± 3.8091	79.1326, 87.1274

n – number of specimens; SD – standard deviation; 95% CI – 95% confidence interval; Group A – ilioaciac plates; Group B – 3D printing acetabular-wing plates; Group C – 2 parallel reconstruction plates.

The stability of the internal fixation is reflected by the load at which failure occurs. These values were 1378.83 ± 34.383 N, 1516.83 ± 30.896 N and 1351.00 ± 26.046 N for Groups A, B and C, respectively (Table 4). Group B was significantly superior to Groups A and C (p < 0.05). No significant differences were evident between Groups A and C (p > 0.05) (Table 5).

Discussion

Acetabular fractures are one of the most difficult fractures to treat due to their complex anatomical structures, morphological differences among individuals and

Table 3. Comparisons of axial stiffness. The Group B constructs were stiffer than the Group A and Group C constructs ($p < 0.05$, $\alpha = 0.05$). Multiple comparisons

Dependent variable: Axial stiffness							
Group		mean difference	SE	p-value	95% CI		
					lower bound	upper bound	
LSD	Group A	Group B	-45.93833	5.88883	0.000	-58.4901	-33.3866
		Group C	39.35000	5.88883	0.000	26.7983	51.9017
	Group B	Group A	45.93833	5.88883	0.000	33.3866	58.4901
		Group C	85.28833	5.88883	0.000	72.7366	97.8401
	Group C	Group A	-39.35000	5.88883	0.000	-51.9017	-26.7983
		Group B	-85.28833	5.88883	0.000	-97.8401	-72.7366
Dunnett T3	Group A	Group B	-45.93833	7.04268	0.000	-66.6754	-25.2013
		Group C	39.35000	3.93268	0.000	27.2371	51.4629
	Group B	Group A	45.93833	7.04268	0.000	25.2013	66.6754
		Group C	85.28833	6.24258	0.000	64.9809	105.5957
	Group C	Group A	-39.35000	3.93268	0.000	-51.4629	-27.2371
		Group B	-85.28833	6.24258	0.000	-105.5957	-64.989

LSD – least significant difference; SE – standard error; 95% CI – 95% confidence interval. The mean difference is significant at the 0.05 level.

Table 4. Failure test in cadaveric specimens used to compare 3 kinds of plate fixations: Compressive force

Groups	n	Compressive force [N]	
		mean ±SD	95% CI
Group A	6	1378.83 ±34.383	1342.75, 1414.92
Group B	6	1516.83 ±30.896	1484.41, 1549.26
Group C	6	1351.00 ±26.046	1323.67, 1378.33

SD – standard deviation; 95% CI – 95% confidence interval.

limitations of surgical approaches. In addition, it is difficult to fix them because of the thinness of quadrilateral plate and bearing area. Pelvic malunion and joint incoordination

are associated with the long-term risk of osteoarthritis, and the greatest challenge in the management of acetabular fractures is to obtain adequate fracture reduction.^{21–23} The ultimate goal of complex acetabular fractures therapy is to reduce complications, improve quality of life, and maximize recovery and post-recovery functional status. It has remained a great challenge to find an effective way to fix a quadrilateral plate for complex acetabular fractures. As is known to all, it is difficult to achieve anatomical contouring intraoperatively due to the complexity of the acetabulum, so surgeons need to pre-contour the conventional reconstruction plate when using it during the operations.¹⁴ However, the repeated bending of the plate will cause

Table 5. Comparisons of compressive force for different fixations. Multiple comparisons

Dependent variable: Compressive force							
Group		mean difference	SE	p-value	95% CI		
					lower bound	upper bound	
LSD	Group A	Group B	-138.000*	17.686	0.000	-175.70	-100.30
		Group C	27.833	17.686	0.136	-9.86	65.53
	Group B	Group A	138.000*	17.686	0.000	100.30	175.70
		Group C	165.833*	17.686	0.000	128.14	203.53
	Group C	Group A	-27.833	17.686	0.136	-65.53	9.86
		Group B	-165.833*	17.686	0.000	-203.53	-128.14
Dunnett T3	Group A	Group B	-138.000*	18.871	0.000	-191.49	-84.51
		Group C	27.833	17.609	0.358	-22.63	78.30
	Group B	Group A	138.000*	18.871	0.000	84.51	191.49
		Group C	165.833*	16.497	0.000	118.93	212.74
	Group C	Group A	-27.833	17.609	0.358	-78.30	22.63
		Group B	-165.833*	16.497	0.000	-212.74	-118.93

The mean difference is significant at the 0.05 level.

fatigue damage and lead to complications of internal fixation failure. In recent years, one possible way to solve this problem is using 3D printing technology to design and assemble anatomical models. Here, we have designed a novel customized wing-shaped plate for the particular acetabulum rupture according to the mirror model of the patient's healthy side of the hemi-pelvis. The customized fixation system designed directly from the specific patient is better adapted to the bone surface when compared with the traditional fixation system, which will reduce the time of bending and fixing the plate during the operation. It contains 3 parts, of which the anterior branch was to be fixed to the pubic branch, the posterior was to be fixed to the above great sciatic notch, and the lower branch was to be fixed to the ischium spine. The lower 2 parts form an arc as a barrier plate on the surface that can effectively fix the quadrilateral area of the comminuted fracture, avoiding medial subluxation of the femoral head. This design concept was consistent with the direction of the acetabular trabecula and can effectively fix the anterior and posterior column of the acetabulum. A personalized bone plate can facilitate better preoperative planning and better intraoperative work. It could greatly reduce the operation time and blood loss during surgery with no need for pre-bending according of the acetabulum surface. And in previous studies, we have demonstrated that the customized acetabular-wing plates had the equivalent hardness, tensile strength, yield strength, and mechanical properties as traditional plates.¹⁸

Quadrilateral surface buttress plates and traditional forms of both column acetabular fracture fixation usually use multiple bone plates during the operation. In this study, we used just 1 plate and fewer screws instead of multiple reconstruction plates to fix the ruptured pelvis, which could decrease the risk of the screws penetrating the acetabulum fossa. Besides, the results presented that a single wing-plate is stable enough, as the axial stiffness of Groups A, B and C were 122.4800 ± 8.8480 N/mm, 168.4830 ± 14.8091 N/mm and 83.1300 ± 3.8091 N/mm, respectively (Table 2). Group B was significantly stiffer than Groups A and C ($p < 0.05$) (Table 3). The novel customized wing-shape plates spanning the posterior and anterior columns are biomechanically comparable and, in some cases, superior to traditional forms of fixation in this cadaveric hemipelvis model. Another advantage is that fracture reduction could be judged according to the surface morphology of the bone plate during the operation, thus avoiding errors caused by intraoperative fluoroscopy.

Computer-aided design (CAD) combined with 3D printing is a novel surgical technique that is frequently applied in the orthopedic field.^{18,24,25} Computer-aided design and 3D printing technology have been used for the design and assembly of anatomical models, the production of surgery assisted instruments and the printing of implants and prostheses.^{26–28} The procedure is typically conducted for preoperative bending of the bone plates to assess the position

and length of the screws using a 3D printing pelvic model. Patient-specific pre-contoured plates in acetabular fracture have been studied by a few researchers, and metal 3D printing technology has been widely used to fabricate customized spinal prostheses, knee joint prostheses, and femoral prostheses,¹⁵ but personalized plate study was lacking. Selective laser welding (SLM) can be used to rapidly prepare customized plates to meet the urgent need of surgical treatment. Using 3D printers as production tools has become known in the industry as additive manufacturing (as opposed to the old, subtractive business of cutting, drilling and bashing metal). Therefore, combined with SLM, a customized plate for complex acetabular fracture fixation can be used in clinics to improve the quality and efficiency of surgery.

Anterior columns can be combined to posterior hemitransverse fractures (ACPHTFs), which commonly occur in geriatric acetabular fractures.²⁹ To assess the stability of anterior columns, posterior columns and quadrilateral plates, we designed complex acetabular fractures on the basis of ACPHTFs and added an additional fracture line across the acetabular dome to the iliosciatic notch, parallel to the posterior fracture line. This fracture model splits the quadrilateral plate into 2 distinct regions, with the rear region and the acetabulum being weight-bearing free, thus fitting our experimental aims. Meanwhile, the complex classical fracture model offers complex acetabulum fracture references for acetabulum biomechanical research. To assess the direct blocking effect of the steel plate on the quadrilateral plate and acetabular dome, we made some artificial upper femur sections. The artificial femoral head was oriented 25° in the retroversion and 45° in the abduction as shown by Khajavi et al.³⁰ Theoretically, the force applied to acetabular fossa from a single stance was equal to the double Body Weight (BW). However, patients were recommended to limit weight-bearing loads to about 20% of their BW during recovery and after surgery.^{31,32} In this study, we selected a rigorous loading scenario (up to 700 N) to simulate the body bearing. Force and displacement data was collected and analyzed to calculate the construction stiffness.

The standard of the “internal fixation failure” was a 3-mm acetabular fracture gap, which easily leads to arthritis.^{4,7,20} In the failure test, we monitored the increase in fracture gap to 3 mm in the presence of a loading force, incrementally increased at 20 N/s. Control groups consisted of intrapelvic buttressing fixation as a method to support the quadrilateral plate. A single group produced an intrapelvic buttressing plate along the arcuate, in combination with an additional pelvic plate and lag screws to fix the anterior and posterior columns. The other group had intrapelvic buttressing from the iliac surface to the sitting joint, and could prevent quadrilateral plate medial displacement and fix the posterior column.










There were limitations to this study. Firstly, we chose to use a fresh frozen cadaver pelvis, with a sample size

of 6 for each group. Although bone mineral density was quantified before the biomechanical test, the accuracy of the experiment may have been affected by the insufficient samples and different specimen quality levels. Cadaveric specimens were from an older population and there were individual differences among them. Secondly, our experiments focused on mechanical studies of the immediate stability of fracture repair and did not simulate a gait loading condition. It is believed that the early stages of healing involving static loading allow for a comparison of the biomechanical properties of implants, and immediate biomechanical stability has an important influence on fracture healing during this period. Thirdly, we excised strong musculature that leads to deforming forces, providing only weak support for the fractures. There are, therefore, deficiencies that require improvement. These include: 1) customized 3D printing acetabular-wing plates designed on the basis of the anatomic reduction of fractures, and if fracture reduction does not occur, the bone surface becomes poorly fitted to the bone plate, and pre-set screws become difficult to position; 2) during the design and production processes, the influence of local soft tissue was not fully considered. The internal fixation method based on the preoperative design may thus not be realized by the soft tissue influence. Therefore, the outcome of wing-plate for acetabular fracture requires long-term follow-up in clinical practice.

Conclusions

The main finding of this study was that treatment of displaced both-column acetabular fractures using a 3D printing wing-plate appears to be a safe option with good stability outcomes. Our method used computer aid design according to the digital pelvic model, to which patient-specific implants were perfectly matched to the ruptured acetabulum. Combined with 3D printing technology, the customized plate with optimal structure can be produced quickly to meet the emergency time requirements.

ORCID iDs

Xiangyuan Wen  <https://orcid.org/0000-0001-9939-4967>
 Hai Huang  <https://orcid.org/0000-0003-0289-9825>
 Canbin Wang  <https://orcid.org/0000-0002-1911-5065>
 Jianghui Dong  <https://orcid.org/0000-0003-3961-1688>
 Xuezhi Lin  <https://orcid.org/0000-0003-1362-515X>
 Fuming Huang  <https://orcid.org/0000-0002-2036-1626>
 Hua Wang  <https://orcid.org/0000-0001-9004-176X>
 Liping Wang  <https://orcid.org/0000-0001-9355-1167>
 Shicai Fan  <https://orcid.org/0000-0002-1993-6074>

References

1. Tile M. Pelvic ring fractures: Should they be fixed? *J Bone Joint Surg Br.* 1988;70(1):1–12.
2. Peter RE. Open reduction and internal fixation of osteoporotic acetabular fractures through the ilio-inguinal approach: Use of buttress plates to control medial displacement of the quadrilateral surface. *Injury.* 2015;46(Suppl 1):S2–S7.
3. Wu XB, Wang JQ, Sun X, Zhao CP. Guidance for treatment of pelvic acetabular injuries with precise minimally invasive internal fixation based on the orthopaedic surgery robot positioning system. *Orthop Surg.* 2019;11(3):341–347.
4. Laflamme GY, Hebert-Davies J, Rouleau D, Benoit B, Leduc S. Internal fixation of osteopenic acetabular fractures involving the quadrilateral plate. *Injury.* 2011;42(10):1130–1134.
5. Culemann U, Holstein JH, Kohler D, et al. Different stabilisation techniques for typical acetabular fractures in the elderly – a biomechanical assessment. *Injury.* 2010;41(4):405–410.
6. Butterwick D, Papp S, Gofton W, Liew A, Beaulé PE. Acetabular fractures in the elderly: Evaluation and management. *J Bone Joint Surg Am.* 2015;97(9):758–768.
7. Boelch SP, Jordan MC, Meffert RH, Jansen H. Comparison of open reduction and internal fixation and primary total hip replacement for osteoporotic acetabular fractures: A retrospective clinical study. *Int Orthop.* 2017;41(9):1831–1837.
8. Letournel E. Acetabulum fractures: Classification and management. *Clin Orthop Relat Res.* 1980(151):81–106.
9. White G, Kanakaris NK, Faour O, Valverde JA, Martin MA, Giannoudis PV. Quadrilateral plate fractures of the acetabulum: An update. *Injury.* 2013;44(2):159–167.
10. Sen RK, Tripathy SK, Aggarwal S, Goyal T, Mahapatra SK. Commi-nuted quadrilateral plate fracture fixation through the iliofemoral approach. *Injury.* 2013;44(2):266–273.
11. Russell GV Jr, Nork SE, Chip Rott ML Jr. Perioperative complications associated with operative treatment of acetabular fractures. *J Trauma.* 2001;51(6):1098–1103.
12. Bott A, Odutola A, Halliday R, Acharya MR, Ward A, Chesser TJS. Long-term patient-reported functional outcome of polytraumatized patients with operatively treated pelvic fractures. *J Orthop Trauma.* 2019;33(2):64–70.
13. Mehin R, Jones B, Zhu Q, Broekhuysen H. A biomechanical study of conventional acetabular internal fracture fixation versus locking plate fixation. *Can J Surg.* 2009;52(3):221–228.
14. Maini L, Sharma A, Jha S, Sharma A, Tiwari A. Three-dimensional printing and patient-specific pre-contoured plate: Future of acetabulum fracture fixation? *Eur J Trauma Emerg Surg.* 2018;44(2):215–224.
15. Malik HH, Darwood AR, Shaunak S, et al. Three-dimensional printing in surgery: A review of current surgical applications. *J Surg Res.* 2015;199(2):512–522.
16. Fang C, Cai H, Kuong E, et al. Surgical applications of three-dimensional printing in the pelvis and acetabulum: From models and tools to implants. *Unfallchirurg.* 2019;122(4):278–285.
17. Letournel E. Fractures of the acetabulum: A study of a series of 75 cases – Les fractures du cotyle, etude d’une serie de 75 cas. *J de Chirurgie.* 1961; 82:47–87 [translated and substantially abridged]. *J Orthop Trauma.* 2006;20(1 Suppl):S15–S19.
18. Wang D, Wang Y, Wu S, et al. Customized a Ti6Al4V bone plate for complex pelvic fracture by selective laser melting. *Materials (Basel).* 2017;10(1):35.
19. Gillispie GJ, Babcock SN, McNamara KP, et al. Biomechanical comparison of intrapelvic and extrapelvic fixation for acetabular fractures involving the quadrilateral plate. *J Orthop Trauma.* 2017;31(11): 570–576.
20. Barnes SN, Stewart MJ. Central fractures of the acetabulum: A critical analysis and review of literature. *Clin Orthop Relat Res.* 1976;(114):276–281.
21. Matta JM. Fractures of the acetabulum: Accuracy of reduction and clinical results in patients managed operatively within three weeks after the injury. *J Bone Joint Surg Am.* 1996;78(11):1632–1645.
22. Mears DC, Velyvis JH, Chang CP. Displaced acetabular fractures managed operatively: Indicators of outcome. *Clin Orthop Relat Res.* 2003; (407):173–186.
23. Ziran N, Soles GLS, Matta JM. Outcomes after surgical treatment of acetabular fractures: A review. *Patient Saf Surg.* 2019;13:16. doi: 10.1186/s13037-019-0196-2
24. Boudissa M, Courvoisier A, Chabanas M, Tonetti J. Computer assisted surgery in preoperative planning of acetabular fracture surgery: State of the art. *Expert Rev Med Devices.* 2018;15(1):81–89.
25. Cromeens BP, Ray WC, Hoehne B, Abayneh F, Adler B, Besner GE. Facilitating surgeon understanding of complex anatomy using a three-dimensional printed model. *J Surg Res.* 2017;216:18–25.

26. Aimar A, Palermo A, Innocenti B. The role of 3D printing in medical applications: A state of the art. *J Healthc Eng.* 2019;2019:5340616.
27. Wan L, Zhang X, Zhang S, et al. Clinical feasibility and application value of computer virtual reduction combined with 3D printing technique in complex acetabular fractures. *Exp Ther Med.* 2019;17(5):3630–3636.
28. Weidert S, Andress S, Suero E, et al. 3D printing in orthopedic and trauma surgery education and training: Possibilities and fields of application [in German]. *Unfallchirurg.* 2019;122(6):444–451. doi:10.1007/s00113-019-0650-8
29. Karim MA, Abdelazeem AH, Youness M, El Nahal WA. Fixation of quadrilateral plate fractures of the acetabulum using the buttress screw: A novel technique. *Injury.* 2017;48(8):1813–1818.
30. Khajavi K, Lee AT, Lindsey DP, Leucht P, Bellino MJ, Giori NJ. Single column locking plate fixation is inadequate in two column acetabular fractures. A biomechanical analysis. *J Orthop Surg Res.* 2010;5:30.
31. Ryken TC, Owen BD, Christensen GE, Reinhardt JM. Image-based drill templates for cervical pedicle screw placement. *J Neurosurg Spine.* 2009;10(1):21–26.
32. Ma T, Xu YQ, Cheng YB, et al. A novel computer-assisted drill guide template for thoracic pedicle screw placement: A cadaveric study. *Arch Orthop Trauma Surg.* 2012;132(1):65–72.

Social participation of patients with multiple sclerosis

Anna Pokryszko-Dragan^{1,A–F}, Karol Marschollek^{2,B,C,F}, Aleksandra Chojko^{2,B,C,F}, Magdalena Karasek^{2,B,C,F}, Adam Kardys^{2,B,C,F}, Paweł Marschollek^{2,B,C,F}, Ewa Gruszka^{1,B,C,F}, Marta Nowakowska-Kotas^{1,B–D,F}, Sławomir Budrewicz^{1,A,E,F}

¹ Clinical Department of Neurology, Wrocław Medical University, Poland

² Students' Scientific Club, Department of Neurology, Wrocław Medical University, Poland

A – research concept and design; B – collection and/or assembly of data; C – data analysis and interpretation;

D – writing the article; E – critical revision of the article; F – final approval of the article

Advances in Clinical and Experimental Medicine, ISSN 1899–5276 (print), ISSN 2451–2680 (online)

Adv Clin Exp Med. 2020;29(4):469–473

Address for correspondence

Anna Pokryszko-Dragan
E-mail: annapd@interia.pl

Funding sources

None declared

Conflict of interest

None declared

Received on May 17, 2019

Reviewed on June 26, 2019

Accepted on December 12, 2019

Published online on April 28, 2020

Abstract

Background. The effect multiple sclerosis (MS) has on the social functioning and integration of patients has been recently considered as an important factor of the disease.

Objectives. To assess social participation of MS patients with regard to demographic and disease-related variables.

Material and methods. The study comprised 201 MS patients: 140 women, 61 men, aged 24–69 years. The World Health Organization Disability Assessment Schedule (WHODAS 2.0) was applied to assess the aspects of social functioning and the Beck Depression Inventory (BDI) was applied to evaluate the level of depression. Disease duration, degree of disability in Expanded Disability Status Scale (EDSS), most disabling symptoms and type of treatment were determined. WHODAS 2.0 scores (total and within particular domains) and their relationships with age, gender, disease-related variables and level of depression were analyzed.

Results. The results of WHODAS 2.0 for 27.4% of patients exceeded the 90th percentile compared to the population norms (with the highest scores for “getting around” and “participation in society” domains). The results of BDI and WHODAS 2.0 were strongly correlated ($p < 0.001$; $\beta = 0.73$) and mobility impairment was related to both of them ($p < 0.001$; $\beta = -0.12$ and 0.25 , respectively). Other disabling symptoms were associated with scores in domains “understanding and communicating”, “getting around” and “participation in society”.

Conclusions. Social participation of the MS patients is affected by the impact of disease and associated with depression. Particular symptoms of neurological deficit (motor and visual impairment, fatigue) influence social functioning more than general disease-related variables.

Key words: depression, disability, multiple sclerosis, social participation

Cite as

Pokryszko-Dragan A, Marschollek K, Chojko A, et al.
Social participation of patients with multiple sclerosis.
Adv Clin Exp Med. 2020;29(4):469–473.
doi:10.17219/acem/115237

DOI

10.17219/acem/115237

Copyright

© 2020 by Wrocław Medical University
This is an article distributed under the terms of the
Creative Commons Attribution 3.0 Unported (CC BY 3.0)
(<https://creativecommons.org/licenses/by/3.0/>)

Introduction

Multiple sclerosis (MS) is a chronic, multiphasic disorder of the central nervous system. The complex background of the disease includes dysfunction of immune-mediated mechanisms, which is affected by interacting genetic predisposition and environmental factors. Multifocal damage to myelin and axonal loss within the brain and spinal cord may result in a wide range of symptoms and in accumulating physical and mental disability.

The most typical MS onset occurs in young adults and long-lasting course of the disease affects further stages of life. Therefore, MS impact upon the patients' social functioning constitutes an essential problem.¹ Multiple sclerosis may influence the patients' ability to fulfill family and social roles according to their expectations² and may cause barriers to successful employment.³ The patients may prioritize self-care, health-promoting and daily activities to leisure and other aspects of social functioning.⁴ They may also feel stigmatized and isolated, which further affects their involvement in community activities.^{5,6}

Within recent years, the effect MS has on social participation and integration of the patients has been recognized as an important multidimensional factor of the disease.⁷ According to the World Health Organization (WHO) and International Classification of Functioning, Disability and Health (ICF), participation can be defined as engagement in major life activities in the lived environment and involvement in life situations.^{8,9} The evaluated dimensions of participation may include the frequency and range of activities, their importance and associated self-efficacy or satisfaction.^{5,10} The concept of social participation in MS patients has been already elaborated in some studies,^{1,2,4,10,11} which differed in analyzed issues and their measures.

The aim of the study was to assess the assessment of social functioning and participation in MS patients with regard to the demographic and disease-related variables.

Material and methods

Consecutive patients with MS diagnosed according to McDonald's criteria,¹² consulted in the outpatient clinic at the Department of Neurology during January–March 2018, who had regular follow-ups documented in the medical records, were included in the study. Exclusion criteria comprised relapse of the disease or switch to another type of treatment within the preceding 3 months, as well as cognitive impairment which would interfere with filling out the self-administered questionnaires.

The studied group consisted of 201 patients: 140 women and 61 men aged 24–69 years (mean: 41.3 years). A relapsing-remitting (RRMS) course of disease was diagnosed in 91.5% and a secondary progressive (SPMS) course in 8.5%. All the patients with RRMS were being treated

with disease-modifying therapies (DMTs): 115 – interferon beta, 22 – glatiramer acetate, 24 – dimethylfumarate, 18 – fingolimod, 3 – natalizumab.

The assessment of social functioning was carried out using the World Health Organization Disability Assessment Schedule (WHODAS 2.0),¹³ Beck Depression Inventory (BDI)¹⁴ was used to evaluate the level of depression. The self-administered questionnaire was also applied, and included questions concerning the patients' major complaints (symptoms perceived as most disabling) and their perception of the effectiveness and tolerability of treatment. Data on MS duration and its course, disease-modifying treatment and degree of disability (measured in Expanded Disability Status Scale – EDSS)¹⁵ were obtained from the medical records.

The project of the study was approved by Bioethical Committee of Wroclaw Medical University. All the subjects gave their informed consent to participate in the study.

The total result of WHODAS 2.0 was calculated and compared to population norms. Scores in particular domains were presented as percentages. Relationships were analyzed between WHODAS 2.0 results and age, gender, duration of MS, EDSS, most disabling symptoms, type of medication used and BDI.

Statistical analysis was performed using STATISTICA v. 13.0 (StatSoft Polska, Cracow, Poland), with a significance level $\alpha = 0.05$. Categorical variables were presented as numerical and percentage values and continuous ones – as the mean and standard deviation (SD) or median and interquartile range. Spearman's rank correlation was used to assess relationship between WHODAS 2.0 total score and BDI score and general linear models were conducted to establish predictors of WHODAS 2.0 results (total score and scores in each domain).

Results

In the studied group, MS duration ranged from 1 to 39 years (mean: 10.07) and EDSS from 1.0 to 7.0 (median: 3, Q1–Q3: 2–4). Mobility problems, fatigue and visual dysfunction were most common symptoms perceived by the patients as most disabling (Table 1). A total of 158 subjects (78.6%) considered their treatment as effective, 88 (43.8%) noticed side effects of DMTs.

The results of WHODAS 2.0 for 27.36% of patients were above 90th percentile comparing to the population norms. Mean scores in particular domains are presented in Fig. 1.

Beck Depression Inventory score ranged from 0 to 63 (median: 7, Q1–Q3: 2–16); 64 (31.84%) patients scored more than 13, which indicates depressive symptoms (Table 2).

Total score of WHODAS 2.0 or scores in particular domains showed no significant relationships with age and gender of the patients. No significant relationships were found between WHODAS 2.0 results and MS duration or EDSS.

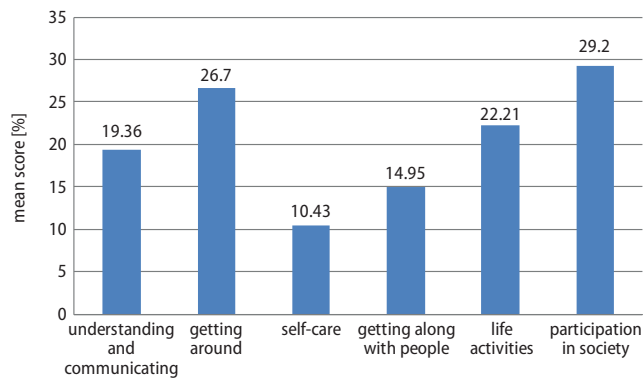


Fig. 1. Mean score in each WHODAS 2.0 domain (as a percentage of total amount of points possible to score)

WHODAS 2.0 – the World Health Organization Disability Assessment Schedule.

Table 1. Major complaints of MS patients (symptoms reported as most disabling). A patient could report more than 1 symptom

Symptoms reported as most disabling	Number (percentage) of patients
Mobility problems	80 (39.8)
Fatigue	48 (23.9)
Visual deficit	35 (17.4)
Headache/vertigo	28 (13.9)
Musculoskeletal pain/stiffness	28 (13.9)
Hand/foot numbness	22 (10.9)
Upper limb weakness	13 (6.5)
Urinary incontinence	10 (5)
Memory problems	9 (4.5)

MS – multiple sclerosis.

Table 2. Distribution of BDI scores in the MS patients. Total score indicates: minimal depression (0–13), mild depression (14–19), moderate depression (20–28), severe depression (29–63)

BDI score	Number (percentage) of patients (N = 201)
0–13	137 (68.2)
14–19	29 (14.4)
20–28	26 (12.9)
29–63	9 (4.5)

BDI – Beck Depression Inventory.

Beck Depression Inventory and WHODAS scores were strongly correlated ($p < 0.01$; $R = 0.73$) and the problem with mobility as the most disabling symptom was a predictor for both of them ($p < 0.001$; $\beta = -0.12$ and $\beta = 0.26$, respectively). Specific symptoms claimed as the most disabling appeared to be the risk factors for higher score particularly in WHODAS domains. All significant associations are shown in Table 3.

No significant relationships were found between WHODAS 2.0 score and the type of medication used in MS therapy or the presence of side effects of treatment.

Table 3. Significant correlations between WHODAS 2.0 scores (total and in particular domains), most disabling symptoms and BDI score in the studied group of MS patients

Total WHODAS 2.0 score
• Mobility problems as most disabling symptom ($p < 0.001$; $\beta = 0.26$)
“Understanding and communicating” domain
• BDI score ($p < 0.001$; $\beta = 0.56$)
• Visual deficit as most disabling symptom ($p = 0.006$; $\beta = 0.16$)
• Fatigue as most disabling symptom ($p = 0.016$; $\beta = 0.14$)
“Getting around” domain
• BDI score ($p < 0.001$; $\beta = 0.46$)
• Mobility problems as most disabling symptom ($p < 0.001$; $\beta = 0.43$)
• Musculoskeletal pain/stiffness as most disabling symptom ($p = 0.04$; $\beta = 0.12$)
“Participation in society” domain
• BDI score ($p < 0.001$; $\beta = 0.65$)
• Mobility problems as most disabling symptom ($p < 0.001$; $\beta = 0.26$)
• Headache/vertigo ($p = 0.02$; $\beta = 0.13$)
BDI score
• Score in “getting along with people” domain ($p < 0.001$; $\beta = 0.31$)
• Score in “life activities” domain ($p = 0.03$; $\beta = 0.19$)
• Score in “participation in society” domain ($p < 0.001$; $\beta = 0.41$)
• Mobility problems as most disabling symptom ($p = 0.05$; $\beta = -0.12$)

Discussion

There is a wide range of instruments to evaluate social functioning and participation which were used in the studies focused on MS patients.^{1,4,7,11} We chose WHODAS 2.0 because of its validation for MS¹⁶ and availability in the Polish language version. WHODAS 2.0 questionnaire addresses the difficulties and problems perceived by a respondent in particular domains. In view of that, the scale results provide better insight in the aspects of the patients’ self-efficacy and satisfaction than a pure measure of frequency or range of social activities.^{5,10}

The findings in our group of MS patients, compared to the population norms, revealed a high percentage of responses with a score above the 70th percentile. The highest scores were reached in the domains “participating in society” and “life activities” and moderate ones in “getting along with people” and “understanding and communicating”. Thus, important aspects of social functioning seemed significantly affected in the studied group. The previous studies in this field^{1,2,4,7,11,17} also showed relevant findings for various measures of social participation, including maintaining relationships, employment status and community integration.

No correlations were found in our MS group between WHODAS 2.0 scores and demographic variables. In other studies,^{1,18} age was not directly related to social functioning measures, but appeared as an interacting factor, linked with quality of life indices and employment status. Hughes et al.⁷ reported better scores for females in social domain of Community Integration Questionnaire, but no other gender-specific relationships were described in this field.

In the studied group, over 90% of patients had a relapsing-remitting course of MS and were being treated with DMTs, which were perceived as effective by the majority of the subjects. Mean level of disability in EDSS in the whole group was relatively mild. Considering these apparently favorable outcomes of the disease, high scores of WHODAS 2.0 certainly deserve attention. Furthermore, there were no significant correlations between WHODAS 2.0 results and MS duration and EDSS. Such relationships were not found for types of DMTs or their side effects, either. Other authors^{2,7,11,17} observed links between disability score and measures of community integration, social participation and employment status. However, their studies used various tools to evaluate social functioning, and they also differed in the sample size.

On the contrary to general indices of MS course, particular symptoms regarded by our patients as most disabling showed significant correlations with WHODAS 2.0 results. The most frequent major complaints (motor impairment, fatigue and visual dysfunction) correlated with scores in all the main domains of WHODAS, while less frequently reported headaches, vertigo, stiffness and pain were related to aspects of mobility and participating in social activities. Mobility impairment, fatigue and occasionally also visual impairment have been indeed shown to affect social participation, employment status and related satisfaction.^{3,19,20} Many authors^{2,4,7,17,18} highlighted the role of cognitive impairment which would have greater impact upon patients' social functioning than physical disability. Only a small percentage of our patients counted cognitive decline among their major complaints. Our methods did not include objective measures of cognitive performance, because its reliable assessment would require widening the questionnaire, possibly discouraging the patients from responding. However, we did consider the role of depression in the evaluation of social functioning issues. Indeed, almost 1/3 of our patients had a BDI score indicating depressive symptoms and a significant correlation was found between the results of BDI and WHODAS. Although other studies^{2,7} reported less frequent depressive symptoms assessed with BDI or Hospital Anxiety and Depression Scale (HADS), their authors confirmed relevant influence of depression upon measures of social participation.^{7,10} It has been highlighted that apart from disease-related variables, social functioning of MS patients is affected by many interacting factors, including personal and environmental ones.^{1,3,10,20}










Overall, our findings, which were obtained with specific and validated tools, show a relevant prospect of social participation in a representative group of MS patients, with contributing factors. Limitations of the study include homogeneity of the studied group (predominating patients with RRMS were probably more likely both to participate in social activities and to respond to the questionnaire than those with SPMS) and only single evaluation of the analyzed issues (without considering dynamics of the disease over time). These aspects could be addressed in the further

studies planned in this field. Furthermore, other factors possibly affecting social participation of MS patients (including cognitive performance and level of education, socioeconomic status, etc.) should be also considered in the analyses.

Conclusions

Social functioning and participation of MS patients are substantially affected by the impact of the disease and show an association with depression. Particular symptoms of neurological deficit (motor and visual impairment, fatigue) seem to influence social functioning more than general disease-related variables. These aspects deserve attention during individualized follow-ups of MS patients.

ORCID iDs

Anna Pokryszko-Dragan  <https://orcid.org/0000-0002-5203-112X>
 Karol Marschollek  <https://orcid.org/0000-0001-9093-180X>
 Aleksandra Chojko  <https://orcid.org/0000-0003-1233-887X>
 Magdalena Karasek  <https://orcid.org/0000-0002-1066-0876>
 Adam Kardys  <https://orcid.org/0000-0001-8230-1904>
 Paweł Marschollek  <https://orcid.org/0000-0003-4588-309X>
 Ewa Gruszka  <https://orcid.org/0000-0002-9800-5461>
 Marta Nowakowska-Kotas  <https://orcid.org/0000-0002-3173-8337>
 Sławomir Budrewicz  <https://orcid.org/0000-0002-2044-6347>

References

1. Mikula P, Sc M, Nagyova I, et al. Social participation and health-related quality of life in people with multiple sclerosis. *Disabil Health J*. 2015;8(1):29–34. <http://dx.doi.org/10.1016/j.dhjo.2014.07.002>
2. Hakim AE, Bakheit AMO, Bryant TN, et al. The social impact of multiple sclerosis – a study of 305 patients and their relatives. *Disabil Rehabil*. 2000;22(6):288–293. <http://www.tandfonline.com/doi/full/10.1080/096382800296755>
3. Messmer Uccelli M, Specchia C, Miller D, Battaglia M. Factors that influence the employment status of people with multiple sclerosis: A multi-national study. *J Neurol*. 2009;256:1989–1996.
4. Plow MA, Finlayson M, Ont OTR, Gunzler D, Heinemann AW. Correlates of participation in meaningful activities among people with multiple sclerosis. *J Rehabil Med*. 2015;47:538–545.
5. Sparling A, Stutts LA, Sanner H, Eijkholt MM. In-person and online social participation and emotional health in individuals with multiple sclerosis. *Qual Life Res*. 2017;26(11):3089–3097.
6. Cook JE, Germano AL, Stadler G. An exploratory investigation of social stigma and concealment in patients with multiple sclerosis. *Int J MS Care*. 2016;18(2):78–84.
7. Hughes AJ, Hartoonian N, Parmenter B, et al. Cognitive impairment and community integration outcomes in individuals living with multiple sclerosis. *Arch Phys Med Rehabil*. 2015;96(11):1973–1979. <http://dx.doi.org/10.1016/j.apmr.2015.07.003>
8. World Health Organization. International classification of functioning, disability and health. 2001. <https://www.who.int/classifications/icf/en/>.
9. Resnik L, Plow MA. Measuring participation as defined by the International Classification of Functioning, Disability and Health: the evaluation of existing measures. *Arch Phys Med Rehabil*. 2009;90:856–866.
10. Yorkston KM, Kuehn CM, Johnson KL, Ehde DM, Jensen MP, Amtmann D. Measuring participation in people living with multiple sclerosis: A comparison of self-reported frequency, importance and self-efficacy. *Disabil Rehabil*. 2008;30(2):88–97.
11. Kwiatkowski A, Marissal J, Pouyfaucou M, Vermersch P, Hauteceur P, Dervaux B. Social participation in patients with multiple sclerosis: Correlations between disability and economic burden. *BMC Neurol*. 2014;14:115.

12. Polman C, Reingold S, Banwell B, et al. Diagnostic criteria for multiple sclerosis: 2010 revisions to the McDonald criteria. *Ann Neurol*. 2011;69:292–302.
13. World Health Organization. http://www.who.int/classifications/icf/WHODAS2.0_36itemsSELF.pdf. Accessed on December 15, 2017.
14. Beck AT, Ward CH, Medelson M, Mock J, Erbaugh J. An inventory for measuring depression. *Arch Gen Psychiatry*. 1961;4: 561–571.
15. Kurtzke J. Rating neurologic impairment in multiple sclerosis: an expanded disability status scale (EDSS). *Neurology*. 1983;33(11): 1444–1452.
16. Garin O, Ayuso-Mateos JL, Almansa J, et al. Validation of the “World Health Organization Disability Assessment Schedule, WHODAS-2” in patients with chronic diseases. *Heal Qual Life Outcomes*. 2010;8:51.
17. Cattaneo D, Lamers I, Bertoni R, Feys P, Jonsdottir J. Participation restriction in people with multiple sclerosis: Prevalence and correlations with cognitive, walking, balance, and upper limb impairments. *Arch Phys Med Rehabil*. 2017;98(7):1308–1315. <http://dx.doi.org/10.1016/j.apmr.2017.02.015>
18. Pompeii LA, Moon SD, McCrory DC. Measures of physical and cognitive function and work status among individuals with multiple sclerosis: A review of the literature. *J Occup Rehabil*. 2005;15(1):69–84.
19. Yorkston KM, Baylor C, Amtmann D. Journal of Communication Disorders Communicative participation restrictions in multiple sclerosis: Associated variables and correlation with social functioning. *J Commun Disord*. 2014;52:196–206. <http://dx.doi.org/10.1016/j.jcomdis.2014.05.005>
20. Hollingsworth H, Gray DB. Structural equation modeling of the relationships between participation in leisure activities and community environments by people with mobility impairments. *Arch Phys Med Rehabil*. 2010;91(8):1174–1181. <http://dx.doi.org/10.1016/j.apmr.2010.04.019>

Evaluation of the relationship between splenic iron overload and liver, heart and muscle features evident on T2*-weighted magnetic resonance imaging

Mehmet Güli Çetinçakmak^{1,A-E}, Salih Hattapoğlu^{1,A,B,D}, Murat Söker^{2,B,C},
Faysal Ekici^{1,A,B,D}, Kamil Yılmaz^{2,B,C}, Cemil Göya^{1,A-C}, Cihad Hamidi^{1,A,D-F}

¹ Department of Radiology, Medical School, Dicle University, Diyarbakir, Turkey

² Department of Pediatrics, Medical School, Dicle University, Diyarbakir, Turkey

A – research concept and design; B – collection and/or assembly of data; C – data analysis and interpretation;

D – writing the article; E – critical revision of the article; F – final approval of the article

Advances in Clinical and Experimental Medicine, ISSN 1899–5276 (print), ISSN 2451–2680 (online)

Adv Clin Exp Med. 2020;29(4):475–480

Address for correspondence

Mehmet Güli Çetinçakmak
E-mail: drmehmetguli@gmail.com

Funding sources

None declared

Conflict of interest

None declared

Received on September 22, 2017

Reviewed on April 16, 2018

Accepted on January 21, 2020

Published online on May 5, 2020

Abstract

Background. Splenic iron overload is the most common clinical condition in patients with thalassemia. However, few studies of the effects of splenectomy have been published.

Objectives. To evaluate the relationship between splenic iron overload and liver, heart and muscle features visible in T2*-weighted magnetic resonance imaging, and to investigate the effects of splenectomy on these tissues in patients with beta-thalassemia major (TM).

Material and methods. We retrospectively included 131 patients (76 male and 55 female) diagnosed with TM. All radiological assessments were performed with the aid of a Philips Achieva 1.5T scanner running a multiecho gradient-echo sequence. Hepatic and splenic T2* values were assessed in the same gradient multiecho series. Muscle T2* values were assessed in the shoulder girdle muscles adjacent to the heart area. The relationships among splenic T2*, hepatic T2*, cardiac T2* and muscle T2* parameters, serum ferritin levels, age and other parameters were evaluated.

Results. The splenic T2* value correlated with serum ferritin level and the hepatic T2* value ($p < 0.001$ and $p < 0.001$, respectively). The splenic T2* value did not correlate with age, cardiac or muscle T2* values, or with spleen size ($p = 0.27, 0.21, 0.99$, and 0.39 , respectively). The muscle T2* value correlated weakly with the serum ferritin level ($p = 0.022$). The cardiac T2* value was lower and the liver size greater in patients who had undergone splenectomy compared with those who had not ($p < 0.001$ and 0.001 , respectively).

Conclusions. Splenic iron overload correlated with hepatic overload and the serum ferritin level. Splenectomy increased cardiac iron overload and triggered liver enlargement. However, the muscle iron overload was low and the muscles were therefore unaffected by splenectomy.

Key words: spleen, iron overload, MR imaging, thalassemia

Cite as

Güli Çetinçakmak MG, Hattapoğlu S, Söker M, et al.
Evaluation of the relationship between splenic iron overload and liver, heart and muscle features evident on T2*-weighted magnetic resonance imaging. *Adv Clin Exp Med.* 2020;29(4):475–480. doi:10.17219/acem/116758

DOI

10.17219/acem/116758

Copyright

© 2020 by Wrocław Medical University

This is an article distributed under the terms of the Creative Commons Attribution 3.0 Unported (CC BY 3.0) (<https://creativecommons.org/licenses/by/3.0/>)

Introduction

Beta-thalassemia major (TM) is a hereditary form of hemolytic anemia characterized by impaired globin B-chain output. Patients with TM require red blood cell transfusions every 2 to 3 weeks. In these patients, senescent native and transfusional erythrocytes are eliminated by the Kupffer cells (phagocytic macrophages) of the spleen and liver, and the released iron is subsequently transported to the plasma by ferroportin.¹ As the total body iron level increases after multiple transfusions and enhanced intestinal absorption, excess iron is stored in the liver and spleen.^{1,2} In thalassemia, the transfusion requirements are increased by spleen hyperactivity, which is often evident in the first decade of life. This condition is termed “hypersplenism” and is treated with splenectomy.³

Assessments of tissue iron overload may be either invasive or noninvasive. Biopsies can be used to assess hepatic iron overload,^{4,5} but are compromised by standardization problems and the risk of complications. Magnetic resonance imaging (MRI) is a noninvasive method frequently used to assess tissue iron overload, and is the only option for assessing iron overload in the heart, since cardiac biopsies are more variable and more dangerous than hepatic biopsies.⁶

Many studies have been conducted on cardiac and hepatic iron overload.^{5,7–10} The spleen is the second most common iron deposition site, after the liver. However, in some studies on splenic iron overload, contradictory results have been reported.^{11–14}

In the present study, we evaluated the relationships among splenic iron overload and that of the liver, heart and muscles, as well as the effects of splenectomy on these tissues in TM patients using T2*-weighted MRI.

Material and methods

Patients

We retrospectively studied 131 TM patients – 76 (58%) men and 55 (42%) women – referred to our clinic between April 2014 and December 2016 for assessments of cardiac and hepatic iron overload using gradient echo (GRE) T2*-weighted MRI. Patients with thalassemia intermedia and primary hemochromatosis were excluded, as were those yielding poor quality MR images. The study was approved by our local ethics committee.

Cardiomuscular and hepatic-splenic examinations

All radiological assessments were performed using an Achieva 1.5-T scanner (Philips, Amsterdam, the Netherlands). Cardiac and hepatic T2*-weighted sequences were obtained using an RC SENSE-body coil (Philips) with electrocardiographic (ECG) respiratory gating. Multiecho gradient echo sequences were obtained from the central liver

Table 1. Splenic, hepatic, cardiac, and muscle multiecho gradient-echo sequences obtained with MRI parameters

MRI parameters	Cardiac and muscle	Liver and spleen
Slace thickness	10 mm	10 mm
FOV	320 × 320	320 × 320
Flip angle	30	45
RT	16 ms	400 ms
Echo times	7 (3, 5, 7, 10, 12, 14 ms)	14 (from 1 to 14 ms with 1 ms increment)

MRI – magnetic resonance imaging; FOV – field of view; RT – repetition time.

zones with transverse plane for the assessment of hepatic T2* values. A short-axis, midventricular, cardiac-gated multiecho gradient echo sequence was used to derive cardiac T2* values (Table 1).

Splenic T2* values were calculated using CMR software (Cardiovascular Imaging Solutions, London, UK). Hepatic and splenic T2* values were calculated using the same echo series. The regions of interest in the spleen and liver covered only tissue. The tissue did not move artifacts outside of vascular and subcapsular spaces. (Fig. 1–2).

The cardiac and muscle T2* values were calculated using the same echo series. Cardiac T2* values were calculated in the mid-ventricular septum (Fig. 3). The muscle T2* values were from shoulder girdle muscles (the subscapular, infrascapular, deltoid, and pectoral muscles) examined in short-axis cardiac sequences (Fig. 4). The calculations were performed using data from regions with no motion artifacts. Within 7 days from the MRI, abdominal ultrasonography (USG) was performed in all the patients; the images were recorded and liver sizes were measured from the midclavicular line of the craniocaudal diameter. Spleen size was taken as the largest diameter on the plane in which the splenic notch was visible. Splenectomy status was recorded. Clinical data including the patients’ ages and serum ferritin levels within the previous 2 months was retrieved from their medical records.

Statistical analysis

All the data was evaluated using SPSS v. 18.0 for Windows (SPSS Inc., Chicago, USA). Only the cardiac T2* values and spleen sizes were normally distributed. We used Spearman’s rank-order method to seek correlations between the splenic T2* value and age, cardiac and hepatic T2* values, liver and spleen sizes, and serum ferritin levels. The Mann–Whitney U test was used to compare cardiac and hepatic T2* values, liver sizes and serum ferritin levels between patients who had and had not undergone splenectomies.

Results

The 131 patients had a mean age of 12.8 years (range: 4–34 years). There were 39 patients who had undergone splenectomies. The mean splenic T2* value was 9.24

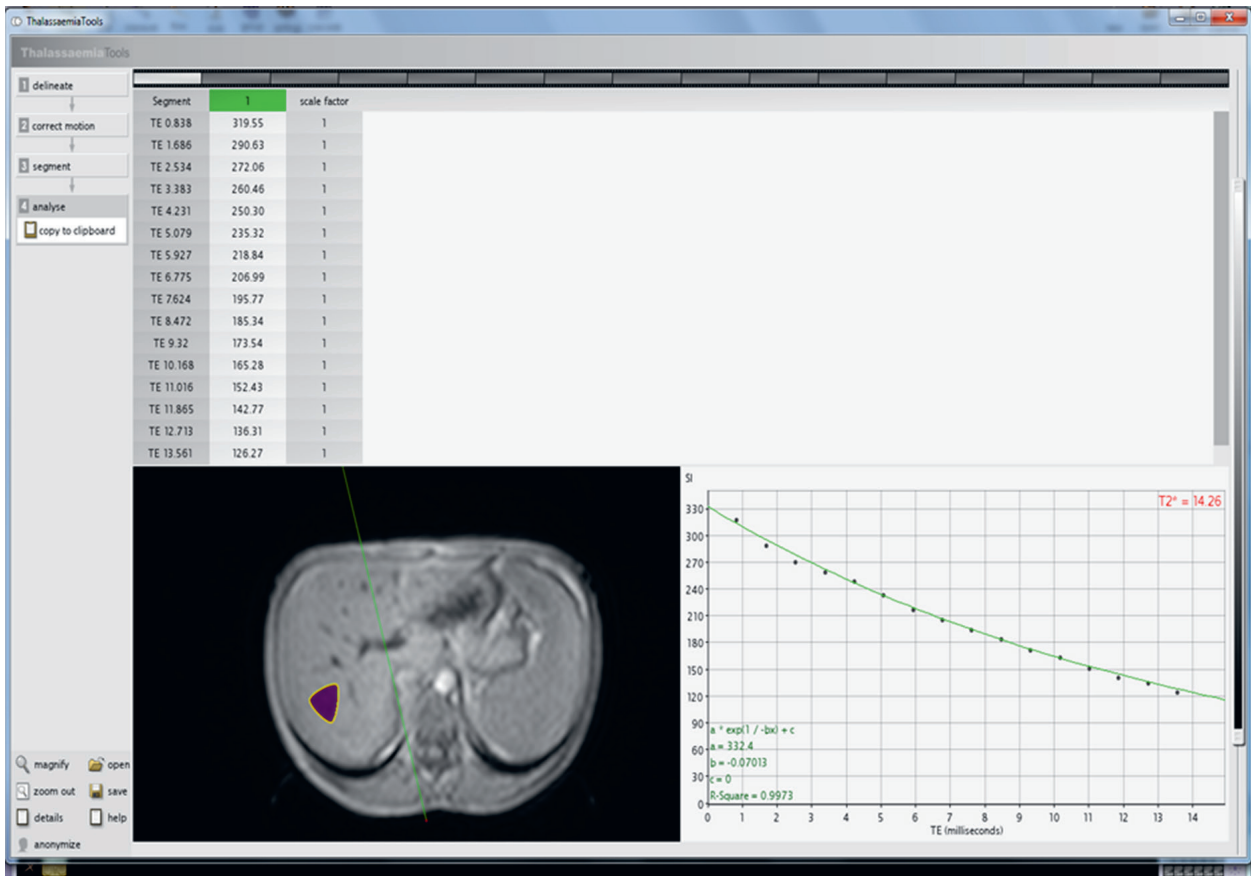
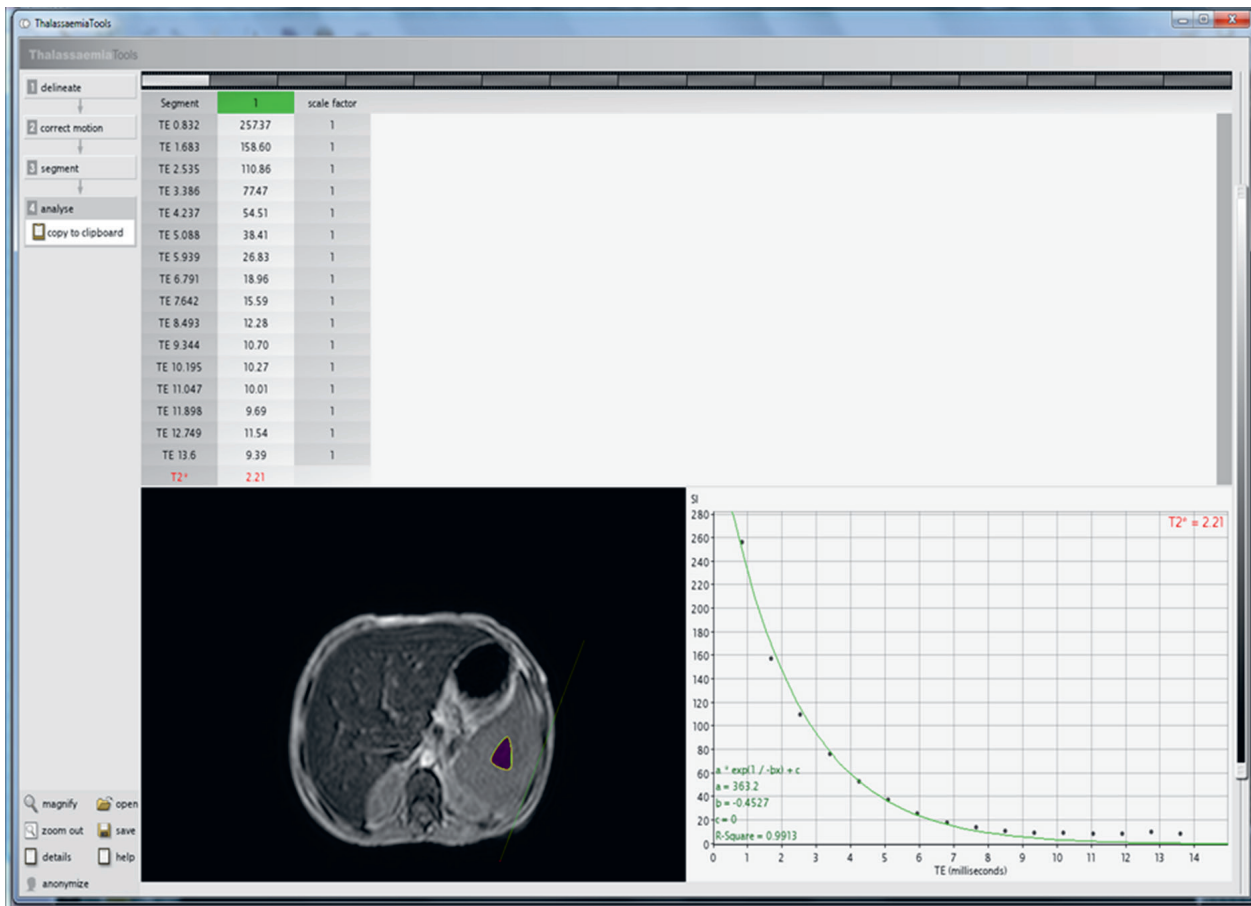


Fig. 1–2. Splenic and hepatic T2* assessments were performed on the central liver zones using a transverse plane multiecho gradient echo sequence. Region of interest (ROI) areas covered only tissue exhibiting no motion artifacts outside of vascular and subcapsular spaces

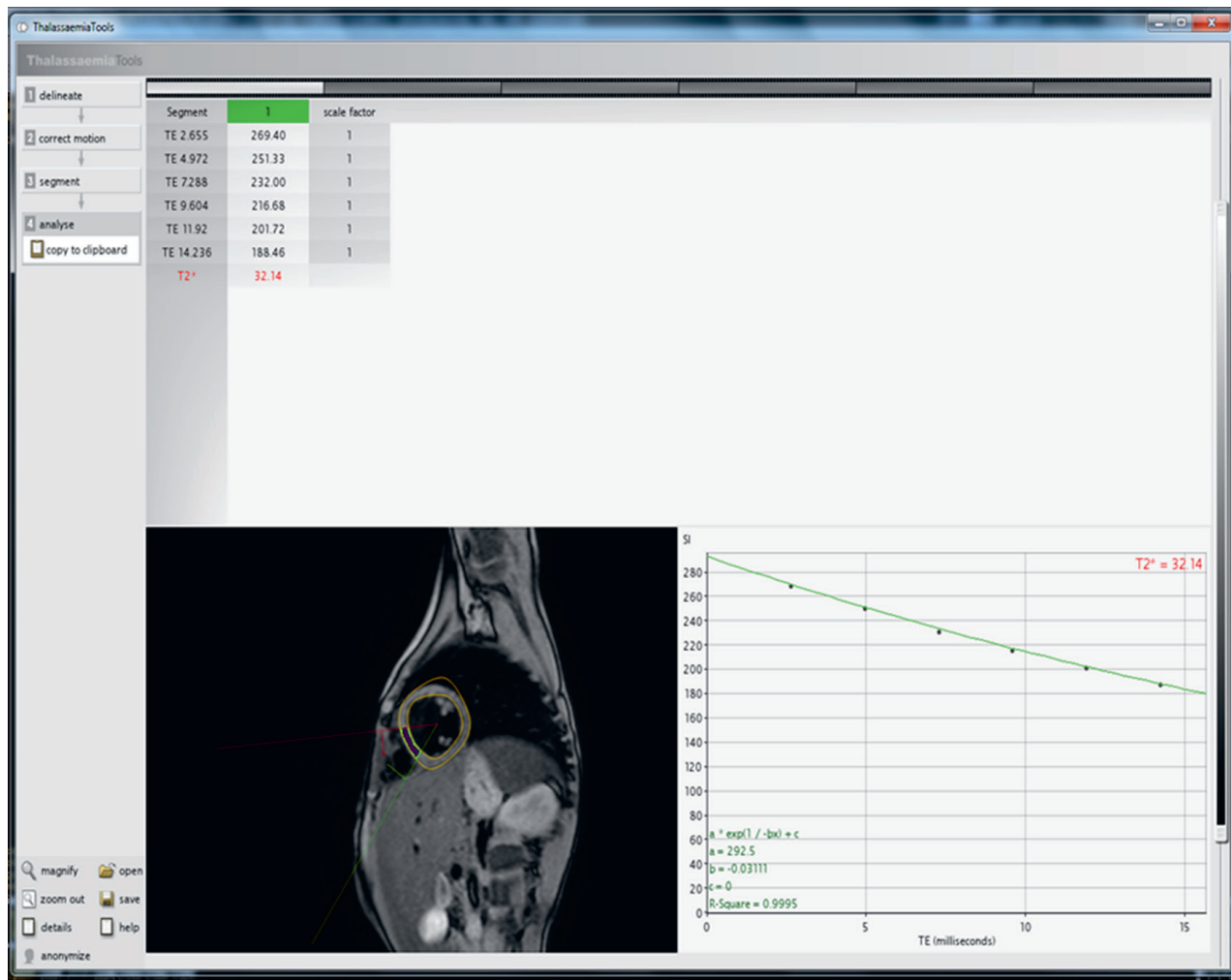


Fig. 3. Cardiac T2* assessments were performed on the ventricular septum using a short-axis, midventricular, cardiac-gated multiecho gradient echo sequence

(range: 0.75–48.75) in the 92 patients who had not undergone splenectomies. Splenic T2* values correlated moderately with hepatic T2* values ($p < 0.001$, $r = 0.516$) (Fig. 5). Serum ferritin levels correlated strongly with both splenic and hepatic T2* values ($p < 0.001$ and 0.001 ; $r = -0.728$ and -0.707 , respectively). Splenic T2* values correlated weakly with liver size ($p = 0.014$), but not with age, cardiac or muscle T2* values, or spleen size ($p = 0.27, 0.21, 0.99$, and

Table 2. Relationships among splenic T2* values, liver and heart features, and serum ferritin levels

Tissue characteristics and serum ferritin	Median (min–max)	p-value	r-value	n
Splenic size [mm]	122 (68–230)	0.393	-0.9	92
Liver T2* [ms]	2.37 (0.6–28.54)	<0.001	0.516	92
Liver size [mm]	145 (98–206)	0.14	-0.255	92
Cardiac T2* [ms]	27.13 (3.95–51.45)	0.211	0.132	92
Muscle T2* [ms]	28.14 (13.93–38.68)	0.992	0.001	73
Serum ferritin	1,969 (302–19,030)	<0.001	-0.728	55

n – number of patients.

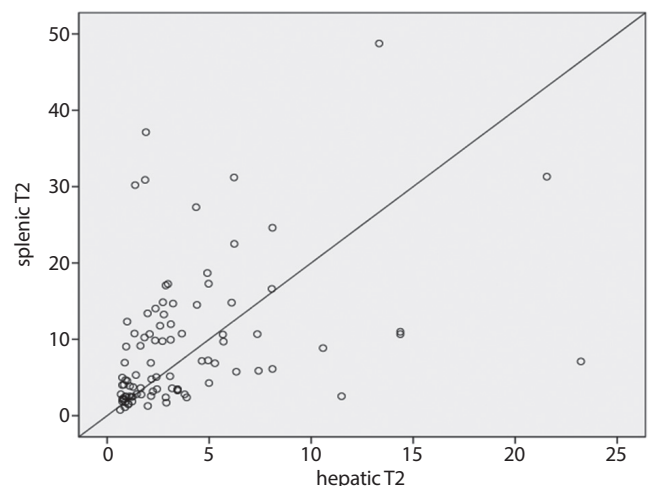


Fig. 5. Scatterplot of the positive correlation between splenic T2* and hepatic T2* values

0.39, respectively) (Table 2). Muscle T2* values correlated with serum ferritin levels ($p = 0.022$, $r = -0.297$) (Table 2).

Cardiac T2* values were lower and liver sizes greater in patients who had undergone splenectomy ($p < 0.001$

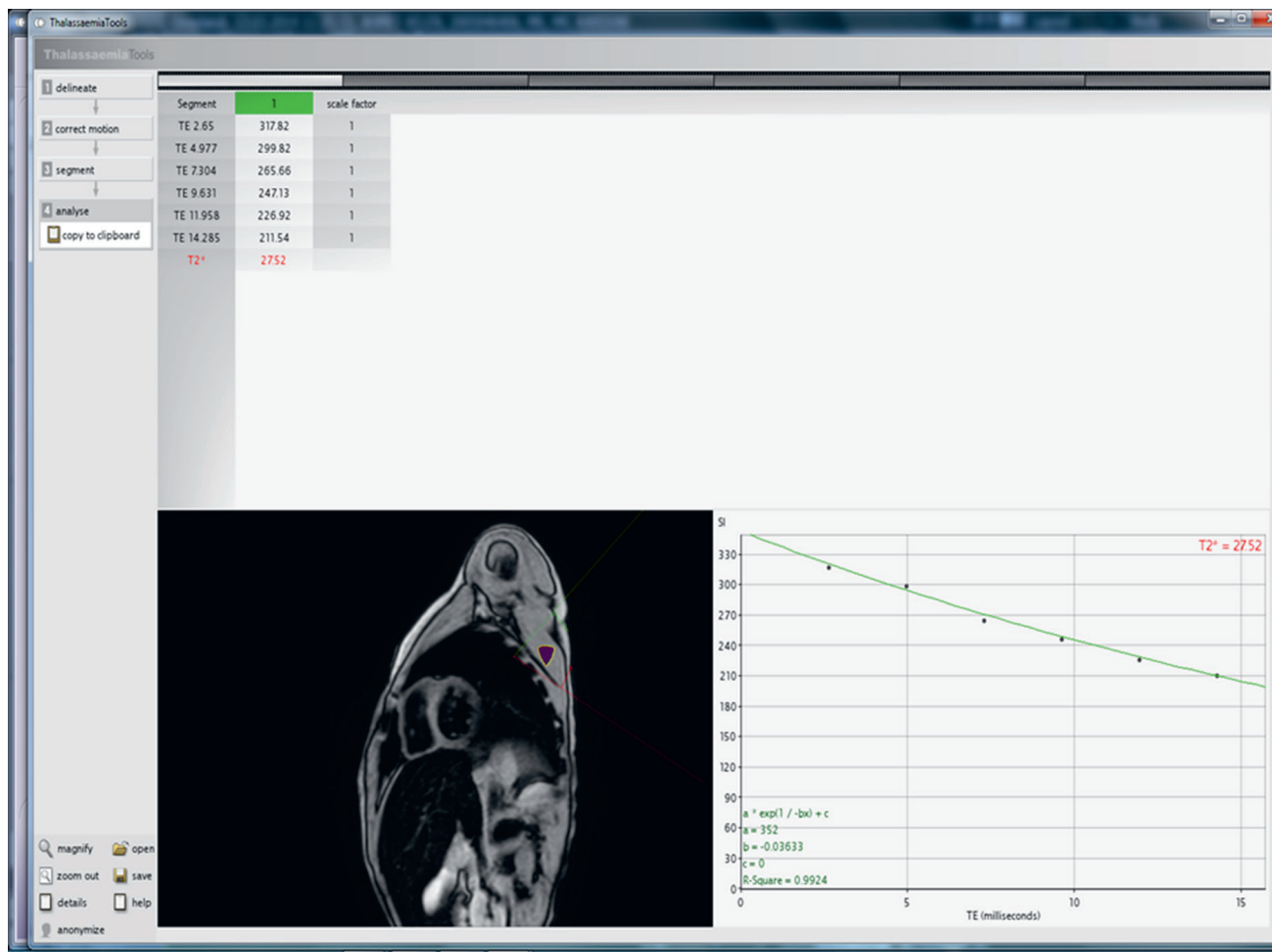


Fig. 4. T2* assessments of the left shoulder girdle muscles were done using short-axis cardiac sequences

Table 3. Comparison of iron loads and serum ferritin levels in patients who had and had not undergone splenectomies

Tissue characteristics and serum ferritin	Patients with splenectomy		Patients without splenectomy		p-value
	median	n	median	n	
Liver T2* [ms]	1.86	37	2.42	92	0.421
Liver size [mm]	161	39	141	92	0.001
Cardiac T2* [ms]	22.27	39	29.45	92	<0.001
Muscle T2* [ms]	28.15	30	28.13	73	0.89
Serum ferritin	2,800	18	1,966	37	0.468

n – number of patients.

and 0.001, respectively). However, no significant between-group differences were evident in terms of muscle or hepatic T2* values or serum ferritin level (p = 0.85, 0.42 and 0.47, respectively) (Table 3).

Discussion

Iron is an essential element involved in oxidative processes and is present in hemoglobin, myoglobin and many enzymes. The iron balance is regulated by increasing

or reducing iron absorption. Humans cannot excrete excess iron. In TM patients, the total body iron level increases upon repeated transfusions in association with enhanced intestinal absorption.^{1,15} Moreover, intestinal iron absorption is accelerated by ineffective erythropoiesis and hypoxia. Senescent erythrocytes from transfused blood and cells resulting from ineffective erythropoiesis are digested by the Kupffer cells of the spleen and liver,^{16,17} increasing iron loading and the blood level of non-transferrin bound iron (NTBI). Non-transferrin bound iron triggers iron poisoning. High levels of NTBI often trigger iron accumulation in various organs, particularly the heart, pancreas and pituitary gland. Iron-mediated cardiac toxicity is a major cause of heart failure and death, particularly in TM patients.^{9,18,19} Excess iron in the pituitary gland and other organs triggers major complications including diabetes mellitus and hypogonadism.²⁰

We found strong correlations between splenic T2* and hepatic T2* values and serum ferritin levels, attributable to the presence of Kupffer cells (phagocytosing erythrocytes) in both the liver and spleen. Few prior studies have sought these correlations. Papakonstantinou et al. used T2*-weighted multiecho gradient-echo sequences to compare the signal intensity ratios of the spleen and

liver to that of the right paraspinal muscle. No correlation was apparent, although all signal intensities correlated with the serum ferritin level.¹¹ Brewer et al. found a weak correlation between the extent of splenic and hepatic iron deposition in thalassemia patients.¹² Our present findings differ, perhaps due to the fact that the mean patient ages in both of the studies cited (16.4 and 24.2 years, respectively) were higher than that of our patients (the mean age of patients who had not undergone splenectomy was 11.4 years). Also, the study by Papakonstantinou et al. had a smaller patient series than ours.¹¹

In our study a moderate correlation was apparent between hepatic and cardiac T2* values, but not between splenic and cardiac T2* values. Excessive liver iron overload reduces the accuracy of T2* imaging, attributable to signal constriction and loss. Although the T2* value is a strong indicator of hepatic iron overload, it does not correlate with liver iron concentrations.^{17,21,22} We suggest that the extent of splenic iron overload may be similar to that of the liver.

Splenectomy may have various effects on tissues. We found that although the cardiac T2* value was lower in patients who had undergone splenectomy, no significant between-group differences were evident in terms of muscle T2* values. This indicated that cardiac iron overload increases after a splenectomy, because cardiac energy metabolism is faster than muscle energy metabolism. Moreover, the muscle T2* value correlated only weakly with the serum ferritin level, indicating that iron accumulation by muscles is low. Liver size was increased in patients who had undergone splenectomy, perhaps due to extramedullary hematopoiesis and a response to the iron overload. The spleen and liver are the primary iron deposition tissues in patients with thalassemia and play important roles in protection against increased iron levels.^{11,21} The spleen also eliminates old and defective erythrocytes. However, this function is performed by the liver in patients who have undergone splenectomy. To our knowledge, the study by Brewer et al. is the only work to explore iron overload in patients who have undergone splenectomy. Cardiac iron overload increased in 40 such patients, but the total hepatic iron load did not.¹²

The limitations of our study include the fact that hepatic iron overload was not confirmed by biopsy and we had no control group.

Conclusions

We found that splenic iron overload was strongly correlated with hepatic iron overload and the serum ferritin level. Splenectomy increased cardiac iron overload and liver size in TM patients. However, as the iron overload in muscles was low, this tissue was not affected by splenectomy.

References

- Ganz T. Molecular control of iron transport. *J Am Soc Nephrol.* 2007; 18(2):394–400.
- Morgan EH, Walters MNI. Iron storage in human disease. *J Clin Pathol.* 1963;16(2):101–107.
- Rodeghiero F, Ruggeri M. Short- and long-term risks of splenectomy for benign haematological disorders: Should we revisit the indications? *Br J Haematol.* 2012;158(1):16–29.
- Garbowski MW, Carpenter JP, Smith G, et al. Biopsy-based calibration of T2* magnetic resonance for estimation of liver iron concentration and comparison with R2 Ferriscan. *J Cardiovasc Magn Reson.* 2014;16:40.
- Hankins JS, McCarville MB, Loeffler RB, et al. R2* magnetic resonance imaging of the liver in patients with iron overload. *Blood.* 2009; 113(20):4853–4855.
- Wood JC. Guidelines for quantifying iron overload. *ASH Educ Program Book.* 2014;2014(1):210–215.
- Christoforidis A, Haritandi A, Tsatra I, Tsitourides I, Karyda S, Athanassiou-Metaxa M. Four-year evaluation of myocardial and liver iron assessed prospectively with serial MRI scans in young patients with β -thalassaemia major: Comparison between different chelation regimens. *Eur J Haematol.* 2007;78(1):52–57.
- Noetzli LJ, Carson SM, Nord AS, Coates TD, Wood JC. Longitudinal analysis of heart and liver iron in thalassemia major. *Blood.* 2008; 112(7):2973–2978.
- Carpenter JP, Roughton M, Pennell DJ. International survey of T2* cardiovascular magnetic resonance in β -thalassaemia major. *Haematologica.* 2013;98(9):1368–1374.
- Wang ZJ, Fischer R, Chu Z, et al. Assessment of cardiac iron by MRI susceptometry and R2* in patients with thalassemia. *Magn Reson Imaging.* 2010;28(3):363–371.
- Papakonstantinou O, Drakonaki EE, Maris T, Vasiliadou A, Papadakis A, Gourtsoyiannis N. MR imaging of spleen in beta-thalassemia major. *Abdom Imaging.* 2015;40(7):2777–2782.
- Brewer CJ, Coates TD, Wood JC. Spleen R2 and R2* in iron-overloaded patients with sickle cell disease and thalassemia major. *JMRI.* 2009; 29(2):357–364.
- Kolnagou A, Natsiopoulou K, Kleanthous M, Ioannou A, Kontoghiorghes GJ. Liver iron and serum ferritin levels are misleading for estimating cardiac, pancreatic, splenic and total body iron load in thalassemia patients: Factors influencing the heterogenic distribution of excess storage iron in organs as identified by MRI T2*. *Toxicol Mech Methods.* 2013;23(1):48–56.
- Papakonstantinou O, Alexopoulou E, Economopoulos N, et al. Assessment of iron distribution between liver, spleen, pancreas, bone marrow, and myocardium by means of R2 relaxometry with MRI in patients with beta-thalassemia major. *J Magn Reson Imaging.* 2009; 29(4):853–859.
- Tziomalos K, Perifanis V. Liver iron content determination by magnetic resonance imaging. *WJG.* 2010;16(13):1587–1597.
- Siegelman ES, Mitchell DG, Semelka RC. Abdominal iron deposition: Metabolism, MR findings, and clinical importance. *Radiology.* 1996; 199(1):13–22.
- Gandon Y, Olivie D, Guyader D, et al. Non-invasive assessment of hepatic iron stores by MRI. *The Lancet.* 2004;363(9406):357–362.
- Wood JC. Estimating tissue iron burden: Current status and future prospects. *Br J Haematol.* 2015;170(1):15–28.
- Matter RM, Allam KE, Sadony AM. Gradient-echo magnetic resonance imaging study of pancreatic iron overload in young Egyptian beta-thalassemia major patients and effect of splenectomy. *Diabetol Metab Syndr.* 2010;2:23.
- Galanello R, Origa R. Beta-thalassemia. *Orphanet J Rare Dis.* 2010;5:11.
- Queiroz-Andrade M, Blasbalg R, Ortega CD, et al. MR imaging findings of iron overload. *Radiogr Rev Publ Radiol Soc N Am Inc.* 2009;29(6): 1575–1589.
- Westphalen ACA, Qayyum A, Yeh BM, et al. Liver fat: Effect of hepatic iron deposition on evaluation with opposed-phase MR imaging. *Radiology.* 2007;242(2):450–455.

The impact of health education on treatment outcomes in heart failure patients

Natalia Alicja Świątoniowska-Lonc^{1,B-D}, Agnieszka Sławuta^{2,B-D}, Krzysztof Dudek^{3,B,C}, Katarzyna Jankowska^{4,B,D}, Beata Katarzyna Jankowska-Polańska^{1,A,E,F}

¹ Faculty of Health Sciences, Wrocław Medical University, Poland

² Department of Internal Medicine, Occupational Diseases, Hypertension, and Clinical Oncology, Wrocław Medical University, Poland

³ Department of Logistic and Transportation Systems, Wrocław University of Science and Technology, Poland

⁴ Department of Conservative Dentistry and Pedodontics, Wrocław Medical University, Poland

A – research concept and design; B – collection and/or assembly of data; C – data analysis and interpretation;

D – writing the article; E – critical revision of the article; F – final approval of the article

Advances in Clinical and Experimental Medicine, ISSN 1899–5276 (print), ISSN 2451–2680 (online)

Adv Clin Exp Med. 2020;29(4):481–492

Address for correspondence

Natalia Alicja Świątoniowska-Lonc

E-mail: natalia.swiatoniowska@student.umed.wroc.pl

Funding sources

None declared

Conflict of interest

None declared

Received on September 20, 2019

Reviewed on October 28, 2019

Accepted on December 5, 2019

Published online on April 29, 2020

Abstract

Background. In 2016 heart failure (HF) affected between 600,000 and 700,000 people in Poland being one of the most common causes of hospitalization and death. Health education is an element of patient treatment aimed at improving the level of self-care and adherence to the treatment recommendations.

Objectives. To perform a systematic review and meta-analysis of the available literature in order to determine the role of health education in HF treatment and its impact on outcomes in patients with chronic HF.

Material and methods. A search was performed in the MEDLINE, PubMed and Scopus databases from January 2010 to January 2019 for the impact of health education on treatment outcomes in HF patients.

Results. A total of 16 studies from 12 countries on 5 continents were analyzed. The meta-analysis focused on the impact of education on outcomes in 944 study group patients. We found that the overall impact of education on outcomes was positive (+1 standard deviation (SD); 95% confidence interval (95% CI) >0). After education was provided, the target patients improved in terms of self-care (mean change (MC) = 13.49; $p = 0.003$; $I^2 = 99.47\%$). Self-care also improved in the controls, but the improvement was less marked (MC = 9.56; $p = 0.001$; $I^2 = 98.33\%$). No impact of education on quality of life (QoL) was confirmed (95% CI = 0).

Conclusions. The greatest benefit of education is seen in terms of adherence to pharmaceutical treatment and self-care, while QoL was not associated with education.

Key words: treatment, education, outcome, heart failure

Cite as

Świątoniowska-Lonc NA, Sławuta A, Dudek K, Jankowska K, Jankowska-Polańska BK. The impact of health education on treatment outcomes in heart failure patients. *Adv Clin Exp Med.* 2020;29(4):481–492. doi:10.17219/acem/115079

DOI

10.17219/acem/115079

Copyright

© 2020 by Wrocław Medical University

This is an article distributed under the terms of the Creative Commons Attribution 3.0 Unported (CC BY 3.0) (<https://creativecommons.org/licenses/by/3.0/>)

Introduction

Depending on the diagnostic criteria used and the population studied, worldwide heart failure (HF) incidence is 100–900 cases per 100,000 person-years. Its global prevalence is estimated at 37.7 million cases. In developed countries, HF affects 1–2% of the adult population.¹ The number of HF patients in the USA currently stands at 5.8 million, and is expected to exceed 8 million by the year 2030. One in 5 individuals can be expected to develop HF at some point in their life.² Heart failure is a clinical syndrome associated with frequent hospitalizations and a complex treatment regimen. Despite advances in HF diagnosis and treatment, 50% of patients globally are rehospitalized within 6 months of discharge, and approx. 300,000 die annually due to HF decompensation.^{3,4} Non-adherence to treatment is the primary cause of mortality and rehospitalization in HF patients.⁵ Out of these rehospitalizations, between 1/3 and 1/2 may be preventable.⁶

Heart failure treatment guidelines produced by scientific societies emphasize the role of multidisciplinary care, comprising self-care, compliance with treatment and follow-up visits as major factors that improve patient outcomes. In HF treatment, lifestyle changes, self-care, health-promoting practices, and symptom monitoring and management are as important as pharmaceutical treatment. The objective of the entire treatment regimen is to improve the patient's physical fitness and quality of life (QoL), prevent rehospitalization and reduce overall mortality.⁷ Considering the complexity of HF and its treatment, relevant knowledge is a major factor in effective therapy. Education is therefore a component of the treatment process in HF, and its main areas include preparing the patient for cooperation with the treatment team, flexible dosages of diuretics, adherence to a low-sodium diet, exercise, daily weighing, fluid intake restrictions, recommended vaccinations, monitoring symptoms, and reacting to exacerbations.

Effective education programs for HF patients have been shown to enhance the patients' knowledge, improve their self-care capabilities, reduce the number of hospitalizations, and improve outcomes and QoL.⁸ In HF patients, self-care has been defined as a naturalistic decision-making process with 2 components: self-care maintenance and self-care management.

Traditional patient education focuses on providing learning material. However, this form of education is often insufficient to influence patients' self-care behavior. The available study results remain unsatisfactory, demonstrating little impact of education on better HF patient outcomes. The overall objective of the implemented educational projects is the development of the patients' self-management skills and capabilities of improving their own QoL. The studies that are available do not describe education as a specific intervention; it is typically part of the HF management program. The benefits of education

are well understood, but it is difficult to tell which education method is the most effective.

According to the World Health Organization (WHO), health education is a process consisting of planned learning and communication opportunities that improve knowledge on health, health-related skills and life skills conducive to health in individuals and communities. Patient counseling is based on behavioral therapy and social cognitive therapy.⁹

The available study results highlight the importance of motivational education. Motivational conversations represent an individual-focused approach, in which thoughtful listening is used rather than confrontation. Medical professionals preparing a patient for performing self-care should use the "education through motivation" approach, as this form of education has been found to be more effective than other methods. Patients demonstrate a willingness to change their behavior and employ strategies aimed at actively taking responsibility for their own health. Education is even more effective if the process is personalized, and patients receiving individualized education show more clinical improvement than those under routine care.^{10,11}

Publications on the effectiveness of education and its association with the effectiveness of HF treatment remain scarce. Authors with an interest in HF report a need for further studies that would evaluate the effectiveness of education with regard to secondary outcomes in HF patients.

Objectives

The aim of the study was to perform a systematic review and meta-analysis of the available literature in order to determine the role of health education in HF treatment and its impact on outcomes in patients with chronic HF.

Methods

The present study investigated the impact and effectiveness of health education in any form with regard to chronic HF treatment outcomes. The outcomes analyzed include QoL, compliance, self-care behavior, and rehospitalization.

Search strategies

The MEDLINE, PubMed and Scopus databases were searched using the following keywords: "education", "chronic heart failure", "self-care" OR "self-management" OR "persistence" OR "adherence" OR "compliance" AND "outcomes". Additional criteria were used to restrict the search scope to research papers published in English between January 2010 and January 2019. Review papers, duplicates and other meta-analyses were excluded.

The final material consisted of 17 papers. Subsequent analyses were performed using the Cochrane Review Manager guidelines.¹² Adherence and compliance, self-care, self-management, QoL, and HF-associated rehospitalizations were understood as secondary outcomes. The search procedure is presented in detail in Fig. 1.

Description of the studies included

The 17 studies included in the meta-analysis were performed in 12 countries on 5 continents. The meta-analysis focused on the impact of education on outcomes in 944 HF patients (out of 3,567 patients in total). Sixteen of the studies analyzed were randomized. The most common randomization procedures included the use of a computer-generated sequence (5 studies) or a randomization center office (2 studies). In 3 studies, randomization was performed by nurses, and in 2 by physicians. One study used sealed envelopes, and another used the website www.randomization.com (Table 1).

Twelve of the studies enrolled hospitalized patients following an acute event, and 5 enrolled outpatients. Male patients comprised 57.5% of the study groups. The mean patient age was 66.9 ±13.2 years. Exclusion criteria were as follows: cognitive impairment (9 studies), severe comorbidities (11 studies), kidney disease (3 studies), life expectancy up to 6 months (1 study) or up to 12 months (3 studies), and surgery within 6 months preceding the study (2 studies).

Questionnaires used to assess the quality of life

The following questionnaires were used:

1. The Kansas City Cardiomyopathy Questionnaire (KCCQ) is a 23-item (15 questions), self-administered, disease-specific instrument that quantifies 6 domains (scales) and 2 summary scores of the patient’s health status. The 6 domains are physical limitations, symptom score, symptom change, self-efficacy, social interference, and QoL. The 2 summary scores are labelled clinical summary scores and overall summary scores. All scale scores are transformed to 0–100 scale, in which a higher score indicates a better health-related quality of life (HRQoL).

2. The Iranian Heart Failure QoL questionnaire (IHF-QoL), a 16-item questionnaire in which questions 1–4 and 6 measure the symptoms of the disease and their severity (score 5–20); question 7 is about physical limitations in performing activities (score 5–15); questions 8, 10, 12, and 13 are about social interference (score 4–12); questions 5, 9 and 11 are about psychological conditions (score 3–10); questions 14 and 15 are about knowledge and self-efficacy (score 2–6); and question 16 is about the patient’s life satisfaction (score 1–3). The questions are answered using a 3- or 4-point Likert scale. The total QoL scores range from 15 to 63 and are calculated by summing the scores of the questions. Higher scores indicate a higher QoL in total and in each dimension.

3. The Minnesota Living with Heart Failure Questionnaire (MLHFQ) has 21 items, which cover the physical

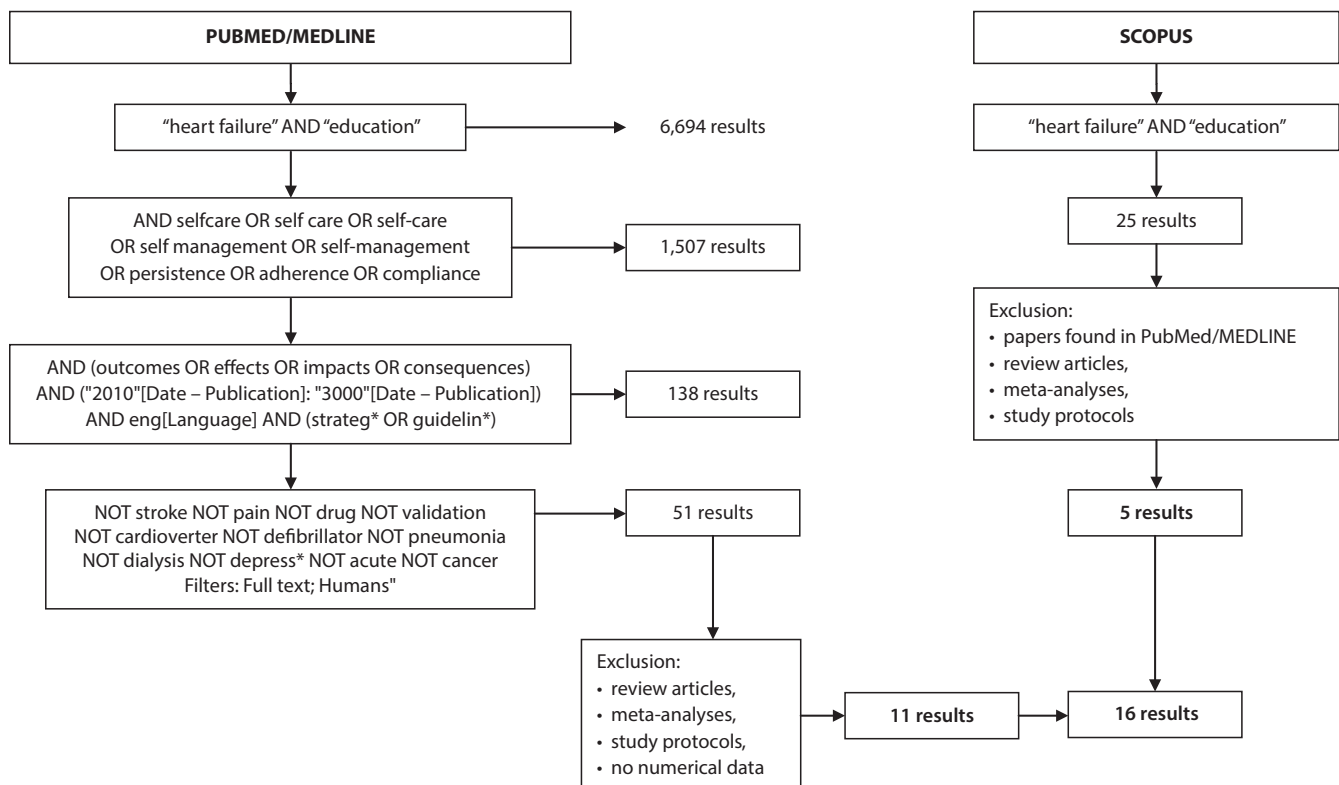


Fig. 1. Study flow diagram

Table 1. Summary of studies of the impact of education on outcomes in HF

No. of study	Reference and year	Educator	Study group		Intervention	Results	
						follow-up	(IG vs CG)
1.	Deka et al., 2018 ¹⁴	N/o	total	30 stable HF patients NYHA class I–III aged 64.7 ±11.5 years	IG: education via Internet, FCHR, weekly Internet-based education/discussion meeting CG: education via Internet, FCHR	8 weeks	compliance to physical activity: 399 ±96 vs 368 ±131
			IG	n = 15			
			CG	n = 15			
2.	Boyde et al., 2018 ⁶	HF nurse	total	200 HF patients	IG: the DVD with manual, teaching sessions CG: written materials	28 days	unplanned hospital readmission: 97 (7) vs 98 (4 – HF-related)
			IG	n = 100 aged 64 ±12.4 years NYHA: II – 34, III – 60, IV – 5		3 months	unplanned hospital readmission: 92 (8) vs 94 (10) knowledge: 13 (12–14) vs 13 (11–14) management: 62.5 (IQR 45 – 70) vs 55 (IQR 40–70)
			CG	n = 100 aged 64 ±12.9 years NYHA: II – 30, III – 64, IV – 5		12 months	unplanned hospital readmission: 83 (8) vs 88(14) post-recruitment knowledge: 13 (IQR 11–14) vs 13 (IQR 12–14) management: 55 (IQR 31.25–65.00) vs 50 (IQR 35–75)
3.	Kato et al., 2016 ¹⁵	nurses, dietician, pharmacist	total	32 HF patients	IG: face-to-face education, written materials CG: standard care without special education	1 month	self-care level: IG: 37 baseline vs 20 after 1 month vs CG: 37 vs 30 (the lower the score, the higher the level) knowledge: 13.1 ±1.7 vs 8.7 ±4.8
			IG	n = 15 aged 64 ±15 years NYHA: II – 5		6 months	self-care level: no significant changes between CG and IG (F = 0.44; p = 0.65) knowledge: 11.5 ±2.0 vs 9.7 ±2.6
			CG	n = 17 aged 65 ±17 years NYHA: II – 9			
4.	Hägglund et al., 2015 ¹⁶	healthcare providers	total	72 HF patients aged 75 ±8 years	IG: table (HIS), phone calls CG: the standardized discharge information	3 months	self-care: 17 (IQR: 13, 22) vs 21 (IQR: 17, 25) (the lower the score, the higher the level) QoL: 65.1 (IQR: 38.5, 83.3) vs 52.1 (IQR: 41.1, 64.1) knowledge: 13 (IQR 12–14) vs 13 (IQR 12–14) hospital days related with HF: 34 vs 113
			IG	n = 32 aged 75 ±8 years NYHA: II – 38%, III – 62%			
			CG	n = 40 aged 76 ±7 years NYHA: II – 18%, III – 82%			
5.	Kinugasa et al., 2014 ¹⁷	nurse, pharmacist, dietitian	overall	277 HF inpatients aged 74 ±13 years	IG: oral teaching sessions	3 months	HF hospitalization: 16% vs 36.8%
			IG	n = 144 aged 75 ±13 years NYHA: III/IV – 11.8		12 months	IG: 50% reduction risk of all-case mortality and unplanned HF-rehospitalization (management program). Multidisciplinary intensive education as the most effective intervention to reduce the risk of the primary endpoint among all medical and non-medical interventions: HR 0.387; 95% CI: 0.200–0.738; p < 0.001.
			CG	n = 131 aged 74 ±13 years NYHA: III/IV – 9			

Table 1. Summary of studies of the impact of education on outcomes in HF – cont.

No. of study	Reference and year	Educator	Study group		Intervention	Results	
						follow-up	(IG vs CG)
6.	Boyne et al., 2014 ¹³	HF nurses and cardiologist	total	382 HF patients aged 71 ±11.2 years	IG: oral and written information, planned outpatient clinic visits, telemonitoring system CG: oral and written information, clinic visits	3 months	self-care level: 17.4 ±6.1 vs 20 ±5.1 (the lower the score, the higher the level) knowledge: 13.3 ±1.1 vs 12.5 ±1.8
			IG	n = 197 aged 71 ±11.9 years NYHA: II – 110, III – 79, IV – 8		6 months	self-care level: 17.1 ±4.4 vs 20 ±5.7 knowledge: 13.2 ±1.2 vs 12.4 ±1.9
			CG	n = 185 aged 71.9 ±10.5 years NYHA: II – 109, III – 74, IV – 2		12 months	Self-care level: 17.4 ±4.5 vs 20.8 ±5.8 (self-care abilities improved with 1.5 points, whereas no changes were found in patients receiving usual care (p < 0.001)). knowledge: 13.5 ±1.2 vs 12.6 ±1.8 (knowledge of patients in the telemonitoring group significantly improved with 0.9 point on a 15-point scale (p < 0.001)). Adherence for activity recommendations improved (p = 0.023) after 3 months and importance of medication adherence increased after 6 (p = 0.012) and 12 months (p = 0.037).
7.	Donner Alves et al., 2012 ¹⁸	medical and nursing staff	total	46 HF patients aged 58 ±10 years	IG: training session, written materials	6 weeks	knowledge about diet in HF: 15.4 vs 12.4 QoL: 23.5 ±17.8 vs 27.3 ±18.1
			IG	n = 23 aged 55 ±10 years NYHA: I e II – 17		6 months	knowledge about diet in HF: 15.8 vs 12.6 QoL: 21.1 ±17.1 vs 29.2 ±14.9
			CG	n = 23 aged 61 ±9 years NYHA: I e II – 19			
8.	Mussi et al., 2013 ¹⁹	HF nurses	total	200 HF patients	IF: home visits and phone calls	6 months	self-care: 22.36 ±6.46 vs 30.91 ±7.3 (the lower the score, the higher the level) knowledge: 71.5% vs 54.95% adherence: 73.52% vs 57.44%
			IG	n = 101 aged 62.49 ±13.65 years NYHA: I – 7, II – 38, III – 41, IV – 13			
			CG	n = 99 aged 63.37 ±12.05 years NYHA: I – 6, II – 44, III – 40, IV – 8			
9.	Leventhal et al., 2011 ²⁰	HF nurses	total	42 HF patients aged 77 ±6.5 years	IG: written materials, face-to-face education at home, phone calls	12 months	Readmission: 22 (52%) patients had an all-cause readmission or died. Only 3 patients were hospitalized with HF decompensation. QoL: no significant effect of the intervention was found on HF related to QoL.
			IG	n = 22 aged 76.7 ±7.1 years LVEF: <45% n = 10			
			CG	n = 20 aged 77.6 ±6 years LVEF: <45% n = 11			

Table 1. Summary of studies of the impact of education on outcomes in HF – cont.

No. of study	Reference and year	Educator	Study group		Intervention	Results	
						follow-up	(IG vs CG)
10.	Ciccone et al., 2010 ²¹	nurses, general practitioners, family physicians, specialist	total	1,160 patients with CVD, diabetes, HF, and/or at risk of CVD aged 64 ±11.2 years	IG: home visit, written materials	18 months	compliance (physical activity): an increase in the number of days per week of physical activity for the entire group from 2.53 to 4.18 days and in exercise time from 19.87 to 32.9 h per session good quality of diet: an increase from 39.4% to 80.7%
11.	Athar et al., 2018 ²²	physician	total	97 HF patients	IG: written materials	30 days	self-care: 11.8 ±2.8 vs 11.7 ±3 30-day survival without readmission or ED visit: 82.6% vs 84.1%
			IG	n = 50 aged 70.3 ±13.7 years LVEF: 45.8 ±16.1			
			CG	n = 47 aged 72.4 ±11.7 years LVEF: 46.5 ±17.5			
12.	Loghmani and Monfared, 2018 ⁴	N/o	total	150 HF patients aged 55 ±14.52 years	IG: dietary notes and motion exercises, lecture, poster and educational pamphlets	1 month	knowledge: 47.24 vs 32.86 function: 36.45 vs 32.56
13.	Wang et al., 2017 ²³	N/o	total	62 HF patients	IG: face-to-face interviews, written materials, lectures	3 months	self-care: 2.71 ±2.72 vs 6.94 ±4.7 (the lower the score, the higher the level) QoL: 20.74 ±14.66 vs 35.29 ±13.67 knowledge: 9.24 ±1.03 vs 5.02 ±1.11
			IG	n = 31 aged 63.97 ±14.47 years			
			CG	n = 31 aged 62.84 ±13.4 years			
14.	Vaillant-Roussel et al., 2016 ²⁴	GPs	total	241 HF patients	IG: education sessions, written materials	19 months	QoL: 33.4 ±22.1 vs 27.2 ±23.3
			IG	n = 115 aged 74.7 ±10.3 years NYHA: I – 14, II – 69, III – 32			
			CG	n = 126 aged 73.54 ±10.8 years NYHA: I – 25, II – 67, III – 34			
15.	Korzhan and Krasnokutskiy, 2016 ²⁵	family physicians	total	371 HF patients, NYHA II or III	IG: training program	6 months	compliance (salt and fluids): 50% vs 19% compliance (physical activity): 61% vs 20%
			IG	n = 173 aged 63 ±8.1 years			
			CG	n = 198 aged 64 ±8.4 years			
16.	Abbasi et al., 2018 ²⁶	nurses, cardiovascular specialist	total	60 HF patients	IG: self-management education program, written and interactive materials, phone calls, follow-up visits CG: the routine education	3 months	QoL: 46.2 ±5.74 vs 42.83 ±7.24
			IG	n = 30 aged 45.23 ±15.93 years NYHA: I – 16 ±53.3, II – 14 ±46.7			
			CG	n = 30 aged 52.3 ±15.88 years NYHA: I – 17 ±56.6, II – 13 ±43.4			

N/o – no information; NYHA – New York Heart Association; GP – general practitioner; CG – control group; IG – intervention group; FCHR – the Fitbit Charge HR; LVEF – left ventricular ejection fraction; CVD – cardiovascular disease; HF – heart failure; ED – emergency department; IQR – interquartile range; 95% CI – 95% confidence interval; HR – hazard ratio; QoL – quality of life.

dimension (8 items), emotional dimension (5 items) and additional dimension (8 items). Each item is scored from 0 to 5, and the total score ranges from 0 to 105. A lower score indicates better QoL.

Statistical analysis

In the case of continuous-scale studies (comparing means between cases and controls), the meta-analysis used Hedges' *g* to calculate the standardized mean difference in the fixed effects model. Heterogeneity statistics were subsequently used to calculate the total standardized mean difference in the random effects model.

In each meta-analysis, the mean change (MC) in outcomes measured before and after the educational intervention was used. Positive MC values indicate higher outcome scores after the educational intervention (i.e., improved outcome compared to that measured before the intervention), while negative MC values indicate higher outcome scores before the educational intervention (i.e., deteriorated outcomes).

As the authors of the papers included in the meta-analysis used a variety of questionnaires, all the scales were converted into a 0–100 scale using the following formula:

$$\frac{x - \min}{\max - \min} \times 100$$

where *min* and *max* stand for the minimum and maximum number of points that could be obtained in a given questionnaire.

Additionally, if a higher score represented a lower level of self-care/knowledge/QoL, the scale was reversed for the purpose of this meta-analysis.

An I^2 parameter was used to assess the degree of heterogeneity. The I^2 value was calculated as $I^2 = 100\% \times (Q - df)/Q$, where *Q* is the statistics of Cochran heterogeneity and *df* is degrees of freedom. The I^2 values are percentages. The 95% uncertainty intervals were calculated according to the proposals set forth by Higgins and Thompson.²⁷

Results

Educational interventions

The studies analyzed included the following types of educational interventions:

1. Training/education sessions for patients (educational sessions: 8 studies; written materials or DVDs: 8 studies; online learning: 2 studies). The sessions included such topics as diet, fluid restriction, exercise, pharmaceutical treatment, and knowledge related to HF. Educational sessions were provided by specialized nurses, physicians, dietitians, pharmacists, physical therapists, and social workers. A variety of methods and materials were used,

such as booklets, discussion services, brochures, lectures, newsletters, multimedia presentations, as well computer programs and software.

2. Patient reminder systems (phone calls: 3 studies; home visits: 3 studies). Regular telephone calls or home visits were conducted by HF nurses and/or physicians. During the phone calls, self-care and the application of knowledge provided in the sessions were discussed. Home visits involved physical, psychosocial and environmental evaluations; repeat education to improve self-care; and setting individual treatment objectives.

3. Telemonitoring systems (2 studies), involving 2 methods. In the first method, patients were presented with pre-set dialogs and questions about their symptoms, knowledge and behavior on a daily basis, and provided answers using touch keys. In the event of any problems, an HF nurse contacted the patient.¹³ In the other method, Fitbit Charge HR (FCHR), information on step count, heart rate, and minutes of exercise were tracked, recorded and transmitted in real time. Exercise sessions could also be recorded using a built-in stopwatch.¹⁴

The effectiveness of the interventions

The impact of education on knowledge about the illness

The impact of education on patients' knowledge about the illness was measured in 7 studies (Fig. 2). In the meta-analysis, the total effect of education was positive (+1 standard deviation (SD) to the right of 0, where 0 indicates no impact), and the lower bound of the 95% confidence interval (95% CI) was greater than 0.

The impact of education on adherence and compliance

Adherence and compliance in HF patients was evaluated in 7 studies (Fig. 3). Due to the lack of control groups

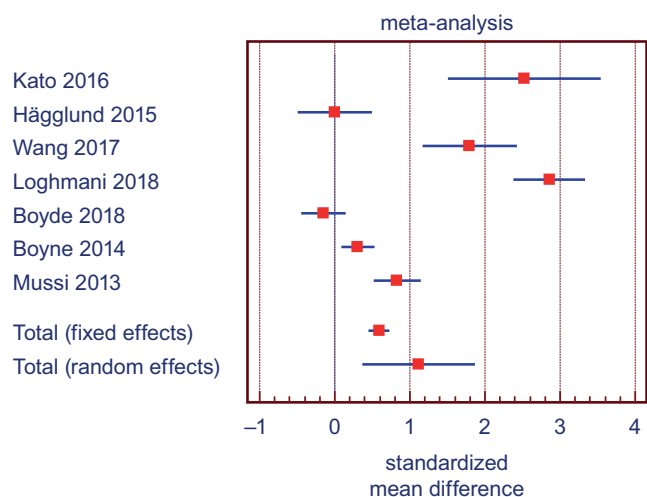


Fig. 2. The impact of education on knowledge (means and 95% CI values)

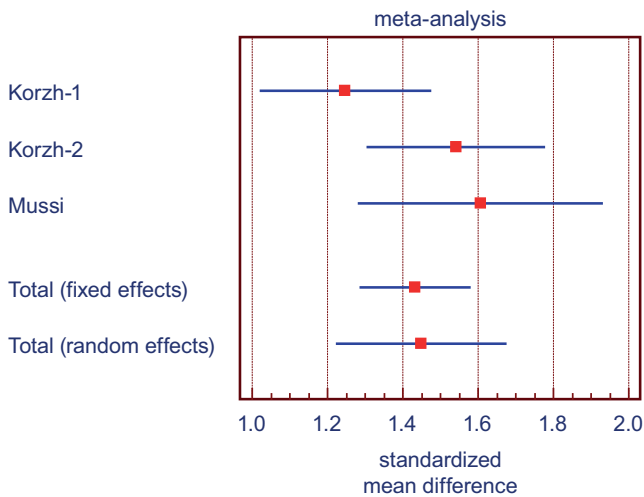


Fig. 3. The impact of education on adherence and compliance (means and 95% CI values)

and discrepancies in the reported data, only 3 papers were ultimately included in this part of the meta-analysis. The total effect of education was positive (over +1 SD to the right of 0, where 0 indicates no impact), and the lower bound of the 95% CI was greater than 0 (the left end point of the horizontal segment).

The impact of education on self-care

Patients who received education

The impact of education on self-care in HF patients was evaluated in 6 studies (Fig. 4). The meta-analysis result was statistically significant ($p = 0.003$), which means that evidence of significant changes in self-care was found among those patients who received education. An MC value of 13.49 indicates that the mean increase in the self-care score resulting from educational interventions was 13.49 points. The test for heterogeneity demonstrated considerable heterogeneity of the studies analyzed ($p < 0.001$), and therefore these results were obtained using the random effects model. The heterogeneity coefficient was $I^2 = 99.47\%$.

The forest plot shows a total MC value of 13.49 points from the meta-analysis (95% CI = 4.52–22.46). This means that after

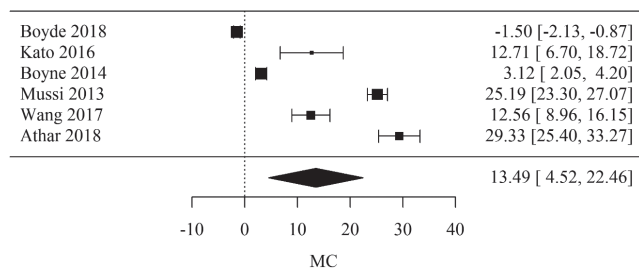


Fig. 4. The impact of education on self-care in the group of patients who received education

MC – mean change.

educational interventions, the targeted patients in the studies improved their self-care scores by a mean of 13.49 points. Self-care improved after education in all the studies included in the meta-analysis except for Boyde et al.⁶

Patients who did not receive education

Significant evidence of changes in the self-care level was found among patients who were not targeted by the educational interventions (Fig. 5). An MC value of 9.56 indicates that after the period designated for the educational intervention, these patients scored, on average, 9.56 points higher on the self-care scale. The test for heterogeneity demonstrated considerable heterogeneity of the studies analyzed ($p < 0.001$), and therefore these results were obtained using the random effects model. The heterogeneity coefficient was $I^2 = 98.33\%$.

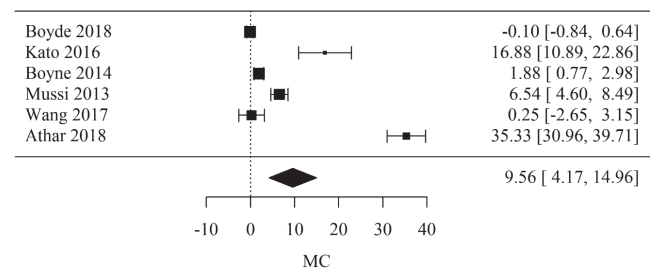


Fig. 5. Changes in self-care in the group of patients who did not receive education

The impact of education on QoL

The impact of education on QoL in HF patients was evaluated in 6 studies (Fig. 6) on the basis of the results of questionnaires evaluating QoL at the baseline and the follow-up points. Due to the lack of a control group in Donner Alves et al. and Leventhal et al., only 4 studies were included in the further analysis.^{18,20} No impact of education on QoL

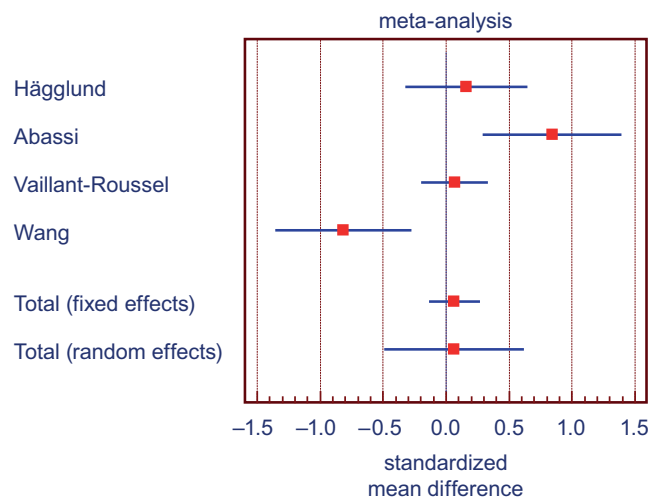


Fig. 6. The impact of education on QoL (means and 95% CI values)

was found in the studies analyzed. In all the studies, 95% CI was 0, except for the study by Wang, who found a negative impact of education on QoL.²³

The impact of education on HF-associated rehospitalizations

The impact of education on the number of HF-associated rehospitalizations in HF patients was evaluated in only 3 studies. Hägglund et al. measured the number of days between subsequent hospitalizations for HF (intervention group 113 days vs control group 64 days).¹⁶ Leventhal et al. reported the number of HF-related readmissions.²⁰ In a study by Vaillant-Roussel, 18 patients in the intervention group and 22 patients in the control group had hospitalizations for CHF decompensation.²⁴ Due to the lack of complete data, a meta-analysis could not be performed for this variable.

Discussion

Factors interfering with HF care include insufficient knowledge on the part of the patients, which results in inadequate self-control and self-care, as well as a lack of a comprehensively integrated care system. Therefore, a new model of care for HF patients is required – one that would include education focused on the implementation of standards to lower the rate of rehospitalizations and mortality, reduce costs, and improve the QoL of patients and their families.

The purpose of the present meta-analysis was to investigate the impact and effectiveness of health education in any form with regard to chronic HF treatment outcomes. The outcomes that were analyzed included QoL, compliance, self-care behavior, and rehospitalization. This meta-analysis confirmed that studies on the role of education for HF patients and its impact on outcomes remain insufficient. Knowledge and education are presented by many authors as important factors in HF treatment, but the studies published report few actual educational interventions and their effects. Out of all the available publications, only 16 met the selection criteria for the present meta-analysis. The meta-analysis only included studies that compared the impact of education using an intervention group and a control group, which makes it unique.

Through the meta-analysis, we confirmed the significance of education in patients with HF and its beneficial role in outcomes. In many cases, patients after an educational intervention experienced a greater improvement of outcomes than the controls. The few studies included in the meta-analysis demonstrate that most education methods and forms offer good results and positively affect outcomes. Improved outcomes were found in terms of compliance, self-care, the rehospitalization rate, and knowledge. Masterson Creber et al. reported that motivational interventions are better than traditional education

programs that focus on providing didactic information.¹¹ The authors emphasized that overall educational approaches for improving self-care in HF had been developed and tested with little impact on HF outcomes. Riegel et al. stated that the motivational approach improves patients' involvement in discussions regarding self-care, while Paradis et al. asserted that it promotes awareness and prepares patients for performing self-care behavior.^{10,28} In the papers that met the inclusion criteria for the present meta-analysis, education was provided in various forms. However, the dominant approaches included face-to-face educational sessions and the use of written materials. Online learning, home visits or phone calls were also used, albeit less commonly. Unfortunately, the variety of educational methods applied precludes the identification of the best approach or the formulation of clear conclusions.

By “motivational interventions”, the authors mean counseling focused on cognitive-behavioral therapy and cognitive therapy, whereby the patients' willingness to change their behavior is assessed and strategies are developed to promote efforts to change this behavior in the desired way. Logically, effective self-care may prevent rehospitalization and enhance QoL. In the literature, most studies focus on evaluating the impact of self-care interventions on patient-related and clinical outcomes, such as self-care behavior, self-efficacy, QoL, exercise, health status, hospitalization, mortality, myocardial stress and systemic inflammation; the impact of education is less commonly investigated. Masterson Creber et al. pointed out that the efficiency of education among HF patients may be limited due to the patients' elderly age, cognitive impairment, drowsiness during the day, poor health awareness, and low motivation.¹¹

In the present meta-analysis, self-care improved both in the intervention groups and in the controls, but the improvement was markedly greater in patients targeted by the educational interventions. These findings contribute to the ongoing discussions on the subject. In Masterson Creber et al., the implemented motivational interventions did not improve self-care in relation to routine care, while in Paradis et al., 1 month after motivational interventions including face-to-face meetings and phone calls, there was an improvement in self-efficacy, though not in self-care maintenance.^{28,29} The differences between the studies may result from differences in intervention duration and follow-up time. Thus, the lack of clear indications from the present meta-analysis may be due to the diverse methodologies in the studies analyzed, the types of education offered and the protocols for evaluating intervention effectiveness. Additionally, the effects of education are influenced by the patients' health literacy and social support.³⁰ Researchers indicate that the elderly age of HF patients affects their capacity to obtain, read, understand and process health-related information.³¹

In our analysis, the mean patient age was 66.9 ± 13.2 years (range: 45.23–77.6 years). Our research demonstrated that no impact of education on QoL was found in the oldest age

group, while in younger patients such an impact was indeed found.^{20,26} Many older adults have low levels of health literacy, which results in poor treatment outcome. Additionally, older HF patients are often depressed, which also significantly affects their self-care capabilities. Poor self-care and the presence of depressive symptoms are very common among HF patients. Depression results in low motivation, a lack of enthusiasm and poor adherence to treatment. Insufficient self-care and motivation levels predict lower QoL, frequent rehospitalization and higher mortality.²³

In our meta-analysis, no significant correlation was found between education and QoL improvement. The studies available consistently show no significant differences in terms of reported QoL between HF patients included in educational interventions and those receiving standard care. In these studies, QoL improves following treatment, regardless of any educational activities. Similar conclusions on the role of education in QoL were reported by Masterson Creber et al., who found that QoL improved both in the intervention group and in the control group, with no statistically significant differences between the 2 groups.¹¹ Likewise, in a study by Vaillant-Roussel et al., no differences in terms of QoL improvement were found between patients receiving education and those treated in the standard manner.²⁴ Wang et al. and Tung et al. demonstrated positive correlations of QoL with self-care behavior and symptom severity.^{23,32} Greater improvement in self-care behavior was associated with a greater improvement in QoL. In other studies, educational strategies were correlated with QoL benefits, as well as with more satisfaction with treatment and less fatigue. No improvement in terms of exercise was found, which is likely to be due to the old age of the HF patients surveyed. Quality of life in this population can also be expected to change with each patient's clinical condition, symptom severity and ability to cope with the difficulties associated with the illness. Abbasi et al. cite findings from a meta-analysis of 6 papers, demonstrating that a self-management education program resulted in shorter hospital stays, fewer hospitalizations and better adherence to medication in HF patients. It did not, however, impact mortality, functional abilities, symptoms, or QoL. These differences may result from the variety of interventions, methodologies, educational methods and follow-up durations.²⁶

As we have suggested, QoL improvement may depend on a given patient's condition and the type of intervention. We agree that motivational interventions alone are not sufficient to improve the QoL of cardiovascular patients. When studying chronically ill patients, one must consider specific factors affecting their reported QoL, and a possible ceiling effect on how much QoL can improve over time as the disease severity worsens.

In the present meta-analysis, education had the strongest significant impact on adherence to treatment. In this aspect, the published data are consistent, confirming

the association between compliance and knowledge. In the meta-analysis by Ruppert et al. on the effectiveness of interventions aimed at improving compliance, an association was indeed found between the effectiveness of supportive activities and adherence levels.³³ The authors suggested that the observed effects were age-dependent. They also pointed out that motivational interventions were more successful when focusing on just a single effect (in this case compliance) than when addressing additional aspects of health behavior.³³ Furthermore, the authors emphasize the role of multimorbidity in HF patients as an adverse factor for the effectiveness of any educational intervention. Likewise, they point to potential cultural differences in specific countries and regions, which were not considered in our meta-analysis.³³

The rehospitalization rate was another outcome investigated here in conjunction with education and intervention effectiveness. However, out of all the studies included in the meta-analysis, only 3 addressed rehospitalization, and therefore further analyses could not be performed. Notably, though, the available data point to a lower number of rehospitalizations as a benefit of the educational interventions undertaken. Clearly, as in the case of the previously discussed aspects, the impact of education on self-care and symptom monitoring capabilities is a factor.

Promoting knowledge on HF is essential for improving adherence and self-care and for preventing rehospitalization, particularly in the case of HF patients living in rural areas.^{34,35} Some papers have also reported that patient education that increases knowledge about the illness is more effective than other interventions in improving adherence to self-care in HF patients. In this context, Uverzagt et al. and Shah et al. showed that adherence to HF self-care recommendations was affected by the availability of an interdisciplinary team consisting of a nurse, a pharmacist, a dietitian, a social worker, and a physician, as well as by regular follow-up.^{36,37}

Conclusions

Education of patients with HF is a key strategy that has a positive impact on outcomes. The greatest benefit is seen in terms of adherence to pharmaceutical treatment and self-care, while QoL was not associated with education.

There are still too few studies on the impact of education on HF outcomes, hence the need for further studies and for interventions adjusted to patients' specific characteristics.

Practical implications

Educational interventions for patients with HF should be patient-centered. Motivational interventions significantly improved self-care behavior, adherence, rehospitalization rate, and knowledge levels in HF patients. It is important to assess the level and ability of education. Further studies


are required to identify the forms of education and the specific behavioral interventions that can successfully improve both clinical and patient-related outcomes in HF.


Study limitations


One limitation of this meta-analysis was the variety of instruments used to measure patient outcomes in the studies analyzed. Inclusion and exclusion criteria were also varied. Further difficulties were associated with comparing results provided in various units (numerical vs percentage data) or measured at various times after the educational intervention, as well as with the lack of a control group in some of the studies analyzed. Also, the meta-analysis did not include studies measuring adherence to pharmaceutical treatment before and after the educational intervention using a direct method (such as blood sample analysis).


ORCID iDs

Natalia Alicja Świątoniowska-Lonc


 <https://orcid.org/0000-0003-4211-9205>

Agnieszka Sławuta  <https://orcid.org/0000-0001-5671-9864>

Krzysztof Dudek  <https://orcid.org/0000-0002-9442-989X>

Katarzyna Jankowska  <https://orcid.org/0000-0002-1437-050X>

Beata Katarzyna Jankowska-Polańska

 <https://orcid.org/0000-0003-1120-3535>

References

- Ziaeeian B, Fonarow GC. Epidemiology and aetiology of heart failure. *Nat Rev Cardiol.* 2016;13(6):368–378.
- Cvetinovic N, Loncar G, Farkas J. Heart failure management in the elderly: A public health challenge. *Wien Klin Wochenschr.* 2016; 128(Suppl 7):466–473.
- Bui AL, Horwich TB, Fonarow GC. Epidemiology and risk profile of heart failure. *Nat Rev Cardiol.* 2011;8(1):30–41.
- Loghmani, L, Monfared MB. The effect of self-care education on knowledge and function of patients with heart failure hospitalized in Kerman city hospitals in 2017. *Electron J Gen Med.* 2018;15(4):em47.
- Navidian A, Yaghoubinia F, Ganjali A, Khoshimaee S. The effect of self-care education on the awareness, attitude, and adherence to self-care behaviors in hospitalized patients due to heart failure with and without depression. *PLoS One.* 2015;10(6):e0130973. doi:10.1371/journal.pone.0130973. eCollection 2015.
- Boyde M, Peters R, New N, Hwang R, Ha T, Korczyk D. Self-care educational intervention to reduce hospitalisations in heart failure: A randomised controlled trial. *Eur J Cardiovasc Nurs.* 2018;17(2):178–185.
- Ponikowski P, Voors AA, Anker SD, et al. 2016 ESC guidelines for the diagnosis and treatment of acute and chronic heart failure. *Kardiol Pol.* 2016;74(10):1037–1147.
- Jovicic A, Holroyd-Leduc JM, Straus SE. Effects of self-management intervention on health outcomes of patients with heart failure: A systematic review of randomized controlled trials. *BMC Cardiovasc Disord.* 2006;6(1):43.
- Health education: Theoretical concepts, effective strategies and core competencies. A foundation document to guide capacity development of health educators. http://applications.emro.who.int/dsaf/EMRPUB_2012_EN_1362.pdf. Accessed June 5, 2019.
- Riegel B, Dickson VV, Garcia LE, Masterson Creber R, Streur M. Mechanisms of change in self-care in adults with heart failure receiving a tailored, motivational interviewing intervention. *Patient Educ Couns.* 2017;100(2):283–288.
- Masterson Creber R, Patey M, Dickson VV, DeCesaris M, Riegel B. Motivational Interviewing Tailored Interventions for Heart Failure (MITI-HF): Study design and methods. *Contemp Clin Trials.* 2015;41: 62–68.
- Lutje V. Guide to the search strategy. https://cidg.cochrane.org/sites/cidg.cochrane.org/files/public/uploads/search-strategy-guide_modified_8mar2013_1.pdf. Accessed January 2, 2019.
- Boyne JJ, Vrijhoef HJ, Spreeuwenberg M, De Weerd G, Kragten J, Gorgels AP; TEHAF investigators. Effects of tailored telemonitoring on heart failure patients' knowledge, self-care, self-efficacy and adherence: A randomized controlled trial. *Eur J Cardiovasc Nurs.* 2014; 13(3):243–252.
- Deka P, Pozehl B, Williams MA, Norman JF, Khazanchi D, Pathak D. MOVE-HF: An internet-based pilot study to improve adherence to exercise in patients with heart failure. *Eur J Cardiovasc Nurs.* 2018; 18(2):122–131.
- Kato NP, Kinugawa K, Sano M, et al. How effective is an in-hospital heart failure self-care program in a Japanese setting? Lessons from a randomized controlled pilot study. *Patient Prefer Adherence.* 2016; 18(10):171–181.
- Hägglund E, Lyngå P, Frie F, et al. Patient-centred home-based management of heart failure. Findings from a randomised clinical trial evaluating a tablet computer for self-care, quality of life and effects on knowledge. *Scand Cardiovasc J.* 2015;49(4):193–199.
- Kinugasa Y, Kato M, Sugihara S, et al. Multidisciplinary intensive education in the hospital improves outcomes for hospitalized heart failure patients in a Japanese rural setting. *BMC Health Serv Res.* 2014; 19(14):351.
- Donner Alves F, Correa Souza G, Brunetto S, Schweigert Perry ID, Biolo A. Nutritional orientation, knowledge and quality of diet in heart failure: Randomized clinical trial. *Nutr Hosp.* 2012;27(2):441–448.
- Mussi CM, Ruschel K, de Souza EN, et al. Home visit improves knowledge, self-care and adherence in heart failure: Randomized clinical trial HELEN-I. *Rev Lat Am Enfermagem.* 2013;21:20–28.
- Leventhal ME, Denhaerynck K, Brunner-La Rocca HP, et al. Swiss Interdisciplinary Management Programme for Heart Failure (SWIM-HF): A randomised controlled trial study of an outpatient inter-professional management programme for heart failure patients in Switzerland. *Swiss Med Wkly.* 2011;8(141):w13171.
- Cicccone MM, Aquilino A, Cortese F, et al. Feasibility and effectiveness of a disease and care management model in the primary health care-system for patients with heart failure and diabetes (Project Leonardo). *Vasc Health Risk Manag.* 2010;6:297–305.
- Athar, MW, Record JD, Martire C, Hellmann DB, Ziegelstein RC. The effect of a personalized approach to patient education on heart failure self-management. *J Pers Med.* 2018;8(4). pii: E39. doi:10.3390/jpm8040039
- Wang Q, Dong L, Jian Z, Tang X. Effectiveness of a PRECEDE-based education intervention on quality of life in elderly patients with chronic heart failure. *BMC Cardiovasc Disord.* 2017;17(1):262.
- Vaillant-Roussel H, Laporte C, Pereira B, et al. Impact of patient education on chronic heart failure in primary care (ETIC): A cluster randomised trial. *BMC Fam Pract.* 2016;17:80.
- Korzh O, Krasnokutskiy S. Significance of education and self-management support for patients with chronic heart failure in family physician practice. *Family Med Primary Care Rev.* 2016;18(4):432–436.
- Abbasi A, Tahereh NG, Mansoureh AF. Effect of the self-management education program on the quality of life in people with chronic heart failure: A randomized controlled trial. *Electron Physician.* 2018; 10(7):7028–7037.
- Higgins JP, Thompson S, Deeks J, Altman DG. Measuring inconsistency in meta-analyses. *British Medical Journal.* 2003;327:557–560.
- Paradis V, Cossette S, Frasure-Smith N, Heppell S, Guertin MC. The efficacy of a motivational nursing intervention based on the stages of change on self-care in heart failure patients. *J Cardiovasc Nurs.* 2010;25(2):130–141.
- Masterson Creber R, Patey M, Lee CS, Kuan A, Jurgens C, Riegel B. Motivational interviewing to improve self-care for patients with chronic heart failure: MITI-HF randomized controlled trial. *Patient Educ Couns.* 2016;99(2):256–264.
- Lee SY, Arozullah AM, Cho YI. Health literacy, social support, and health: A research agenda. *Soc Sci Med.* 2004;58(7):1309–1321.
- Wu JR, Moser DK, DeWalt DA, Rayens MK, Dracup K. Health literacy mediates the relationship between age and health outcomes in patients with heart failure. *Circ Heart Fail.* 2016;9(1):e002250.

32. Tung HH, Lin CY, Chen KY, Chang CJ, Lin YP, Chou CH. Self-management intervention to improve self-care and quality of life in heart failure patients. *Congest Heart Fail.* 2013;19(4):E9–E16.
33. Ruppert TM, Delgado JM, Temple J. Medication adherence interventions for heart failure patients: A meta-analysis. *Eur J Cardiovasc Nurs.* 2015;14(5):395–404.
34. Lee KS, Moser DK, Pelter MM, Nesbitt T, Dracup K. Self-care in rural residents with heart failure: What we are missing. *Eur J Cardiovasc Nurs.* 2017;16(4):326–333.
35. Dracup K, Moser D, Pelter MM, et al. Rural patients' knowledge about heart failure. *J Cardiovasc Nurs.* 2014;29(5):423–428.
36. Unverzagt S, Meyer G, Mittmann S, Samos F-A, Unverzagt M, Prondzinsky R. Improving treatment adherence in heart failure: A systematic review and meta-analysis of pharmacological and lifestyle interventions. *Dtsch Arztebl Int.* 2016;113(25):423–430.
37. Shah D, Simms K, Barksdale D, Wu J-R. Improving medication adherence of patients with chronic heart failure: Challenges and solutions. *Res Rep Clin Cardiol.* 2015;2015:87–95.

The preservation effect of coronary collateral circulation on left ventricular function in chronic total occlusion and its association with the expression of vascular endothelial growth factor A

Yuxiang Dai^{1,B-D}, Shufu Chang^{1,B-D}, Shen Wang^{2,B,C}, Yi Shen^{3,B,C}, Chenguang Li^{1,B,C}, Zheyong Huang^{1,B}, Hao Lu^{1,B}, Juying Qian^{1,B}, Lei Ge^{1,B,E}, Qibing Wang^{1,B}, Feng Zhang^{1,B}, Junbo Ge^{1,A,F}

¹ Department of Cardiology, Fudan University Affiliated Zhongshan Hospital, Shanghai, China

² Department of Cardiology, Xinhua Hospital of Zhejiang Province, the Second Affiliated Hospital of Zhejiang Chinese Medical University, China

³ Department of Geratology, Fudan University Affiliated Zhongshan Hospital, Shanghai, China

A – research concept and design; B – collection and/or assembly of data; C – data analysis and interpretation;

D – writing the article; E – critical revision of the article; F – final approval of the article

Advances in Clinical and Experimental Medicine, ISSN 1899–5276 (print), ISSN 2451–2680 (online)

Adv Clin Exp Med. 2020;29(4):493–497

Address for correspondence

Junbo Ge

E-mail: guoronglang@yeah.net

Funding sources

This work was supported by the National Natural Science Foundation of China (grant No. 81300095).

Conflict of interest

None declared

Received on August 17, 2018

Reviewed on October 28, 2018

Accepted on February 18, 2019

Published online on April 27, 2020

Cite as

Dai Y, Chang S, Wang S, et al. The preservation effect of coronary collateral circulation on left ventricular function in chronic total occlusion and its association with the expression of vascular endothelial growth factor A. *Adv Clin Exp Med.* 2020;29(4):493–497. doi:10.17219/acem/104535

DOI

10.17219/acem/104535

Copyright

© 2020 by Wrocław Medical University

This is an article distributed under the terms of the Creative Commons Attribution Non-Commercial License (<http://creativecommons.org/licenses/by-nc-nd/4.0/>)

Abstract

Background. Patients with coronary chronic total occlusion (CTO) typically have collateralization of the distal vessel, and these collaterals can contribute to the relief of ischemia and anginal symptoms and to the preservation of ventricular function.

Objectives. To investigate the preservation effect of coronary collateral circulation on left ventricular (LV) function in coronary CTO, and to explore the potential mechanism behind the development of coronary collateral circulation.

Material and methods. A total of 102 consecutive patients with coronary CTO were divided into 2 groups: the left ventricular ejection fraction (LVEF)-preserved group (LVEF \geq 50%; n = 46) and the LVEF-decreased group (LVEF < 50%; n = 56). Clinical, angiographic and laboratory data was collected for all patients. The association between LVEF and coronary collateral circulation in coronary CTO patients was analyzed with multivariate logistic regression analysis, and the serum levels of VEGF-A and the mRNA expression levels of the *VEGF-A* gene were compared between different grades of coronary collateral circulation.

Results. Multivariate analysis revealed that Rentrop grades 2–3 and coexisting collateral pathways were independent predictors of LVEF preservation in coronary CTO patients. Patients with Rentrop grades 2–3 had smaller left ventricular end diastolic diameters (LVDd) and left ventricular end systolic diameters (LVSD), and they had larger LVEFs than the patients with Rentrop grades 0–1. Patients with Rentrop grades 2–3 also had higher serum levels of VEGF-A and higher mRNA expression levels of the *VEGF-A* gene in their peripheral blood mononuclear cells (PBMCs) than patients with Rentrop grades 0–1. Patients with coexisting collateral pathways had higher serum levels of VEGF-A and higher mRNA expression levels of the *VEGF-A* gene in PBMCs than patients without coexisting collateral pathways.

Conclusions. Coronary collateral circulation is significantly associated with LVEF preservation, and VEGF-A might promote the formation of coronary collateral circulation.

Key words: chronic total occlusion, left ventricular ejection fraction, coronary collateral circulation, vascular endothelial growth factor A

Introduction

Coronary chronic total occlusion (CTO) is defined as a complete (or nearly complete) occlusion of the coronary vessel with thrombolysis in myocardial infarction (TIMI) flow grade 0 or 1 lasting 3 months or longer.^{1,2} Patients with CTO typically have collateralization of the distal vessel, and these collaterals can contribute to the relief of ischemia and anginal symptoms and to the preservation of ventricular function.^{3,4}

As one of the most important angiogenic factors, vascular endothelial growth factor (VEGF) may promote the development of collateral formation through its ability to maintain the vascular bed, stimulating proliferation/migration of endothelial cells and increasing the permeability of blood vessels.^{5,6} In this study, the association between left ventricular ejection fraction (LVEF) and coronary collateral circulation in coronary CTO patients was analyzed with multivariate logistic regression analysis. The serum levels of VEGF-A and the mRNA expression levels of the *VEGF-A* gene were compared between different grades of coronary collateral circulation. The aim was to evaluate the preservation effect of coronary collateral circulation on left ventricular (LV) function and to explore the potential mechanism behind the development of coronary collateral circulation.

Material and methods

Patients

A total of 102 consecutive patients with coronary CTO from the Department of Cardiology at Fudan University Affiliated Zhongshan Hospital, Shanghai, China, were enrolled between January and April 2014. The inclusion criteria were: 1) age ≥ 18 years; 2) symptomatic angina and/or a positive functional ischemia test; and 3) CTO in at least 1 major epicardial coronary artery detected with diagnostic coronary angiography. The exclusion criteria consisted of: 1) a previous coronary artery bypass graft (CABG); 2) a medical history of cardiogenic shock or cardiopulmonary resuscitation; or 3) an ST-segment elevation myocardial infarction (STEMI) during the previous 48 h. Clinical, angiographic and laboratory data was collected for all patients. This study was approved by the ethics committee of Zhongshan Hospital (approval No. 2013006028) and all patients provided written informed consent.

Angiography and grading of coronary collateral circulation

All angiographies were performed with Axiom-Artis DTA (Siemens, Munich, Germany) or a Innova 2000 system (GE, Evansville, USA) via the radial artery or femoral artery approach. Angiographic results were analyzed using

a GE centricity AI 1000-GE Mnet (v. 4.2.7.05). Coronary collateral circulation was graded according to the Rentrop scoring system (0 = no visible filling of any collateral vessels; 1 = filling of the small side branches; 2 = partial filling of the epicardial artery; 3 = complete filling of the epicardial artery).⁷ The grading of coronary collateral circulation was performed independently by 2 angiographers and a consensus was reached in the case of any disagreement.

Measurement of serum VEGF-A levels

For all patients, 10 mL of whole blood was collected in ethylenediaminetetraacetic acid (EDTA) tubes via peripheral veins immediately after angiography. The samples were then centrifuged at 1,500 g for 10 min at 20°C. The supernatant was collected and serum levels of VEGF-A were measured with a human VEGF-A ELISA Kit (Invitrogen, Waltham, USA) according to the manufacturer's instructions.

Measurement of mRNA expression levels of VEGF-A

Peripheral blood mononuclear cells (PBMCs) were isolated using Ficoll density gradient (Biocoll; Biochrom, Berlin, Germany) centrifugation for 30 min at 500 g. The interphase layer of PBMCs was washed in phosphate-buffered saline (PBS) and then centrifuged for 15 min at 200 g. Total RNA was extracted from the PBMCs using Trizol (Invitrogen). Reverse transcriptase-polymerase chain reaction (RT-PCR) was used to evaluate mRNA expression levels of *VEGF-A* in the PBMCs. Total RNA (1 μ g) was reverse-transcribed into complementary deoxyribonucleic acid (cDNA) with a cDNA synthesis kit (SYBR Premix Ex Taq; Takara Bio Inc., Kusatsu, Japan). The cDNA was denatured at 95°C for 5 min, then amplified for 40 cycles at 94°C for 15 s and at 60°C for 30 s in a Light Cycler (Roche Diagnostics, Rotkreuz, Switzerland). The relative quantification of the mRNA expression levels of *VEGF-A* was performed with the $\Delta\Delta$ Ct method, and *GAPDH* was used as the reference gene. The sense and antisense primers of *VEGF-A* and *GAPDH* used in this study were as follows: *VEGF-A* (sense: 5'-ACTTCTGGGCTGTTCTCG-3'; antisense: 5'-TCCTCTTCCTTCTCTTCTTCC-3') and *GAPDH* (sense: 5'-ACAGTCAGCCGCATCTTC-3'; antisense: 5'-CTCCGACCTTCACCTTCC-3').

Statistical analysis

Categorical variables are expressed as percentages, while continuous variables are expressed as mean \pm standard deviation (SD). Univariate analysis was performed with a χ^2 test or Student's t-test. The variables in the univariate analysis with a p-value < 0.10 were included in the multivariate analysis with a backward stepwise logistic regression model. Multivariate logistic regression analysis was

then performed to identify the association between LVEF and coronary collateral circulation. The left ventricular end diastolic diameters (LVDd), left ventricular end systolic diameters (LVSd), LVEF, serum VEGF-A levels, and mRNA *VEGF-A* expression levels were compared using Student's *t*-test. The IBM SPSS Statistics for Windows v. 19.0 software (IBM Corp., Armonk, USA) was employed to perform all statistical analyses. The significance level was set at $p < 0.05$.

Results

Univariate analysis

The 102 patients were divided into 2 groups according to LVEF: the LVEF-preserved group (LVEF $\geq 50\%$; $n = 46$) and the LVEF-decreased group (LVEF $< 50\%$; $n = 56$). The characteristics of demography, medical history, biochemical parameters and angiography for the 2 groups are shown in Table 1. Univariate analysis showed that prior myocardial infarction, creatinine level, Rentrop grade, and the status of coexisting collateral pathways were statistically significantly different between the LVEF-decreased group and the LVEF-preserved group (Table 1).

Multivariate analysis

Multivariate logistic regression analysis was performed in order to determine the association between LVEF and coronary collateral circulation, adjusting for diabetes mellitus, prior myocardial infarction and creatinine level. According to the results of multivariate analysis, Rentrop grades 2–3 and coexisting collateral pathways were independent predictors for LVEF preservation in coronary CTO patients (Table 2).

LV function of different Rentrop grades

Echocardiography parameters showed that patients with Rentrop grades 2–3 had smaller LVDd (46.83 ± 2.86 mm vs 50.08 ± 3.27 mm; $p = 0.021$) and LVSd (32.79 ± 2.81 mm vs 36.12 ± 3.22 mm; $p = 0.019$), and larger LVEFs ($53.46 \pm 5.18\%$ vs $48.35 \pm 4.29\%$; $p = 0.020$) than patients with Rentrop grades 0–1. These results suggest that high Rentrop grades are associated with proper LV functioning.

Serum VEGF-A levels and mRNA expression levels of the *VEGF-A* gene

Patients with Rentrop grades 2–3 had higher serum levels of VEGF-A (141.92 ± 46.31 pg/mL vs 76.34 ± 32.75 pg/mL; $p = 0.028$) and higher mRNA expression levels of the *VEGF-A* gene in their peripheral blood mononuclear cells (0.93 ± 0.25 vs 0.62 ± 0.19 ; $p = 0.001$) than patients with Rentrop grades 0–1. Patients with coexisting collateral pathways

Table 1. Characteristics of the demography, medical history, biochemical parameters, and angiography in the LVEF-decreased group and the LVEF-preserved group

Parameter	LVEF-preserved group (n = 46)	LVEF-decreased group (n = 56)	p-value
Demographics			
Age [years]	60.4 \pm 8.9	59.4 \pm 9.9	0.665
Male [n/%]	35/76.1	38/67.9	0.387
Body mass index [kg/m ²]	26.6 \pm 1.9	26.6 \pm 1.7	0.734
Medical history			
Diabetes mellitus [n/%]	12/26.1	25/44.6	0.054
Cigarette smoking [n/%]	30/65.2	35/62.5	0.838
Hypertension [n/%]	24/52.2	33/58.9	0.551
Family history of CAD [n/%]	12/26.1	13/23.2	0.819
Hyperlipidemia [n/%]	22/47.8	29/51.8	0.842
Peripheral vascular disease [n/%]	8/17.4	12/21.4	0.803
Prior myocardial infarction [n/%]	8/17.4	21/37.5	0.029
Cerebrovascular disease [n/%]	2/4.4	2/3.6	1.000
Prior PCI [n/%]	8/17.4	7/12.5	0.579
Prior CABG [n/%]	5/10.9	6/10.7	1.000
Biochemical parameters			
Troponin I [ng/mL]	0.01 \pm 0.004	0.01 \pm 0.005	0.860
Creatinine [mg/dL]	73.8 \pm 23.1	82.9 \pm 22.4	0.048
Cholesterol [mmol/L]	5.6 \pm 0.8	5.5 \pm 0.9	0.401
LDL-C [mmol/L]	3.6 \pm 0.7	3.6 \pm 0.6	0.858
HbA _{1c} [%]	6.2 \pm 0.4	6.2 \pm 0.5	0.350
Angiographic findings			
Collateral circulation (Rentrop 2–3) [n/%]	37/80.4	32/57.1	0.019
Coexisting collateral pathways	17/36.9	10/17.9	0.042

CAD – coronary artery disease; CABG – coronary artery bypass grafting; LDL-C – low-density-lipoprotein cholesterol; LVEF – left ventricular ejection fraction; PCI – percutaneous coronary intervention.

Table 2. Association between LVEF and coronary collateral circulation

Parameter	OR	95% CI	p-value
Diabetes mellitus	0.298	0.105–0.843	0.021
Prior myocardial infarction	0.374	0.126–1.091	0.063
Creatinine [mg/dL]	0.526	0.402–1.271	0.184
Collateral grading	3.971	1.472–10.634	0.006
Coexisting collateral pathways	1.842	1.016–4.095	0.043

LVEF – left ventricular ejection fraction; OR – odds ratio; 95% CI – 95% confidence interval.

had higher serum levels of VEGF-A (138.41 ± 45.76 pg/mL vs 83.68 ± 33.29 pg/mL; $p = 0.035$) and higher mRNA expression levels of the *VEGF-A* gene in their PBMCs (0.88 ± 0.23 vs 0.64 ± 0.20 ; $p < 0.001$) than patients without coexisting collateral pathways. These results suggest that VEGF-A is associated with the development of coronary collateral circulation.

Discussion

Collateral circulation, which has the ability to provide blood flow to an area whose original supply vessel is obstructed, can be observed in almost all coronary CTOs.^{8,9} Therefore, collateral blood supply to an ischemic area may maintain metabolic supply and prevent myocardial necrosis.^{4,10} The prognosis is mainly determined by the extent of the myocardial infarction or ischemia in patients suffering from coronary CTOs. Coronary collateral circulation plays a key role in decreasing the size of a myocardial infarct or ischemia.^{11,12} Previous reports have demonstrated that better coronary collateral circulation is associated with smaller infarcts, less ventricular aneurysm formation, improved ventricular function, fewer future cardiovascular events, and improved survival.^{13–15} In our study, 46 of the 102 patients with coronary CTO had preserved LVEF, and they had higher percentages of better-developed coronary collateral circulation (Rentrop grades 2–3) and multiple coexisting collateral pathways. Coexisting collateral pathways may help the region supplied by the obstructed vessel to receive more blood supply, may help to restore more perfusion and may help to preserve systolic function. Multivariate analysis also revealed that Rentrop grades 2–3 and coexisting collateral pathways are independent predictors for LVEF preservation in coronary CTO patients.

The growth of collateral vessels includes the proliferation of capillaries in the ischemic area (angiogenesis) and the maturation of pre-existing collateral vessels (arteriogenesis).^{16,17} Angiogenesis is the sprouting of new capillaries from existing vascular structures; it is triggered by endothelial cell migration and proliferation.^{4,9,17} Vascular endothelial growth factor possesses multiple functions, such as inducing the migration and proliferation of endothelial cells, enhancing vascular permeability and modulating thrombogenicity, all of which have been confirmed experimentally in vivo and in vitro.^{18,19} Vascular endothelial growth factor is secreted by a variety of cells, including aortic smooth muscle cells, macrophages, myocytes, lymphocytes, neutrophils, and platelets.²⁰ In the case of severe coronary stenosis or CTO, the secretion of VEGF is upregulated because of ischemia and hypoxia.^{21,22} The endothelial cells then detach, migrate, proliferate, and finally form a new vessel.²³ In this study, serum VEGF-A levels and mRNA expression levels of the *VEGF-A* gene in PBMCs were measured to determine their association









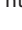
with coronary collateral circulation, and the results showed that well-developed coronary collateral circulation was associated with higher levels of serum VEGF-A and mRNA expression of the *VEGF-A* gene. This is consistent with previous findings that the formation of collateral circulation is regulated by VEGF.^{21,24}

Elevated expression of VEGF is important for the establishment of coronary collateral circulation in CTOs. Furthermore, elevated VEGF expression is conducive to the survival, homing and directional differentiation of endothelial progenitor cells and myocardial repair. Thus, VEGF is an important potential therapeutic target for promoting collateral growth in the treatment of CTOs with no suitable revascularization option. Although animal experiments have confirmed that collateral circulation improves greatly after delivering angiogenic growth factors,^{23,25} further evidence is needed in coronary CTO patients.

Conclusions

Coronary collateral circulation was statistically significantly correlated with LVEF preservation, and VEGF-A might promote the formation of coronary collateral circulation.

ORCID iDs

Yuxiang Dai  <https://orcid.org/0000-0002-2232-9136>
 Shufu Chang  <https://orcid.org/0000-0001-5672-2158>
 Shen Wang  <https://orcid.org/0000-0001-5336-4324>
 Yi Shen  <https://orcid.org/0000-0001-6903-7643>
 Chenguang Li  <https://orcid.org/0000-0001-9708-1289>
 Zheyong Huang  <https://orcid.org/0000-0003-4538-4848>
 Hao Lu  <https://orcid.org/0000-0003-3401-135X>
 Juying Qian  <https://orcid.org/0000-0002-6155-6577>
 Lei Ge  <https://orcid.org/0000-0003-2704-7100>
 Qibing Wang  <https://orcid.org/0000-0002-8033-1840>
 Feng Zhang  <https://orcid.org/0000-0003-1405-2293>
 Junbo Ge  <https://orcid.org/0000-0003-1030-7009>

References

1. Shah PB. Management of coronary chronic total occlusion. *Circulation*. 2011;123(16):1780–1784.
2. Lee CK, Chen YH, Lin MS, et al. Retrograde approach is as effective and safe as antegrade approach in contemporary percutaneous coronary intervention for chronic total occlusion: A Taiwan single-center registry study. *Acta Cardiol Sin*. 2017;33(1):20–27.
3. Seiler C. Assessment and impact of the human coronary collateral circulation on myocardial ischemia and outcome. *Circ Cardiovasc Interv*. 2013;6(6):719–728.
4. Seiler C, Stoller M, Pitt B, Meier P. The human coronary collateral circulation: Development and clinical importance. *Eur Heart J*. 2013;34(34):2674–2682.
5. Bernatchez PN, Soker S, Sirois MG. Vascular endothelial growth factor effect on endothelial cell proliferation, migration, and platelet-activating factor synthesis is Flk-1-dependent. *J Biol Chem*. 1999;274(43):31047–31054.
6. Dulak J, Jozkowicz A, Frick M, et al. Vascular endothelial growth factor: Angiogenesis, atherogenesis or both? *J Am Coll Cardiol*. 2001;38(7):2137–2138.
7. Rentrop KP, Cohen M, Blanke H, Phillips RA. Changes in collateral channel filling immediately after controlled coronary artery occlusion by an angioplasty balloon in human subjects. *J Am Coll Cardiol*. 1985;5(3):587–592.

8. Schaper W. Collateral circulation: Past and present. *Basic Res Cardiol*. 2009;104(1):5–21.
9. Seiler C. The human coronary collateral circulation. *Eur J Clin Invest*. 2010;40(5):465–476.
10. Teunissen PF, Horrevoets AJ, van Royen N. The coronary collateral circulation: Genetic and environmental determinants in experimental models and humans. *J Mol Cell Cardiol*. 2012;52(4):897–904.
11. Karowni W, El Accaoui RN, Chatterjee K. Coronary collateral circulation: Its relevance. *Catheter Cardiovasc Interv*. 2013;82(6):915–928.
12. Małek ŁA, Śpiewak M, Kłopotowski M, Marczak M, Witkowski A. Combined analysis of myocardial function, viability, and stress perfusion in patients with chronic total occlusion in relation to collateral flow. *Kardiol Pol*. 2015;73(10):909–915.
13. McEntegart MB, Badar AA, Ahmad FA, et al. The collateral circulation of coronary chronic total occlusions. *EuroIntervention*. 2016;11(14):e1596–e1603.
14. Choi JH, Chang SA, Choi JO, et al. Frequency of myocardial infarction and its relationship to angiographic collateral flow in territories supplied by chronically occluded coronary arteries. *Circulation*. 2013;127(6):703–709.
15. Meier P, Hemingway H, Lansky AJ, Knapp G, Pitt B, Seiler C. The impact of the coronary collateral circulation on mortality: A meta-analysis. *Eur Heart J*. 2012;33(5):614–621.
16. Chilian WM, Penn MS, Pung YF, et al. Coronary collateral growth: Back to the future. *J Mol Cell Cardiol*. 2012;52(4):905–911.
17. Fujita M, Tambara K. Recent insights into human coronary collateral development. *Heart*. 2004;90(3):246–250.
18. Gerhardt H. VEGF and endothelial guidance in angiogenic sprouting. *Organogenesis*. 2008;4(4):241–246.
19. Cai J, Jiang WG, Ahmed A, Boulton M. Vascular endothelial growth factor-induced endothelial cell proliferation is regulated by interaction between VEGFR-2, SH-PTP1 and eNOS. *Microvasc Res*. 2006;71(1):20–31.
20. Hamamichi Y, Ichida F, Yu X, et al. Neutrophils and mononuclear cells express vascular endothelial growth factor in acute Kawasaki disease: Its possible role in progression of coronary artery lesions. *Pediatr Res*. 2001;49(1):74–80.
21. Toyota E, Warltier DC, Brock T, et al. Vascular endothelial growth factor is required for coronary collateral growth in the rat. *Circulation*. 2005;112(14):2108–2113.
22. Clayton JA, Chalothorn D, Faber JE. Vascular endothelial growth factor-A specifies formation of native collaterals and regulates collateral growth in ischemia. *Circ Res*. 2008;103(9):1027–1036.
23. Schirmer SH, van Nooijen FC, Piek JJ, van Royen N. Stimulation of collateral artery growth: Travelling further down the road to clinical application. *Heart*. 2009;95(3):191–197.
24. Lucitti JL, Mackey JK, Morrison JC, Haigh JJ, Adams RH, Faber JE. Formation of the collateral circulation is regulated by vascular endothelial growth factor-A and a disintegrin and metalloprotease family members 10 and 17. *Circ Res*. 2012;111(12):1539–1550.
25. Degen A, Millenaar D, Schirmer SH. Therapeutic approaches in the stimulation of the coronary collateral circulation. *Curr Cardiol Rev*. 2014;10(1):65–72.

Receptor-mediated attenuation of insulin-like growth factor-1 activity by galactose-1-phosphate in neonate skin fibroblast cultures: Galactosemia pathogenesis

Mazen Al-Essa^{A-F}, Gursev Dhaunsi^{A-F}

Department of Pediatrics, Faculty of Medicine, Kuwait University, Kuwait

A – research concept and design; B – collection and/or assembly of data; C – data analysis and interpretation; D – writing the article; E – critical revision of the article; F – final approval of the article

Advances in Clinical and Experimental Medicine, ISSN 1899–5276 (print), ISSN 2451–2680 (online)

Adv Clin Exp Med. 2020;29(4):499–504

Address for correspondence

Mazen Al-Essa
E-mail: mazen@hsc.edu.kw

Funding sources

None declared

Conflict of interest

None declared

Acknowledgements

Authors would like to thank Mrs. Heba Dalvi and Mrs. Somaya for their technical assistance. This study was supported by a research grant (No. MK 01/16) funded by Research Sector, Kuwait University, Kuwait.

Received on March 14, 2019

Reviewed on April 25, 2019

Accepted on August 18, 2019

Published online on April 30, 2020

Abstract

Background. The pathogenesis of classical galactosemia, a rare metabolic disorder associated with developmental complications in neonates and children due to inherited deficiency of galactose-1-phosphate (Gal-1-P) uridylyltransferase (GALT), is known to be mediated by elevated Gal-1-P levels and involves a cascade of cytokines, reactive oxygen species (ROS) and growth factors.

Objectives. To examine *ex vivo* the effect of Gal-1-P on the mitogenic activity of different growth factors, particularly insulin-like growth factor-1 (IGF-1), known to regulate growth and development from the fetal stage to adulthood.

Material and methods. Fibroblasts derived from the foreskin of 3–8-day-old healthy neonates were cultured for 1–14 days with 0–20 mM galactose or 0–10 mM Gal-1-P and then stimulated with 5% fetal bovine serum (FBS) or 50 ng/mL of platelet-derived growth factor (PDGF) or fibroblast growth factor (FGF) or IGF-1 for 24 h. DNA synthesis was measured and protein expression of PDGFR, FGFR and IGF-1R was assessed with western blotting.

Results. Supra-physiological concentrations of galactose significantly decreased FBS- and IGF-1-induced BrdU incorporation. The presence of Gal-1-P (5–10 mM) in culture medium for 7–14 days significantly ($p < 0.01$) decreased IGF-1-, PDGF- and FBS-stimulated DNA synthesis. While treatment with Gal-1-P selectively and significantly ($p < 0.01$) reduced the protein expression of IGF-1 receptor, galactose treatment did not have any marked effect on examined growth factor receptors.

Conclusions. This study demonstrates that Gal-1-P impairs IGF-1 activity through IGF-1-receptor impairment, thereby providing a new insight into the molecular mechanisms of galactosemia pathogenesis.

Key words: neonates, growth factors, DNA synthesis, IGF-1 receptor, galactosemia

Cite as

Al-Essa M, Dhaunsi G. Receptor-mediated attenuation of insulin-like growth factor-1 activity by galactose-1-phosphate in neonate skin fibroblast cultures: Galactosemia pathogenesis. *Adv Clin Exp Med.* 2020;29(4):499–504. doi:10.17219/acem/111807

DOI

10.17219/acem/111807

Copyright

© 2020 by Wrocław Medical University
This is an article distributed under the terms of the Creative Commons Attribution 3.0 Unported (CC BY 3.0) (<https://creativecommons.org/licenses/by/3.0/>)

Introduction

Classical galactosemia is a metabolic disorder which results from a genetic aberration in galactose-1-phosphate uridylyltransferase (GALT), an enzyme that catalyzes the formation of uridine diphosphate galactose from galactose-1-phosphate (Gal-1-P).¹ The clinical features of classical galactosemia range from cataract, hypoglycemia, hepatomegaly, and hypotonia to sepsis. Clinical symptoms develop in infants during the neonatal period due to consumption of galactose^{2–4} and an early withdrawal of galactose from the diet is known to remarkably reduce the incidence of serious illness among neonates. Dietary restrictions can prove to be life-saving in the first few weeks of life but do not protect from galactosemia-related long-term complications like cognitive impairment or neurological or speech abnormalities. Toxic levels of Gal-1-P in the cells due to continued endogenous galactose synthesis in diet-restricted cases or from abnormal galactosylation of proteins^{5–7} lead to mental retardation, motor abnormalities, dyspraxia, and hypergonadotropic hypogonadism. Though galactosemia-induced cellular dysfunction has been reported to involve the participation of various intracellular and extracellular biomolecules such as reactive oxygen species (ROS), cytokines and growth factors,⁸ the exact molecular mechanism of pathogenesis remains unclear. We recently reported that the nicotinamide adenine dinucleotide phosphate (NADPH) oxidase system is impaired in patients with classical galactosemia and may contribute, at least in part, to increased risk of infection and sepsis due to impaired bactericidal superoxide anion production by the leukocytes.⁹ In addition to the reported role of ROS and cytokines in cellular events of galactosemia, endocrine participation has also been suggested in the pathogenesis of galactosemia, as children with classical galactosemia are reported to have low levels of circulating insulin-like growth factor-1 (IGF-1) levels.¹⁰

We reported earlier that galactosemia is associated with a nitric oxide (NO)-mediated downregulation of IGF-1, a mitogen with a key role in the growth and function of various human organs and tissues.¹¹ Growth hormone, IGF-1, epidermal growth factor (EGF) and fibroblast growth factor (FGF) are known to play a vital role in growth and development at different stages of childhood.^{12,13} The IGF-1 is a peptide that regulates bone growth, cellular differentiation, and metabolic activities, and plays a role in the functioning of the cardiovascular system.¹⁴ A major amount of the circulating IGFs is of hepatic origin, however, physiologically, production of IGF-1 also occurs in other tissues, such as growth plate and bone, with various autocrine and paracrine functions.¹⁵ Though previous studies have demonstrated that IGF-1 production is mitigated under galactosemic conditions along with decreased levels of IGF-1 levels in plasma, our main goal in this study was to investigate if Gal-1-P has any effect on growth factor activity, particularly that of IGF-1.

This study was carried out according to the protocols of the Institutional Ethical Review Committee of Kuwait University, Kuwait (approval No. MK 01/16).

Material and methods

Material

Galactose, Gal-1-phosphate and other chemicals used for the biochemical assays were purchased from Sigma-Aldrich (St. Louis, USA). The chemicals and materials required for the cell cultures, including fetal bovine serum (FBS), were procured from Invitrogen–Thermo Fisher Scientific (Carlsbad, USA). The electrophoresis reagents were purchased from BioRad Laboratories (Hercules, USA), whereas the antibodies for western blot analysis were procured from Santa Cruz Biotechnology (Santa Cruz, USA). The fibroblasts used in this study were cultured from the skin explants of foreskin samples collected from 3–8-day-old healthy neonates.

Methods

Cell cultures and their treatment with experimental materials

Fibroblasts were cultured in a growth medium, Dulbecco's modified Eagle medium (DMEM) F-12 supplemented with 10% FBS and penicillin/streptomycin (5U, 5 µg/mL, respectively), in a humidified atmosphere of 5% CO₂ and 95% air. The cell cultures were grown to confluence before their use for various experiments. Cell cultures were washed twice with RPMI culture medium before the start of each experiment. The cells were treated with varying concentrations (0–20 mM) of galactose and Gal-1-P (0–10 mM) for 1–14 days and the cultures were replenished with galactose/Gal-1-P every 24 h. Lipofectamine was added as a permeating agent to the cell cultures in experiments with the polar molecule Gal-1-P. Growth factors (50 ng/mL), namely platelet-derived growth factor (PDGF), FGF and IGF-1, were added to the culture medium for 24 h in the presence or absence of galactose/Gal-1-P to examine DNA synthesis. Following treatment of the cell cultures with the experimental agents, culture supernatants were collected and cells were harvested and homogenized in 50 mM Tris-HCl buffer, pH 7.4, containing protease inhibitors. In the control experiments, 5–20 mM of mannitol was added to the cell cultures in order to examine its effect on mitogen-induced DNA synthesis and growth factor receptors.

BrdU incorporation

DNA synthesis in the cell cultures was assayed by measuring bromodeoxyuridine (BrdU) incorporation into the cellular DNA. The cell cultures were grown in the presence or absence of galactose or Gal-1-phosphate for

1–14 days and mitogens (FBS and growth factor) were added for 24 h along with BrdU, provided in kits purchased from Calbiochem (Merck, Kenilworth, USA).

Western blot analysis

Following treatment of the fibroblast cultures with the various experimental agents, cell homogenates were prepared and lysed using 50 mM Tris-based buffer (pH 7.6) which contained 5 mM EGTA, 150 mM NaCl, 1% Triton 100, 2 mM Na_3VO_4 , 50 mM sodium fluoride solution (NAF), 1 mM phenylmethanesulfonyl fluoride (PMSF), 20 μM phenylarsine, 10 mM sodium molybdate, 10 $\mu\text{g}/\text{mL}$ leupeptin, and 8 $\mu\text{g}/\text{mL}$ aprotinin. Cell lysates prepared from different treatment groups were subjected to SDS-polyacrylamide gel electrophoresis (SDS-PAGE) in equal amounts of protein and transferred onto a nitrocellulose membrane. The membranes were then incubated with monoclonal antibodies to FGF receptor (FGFR), platelet-derived growth factor (PDGF) receptor and IGF-1 receptor, and washed 3 times before incubation with secondary antibodies conjugated to horseradish peroxidase. The SuperSignal chemiluminescence method was used to detect protein bands and equal loading of the proteins was checked through detection of β -actin using primary rabbit anti-human β -actin antibody. The bands were analyzed and quantified using densitometry.

The amount of protein in each cell homogenate was measured using Bio-Rad protein assay kit (catalogue #500-0006).

Statistical analysis

The results were analyzed using GraphPad Prism software v. 6 (GraphPad, San Diego, USA). The data is presented as mean \pm standard deviation (SD) of number of experiments and the mean values were compared using Student's t-test for significance of variance between the different study groups.

Results

Effect of galactose on growth factor-induced BrdU incorporation into DNA

The addition of 1–20 mM of galactose for 1–14 days induced varied DNA synthesis in response to stimulation by FBS (Fig. 1), with no significant effect of 1-day exposure to galactose. Treatment of the cell cultures with supra-physiological concentrations (10–20 mM) of galactose for 7–14 days significantly ($p < 0.01$) impaired FBS-induced DNA synthesis when compared to cells stimulated with FBS without galactose treatment. The addition of 10 mM galactose to the cell cultures for 1–14 days did not have any significant effect on FGF- or PDGF-induced DNA synthesis (Fig. 2); however IGF-1-induced DNA synthesis was

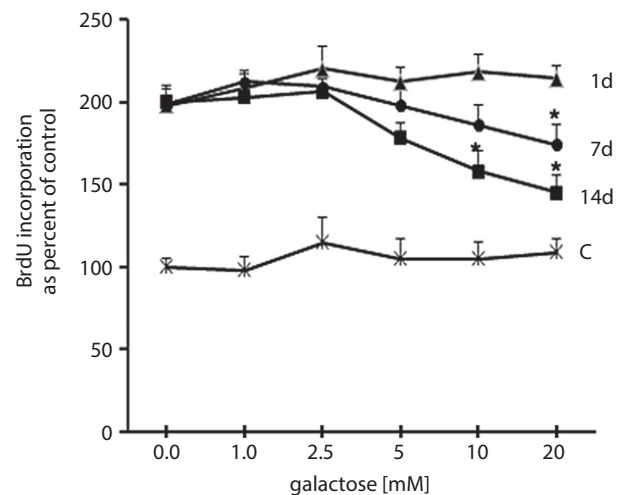


Fig. 1. BrdU incorporation (shown as percent of control) in skin fibroblasts stimulated with FBS for 24 h following treatment with varying concentrations (0–20 mM) of galactose for 1 day (rectangle points), 7 days (round points) or 14 days (square points). The control (star points) is represented by cells treated with varying concentrations of galactose in a mitogen-free medium (MFM). BrdU incorporation in the control cells was 0.58 ± 0.04 absorbance units (Au) at 450 nm per 5×10^3 cells. The data shown in graph is mean \pm SD of at least 6 measurements of BrdU incorporation carried out in duplicate. Statistical significance * $p < 0.01$ when compared to cells stimulated with FBS in the absence of galactose for the respective period of treatment (1, 7 or 14 days)

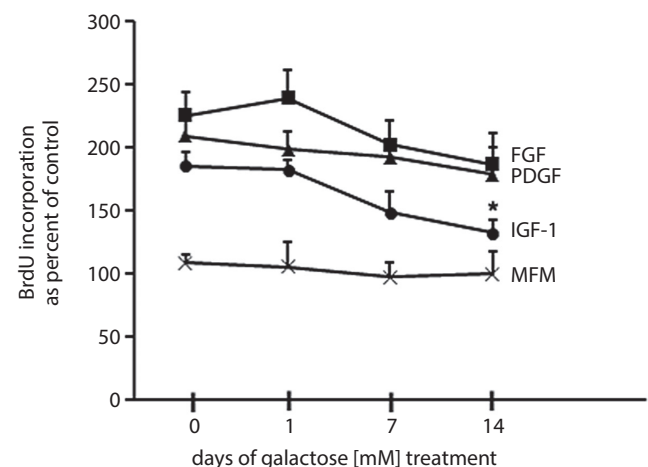


Fig. 2. BrdU incorporation (shown as percent of control) in skin fibroblasts cultured in the presence of 10 mM galactose for 1–14 days and then stimulated for 24 h with 50 ng/mL of PDGF (triangle points), FGF (square points) or IGF-1 (round points). The star points represent cells cultured in the presence of galactose for 1–14 days but not stimulated with any growth factor for BrdU incorporation. The data shown in the graph is the mean \pm SD of at least 6 measurements of BrdU incorporation carried out in duplicate. Statistical significance * $p < 0.01$ when compared to cells stimulated with the respective growth factor in the absence of galactose

markedly impaired by exposure of the cells to galactose for 7 days or longer, as BrdU incorporation was significantly ($p < 0.01$) reduced compared to the cells treated with IGF-1 in a galactose-free medium. Interestingly, the control experiments using cells cultured in the presence of 20 mM mannitol revealed that growth factor-induced DNA synthesis was not markedly altered (data not shown).

Effect of galactose-1-P on IGF-1- or FGF- or PDGF-induced BrdU incorporation into DNA

The addition of physiological or supraphysiological concentrations of Gal-1-P (0.5–10 mM) to the culture medium for 24 h did not have any marked effect on basal (control) or FBS-induced DNA synthesis in the fibroblast cells (Fig. 3). Chronic treatment (7–14 days) with

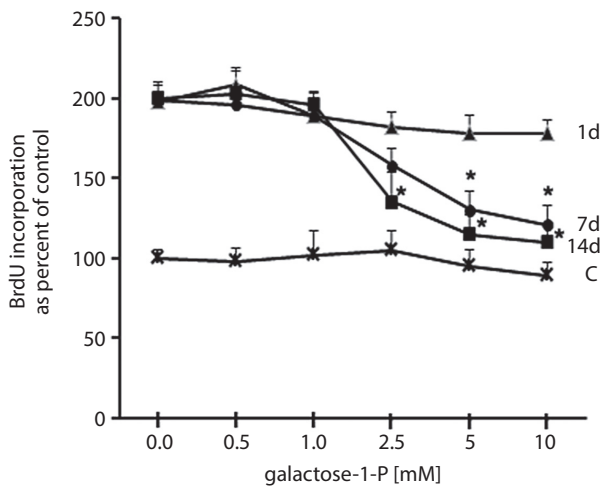


Fig. 3. BrdU incorporation (shown as percent of control) in skin fibroblasts stimulated with FBS for 24 h following treatment with varying concentrations (0–10 mM) of Gal-1-P for 1 day (rectangle points), 7 days (round points) or 14 days (square points). The control (star points) is represented by cells treated with varying concentrations of Gal-1-P in a mitogen-free medium (MFM). The data shown in the graph is the mean \pm SD of at least 6 measurements of BrdU incorporation carried out in duplicate. Statistical significance * $p < 0.01$ when compared to cells stimulated with FBS in the absence of Gal-1-P for the respective period of treatment (1, 7 or 14 days)

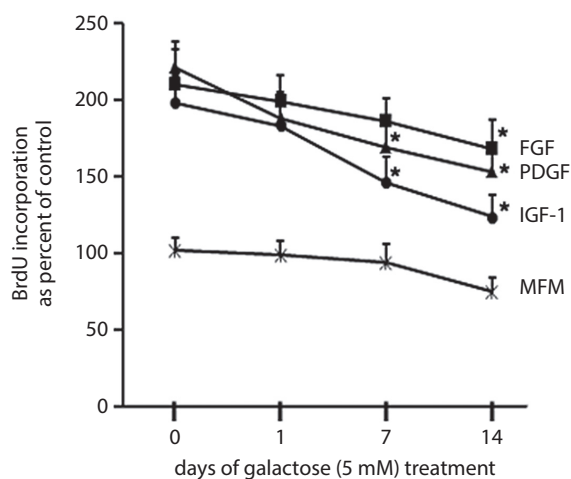


Fig. 4. BrdU incorporation (shown as percent of control) in skin fibroblasts cultured in the presence of 5 mM Gal-1-P for 1–14 days and then stimulated for 24 h with 50 ng/mL of PDGF (triangle points), FGF (square points) or IGF-1 (round points). The star points represent cells cultured in the presence of Gal-1-P for 1–14 days but not stimulated with any growth factor for BrdU incorporation. The data shown in the graph is the mean \pm SD of at least 6 measurements of BrdU incorporation carried out in duplicate. Statistical significance * $p < 0.01$ when compared to cells stimulated with the respective growth factor in the absence of Gal-1-P

supraphysiological concentrations of Gal-1-P (2.5–10.0 mM) significantly reduced ($p < 0.01$) FBS-induced BrdU incorporation in the fibroblast cells while lower concentrations of Gal-1-P did not have any notable effect (Fig. 3). The addition of Gal-1-P to the culture medium at supraphysiological concentrations for 14 days was observed to markedly impair growth factor-induced DNA synthesis in fibroblasts, as BrdU incorporation was significantly ($p < 0.01$) reduced in the cells stimulated with IGF-1 or PDGF (Fig. 4). Selective impairment of growth factor-induced DNA synthesis was also observed in cells cultured with 5 mM Gal-1-P for 7 days, where IGF-1-induced BrdU incorporation was significantly reduced without any marked effect on the mitogenic activity of PDGF and FGF (Fig. 4). Supraphysiological concentrations of Gal-1-P did not have any remarkable effect on basal (mitogen-free culture medium) DNA synthesis except for a notable, but statistically non-significant, reduction in BrdU incorporation following 14 days of treatment.

Effect of galactose and Gal-1-P on IGF-1 receptor and FGF receptor

Protein expression of IGF-1 receptor was significantly ($p < 0.01$) reduced in fibroblasts cultured in the presence of 5 mM Gal-1-P for 14 days (Fig. 5). Galactose treatment did not have any remarkable effect on the protein expression of FGFR or IGF-1R, while the impairment effect of Gal-1-P on IGF-1R was selective as FGFR protein levels remained unaltered. Neither Gal nor Gal-1-P had any marked effect on PDGF receptor expression (data not shown).

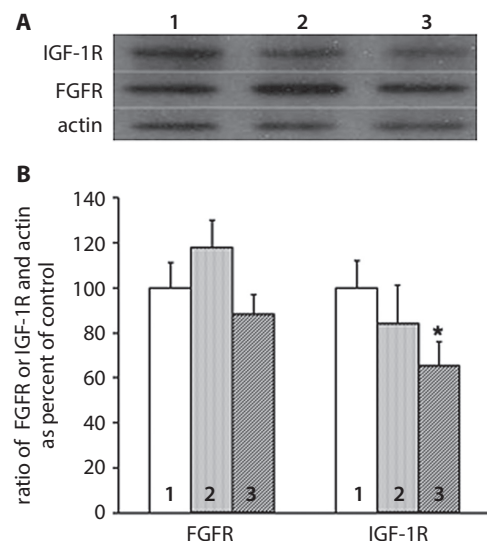


Fig. 5. Western blot analysis for protein expression of FGFR and IGF-1R in the fibroblast cells cultured in the presence of 10 mM of galactose (lane and bar 2) or 5 mM of Gal-1-P (lane and bar 3) for 14 days. The control (lane and bar 1) represents cells without any treatment. The values shown are the mean \pm SD of 6 measurements. Statistical significance * $p < 0.01$ when compared to the control (bar 1). The ratio of the band densities of FGFR/actin or IGF-1R/actin are shown as a percent of the control

Discussion

Endocrine disturbances have been reported to occur in galactosemia, where IGF-1 and its binding proteins are known to contribute toward pathogenesis, and our previous studies^{10,11} on the molecular mechanisms have also demonstrated that galactose/Gal-1-P downregulate the gene expression of IGF-1, a key determinant in the growth and development of children. The bioactivities of growth factors such as IGF-1 and growth hormone are important, in addition to their available content in the body tissues and fluids, for their role in the endocrine system during various developmental stages in children. This study establishes that the mitogenic activity of certain growth factors is profoundly impaired, possibly through receptor impairment, under galactosemic conditions. A marked decrease in FBS-induced mitogenic activity after chronic exposure of fibroblasts to supraphysiological concentrations of galactose under *ex vivo* conditions indicates some modifications in the cascade of molecular events. Our findings that exposure of fibroblast cultures to sub-/supraphysiological concentrations of galactose for 1–14 days did not affect basal (absence of a mitogen) DNA synthesis rules out any direct inhibitory effect of galactose on cell growth/survival. The fact that exposure to supraphysiological concentrations of galactose for up to 7 days did not have any marked effect on FBS-simulated DNA synthesis further points to some molecular modifications in the chronic presence of galactose or its metabolic derivatives where profound impairment of mitogen-induced DNA synthesis was observed. It is well-documented that Gal-1-P, a major metabolite of galactose that accumulates in the tissues and body fluids of galactosemia patients,¹⁶ is responsible for the detrimental effects. Profound impairment of growth factor-induced DNA synthesis by prolonged exposure to Gal-1-P strongly signals that the galactosemia-induced effects on growth factor activity might be mediated by this metabolite.

Though the exact mechanism of pathogenesis remains unknown, molecular galactosylation is a well-reported biochemical feature of galactosemia, which leads to the altered structure and function of cells and its membranes.¹⁷ The observed effect of chronic hypergalactosemic exposure on mitogen-/IGF-1-stimulated DNA synthesis may possibly be due to some kind of molecular galactosylation. The mitogenic activity of a growth factor is dependent upon its respective receptor, which triggers a cascade of signal transduction events to regulate cell growth and survival.¹⁸ The selective impairment of growth factor activity by Gal-1-P as observed in this study suggests a differential regulation of the function of various growth factor receptors under galactosemic conditions. A marked impairment of IGF-1-induced DNA synthesis associated with significantly decreased IGF-1 receptor protein in fibroblasts exposed to chronic treatment with Gal-1-P suggests that either Gal-1-P downregulates the gene expression

of IGF-1 receptor or post-translational modifications might be responsible for the reduction in IGF-1 receptor protein under galactosemic conditions. The fact that FGF receptor levels are increased, though not significantly, and PDGF receptor levels remained unaltered in the fibroblasts after chronic treatment with Gal-1-P indicates that either Gal-1-P selectively regulates the gene expression of various proteins or post-translational modifications such as molecular galactosylation differentially affect the structure and function of various membrane proteins including growth factor receptors. Other factors that might have deleterious effects on cell membrane components include cellular oxidative stress due to an imbalance of cellular ROS/reactive nitrogen species and cytokines.¹⁹


Increased levels of nitrites in the serum of galactosemia patients, as shown in our previous study, in addition to other reports regarding the overproduction of NO and the formation of nitrotyrosine residues in galactosemic tissues, may cause, at least in part, some of the post-translational modifications in membrane receptor proteins. In view of our earlier study, showing the profound effect of Gal-1-P on NO production in comparison to galactose signifies that Gal-1-P may likely be the major molecular trigger to induce deleterious changes in membrane receptor protein, in addition to galactosylation and other factors, to bring about the observed impairment of growth factor activity. Galactose alone did not have any marked effect on IGF-1-induced DNA synthesis, however its metabolite, Gal-1-P significantly reduced IGF-1 receptor protein and profoundly impaired IGF-1-induced DNA synthesis, clearly establishing that Gal-1-P is the key galactose metabolite to regulate growth factor function under hypergalactosemic conditions.

Conclusions

The selective impairment observed of IGF-1 mitogenic function by Gal-1-P through receptor modulation unravels a likely new molecular mechanism of galactosemia pathogenesis.

ORCID iDs

Mazen Al-Essa  <https://orcid.org/0000-0003-4119-3745>

Gursev Dhaunsi  <https://orcid.org/0000-0003-3496-8661>

References

1. Timson DJ. The molecular basis of galactosemia: Past, present and future. *Gene*. 2016;589(2):133–141. doi:10.1016/j.gene.2015.06.077
2. Chung MA. Galactosemia in infancy: Diagnosis, management and prognosis. *Pediatr Nurs*. 1997;23(6):563–569.
3. Bosch AM. Classical galactosemia revisited. *J Inherit Metab Dis*. 2006; 29(4):516–525.
4. Panis B, Forget PP, van Kroonenburgh MJ, et al. Bone metabolism in galactosemia. *Bone*. 2004;35(4):982–987.
5. Coelho AI, Rubio-Gozalbo ME, Vicente JB, Rivera I. Sweet and sour: An update on classic galactosemia. *J Inherit Metab Dis*. 2017;40(3): 325–342.

6. Charlwood J, Clayton P, Keir G, Mian N, Winchester B. Defective galactosylation of serum transferrin in galactosemia. *Glycobiology*. 1998; 8(4):351–357.
7. Cangemi G, Barco S, Barbagallo L, et al. Erythrocyte galactose-1-phosphate measurement by GC-MS in the monitoring of classical galactosemia. *Scand J Clin Lab Invest*. 2012;72(1):29–33.
8. Banerjee AK, Mandal A, Chanda D, Chakraborti S. Oxidant, antioxidant and physical exercise. *Mol Cell Biochem*. 2003;253(1–2):307–312.
9. Al-Essa M, Dhaunsi GS, Al-Qabandi W, Khan I. Impaired NADPH oxidase activity in peripheral blood lymphocytes of galactosemia patients. *Exp Biol Med*. 2013;238(7):779–786.
10. Rubio-Guzalbo ME, Panis B, Zimmerman LJ, Spaapen LJ, Menheere PP. The endocrine system in treated patients with classical galactosemia. *Mol Genet Metab*. 2006;89(4):316–322.
11. Dhaunsi GS, Al-Essa M. Downregulation of insulin-like growth factor-1 via nitric oxide production in a hypergalactosemic model of neonate skin fibroblast cultures. *Neonatology*. 2016;110(3):225–230.
12. LeRoith D, Yakar S. Mechanisms of disease: Metabolic effects of growth hormone and insulin-like growth factor-1. *Nat Clin Pract Endocrinol Metab*. 2007;3(3):302–310.
13. Dhaunsi G. Receptor-mediated selective impairment of insulin-like growth factor-1 activity in congenital disorders of glycosylation patients. *Pediatr Res*. 2017;81(3):526–530.
14. LeRoith D. Seminars in medicine of the Beth Israel Deaconess Medical Center. Insulin-like growth factors. *N Eng J Med*. 1997;336(9):633–640.
15. Lupu F, Terwilliger JD, Lee K, Segre GV, Efstratiadis A. Roles of growth hormone and insulin-like growth factor-1 in mouse postnatal growth. *Dev Biol*. 2001;229(1):141–162.
16. Yuzyuk T, Viau K, Andrews A, Pasquali M, Longo N. Biochemical changes and clinical outcomes in 34 patients with classical galactosemia. *J Inherit Metab Dis*. 2018;41(2):197–208.
17. Coss KP, Byrne JC, Coman DJ, et al. IgG N-glycans as potential biomarkers for determining galactose tolerance in classical galactosemia. *Mol Genet Metab*. 2012;105(2):212–220.
18. Werner H, LeRoith D. Insulin and insulin-like growth factor receptors in the brain: Physiological and pathological aspects. *Eur Neuropsychopharmacol*. 2014;24(12):1947–1953.
19. Pisoschi AM, Pop A. The role of antioxidants in the chemistry of oxidative stress: A review. *Eur J Med Chem*. 2015;97:55–74.

Mayer–Rokitansky–Küster–Hauser syndrome as an interdisciplinary problem

Magdalena Liszewska-Kapłon^{1,A–D}, Mateusz Strózik^{1,2,A–D}, Łukasz Kotarski^{1,A,B}, Maciej Bagłaj^{3,E,F}, Lidia Hirnle^{1,E,F}

¹ 1st Department and Clinic of Gynecology and Obstetrics, Wrocław Medical University, Poland

² Division of Histology and Embryology, Department of Human Morphology and Embryology, Wrocław Medical University, Poland

³ Department of Pediatric Surgery and Urology, Wrocław Medical University, Poland

A – research concept and design; B – collection and/or assembly of data; C – data analysis and interpretation;

D – writing the article; E – critical revision of the article; F – final approval of the article

Advances in Clinical and Experimental Medicine, ISSN 1899–5276 (print), ISSN 2451–2680 (online)

Adv Clin Exp Med. 2020;29(4):505–511

Address for correspondence

Mateusz Strózik

E-mail: juriaa@gmail.com

Funding sources

None declared

Conflict of interest

None declared

Received on February 20, 2019

Reviewed on August 30, 2019

Accepted on March 10, 2020

Published online on April 29, 2020

Abstract

The Mayer–Rokitansky–Küster–Hauser (MRKH) syndrome, also known as Müllerian agenesis or aplasia, is a congenital disease manifested by the aplasia of the uterus and the upper 2/3 of the vagina; its incidence is 1 in 4,000–5,000 female live births. We can distinguish 2 types of the MRKH syndrome: type I, which is characterized by an isolated absence of 2/3 of the vagina and uterus; and type II or MURCS (Müllerian duct aplasia, unilateral renal agenesis and cervicothoracic somite anomalies), which is also associated with other symptoms. The treatment of the MRKH syndrome patients aims at creating a neovagina and enabling sexual intercourse. Non-surgical techniques are the first-choice methods, and more than 90% of patients notice an anatomical and functional improvement if they are well-prepared emotionally. If non-surgical treatment does not bring about the expected results, a surgical procedure remains an option. The surgical method is mainly determined by the surgeon's experience. There are a few types of operations, though none of them seems superior to others. The next challenge is to provide these patients with a chance to become parents. Nowadays, a uterine transplant, a surrogate or adoption are the available solutions. An interdisciplinary approach is required, and the treatment should consist of medical and psychological support. This review presents the current knowledge about the MRKH syndrome with regard to the current methods of non-surgical and surgical treatment as well as a summary of the associated psychological problems.

Key words: MRKH syndrome, treatment, surgical, psychological aspects

Cite as

Liszewska-Kapłon M, Strózik M, Kotarski Ł, Bagłaj M, Hirnle L. Mayer–Rokitansky–Küster–Hauser syndrome as an interdisciplinary problem. *Adv Clin Exp Med.* 2020;29(4):505–511. doi:10.17219/acem/118850

DOI

10.17219/acem/118850

Copyright

© 2020 by Wrocław Medical University

This is an article distributed under the terms of the Creative Commons Attribution 3.0 Unported (CC BY 3.0) (<https://creativecommons.org/licenses/by/3.0/>)

Definition and epidemiology

The Mayer–Rokitansky–Küster–Hauser (MRKH) syndrome is a disorder of congenital anomalies that affects about 1:4,000–1:5,000 live-born girls.^{1,2} This syndrome is characterized by a missing or hypoplastic uterus, the upper 2/3 of the vagina missing, the proper development of external genitalia, properly functioning ovaries, and the appropriate karyotype for women – 46,XX.³

Etiopathogenesis

The etiology of the MRKH syndrome still remains unknown,^{4,5} though family cases have been described, suggesting that the MRKH syndrome may be an inherited disorder. Most of the current research suggests autosomal dominant inheritance, or a multifactorial or polygenic etiology of the MRKH syndrome.⁶ From the genetic point of view, 2 locations have been studied extensively. Among the suspected contributors to the MRKH syndrome are mutations in the homeobox genes. The homeobox genes are a large family of 39 genes, which can be divided into 4 classes: *Hoxa*, *Hoxb*, *Hoxc*, and *Hoxd*.⁷ The most important genes seem to be *Hoxa10*, *Hoxa11* and *Hoxa13*; they are located in the area which is directly responsible for the development of the uterus, cervix and vagina. *Hoxa 10* is expressed in the developing uterus, *Hoxa 11* in the lower uterine segment and cervix, and finally, *Hoxa 13* is expressed in the vagina.⁸ Another interesting genetic abnormality was described in the *WNT4* gene locus. The *WNT4* gene inhibits steroidogenic enzymes like 3 β -hydroxysteroid dehydrogenase and 17 α -hydroxylase, making the MRKH syndrome patients exhibit hyperandrogenism. A study conducted by Biason-Lauber et al., comprising the genetic analysis of an 18-year-old patient with the MRKH syndrome, confirmed the mutation of the *WNT4* gene in the woman.⁹ On the contrary, Philibert et al. examined 28 adolescent girls with the MRKH syndrome, 27 of whom – without hyperandrogenism – had no *WNT4* mutation.¹⁰

Clinical manifestation

Historically, 2 types of the MRKH syndrome have been distinguished: type I is characterized by an isolated absence of 2/3 of the vagina and uterus, whereas type II (MURCS – Müllerian duct aplasia, unilateral renal agenesis and cervicothoracic somite anomalies) is also associated with other symptoms, such as cardiac, urological and otological malformations.^{11–14} The associated malformations can be found in nearly 50% of patients with the MRKH syndrome; in 1/3 of cases, renal anomalies are detected, such as horse-shoe kidney, or ectopic or bilateral ureteropelvic junction

obstruction.¹⁵ In some situations, the term GRES (Genital, Renal, Ear, Skeletal) syndrome may be more appropriate.¹⁶ According to Deng et al., the spectrum of types I and II of the MRKH syndrome varies across different races and geographical locations; in their recent study, MURCS occurred in only 3% of cases.¹⁷

The MRKH syndrome often remains unrecognized until primary amenorrhea is observed; then, the diagnosis of the situation is extended. It is important to emphasize that the MRKH syndrome is the 2nd most common reason for the total absence of menstruation.¹⁸ Many patients have small remnants of endometrial tissue located in the muscular buds, which can lead to cyclical pelvic pain, sometimes requiring surgical or pharmacological management.^{19,20} Lately, there has been reported an increasing number of leiomyomas and fibroids, developing in the Müllerian remnant tissues or in the rudimentary uterus, which also may cause lower abdominal pain.^{21–23}

Diagnostic tools

Women with a diagnosis of the MRKH syndrome present with 46,XX karyotypes and normal external genitalia. They develop secondary sexual characteristics due to functional ovaries.^{24–26} The levels of the follicle-stimulating hormone (FSH) and the lutenizing hormone (LH) are appropriate to their age and to the phase of their menstrual cycle.³ The first suspicion of the MRKH syndrome is based on a medical interview (primary amenorrhea) as well as on a clinical examination revealing the absence of the vagina and a non-palpable uterus. To confirm the initial diagnosis, various diagnostic techniques may be used.²⁷

A highly available method, routinely used in diagnostics, is ultrasound examination. It easily shows the upper level of the vagina as well as the presence or absence of the uterus. Furthermore, it simultaneously allows the assessment of the kidneys and bladder for coexistent abnormalities.¹⁸ In many cases, ultrasonography (USG) findings are incomplete or inconclusive, especially when it comes to differentiation between types I and II of the MRKH syndrome.²⁸

Magnetic resonance imaging (MRI) is the gold standard in the process of diagnosing the MRKH syndrome patients. This technique is more sensitive than USG in detecting rudimentary Müllerian structures, which can be found in 90% of patients with the MRKH syndrome.^{29,30} In a recent study by Wang et al., MRI was crucial in exploring the location of the ovaries, as in 28% of cases, they were abnormally located.³¹ Such knowledge is important in the process of surgical planning and infertility treatment. Additionally, MRI can visualize the associated congenital anomalies, especially in the urinary tract.¹⁸

Differential diagnosis

Symptoms that are most similar to the MRKH phenotype are present in the androgen insensitivity syndrome. In both situations, primary amenorrhea, a shortened vagina and an absent cervix are observed. In patients with the androgen insensitivity syndrome, the gonads are testes. The differentiating symptoms are the androgen insensitivity syndrome patients' serum testosterone levels within the male range and karyotype 46,XY.³²

The most common genetic etiology of pubertal delay and primary amenorrhea is the Turner syndrome, with 45,X karyotype and an elevated FSH level. The final diagnosis of the Turner syndrome is based on the karyotype analysis. Typical clinical signs include a short and webbed neck, a low hairline at the nape of the neck, a short stature, a shield chest, and delayed puberty due to hypogonadism.³³

Another disease with a similar clinical appearance is *CYP17A1* deficiency – congenital adrenal hyperplasia due to 17 α -hydroxylase deficiency. *CYP17A1* is a gene that is necessary for the synthesis of sex steroids and cortisol. Additionally, hypertension and hypokalemia are observed. Females affected by these symptoms will have the uterus and vagina, but males will usually have female external genitalia, a blind vagina and intra-abdominal testes.³⁴ In *CYP17A1* deficiency, reduced sex steroids and elevated gonadotropin and progesterone levels as well as mineralocorticoid hypertension are pathognomonic (Table 1).³⁵

Management

The main goal of the MRKH treatment is to create an appropriate vaginal cavity in order to facilitate sexual intercourse. Throughout the years, a lot of non-surgical and surgical interventions have been developed. Currently, the best management method remains controversial due to the lack of longitudinal studies and prospective evaluation of the interventions undertaken.³⁶ Moreover, there is no general united definition of successful neovagina formation. Studies focus on the anatomical length or functionality which enables satisfactory intercourse. The lack

of guidelines leaves the choice of treatment to the surgeon; it depends on the surgeon's expertise and previous surgical attempts as well as on the patient's genital configuration.

Psychological aspects

Apart from the most common physiological symptoms, the MRKH syndrome patients are very often afflicted with various psychological problems. They suffer from disturbances in perceiving their sex, body, and social or sexual role as a woman.³⁷ Heller-Boersma et al. point to the fact that the MRKH syndrome may contribute to various, often extreme, emotional behaviors, ranging from positive ones – like a high level of motivation for treatment – to negative ones like depression, anxiety, shock, the feeling of isolation, shame, and even suicidal tendencies.³⁷ In 2012, Gupta and Kharb described the first case of suicide related to the MRKH syndrome.³⁸ The woman was in a state of despair due to her illness. She came to the point where she did not care about hygiene and stopped bathing, thus causing infective dermatitis. Then, as a result of the additional stress, she committed a suicide.³⁸ The American College of Obstetricians and Gynecologists (ACOG) indicates that the role of support groups for patients with the MRKH syndrome is crucial. What is also emphasized by ACOG is the importance of the psychological aspect in the whole process of healing.³⁹ Studies have revealed that the best indicator of the emotional acceptance of the diagnosis is the relationship between parents or caretakers and the patient as well as the patient's ability to share their feelings with their family and friends.⁴⁰ Beisert et al. analyzed 31 MRKH patients in comparison with 31 healthy women.⁴¹ They observed partly similar sexual development, whereby the MRKH patients exhibited dyadic sexual activity. It was speculated that this was not only due to the defective biological condition, but was also a psychological consequence of the disease.⁴¹ To our knowledge, there are no studies that have indicated patients affected by the MRKH syndrome deciding to change their gender or having gender dysphoria. Nevertheless, many studies have revealed the patients' doubts about their female identity, and a sense of being defective and incomplete.^{40,42,43} Some women believed that

Table 1. Differential diagnosis of the Mayer–Rokitansky–Küster–Hauser (MRKH) syndrome

Syndrome	Karyotype	Menstruation	Female internal reproductive organs	Laboratory findings
MRKH syndrome	46,XX	primary amenorrhea	– lack/hypoplasia of the uterus – lack of the upper 2/3 of the vagina – normal ovaries	↑ testosterone
Androgen insensitivity syndrome	46,XY	primary amenorrhea	– a shortened vagina – lack of the cervix – testes	↑ FSH
Turner syndrome	45,X	primary amenorrhea	hypogonadism	↑/N FSH
Congenital adrenal hyperplasia	46,XY	irregular menstruation	presence of the vagina and uterus	↑ FSH ↑ progesterone ↓ estrogen

FSH – follicle-stimulating hormone; N – normal.

to be a real woman they must have reproductive abilities.⁴⁴ Unfortunately, fulfilling important life roles is affected by long-lasting and demanding treatment. Professional medical care which focuses not only on the treatment itself, but also on psychological support for the patients, could help overcome these limitations.⁴⁵

Non-surgical treatment

According to the ACOG recommendations, the first-choice treatment should begin with non-surgical methods.³⁹ A multicenter study conducted by Cheikhelard et al. showed that surgery was not superior to non-surgical methods based on dilation.⁴⁶ First described by Frank, the use of dilators of increasing sizes still remains one of the most popular first-line treatment methods as well as the one used after surgical procedures for maintaining the vaginal cavity.⁴⁷ In 1981, Ingram modified Frank's technique to avoid some inconveniences by installing a dilator on a bicycle seat, allowing the patient to perform other activities during the sessions.⁴⁸ Dilators of increasing sizes are placed inside the vaginal dimple and intermittent, progressive, manual pressure is used to create a vaginal cavity. Dilators are supposed to be used 3 times a day for 15–20 min. Both methods are minimally invasive and cost-effective procedures, with a low complication rate, allowing a vagina to be created from normal vaginal tissue.⁴⁹ Non-surgical options are reserved for those patients who are motivated and psychosexually mature, because the success rate depends mainly on the patient's compliance.⁵⁰ According to Edmonds et al., more than 90% of patients will respond to a non-surgical procedure using vaginal dilators with both the anatomical (a neovagina greater than 6 cm in length) and functional success.⁵¹ According to a recent study by Both et al., women with a neovagina after dilation showed a weaker vaginal blood flow response after sexual stimulation, which may be related to lesser innervation and vascularization as compared to a natal vagina.⁵² Despite such findings, patients with the MRKH syndrome did not differ in the level of subjective sexual arousal and satisfaction from the control group.⁵² Ketheeswaran et al. found that adjuvant treatment, such as estriol cream, nitrous oxide and oxygen, diazepam, lidocaine ointment, paracetamol, and naproxen, can improve outcomes in women who used vaginal dilators.⁵³ The adjuvants minimize discomfort and anxiety during progressive dilation. The success rate depends on the patient's compliance and attitude; therefore, multidisciplinary care involving social workers, trained nurses, psychologists, and physicians play a key role.²

Surgical treatment

Surgical methods should be reserved for patients deprecating the dilation technique as well as for those after unsuccessful non-surgical management. There are a number of surgical techniques used to create an artificial vagina.

Intestinal vaginoplasty was first described in 1892 by Sneuguireff, and today utilizes the sigmoid colon in the creation of a neovagina. This technique requires both a perineal approach and laparotomy, demanding the cooperation of a pediatric surgeon and a gynecologist. The sigmoid colon is widely used as a graft due to its larger diameter and close proximity to the perineum. Historically, the ileum, cecum and jejunum segments were used, but due to high morbidity and mortality, the procedure was abandoned. Sigmoid colon tissue, 10–12 cm in length, with its own blood supply, is distended toward the introitus, and then connected with the created cavity. There are a number of advantages of this method, e.g., no dilators are required after the surgery and lubrication is satisfactory.⁵⁴ In a recent study by Özkan et al., 43 cases of sigmoid vaginoplasty were reviewed and the overall success was reported, both anatomical (the mean length of a neovagina was 11.7 ± 1.2 cm) and functional (97% of patients rated their sexual intercourse as satisfactory).⁵⁵ The most concerning flaws are excessive odorous secretion in the beginning, donor site morbidity, defecation problems, postoperative ileus, anastomotic leaks, the development of inflammatory bowel disease, ulcerative colitis, diversion colitis, potential neoplasia and carcinoma in the grafts, neovaginal prolapse, and stenosis.^{56–58} The laparoscopic modification has been gaining more and more popularity, with fewer postoperative pelvic adhesions, less intraoperative blood loss, a better cosmetic effect, a shorter hospital stay, and faster recovery.⁵⁹ Nevertheless, it should be performed only by experienced laparoscopic surgeons.⁶⁰ Robotic approaches are also evolving, but due to high costs, they still remain limited.⁶¹ In the upcoming era of the uterus transplantation, while choosing the method for neovagina creation, performing such transplantation in the future should be taken into consideration. Gauthier et al. raise concerns about sigmoid coloplasty and suggests that this type of surgery should be avoided in neovagina creation.⁶² An increased risk of adhesions, damage to a neovagina and contamination from bowel mucosa can put a uterine transplant at risk and lead to the failure of the procedure.⁶²

One of the most popular types of surgery is the laparoscopic Vecchietti vaginoplasty, first described in 1965 as a laparotomy. This technique is based on progressive passive traction through the external pelvic wall on the retrohymenal fovea with the use of an acrylic "olive". This method preserves natural vaginal tissue, and avoids stenosis complications and excessive mucus production. As compared to other surgical interventions, the Vecchietti procedure boasts the shortest operative time.⁴⁹ Some alternatives to Vecchietti's procedure have been proposed, using balloons or a Foley catheter instead of acrylic olives, or applying a different approach, avoiding vesicorectal tunneling – a safer, shorter, more effective, and less traumatic procedure, with a very low complication rate.^{63,64}

Another type of surgery relies on creating a neovaginal space between the rectum and the bladder by inserting

an inlay graft. McIndoe's approach requires perineal access, avoiding an abdominal incision. A cavity is created between the urethra and the rectum, and a skin graft, usually acquired from the buttock area, is used. McIndoe modifications with different types of grafts have been proposed, e.g., with split-thickness skin grafts and full-thickness skin grafts, an amnion, autologous vaginal tissue cultured in vitro, and artificial grafts. Injury to the neighboring organs, such as the rectum and bladder, are the most serious complications. Skin grafts are often problematic because of inadequate lubrication, resulting in dyspareunia, a high rate of stenosis and excessive hair growth. External visible scars from the graft harvest sites – the buttock, groin or thigh – can also cause the patient's discomfort. Graft methods require the postoperative use of molds in order to prevent possible graft contraction and stenosis. The molds need to be carefully changed to avoid the shearing of the graft, as the secondary healing of lesions is connected with unfavorable long-term results.⁶⁵ According to McQuillan and Grover, graft techniques require the longest hospital stay after the surgery.⁴⁹ Squamous papillomas in the skin graft have been reported in a neovagina, hence there are some concerns about their malignant transformation.⁶⁶

The Davydov procedure, designed as an abdominal approach, is nowadays widely performed laparoscopically.⁶⁷ After dissecting the retrovesical space, the peritoneum is mobilized and an attachment with the neovaginal introitus is created. Postoperative dilation is required to avoid vaginal collapse before epithelialization is complete. Still, peritoneal vaginoplasty is accompanied by a greater number of intra- and postoperative complications, and more frequent rectal injuries than other vaginoplasty techniques.⁶⁸

Another form is Williams vaginoplasty, later modified by Creatas,⁶⁹ where a neovaginal pouch is created with a deep incision extending from the labia majora to the peritoneum, further expanded by dilators or sexual intercourse. A study on 178 women reported a 96% anatomical success rate and a 94% functional success rate.⁷⁰ Wound infection, hematomas and excessive hair growth may complicate the procedure.

The gold standard treatment for the MRKH syndrome has yet to be established, because it is extremely difficult to compare the results of different techniques without prospective long-term studies.⁷¹

Reproductive challenges

Every woman affected by the MRKH syndrome has no reproductive ability, which is one of the main problems for these patients. The possibility of having children is limited to a uterine transplant, or an in vitro method using a surrogate or adoption.^{72–74} In a study on 50 MRKH syndrome women, after reconstructive surgery, nearly 2/3 of the study group were interested in uterus transplantation.⁷⁵ Uterine transplantation can be a real solution

in the future for patients with the MRKH syndrome, especially with the latest report of the first live birth after a uterus transplant in the USA in an MRKH syndrome patient.^{74,76,77} Currently, there are 7 ongoing clinical trials concerning uterine transplantation in the MRKH syndrome patients.⁷⁸


Summary


The MRKH syndrome is certainly a disease that requires an interdisciplinary approach. The congenital defects occurring in the patient modify her own image as a sexual person, but should not necessarily be regarded as impairing sexual satisfaction, since it is affected by many more factors. In recent years, numerous methods of MRKH management for patients have been developed. However, in fact there is no ideal method for all patients. Optimal care for such patients includes both therapeutic and psychological support.


ORCID iDs

Magdalena Liszewska-Kapłon  <https://orcid.org/0000-0002-4116-3530>

Mateusz Strózik  <https://orcid.org/0000-0002-5533-3086>

Łukasz Kotarski  <https://orcid.org/0000-0002-0866-9636>

Maciej Baglaj  <https://orcid.org/0000-0002-6291-1577>

Lidia Hirnle  <https://orcid.org/0000-0001-9789-5370>

References

- Petrozza JC. Mayer–Rokitansky–Küster–Hauser syndrome and associated malformations: Are they as common as we think? *Fertil Steril*. 2016;106(5):1047–1048.
- Patel V, Hakim J, Gomez-Lobo V, Amies Oelschlager AM. Providers' experiences with vaginal dilator training for patients with vaginal agenesis. *J Pediatr Adolesc Gynecol*. 2018;31(1):45–47.
- Boruah DK, Sanyal S, Gogoi BB, et al. Spectrum of MRI appearance of Mayer–Rokitansky–Küster–Hauser (MRKH) syndrome in primary amenorrhea patients. *J Clin Diagnostic Res*. 2017;11(7):TC30–TC35.
- Kobayashi A, Behringer RR. Developmental genetics of the female reproductive tract in mammals. *Nat Rev Genet*. 2003;4(12):969–980.
- Watanabe K, Kobayashi Y, Banno K, et al. Recent advances in the molecular mechanisms of Mayer–Rokitansky–Küster–Hauser syndrome. *Biomed Rep*. 2017;7(2):123–127.
- Herlin M, Højland AT, Petersen MB. Familial occurrence of Mayer–Rokitansky–Küster–Hauser syndrome: A case report and review of the literature. *Am J Med Genet A*. 2014;164A(9):2276–2286.
- Sultan C, Biason-Lauber A, Philibert P. Mayer–Rokitansky–Küster–Hauser syndrome: Recent clinical and genetic findings. *Gynecol Endocrinol*. 2009;25(1):8–11.
- Eun Kwon H, Taylor HS. The role of *HOX* genes in human implantation. *Ann NY Acad Sci*. 2004;1034(1):1–18.
- Biason-Lauber A, Konrad D, Navratil F, Schoenle EJ. A *WNT4* mutation associated with Müllerian-duct regression and virilization in a 46,XX woman. *N Engl J Med*. 2004;351(8):792–798.
- Philibert P, Biason-Lauber A, Rouzier R, et al. Identification and functional analysis of a new *WNT4* gene mutation among 28 adolescent girls with primary amenorrhea and Müllerian duct abnormalities: A French collaborative study. *J Clin Endocrinol Metab*. 2008;93(3):895–900.
- Nakum A, Kumawat K, Chauhan H, Parikh JV. Mayer–Rokitansky–Küster–Hauser (MRKH) syndrome type 2: Atypical presentation of rare case. *Natl J Med Res*. 2013;3(4):409–411.
- Oppelt PG, Lermann J, Strick R, et al. Malformations in a cohort of 284 women with Mayer–Rokitansky–Küster–Hauser syndrome (MRKH). *Reprod Biol Endocrinol*. 2012;10:57.

13. Kapczuk K, Iwaniec K, Friebe Z, Kędzia W. Congenital malformations and other comorbidities in 125 women with Mayer–Rokitansky–Küster–Hauser syndrome. *Eur J Obstet Gynecol Reprod Biol.* 2016;207:45–49.
14. Pan HX, Luo GN. Phenotypic and clinical aspects of Mayer–Rokitansky–Küster–Hauser syndrome in a Chinese population: An analysis of 594 patients. *Fertil Steril.* 2016;106(5):1190–1194.
15. Chandiramani M, Gardiner CA, Padfield CJ, Ikhenia SE. Mayer–Rokitansky–Küster–Hauser syndrome. *J Obstet Gynaecol.* 2006;26(7):603–606.
16. Strübbe EH, Cremers CW, Willemsen WN, Rolland R, Thijn CJ. The Mayer–Rokitansky–Küster–Hauser (MRKH) syndrome without and with associated features: Two separate entities? *Clin Dysmorphol.* 1994;3(3):192–199.
17. Deng S, He Y, Chen N, Zhu L. Spectrum of type I and type II syndromes and associated malformations in Chinese patients with Mayer–Rokitansky–Küster–Hauser syndrome: A retrospective analysis of 274 cases. *J Pediatr Adolesc Gynecol.* 2019;32(3):284–287.
18. Giusti S, Fruzzetti E, Perini D, Fruzzetti F, Giusti P, Bartolozzi C. Diagnosis of a variant of Mayer–Rokitansky–Küster–Hauser syndrome: Useful MRI findings. *Abdom Imaging.* 2011;36(6):753–755.
19. Marsh CA, Will MA, Smorgick N, Quint EH, Hussain H, Smith YR. Uterine remnants and pelvic pain in females with Mayer–Rokitansky–Küster–Hauser syndrome. *J Pediatr Adolesc Gynecol.* 2013;26(3):199–202.
20. Chandini M, Hari Babu Ramineni, Rakesh Y, Babu K, Vidyadhara S. Mayer–Rokitansky–Küster–Hauser syndrome with gonadotropin deficiency: A rare case report. *Int J Res Med Sci.* 2016;4(7):3045–3047.
21. Hoo PS, Norhaslinda AR, Shah Reza JN. Rare case of leiomyoma and adenomyosis in Mayer–Rokitansky–Küster–Hauser syndrome. *Case Rep Obstet Gynecol.* 2016;2016:3725043.
22. Amaratunga T, Kirkpatrick I, Yan Y, Karlicki F. Ectopic pelvic fibroid in a woman with uterine agenesis and Mayer–Rokitansky–Küster–Hauser syndrome. *Ultrasound Q.* 2017;33(3):237–241.
23. Kulkarni MM, Deshmukh SD, Hol K, Nene N. A rare case of Mayer–Rokitansky–Küster–Hauser syndrome with multiple leiomyomas in hypoplastic uterus. *J Hum Reprod Sci.* 2015;8(4):242–244.
24. Leduc B, van Campenhout J, Simard R. Congenital absence of the vagina. Observations on 25 cases. *Am J Obstet Gynecol.* 1968;100(4):512–520.
25. Sarto GE. Cytogenetics of fifty patients with primary amenorrhea. *Am J Obstet Gynecol.* 1974;119(1):14–23.
26. Shane JM, Wilson EA, Schiff I, Naftolin F. A preliminary report on gonadotropin responsiveness in the Mayer–Rokitansky–Küster–Hauser syndrome (congenitally absent uterus). *Am J Obstet Gynecol.* 1977;127(3):326–327.
27. Lermann J, Mueller A, Wiesinger E, et al. Comparison of different diagnostic procedures for the staging of malformations associated with Mayer–Rokitansky–Küster–Hauser syndrome. *Fertil Steril.* 2011;96(1):156–159.
28. Muñoz MdM, Noguero R, Martin S. Mayer–Rokitansky–Küster–Hauser (MRKH) syndrome. Diagnostic and therapeutic approach of a rare disease. *Colomb Med.* 2011;42(3):369–372.
29. Preibsch H, Rall K, Wietek BM, et al. Clinical value of magnetic resonance imaging in patients with Mayer–Rokitansky–Küster–Hauser (MRKH) syndrome: Diagnosis of associated malformations, uterine rudiments and intrauterine endometrium. *Eur Radiol.* 2014;24(7):1621–1627.
30. Wang Y, Lu J, Zhu L, et al. Evaluation of Mayer–Rokitansky–Küster–Hauser syndrome with magnetic resonance imaging: Three patterns of uterine remnants and related anatomical features and clinical settings. *Eur Radiol.* 2017;27(12):5215–5224.
31. Wang Y, Lu J, Zhu L, et al. Increased incidence of abnormally located ovary in patients with Mayer–Rokitansky–Küster–Hauser syndrome: A retrospective analysis with magnetic resonance imaging. *Abdom Radiol (NY).* 2018;43(11):3142–3146.
32. Mendoza N, Motos MA. Androgen insensitivity syndrome. *Gynecol Endocrinol.* 2013;29(1):1–5.
33. Santos V, Marçal M, Amaral D, Pina R, Lopes L, Fonseca G. Turner syndrome. From child to adult... A multidisciplinary approach [in Portuguese]. *Acta Med Port.* 23(5):873–882.
34. Kim SM, Rhee JH. A case of 17 alpha-hydroxylase deficiency. *Clin Exp Reprod Med.* 2015;42(2):72–76.
35. Fontenele R, Costa-Santos M, Kater CE. 17 α -hydroxylase deficiency is an underdiagnosed disease: High frequency of misdiagnoses in a large cohort of Brazilian patients. *Endocr Pract.* 2018;24(2):170–178.
36. Callens N, De Cuyper G, De Sutter P, et al. An update on surgical and non-surgical treatments for vaginal hypoplasia. *Hum Reprod Update.* 2014;20(5):775–801.
37. Heller-Boersma JG, Edmonds DK, Schmidt UH. A cognitive behavioural model and therapy for utero-vaginal agenesis (Mayer–Rokitansky–Küster–Hauser syndrome: MRKH). *Behav Cogn Psychother.* 2009;37(4):449–467.
38. Gupta M, Kharb V. MRKH syndrome: Psychological disturbances and suicide. *J Indian Acad Forensic Med.* 2012;34(1):86–88.
39. Committee on Adolescent Health Care. ACOG Committee opinion No. 728: Müllerian agenesis: Diagnosis, management, and treatment. *Obstet Gynecol.* 2018;131(1):e35–e42.
40. Poland ML, Evans TN. Psychologic aspects of vaginal agenesis. *J Reprod Med.* 1985;30(4):340–344.
41. Beisert MJ, Szymańska-Pytlińska ME, Kapczuk K, Chodecka A, Walczyk-Matyja K, Kędzia W. Sexual activity of women with Mayer–Rokitansky–Küster–Hauser syndrome (MRKHS) – preliminary study. *Ginek Pol.* 2015;86(9):648–652.
42. Freundt I, Toolenaar TA, Huikeshoven FJ, Jeekel H, Drogendijk AC. Long-term psychosexual and psychosocial performance of patients with a sigmoid neovagina. *Am J Obstet Gynecol.* 1993;169(5):1210–1214.
43. Holt R, Slade P. Living with an incomplete vagina and womb: An interpretative phenomenological analysis of the experience of vaginal agenesis. *Psychol Health Med.* 2003;8(1):19–33.
44. David A, Carmil D, Bar-David E, Serr DM. Congenital absence of the vagina. Clinical and psychologic aspects. *Obstet Gynecol.* 1975;46(4):407–409.
45. Delaine M, Ohl J. Sexual activity and quality of life in patients with Mayer–Rokitansky–Küster–Hauser [in French]. *Gynecol Obstet Fertil.* 2014;42(12):865–871.
46. Cheikhelard A, Bidet M, Baptiste A, et al. Surgery is not superior to dilation for the management of vaginal agenesis in Mayer–Rokitansky–Küster–Hauser syndrome: A multicenter comparative observational study in 131 patients. *Am J Obstet Gynecol.* 2018;219(3):281.e1–281.e9.
47. Frank RT. The formation of an artificial vagina without operation. *Am J Obstet Gynecol.* 1938;35(6):1053–1055.
48. Ingram JM. The bicycle seat stool in the treatment of vaginal agenesis and stenosis: A preliminary report. *Am J Obstet Gynecol.* 1981;140(8):867–873.
49. McQuillan SK, Grover SR. Dilation and surgical management in vaginal agenesis: A systematic review. *Int Urogynecol J.* 2014;25(3):299–311.
50. Adeyemi-Fowode OA, Dietrich JE. Assessing the experience of vaginal dilator use and potential barriers to ongoing use among a focus group of women with Mayer–Rokitansky–Küster–Hauser syndrome. *J Pediatr Adolesc Gynecol.* 2017;30(4):491–494.
51. Edmonds DK, Rose GL, Lipton MG, Quek J. Mayer–Rokitansky–Küster–Hauser syndrome: A review of 245 consecutive cases managed by a multidisciplinary approach with vaginal dilators. *Fertil Steril.* 2012;97(3):686–690.
52. Both S, Kluijvers K, Ten Kate-Booij M, Weijnenborg P. Sexual response in women with Mayer–Rokitansky–Küster–Hauser syndrome with a non-surgical neo-vagina. *Am J Obstet Gynecol.* 2018;219(3):283.e1–e283.e8.
53. Ketheeswaran A, Morrisey J, Abbott J, Bennett M, Dudley J, Deans R. Intensive vaginal dilation using adjuvant treatments in women with Mayer–Rokitansky–Küster–Hauser syndrome: Retrospective cohort study. *Aust N Z J Obstet Gynaecol.* 2018;58(1):108–113.
54. Georgas K, Belgrano V, Andréasson M, Elander A, Selvaggi G. Bowel vaginoplasty: A systematic review. *J Plast Surg Hand Surg.* 2018;52(5):265–273.
55. Özkan Ö, Özkan Ö, Çinpolat A, et al. Vaginal reconstruction with the modified rectosigmoid colon: Surgical technique, long-term results and sexual outcomes. *J Plast Surg Hand Surg.* 2018;52(4):210–216.
56. van der Sluis WB, Bouman MB, Meijerink WJHJ, et al. Diversion neovaginitis after sigmoid vaginoplasty: Endoscopic and clinical characteristics. *Fertil Steril.* 2016;105(3):834–839.e1.
57. Djordjevic ML, Stanojevic DS, Bizic MR. Rectosigmoid vaginoplasty: clinical experience and outcomes in 86 cases. *J Sex Med.* 2011;8(12):3487–3494.

58. Kisku S, Varghese L, Kekre A, et al. Bowel vaginoplasty in children and young women: An institutional experience with 55 patients. *Int Urogynecol J*. 2015;26(10):1441–1448.
59. Zhang M, Li S, Huang X, et al. Transumbilical single-incision laparoscopic vaginoplasty hybrid transperineal approach using a sigmoid colon segment: Initial twenty-five cases. *Int Urol Nephrol*. 2016;48(9):1401–1406.
60. Bouman MB, Buncamper ME, van der Sluis WB, Meijerink WJ. Total laparoscopic sigmoid vaginoplasty. *Fertil Steril*. 2016;106(7):e22–e23.
61. Boztosun A, Olgan S. Robotic sigmoid vaginoplasty in an adolescent girl with Mayer–Rokitansky–Küster–Hauser syndrome. *Female Pelvic Med Reconstr Surg*. 2016;22(5):e32–e35.
62. Gauthier T, Lavoue V, Piver P, et al. Which neovagina reconstruction procedure for women with Mayer–Rokitansky–Küster–Hauser syndrome in the uterus transplantation era? Editorial from the French Uterus Transplantation Committee (CETUF) of CNGOF. *J Gynecol Obstet Hum Reprod*. 2018;47(4):175–176.
63. Brucker SY, Gegusch M, Zubke W, Rall K, Gauwerky JF, Wallwiener D. Neovagina creation in vaginal agenesis: Development of a new laparoscopic Vecchietti-based procedure and optimized instruments in a prospective comparative interventional study in 101 patients. *Fertil Steril*. 2008;90(5):1940–1952.
64. Rall K, Schickner MC, Barresi G, et al. Laparoscopically assisted neovaginoplasty in vaginal agenesis: A long-term outcome study in 240 patients. *J Pediatr Adolesc Gynecol*. 2014;27(6):379–385.
65. Han SE, Go JY, Choi DS, Seo GH, Lim SY. Experience with specially designed pored polyacetal mold dressing method used in McIndoe-style vaginoplasty. *J Pediatr Urol*. 2017;13(6):621.e1–e621.e6.
66. Idrees MT, Deligdisch L, Altchek A. Squamous papilloma with hyperpigmentation in the skin graft of the neovagina in Rokitansky syndrome: Literature review of benign and malignant lesions of the neovagina. *J Pediatr Adolesc Gynecol*. 2009;22(5):e148–e155.
67. Davydov SN, Zhvitiashvili OD. Formation of vagina (colpopoiesis) from peritoneum of Douglas pouch. *Acta Chir Plast*. 1974;16(1):35–41.
68. Le A, Wang Z, Shan L, Xiao T, Luo G, Shen Y. Analysis of rectal injuries resulting from laparoscopic peritoneal vaginoplasty (Luohu operation). *Clin Exp Obstet Gynecol*. 2016;43(2):250–253.
69. Creatsas G, Deligeorglou E, Makrakis E, Kontoravdis A, Papadimitriou L. Creation of a neovagina following Williams vaginoplasty and the Creatsas modification in 111 patients with Mayer–Rokitansky–Küster–Hauser syndrome. *Fertil Steril*. 2001;76(5):1036–1040.
70. Creatsas G, Deligeorglou E. Vaginal aplasia and reconstruction. *Best Pract Res Clin Obstet Gynaecol*. 2010;24(2):185–191.
71. Torres-de la Roche LA, Devassy R, Gopalakrishnan S, et al. Plastic neo-vaginal construction in Mayer–Rokitansky–Küster–Hauser syndrome: An expert opinion paper on the decision-making treatment process. *GMS Interdiscip Plast Reconstr Surg DGPW*. 2016;5:Doc08.
72. Friedler S, Grin L, Liberti G, Saar-Ryss B, Rabinson Y, Meltzer S. The reproductive potential of patients with Mayer–Rokitansky–Küster–Hauser syndrome using gestational surrogacy: A systematic review. *Reprod Biomed Online*. 2016;32(1):54–61.
73. Stadnicka G, Łepecka-Klusek C, Pilewska-Kozak AB, Pawłowska-Muc AK, Bałduga-Bałanda-Bałdyga A. The care of patients with Mayer–Rokitansky–Küster–Hauser syndrome (MRKH) [in Polish]. *J Educ Health Sport*. 2017;7(3):361–370.
74. Suganuma N, Hayashi A, Kisu I, Banno K, Hara H, Mihara M. Uterus transplantation: Toward clinical application in Japan. *Reprod Med Biol*. 2017;16(4):305–313.
75. Chmel R, Novackova M, Pastor Z, Fronek J. The interest of women with Mayer–Rokitansky–Küster–Hauser syndrome and laparoscopic Vecchietti neovagina in uterus transplantation. *J Pediatr Adolesc Gynecol*. 2018;31(5):480–484.
76. Testa G, McKenna GJ, Gunby RT Jr, et al. First live birth after uterus transplantation in the United States. *Am J Transplant*. 2018;18(5):1270–1274.
77. Brännström M, Dahm Kähler P, Greite R, Mölne J, Díaz-García C, Tullius SG. Uterus transplantation: A rapidly expanding field. *Transplantation*. 2018;102(4):569–577.
78. Search of: MRKH – list results. Home - ClinicalTrials.gov. <https://clinicaltrials.gov/ct2/results?cond=MRKH&term=&cntry=&state=&city=&dist=>. Accessed February 19, 2029.

IgA vasculitis with nephritis in children

Katarzyna Dyga^{1,B,D}, Maria Szczepańska^{2,E,F}

¹ Department of Pediatric Nephrology, Teaching Hospital No. 1, Medical University of Silesia, Zabrze, Poland

² Chair and Department of Pediatrics, School of Medicine with the Division of Dentistry in Zabrze, Medical University of Silesia, Poland

A – research concept and design; B – collection and/or assembly of data; C – data analysis and interpretation;

D – writing the article; E – critical revision of the article; F – final approval of the article

Advances in Clinical and Experimental Medicine, ISSN 1899–5276 (print), ISSN 2451–2680 (online)

Adv Clin Exp Med. 2020;29(4):513–519

Address for correspondence

Katarzyna Dyga

E-mail: katarzynadyga@wp.pl

Funding sources

None declared

Conflict of interest

None declared

Received on June 18, 2019

Reviewed on August 27, 2019

Accepted on September 24, 2019

Published online on April 30, 2020

Abstract

Immunoglobulin A vasculitis (IgAV), formerly known as Henoch–Schönlein purpura (HSP), is the most common form of systemic vasculitis in children. Although the first case of IgAV was described more than 200 years ago, its etiology still remains unclear. Nephrological symptoms are observed in 30–50% of children during the course of the disease, and in up to 91% of cases within 6 weeks of the onset of the first symptoms. Whereas other organ manifestations of IgAV are mostly benign and self-limiting, nephritis may lead to chronic kidney disease (CKD) and end-stage renal disease (ESRD). Appropriate treatment commenced early enough can stop the disease progression. However, even in severe cases there are no evidence-based guidelines, which makes the therapeutic decisions more difficult. In this article, which is the most up-to-date overview regarding IgAV, we discuss the disease's pathogenesis, the clinical forms of renal involvement in the course of the disease, the risk factors for adverse prognosis and treatment options in accordance with current recommendations.

Key words: children, nephritis, immunoglobulin A vasculitis

Cite as

Dyga K, Szczepańska M. IgA vasculitis with nephritis in children. *Adv Clin Exp Med.* 2020;29(4):513–519.

doi: 10.17219/acem/112566

DOI

10.17219/acem/112566

Copyright

© 2020 by Wrocław Medical University

This is an article distributed under the terms of the Creative Commons Attribution 3.0 Unported (CC BY 3.0)

(<https://creativecommons.org/licenses/by/3.0/>)

Introduction

Immunoglobulin A vasculitis (IgAV), formerly known as Henoch–Schönlein purpura (HSP), is a type of small-vessel vasculitis and is the most common form of systemic vasculitis in children.¹ The eponym “Henoch–Schönlein purpura” comes from the names of the 2 researchers, Johann Schönlein and his student Eduard Henoch, who first made a detailed analysis of this disease. According to the new nomenclature established during the International Chapel Hill Consensus Conference in 2012 (CHCC2012), the proper name of the disease is immunoglobulin A vasculitis (IgAV). The consensus to replace the former name (HSP) with IgAV was based on the pathophysiological feature of this disease whereby abnormal immunoglobulin A (IgA) is deposited in blood vessel walls.² The most typical symptom of IgAV is skin involvement – mainly presenting as a palpable purpura – which is often associated with systemic manifestations, including gastrointestinal pain and bleeding, arthralgia and/or arthritis and glomerulonephritis. Although most symptoms are self-limiting, renal disease is the most likely to result in long-term morbidity.

Epidemiology

The annual incidence of IgAV in children and infants is estimated to be 3–26.7 per 100,000, depending on the country studied; it is 2–33 times more common in children than in adults.³ The disease occurs in children aged 3–15 years, though 90% of cases concern children under the age of 10 years; the mean age is 6 years.^{4,5} Immunoglobulin A vasculitis is more often diagnosed in boys,^{1,4–6} with a lower incidence in African-origin children compared with Caucasian or Asian.¹ Immunoglobulin A vasculitis is also more common in children with familial Mediterranean fever.⁷

Diagnostic criteria

Immunoglobulin A vasculitis diagnosis should be based on the new classification criteria developed jointly by the European League Against Rheumatism (EULAR), the Pediatric Rheumatology International Trials Organization (PRINTO) and the Pediatric Rheumatology European Society (PRES) in 2008 and published in 2010, which have a sensitivity of 100% and a specificity of 87%. The criteria include a diagnosis of non-thrombocytopenic skin purpura with lower limb predominance as the main symptom and 1 of 4 additional criteria: abdominal pain, arthritis or joint pain, symptoms of nephropathy (proteinuria >0.3 g/24 h or a urine protein/creatinine ratio (UP/UC ratio) >30 mg/mmol on a spot morning sample or hematuria of >5 erythrocytes/high-power field), and a typical

picture in histopathological examination of the skin showing leukocytoclastic vasculitis with predominant IgA deposits or kidney biopsy presenting proliferative glomerulonephritis with predominant IgA deposits. In cases of purpura with an atypical distribution, the presence of IgA deposits in the biopsy specimen is required.⁸ Ultrasonography is non-specific for IgAV (mesenteric lymphadenopathy and ascites detection), but along with computed tomography imaging is useful in diagnosing abdominal complications, such as intussusception, kidney parenchymal disease, and epididymal and testicular inflammation.⁹

Pathogenesis

Although the first case of this disease was described more than 200 years ago, its etiology still remains unclear. The current etiopathogenetic hypothesis for IgAV assumes an abnormal immune response to various antigens in genetically susceptible individuals.⁴ This theory is supported by the fact that IgAV mainly appears outside of the summer months, which is likely due to the relationship with infections and the lower risk of transmitting microbes among children during the summertime.^{1,4,10} In addition, symptoms of upper respiratory tract infection during the 3 weeks preceding the disease are reported in 90% of patients.^{4,11} In studies conducted independently by Calvino et al. and Saulsbury, a positive throat culture for group A beta-hemolytic streptococci (GAS) was found in 20–35% of IgAV patients.^{5,12} Interestingly, Masuda et al. suggest that glomerular deposition of nephritis-associated plasmin receptor (NAP1r), a GAS antigen, may be responsible for some cases of IgAV nephritis.¹³ There is also an assumption that microorganisms could harbor antigenic structures resembling those of human small-vessel endothelial cells, consequently leading to the production of IgA cross-reactive anti-endothelial cell antibodies (AECA), which promote vascular damage by the activation of the complement system and antibody-dependent cellular cytotoxicity (ADCC).¹⁴

In the literature, non-infectious agents are also reported to initiate the development of IgAV, such as medications (e.g., non-steroidal anti-inflammatory drugs (NSAIDs)), angiotensin converting enzyme inhibitors (ACEi), angiotensin receptor blockers (ARB), vaccines (e.g., the influenza vaccine or the hepatitis A and B vaccines) and malignancies, in this case mainly affecting adults (e.g., non-small cell lung cancer or prostate cancer).^{15,16}

It is also possible that there is a genetic predisposition to developing IgAV and subsequent renal involvement. The genetic studies carried out so far indicate that the HLA-DRB1*01:03 allele in Europeans and the HLA-B*41:02 allele in Caucasians are associated with increased susceptibility to IgAV.¹⁷ López-Mejías et al. reported that a protective effect against the development of IgAV

appears to exist in Caucasians with the HLA-DRB1:03 phenotype.¹⁸ Moreover, several molecular and genetic polymorphisms relating to disease susceptibility, severity and/or the risk of renal involvement have recently been described. An increased risk of nephritis in the course of IgAV is associated with the polymorphism of genes encoding vascular endothelial growth factor (VEGF), interleukin 1 receptor antagonist (IL-1Ra), interleukin 1 β (IL-1 β) and interleukin 8 (IL-8) and the presence of the HLA-B35 allele.^{19,20} However, most of the above studies were conducted on a relatively small number of patients, which means they lack the power to be definitive or necessarily applicable to all racial groups.²¹

Although the detailed pathogenic mechanism of IgAV with nephritis (IgAVN) has not been fully elucidated, it seems to be identical to IgA nephropathy (IgAN) with only quantitative differences, possibly accounting for the different clinical presentation with more acute signs of nephritis in IgAV and a more insidious onset of IgAN. However, the latest hypothesis, created by Heineke et al., suggests that renal and systemic symptoms in IgAV, IgAVN and IgAN may have different origins.²² Moreover, the authors anticipated that IgAVN is a dual disease which has components of both IgAV and IgAN.

The current hypothesis for glomerulonephritis in IgAN and IgAVN assumes that the symptoms are due to the deposition of immune complexes in small blood vessels (predominantly capillaries, venules or arterioles) which mainly consist of subclass 1 of immunoglobulin A, IgA1. The proposed mechanism of this phenomenon includes the disturbance of the glycosylation of oligosaccharides located in the hinge region of IgA1 by the failure of galactose to attach to the N-acetylgalactosamine residues found at this site.²³ The primary defect that leads to the production of such abnormally glycosylated IgA1 is probably heritable^{24,25} and might be due to a reduced activity of core 1 β 1,3-galactosyltransferase (C1GalT1) and an elevated expression and activity of α -N-acetylgalactosaminide α -2,6-sialyltransferase 2 (ST6GalNAc-II) in peripheral B cells.^{23,26} There is also a hypothesis that mucosal infection and concomitant interleukin 6 (IL-6) and interleukin 4 (IL-4) production may lead to aberrant glycosylation by modifying the glycosylation machinery.²⁶

These aberrantly glycosylated IgA1 antibodies, called galactose-deficient IgA1 (Gd-IgA1), have been shown to form immune complexes with naturally occurring anti-glycan IgA1 or IgG antibodies, whose origin is poorly understood.^{22,23} It was noted that all IgAV patients have IgA1-containing circulating immune complexes (CIC) of low molecular mass, but only those with nephritis have additional high-molecular-mass IgA1- or IgG-containing CICs.^{16,23} There is an assumption that the presence of IgG in immune complexes facilitates deposition on the glomerular mesangium.²² It was also observed that IgA1-containing immune complexes are present at higher concentrations in the urine of patients with IgAN and IgAVN

and can form a specific marker for disease activity and/or severity in these patients.^{23,27}

Due to the large size of CICs, their binding to the asialoglycoprotein receptors on hepatocytes (ASGP-R) and their internalization and degradation by hepatic cells are inhibited, which leads to their increased amounts in circulation.¹⁶ In the kidneys they bind to transferrin receptor (CD71, TfR) on mesangial cells,^{28,29} which enhances immune complex deposition and stimulates mesangial cells to proliferate and overproduce cellular matrix components and to secrete chemokines such as transforming growth factor beta (TGF β) or tumor necrosis factor alpha (TNF- α) – which alter podocyte function³⁰ – and IL-8, which recruits and activates polymorphonuclear neutrophils (PMNs).³¹ Accompanying glomerular complement activation through both the alternative and mannan-binding lectin pathways³² initiates the inflammatory cascade and enhances glomerular injury, contributing to the development of proliferative glomerulonephritis. Additionally, recent reports have assumed that IgA immune complexes directly induce neutrophils' migration and activation into affected tissues by binding to their IgA receptor, Fc α RI, worsening tissue damage.²²

Nephropathy

The course of IgAV is usually mild and self-limiting, but in 30–50% of patients it may lead to renal complications,^{5,6,12} which vary from asymptomatic microscopic hematuria with or without proteinuria and macroscopic hematuria, through fully expressed nephritic or nephrotic syndrome to rapidly progressive glomerulonephritis (RPGN). As for hypertension, it may be isolated or related to renal impairment.⁷ The most often symptom of nephritis is isolated microscopic hematuria with or without proteinuria.^{5,12} According to Pohl, either nephritic or a nephrotic syndrome develop in about 20% of IgAVN patients (7% of all IgAV cases).⁶

Nephrological symptoms usually appear early: in the 1st month of the disease in 85% of cases, within 6 weeks in 91% and within 6 months of the onset of the first symptoms in 97% of cases.³³ It is noteworthy that, according to several retrospective studies, nephritis never precedes the onset of skin lesions.^{5,12} Moreover, Saulsbury reports that the incidence of nephritis is significantly lower in children under the age of 2 years than in older children.⁵

The risk factors for developing nephropathy in the course of IgAV, according to a meta-analysis carried out by Chan et al., include male gender, an age of over 10 years, the presence of severe gastrointestinal symptoms (abdominal pain, gastrointestinal bleeding and ischemic intestinal injury), persistent purpura, the occurrence of relapses, arthritis/arthritis, and certain laboratory abnormalities, such as leukocytosis above $15 \times 10^9/L$, thrombocytosis above $500 \times 10^9/L$, elevated serum antistreptolysin O

(ASO) titer, and decreased serum c3 of the complement concentration.³⁴

A kidney biopsy in IgAV should be considered when acute renal impairment or nephritic syndrome is observed at the initial stage; moreover, when nephrotic syndrome with normal renal function persists for 4 weeks, nephrotic range proteinuria (a UP/UC ratio >250 mg/mmol) is observed for 4–6 weeks or persistent proteinuria (a UP/UC ratio >100 mg/mmol) occurs for more than 3 months.⁷ Interestingly, a study carried out by Halling et al. revealed that severe morphological changes found in renal biopsy occurred not only in patients with proteinuria in the nephrotic range but also in those with mild proteinuria. This observation allowed the authors to conclude that the clinical findings at the onset of the disease cannot predict the morphological changes.³⁵ Likewise, a long-term study conducted by Ronkainen et al. confirmed that severity of findings on the first kidney biopsy did not correlate with the risk of a poor outcome (hypertension, persistent proteinuria or end-stage renal disease (ESRD)).³⁶

As an alternative to kidney biopsy, Hara et al. showed that the podocyturia as well as hematuria and proteinuria had significant correlations with acute renal lesions – such as acute extracapillary, intracapillary and tubulointerstitial lesions – in biopsy. They also suggested that the cumulative excretion of urinary podocytes may be a predictor for histologic disease progression among children with IgAN and IgAVN.³⁷

In a review conducted by Jelusic et al., the authors emphasized the role of appropriate histological classification in establishing guidelines for treating patients with IgAVN. However, a current problem of classifying IgAVN is that the classifications have not been validated in children or they have only been validated in IgAN.³⁸ It is worth pointing out that, compared to IgAN, in IgAVN renal biopsy samples show increased endocapillary proliferation, epithelial crescents, neutrophil infiltration, perivascular glomerular IgA, subendothelial/subepithelial IgA deposits and fibrin deposits,^{6,16,38,39} which indicates the use of a different classification.

Currently, histological changes are graded in a classification which was published in 1977 by the International Study for Kidney Disease in Children (ISKDC), with 6 categories (I–V, according to the presence and number of crescents, and VI, for a membranoproliferative aspect). In this classification, only mesangial proliferation and the percentage of crescents is used to estimate disease severity and to predict outcome. However, the latest retrospective study, carried out on adults with IgAVN by Huang et al., showed that patients with more crescents had more severe renal manifestations and worse treatment response, whereas the proportion of crescents did not correlate with a higher risk for ESRD or a 50% decline in renal function.⁴⁰ According to Davin, the main failing of the ISKDC classification is that it does not consider some other important prognostic factors, such as mesangial and endocapillary

hypercellularity, tubular atrophy, interstitial fibrosis, interstitial inflammation, crescent features (fibrotic or not), segmental and global glomerulosclerosis and arterio- and arteriolosclerosis.⁴¹

Due to these all disadvantages of the ISKDC, some investigators prefer to apply the Oxford classification in updated in 2016 form called the MEST-C score, which includes 5 parameters: mesangial hypercellularity (M), endocapillary hypercellularity (E), segmental glomerulosclerosis (S), tubular atrophy/interstitial fibrosis (T), and cellular/fibrocellular crescents (C). However, this classification was originally created for IgAN and is currently not recommended for use in IgAVN.^{38,39} In 2017, Xu et al. estimated the value of the Oxford classification in children with IgAVN on the basis of a retrospective study including 104 patients. They found that segmental glomerulosclerosis (S) was strongly associated with impaired renal function and tubular atrophy/interstitial fibrosis (T) was significantly associated with proteinuria and clinical remission. The authors suggested that this classification may help to identify histological variables that have independent predictive value for a patient's response to therapy.⁴² Moreover, the latest study, conducted by Huang et al. on a larger group of IgAVN patients, revealed that the assessment of segmental glomerulosclerosis was an independent risk factor for renal endpoints, defined as a $\geq 30\%$ reduction in baseline estimated glomerular filtration rate in 2 years or a doubling of serum creatinine or ESRD, and confirmed that an updated Oxford classification can be valuable in predicting renal outcomes in IgAVN.⁴³ The classification developed by Koskela et al. in 2017 is the modified semiquantitative classification (SQC), which includes activity index, chronicity index and focal or diffuse mesangial proliferation. The authors demonstrated that the SQC was more coherent and more sensitive in terms of predicting IgAVN patient outcomes than the ISKDC.⁴⁴ Although their research revealed promising results, a study on a larger number of patients is needed to properly validate this classification.³⁸

Treatment

Treatment decisions in IgAV are difficult due to the large proportion of patients with a favorable prognosis and an unpredictable course in individual patients. Most reports in the literature consist of series or retrospective studies involving small numbers of patients, which makes the creation of standards of treatment more difficult.

In 2009, Zaffanello and Fanos published a review of literature from 1988 to 2008, which included reports of treatment with prednisolone, methylprednisolone, cyclophosphamide, azathioprine, cyclosporine, dypiridamole, warfarine and plasma exchange. The authors concluded that there was a lack of properly designed, randomized, placebo-controlled trials which could serve as a basis

for appropriate standards of treatment for patients with IgAVN.⁴⁵

In 2012, Kidney Disease: Improving Global Outcomes (KDIGO) published a practical guideline for the treatment of glomerulonephritis. According to their recommendations, in the case of persistent proteinuria of more than 0.5–1 g/day/1.73 m² in patients with IgAV, treatment with ACEi or ARB should be administered for 3–6 months, due to the renoprotective effects of these drugs, including delayed progression of renal failure and reduction of proteinuria. When this treatment is ineffective and the estimated glomerular filtration rate (eGFR) value remains higher than 50 mL/min/1.73 m², it is recommended to use the procedure as in IgA nephropathy (IgAN), involving the introduction of steroid therapy for a period of 6 months. In children with glomerular crescents in renal biopsy (more than 50% of glomeruli) and clinical manifestations of nephrotic syndrome and/or worsened renal function, the recommended treatment is similar of that for crescent IgA nephropathy, involving the use of steroids with simultaneous application of cyclophosphamide (CYP).⁴⁶ Kidney Disease: Improving Global Outcomes do not advise the use of steroids to prevent the development of nephropathy in the course of IgAV. Similarly, in several other studies it was demonstrated that steroid therapy does not protect against kidney involvement in the course of IgAV.^{5,45,47,48} However, these guidelines recommend an approach similar to treatment of IgAN patients, without taking into account the more acute onset of IgAV nephritis with more aggressive lesions in renal histology. In the opinion of Davin et al. the approach proposed by KDIGO may lead to undertreatment, mainly because acute and potentially aggressive glomerular inflammation either goes untreated or its immunosuppressive treatment is delayed for several months.⁴⁹ Interestingly, the largest longitudinal observational study, including 506 patients with IgAN and 161 patients with IgAV conducted by The Cure Glomerulonephropathy Network (Cure GN), revealed that in comparison to patients with IgAN, those with IgAVN were more likely to receive immunosuppressive therapy (79.5% vs 54%; $p < 0.001$), of which 35% were being treated with ≥ 2 immunosuppressive agents at the time of diagnosis.⁵⁰ This fact may indirectly suggest that a more severe course of IgAV requires more aggressive treatment than IgAN. The latest nationwide, longitudinal follow-up study from Finland confirms that early treatment may have a favorable effect on final renal prognosis.⁵¹

Recently, the European initiative SHARE (Single Hub and Access point for paediatric Rheumatology in Europe) released the long-awaited international recommendations for the diagnosis and treatment of IgAV. The panel of experts divided IgAV with nephritis into 3 categories, depending on the severity: mild, moderate and severe. For patients with mild IgAVN (normal eGFR and mild proteinuria – a UP/UC ratio < 100 mg/mmol – or moderate proteinuria – a UP/UC ratio of 100–250 mg/mmol), SHARE

recommends the use of oral prednisolone as a first-line treatment. However, the addition of other immunosuppressive agents, such as azathioprine (AZA), mycophenolate mofetil (MMF) or pulse iv. methylprednisolone (MP), may be considered as a second-line treatment. In moderate IgAVN ($< 50\%$ crescents on renal biopsy and impaired eGFR or severe persistent proteinuria – a UP/UC ratio > 250 mg/mmol for at least 4 weeks), oral prednisolone or pulse iv. methylprednisolone should be used as first-line treatment. In this case, the addition of AZA, MMF or iv. cyclophosphamide (CYP) may be used in first- or second-line treatment according to the histopathological findings of renal biopsy. In severe IgAVN ($> 50\%$ crescents on renal biopsy and impaired eGFR or severe persistent proteinuria) patients should be treated with iv. CYP and pulsed MP and/or oral prednisolone like patients with other forms of severe systemic small-vessel vasculitis. According to these recommendations patients with persistent proteinuria (a duration > 3 months) should be treated with ACEi or ARB irrespective of whether they are receiving prednisolone or other immunosuppressive treatment.⁵²

Both KDIGO and the latest SHARE recommendations are based mainly on expert opinions, because there is a lack of high-level controlled trials for severe IgAVN. Many authors emphasize the need to conduct well-designed, multicenter studies to provide evidence-based recommendations.^{39,45,46,52}

Prognosis

The progression of renal impairment in the course of IgAV is unpredictable in patients at the individual level, and active renal disease may develop after an initially mild nephritis or many years after stable, minor urinary abnormalities.^{36,39,53,54} A study conducted by Nussinovitch et al. suggests that even patients with no urinary abnormalities at onset may develop hypertension later on.⁵⁴ The occurrence of nephrological symptoms in some cases even long after the diagnosis of IgAV may be explained by the finding that the majority of children who underwent kidney re-biopsy within 2–9 years still have IgA deposits.²¹

While other organ manifestations of IgAV are mostly benign and self-limiting, nephritis might lead to chronic kidney disease (CKD) and ESRD. Long-term renal outcome correlates to the severity of the initial clinical presentation and to the extent of renal biopsy changes.^{35,39,53} A systematic review carried out by Narchi confirmed that the risk of long-term renal impairment, defined as persistent nephritic or nephrotic syndrome, renal insufficiency or hypertension, was low (1.6%) in patients with only isolated proteinuria or hematuria, but was much higher (19.5%) if the initial presentation was complicated by nephritic or nephrotic syndrome, with the risk being 2.5 times greater in women than in men.³³ Other studies evaluating patients from tertiary care centers with pediatric

nephrology wards found that the patients with nephritic, nephrotic or nephritic/nephrotic syndrome at onset had an even higher risk of long-term renal impairment, estimated at 35–44%.^{36,53}

Adverse prognostic factors for ESRD in adults with IgAV include renal dysfunction which persists from the onset of the disease (a creatinine level >1.35 mg/dL), proteinuria of over 1 g/day, macroscopic hematuria, hypertension and some degree of interstitial fibrosis, the presence of sclerotic glomeruli and fibrinoid necrosis on histopathology from a kidney biopsy.^{55,56}

Immunoglobulin A vasculitis recurs in about 1/3 of all cases,⁵ generally within 4 months of the resolution of the original symptoms. Recurrences are more frequent in patients with renal involvement, but are usually milder and of shorter duration than the original episode.^{5,12,21}

The follow-up period for children presenting with IgAV should last at least 6–12 months and should include regular urine testing for proteinuria and hematuria as well as blood pressure monitoring.^{33,52} According to a review carried out by Narchi, there is no need to follow up after the first 6 months with patients whose urinalysis remains normal, but measurements of serum urea and creatinine need to be continued in the presence of persistent isolated hematuria and/or proteinuria.³³

Women with a history of IgAV during childhood are at a higher risk of complications such as proteinuria and hypertension during pregnancy and should be monitored closely.^{33,36,53} In a study carried out by Ronkainen et al., up to 70% of pregnancies had complications of hypertension and/or proteinuria, even in the absence of active renal disease, which led to the conclusion that all women with a history of IgAV and even mild renal symptoms should be carefully observed, not only during pregnancy but also afterwards.³⁶


Regarding the risk of relapse of IgAV after kidney transplantation, depending on the source it is 33% to 50%,¹⁵ whereas the risk of graft loss from the recurrence of the disease, as reported by Kanaan et al, is 7.5% during 10-year follow-up period.⁵⁷

Conclusions

The authors emphasize that whereas other organ manifestations of IgAV are mostly benign and self-limiting, nephritis might lead to CKD, in its terminal stage as well. Appropriate treatment commenced early enough can stop the progression of the disease. However, even for the most severe cases, there are no evidence-based guidelines, which makes therapeutic decisions more difficult.

ORCID iDs

Katarzyna Dyga  <https://orcid.org/0000-0002-7172-9179>

Maria Szczepańska  <https://orcid.org/0000-0002-6772-1983>

References

- Gardner-Medwin JM, Dolezalova P, Cummins C, Southwood TR. Incidence of Henoch–Schönlein purpura, Kawasaki disease and rare vasculitides in children of different ethnic origins. *Lancet*. 2002;360(9341):1197–1202.
- Jannette JC, Falk RJ, et al. 2012 Revised International Chapel Hill Consensus Conference of Nomenclature of Vasculitides. *Arthritis Rheum*. 2013;65(1):1–11.
- Piram M, Mahr A. Epidemiology of immunoglobulin A vasculitis (Henoch–Schönlein): Current state of knowledge. *Curr Opin Rheumatol*. 2013;25(2):171–178.
- Piram M, Maldini C, Biscardi S, et al. Incidence of IgA vasculitis in children estimated by four-source capture-recapture analysis: A population-based study. *Rheumatology (Oxford)*. 2017;56(8):1358–1366.
- Saulsbury FT. Henoch–Schönlein purpura in children. Report of 100 patients and review of the literature. *Medicine (Baltimore)*. 1999;78(6):395–409.
- Pohl M. Henoch–Schönlein purpura nephritis. *Pediatr Nephrol*. 2015;30(2):245–252.
- McCarthy HJ, Tizard EJ. Clinical practice: Diagnosis and management of Henoch–Schönlein purpura. *Eur J Pediatr*. 2010;169(6):643–650.
- Ozen S, Pistorio A, Iusan SM, et al. EURAL/PRINTO/PRES criteria for Henoch–Schönlein purpura, childhood polyarteritis nodosa, childhood Wegener granulomatosis and childhood Takayasu arteritis: Ankara 2008. Part II: Final classification criteria. *Ann Rheum Dis*. 2010;69(5):798–806.
- Singhal M, Gupta P, Sharma A. Imaging in small and medium vessel vasculitis. *Int J Rheum Dis*. 2019;22(Suppl 1):78–85.
- Hwang HH, Lim IS, Choi BS, Yi DY. Analysis of seasonal tendencies in pediatric Henoch–Schönlein purpura and comparison with outbreak of infectious diseases. *Medicine (Baltimore)*. 2018;97(36):e12217.
- Jamrozik A, Sybilski A, Pohorecka M, Patena K. Zespół Schönleina-Henocha – nowe wyzwania diagnostyczne w starej chorobie. *Pediatr Med Rodz*. 2012;8(3):214–221.
- Calvino MC, Llorca J, Garcia-Porrua C, et al. Henoch–Schönlein purpura in children from northwestern Spain: A 20-year epidemiologic and clinical study. *Medicine (Baltimore)*. 2001;80(5):279–290.
- Masuda M, Nakanishi K, Yoshizawa N, Iijima K, Yoshikawa N. Group A streptococcal antigen in the glomeruli of children with Henoch–Schönlein nephritis. *Am J Kidney Dis*. 2003;41(2):366–370.
- Yang YH, Wang SJ, Chuang YH, Lin YT, Chiang BL. The level of IgA antibodies to human umbilical vein endothelial cells can be enhanced by TNF- α treatment in children with Henoch–Schönlein purpura. *Clin Exp Immunol*. 2002;130(2):352–357.
- Grenda R. Nefropatia w przebiegu plamicy Henocha–Schönleina. *Nefrol Dial Pol*. 2008;12(3):186–192.
- Davin JC, Ten Berge IJ, Weening JJ. What the difference between IgA nephropathy and Henoch–Schönlein purpura nephritis? *Kidney Int*. 2001;59(3):823–834.
- González-Gay M, López-Mejías R, Pina T, Blanca R, Castañeda S. IgA vasculitis: Genetics and clinical and therapeutic management. *Curr Rheumatol Rep*. 2018;20(5):24.
- López-Mejías R, Genre F, Pérez BS, et al. HLA-DRB1 association with Henoch–Schönlein purpura. *Arthritis Rheumatol*. 2015;67(3):823–827.
- Brogan PA. What's new in the aetiopathogenesis of vasculitis? *Pediatr Nephrol*. 2007;22(8):1083–1094.
- Amoli MM, Thomson W, Hajeer AH, et al. HLA-B35 association with nephritis in Henoch–Schönlein purpura. *J Rheumatol*. 2002;29(5):948–949.
- Brogan P, Eleftheriou D, Dillon M. Small vessel vasculitis. *Pediatr Nephrol*. 2010;25(6):1025–1035.
- Heineke MH, Ballering AV, Jamin A, Ben Mkaddem S, Monteiro RC, Van Egmond M. New insights in the pathogenesis of immunoglobulin A vasculitis (Henoch–Schönlein purpura). *Autoimmunity Rev*. 2017;16(12):1246–1253.
- Lau K, Suzuki H, Novak J, Wyatt RJ. Pathogenesis of Henoch–Schönlein purpura nephritis. *Pediatr Nephrol*. 2010;25(1):19–20.
- Gharavi AG, Moldoveanu Z, Wyatt RJ, et al. Aberrant IgA1 glycosylation is inherited in familial and sporadic IgA nephropathy. *J Am Soc Nephrol*. 2008;19(5):1008–1014.

25. Kyrlyuk K, Moldoveanu Z, Sanders JT, et al. Aberrant IgA1 glycosylation is inherited in pediatric IgA Nephropathy and in Henoch–Schönlein Purpura nephritis. *Kidney Int.* 2011;80(1):79–87.
26. Suzuki H, Raska M, Yamada K, et al. Cytokines alter IgA1 O-glycosylation by dysregulating C1GalT1 and ST6GalNAc-II enzymes. *J Biol Chem.* 2014;289(8):5330–5339.
27. Mizerska-Wasiak M, Gajewski Ł, Cichoń-Kawa K, et al. Serum GDIG1 levels in children with IgA nephropathy and Henoch–Schönlein nephritis. *Cent Eur J Immunol.* 2018;43(2):162–167.
28. Moura IC, Acros-Fajardo M, Sadaka C, et al. Glycosylation and size of IgA1 are essential for interaction with mesangial transferrin receptor in IgA nephropathy. *J Am Soc Nephrol.* 2004;15(3):622–634.
29. Haddad E, Moura IC, Arcos-Fajardo M, et al. Enhanced expression of the CD71 mesangial IgA1 receptor in Berger disease and Henoch–Schönlein nephritis: Association between CD71 expression and IgA deposits. *J Am Soc Nephrol.* 2003;14(2):327–337.
30. Lai KN, Leung JC, Chan Ly, et al. Activation of podocytes by mesangial-derived TNF-alpha: glomerulo-podocytic communication in IgA nephropathy. *Am J Physiol Renal Physiol.* 2008;294(4):F945–F955.
31. Yang YH, Chuang YH, Wang LC, Huang HY, Gershwin ME, Chiang BL. The immunobiology of Henoch–Schönlein purpura. *Autoimmun Rev.* 2008;7(3):179–184.
32. Roos A, Bouwman LH, Van Gijlswijk-Janssen DJ, Faber-Krol MC, Stahl GL, Daha MR. Human IgA activates the complement system via the mannan-binding lectin pathway. *J Immunol.* 2001;167(5):2861–2868.
33. Narchi H. Risk of long term renal impairment and duration of follow up recommended for Henoch–Schönlein purpura with normal or minimal urinary findings: A systematic review. *Arch Dis Child.* 2005;90(9):916–920.
34. Chan H, Tang YL, Lv XH, et al. Risk Factors Associated with renal involvement in childhood Henoch–Schönlein purpura: A meta-analysis. *PLoS One.* 2016;11(11):e0167346.
35. Halling SF, Söderberg MP, Berg UB. Henoch Schonlein nephritis: Clinical findings related to renal function and morphology. *Pediatr Nephrol.* 2005;20(1):46–51.
36. Ronkainen J, Nuutinen M, Koskimies O. The adult kidney 24 years after childhood Henoch–Schönlein purpura: A retrospective cohort study. *Lancet.* 2002;360(9334):666–670.
37. Hara M, Yanagihara T, Kihara I. Cumulative excretion of urinary podocytes reflects disease progression in IgA nephropathy and Schönlein-Henoch purpura nephritis. *Clin J Am Soc Nephrol.* 2007;2(2):231–238.
38. Jelusic M, Sestan M, Cimaz R, Ozen S. Different histological classifications for Henoch–Schönlein purpura nephritis: Which one should be used? *Pediatr Rheumatol Online J.* 2019;17(1):10.
39. Nicoara O, Twombly K. Immunoglobulin A nephropathy and immunoglobulin A vasculitis. *Pediatr Clin North Am.* 2019;66(1):101–110.
40. Huang X, Wu J, Wu XW, et al. Significance of histological crescent formation in patients with IgA vasculitis (Henoch–Schönlein purpura)-related nephritis: A cohort in the adult Chinese population. *BMC Nephrol.* 2018;19(1):334.
41. Davin JC. Henoch–Schönlein purpura nephritis: Pathophysiology, treatment, and future strategy. *Clin J Am Soc Nephrol.* 2011;6(3):679–689.
42. Xu K, Zhang L, Ding J, et al. Value of the Oxford classification of IgA nephropathy in children with Henoch–Schönlein purpura nephritis. *J Nephrol.* 2018;31(2):279–286.
43. Huang X, Ma L, Ren P, et al. Updated Oxford classification and the international study of kidney disease in children classification: Application in predicting outcome of Henoch–Schönlein purpura nephritis. *Diagnostic Pathol.* 2019; doi:10.1186/s13000-019-0818-0.
44. Koskela M, Ylinen E, Ukonmaanaho EM, et al. The ISKDC classification and a new semiquantitative classification for predicting outcomes of Henoch–Schönlein purpura nephritis. *Pediatr Nephrol.* 2017;32(7):1201–1209.
45. Zaffanello M, Fanos V. Treatment-based literature of Henoch–Schönlein purpura nephritis in childhood. *Pediatr Nephrol.* 2009;24(10):1901–1911.
46. Kidney Disease: Improving global outcomes (KDIGO). Henoch–Schönlein purpura. *Kidney Int Suppl.* 2012(11):218–220.
47. Hahn D, Hodson EM, Willis NS, Craig JC. Interventions for preventing and treating kidney disease in Henoch–Schönlein purpura (HSP). *Cochrane Database Syst Rev.* 2015;7(8):CD005128.
48. Dudley J, Smith G, Llewelyn-Edwards A, Bayliss K, Pike K, Tizard J. Randomised, double-blind, placebo-controlled trial to determine whether steroids reduce the incidence and severity of nephropathy in Henoch–Schönlein purpura (HSP). *Arch Dis Child.* 2013;98(10):756–763.
49. Davin JC, Coppo R. Pitfalls in recommending evidence-based guidelines for protean disease like Henoch–Schönlein purpura nephritis. *Pediatr Nephrol.* 2013;28(10):1897–1903.
50. Salewski D, Ambruzs J, Appel G, et al. Clinical characteristics and treatment patterns of children and adults with IgA nephropathy or IgA vasculitis: Findings from CureGN Study. *Kidney Int Rep.* 2018;3(6):1373–1384.
51. Koskela M, Jahnukainen T, Endén K, et al. Methylprednisolone or cyclosporine a in the treatment of Henoch–Schönlein nephritis: A nationwide study. *Pediatr Nephrol.* 2019;34(8):1447–1456.
52. Ozen S, Marks SD, Brogan P, et al. European consensus-based recommendations for diagnosis and treatment of immunoglobulin A vasculitis – the SHARE initiative. *Rheumatology (Oxford).* 2019. doi:10.1093/rheumatology/kez041
53. Goldstein AR, White RH, Akuse R, Chantler C. Long-term follow-up of childhood Henoch–Schönlein nephritis. *Lancet.* 1992;339(8788):280–282.
54. Nussinovitch N, Elishkevitz K, Volovitz B, Nussinovitch M. Hypertension as a late sequela of Henoch–Schönlein purpura. *Clin Pediatr.* 2005;44(6):543–547.
55. Audemard-Verger A, Pillebout E, Guillevin L, Thervet E, Terrier B. IgA vasculitis (Henoch–Schönlein purpura) in adults: Diagnostic and therapeutic aspects. *Autoimmun Rev.* 2015;14(7):579–585.
56. Heleniak Z, Dębska-Ślizień A, Ptasńska-Perkowska A, Rutkowski B. Zapalenie naczyń związane z IgA (plamica Henocha-Schönleina) a nerki. *Forum Nefro.* 2014;7(3):159–168.
57. Kanaan N, Mourad G, Thervet E, et al. Recurrence and graft loss after kidney transplantation for Henoch–Schönlein purpura nephritis: A multicenter analysis. *Clin J Am Soc Nephrol.* 2011;6(7):1768–1772.

